THÈSE

Pour obtenir le grade de

Docteur de l'Université Paris Descartes

Specialité: Biophysique

École Doctoral: Frontières du Vivant, ED 474

Présentée par:

Ester ANON

Sujet de la thèse:

Dynamique de la fermeture des trous épithéliaux en utilisant des techniques de micromécanique et de microfabrication

Dynamics of epithelial gap closure using microfabrication and micromechanical approaches

Thèse dirigée par Benoit LADOUX

Soutenue le 5 octobre 2012 davant le jury composé par:

Mme. Cecile Sykes,	présidente
M. James W. Nelson,	rapporteur
M. Michel Labouesse,	rapporteur
M. Nir Gov,	examinateur
M. Matthieu Piel,	examinateur
M. Benoit Ladoux,	directeur de thèse
M. Xavier Trepat,	co-directeur de thèse

A qui veu llum en mi, fins i tot quan estic a les fosques

To all who believed in me

A la iaia, perquè el seu record m'ha acompanyat
durant la redacció de la tesi,
i estaria orgullosa de veure on he arribat.

Acknowledgments

You are now starting this thesis manuscript, reading page 4 of the thesis. However, these lines are written at the very end of my PhD, after 4 years of absorbing work, filled with many enriching scientific experiences, acquired knowledge, and emotions. Only now I look back at these years with some perspective. In my opinion, a PhD can be compared to a roller-coaster: you feel very excited to jump in, it is full of ups and downs, it is very intense but goes by very fast. Sometimes you can feel scared of a huge slope, although I am not easily scared and prefer to laugh of excitement rather than close my eyes.

But more importantly, this is a ride where you do not go alone. Many people have been by my side all along the PhD, others have crossed my path at some points. First of all, I thank my PhD supervisors, who are great scientists and great persons that I admire for their impeccable scientific career. I thank Benoit for giving me the opportunity of going into the PhD adventure and make it international, allowing me to stay in Paris, Barcelona, and Singapore, which I truly enjoyed. Thanks for introducing me to the world of pillars and PDMS, for his scientific guidance, for helping me solve the problems that popped-up (especially when bent pillars where bending my mind) and for his always-supportive words. I thank my co-director Xavi, who mentored me and transmitted me his passion for research, for being always available for me, and for being strict with me, because this means he cares for me. I truly thank you for sending me back my writings all in red, because I learned a lot from your corrections and advices. Thanks for making me something close to a scientist.

Un grand remerciement à mes camarades du MSC: Amsha, Jimmy, Pierre, j'ai passé des très bons moments avec vous pendant les prèmieres années de thèse à Paris. Merci pour votre aide au labo, pour votre patience avec mon français, pour des longes conversations, pour les verres dehors le labo. Mes mémoires aussi pour ceux qui j'ai rencontrés au début de la thèse : Guillaume, Démosthène, Damien, Léa, Felix, Agnès, et autres.

To the lab in Barcelona, infinite thanks for all the great moments we had. Un gràcies enorme al Xevi ; han estat 4 anys intensos treballant colze a colze, dels quals he après molt de tu, científicament i personalment. Gràcies pels teus consells, per la teva ajuda, per les nostres converses, per la teva rialla, i per fer tan agradable el treballar junts. I això no ha fet més que començar, llarga vida al colze a colze ! Agustí, gràcies per haver aparegut. Has estat clau en la última part de la tesi, crec que hem fet un bon equip : ets un mecànic *digno de admirá* ! He après molt de

tu, *yo soy una simple ganadera,* i hem compartit molts bons moments dins i fora del lab. T'auguro una molt bona tesi, que m'aniras explicant mentre patinem, fem mojitos, o durant concerts. Muchas gracias también a Elsa, una pieza muy importante en el lab, he aprendido mucho de tu parte científica, y he encontrado una muy buena amiga en ti, y también en Nathalie. Gràcies Mari, per tota la feina imprescindible que fas al lab, per cuidar-me les cèl.lules, i per les quedades fora del lab. Merci à Romaric (for your easy-goingness), a Laura (con quien he compartido algunas de mis inquietudes), a la Sònia (la més autèntica), l'Anita (que sempre alegra el laboratori), el Pere (un jove cientific que també admiro molt), l'Alberto (gran fichaje, pero no te me estreses !). Grazzie Don Vito, my model(ler), for being a charming italian English-man or English italian-man, for your corrections on my English, and for our shared loud laughs. I wish you and Antonia all the best and a long life in Barcelona. General thanks also to UBBs lab, with whom I shared some great scientific discussions and nice moments. Ha estat un plaer coincidir amb la Irene, l'Esther, l'Alicia, la Marta, i tota la resta, en els intensos (i potser interminables ?) lab meetings, i en la Mojito Pool party ! No descarto deixar-m'hi caure en les properes edicions…

Also, unforgettable people I met at Mechanobiology Institute (MBI) in Singapore. First I thank Mike Sheetz for allowing me to spend few months in 2010 and in 2012 in such an amenable scientific environment, terrific place they have put together. Thanks to Man Chun, who guided me to find my way around the lab, supplied me with all reagents and cells I needed, and was always there to help me. Likewise, thanks to Surabhi, Vedula, Soumya, for being there when I was lost in the lab. Thanks to the Indian gang for the great moments we spent there : Soumya again, Shefali, Nikhil, Abishek, Madduresh. Thanks to Cheng-han for great moments we shared, and being an inspiring scientist. Thanks to all the others with whom I shared moments in the intense months in Singapore : Thomas, Andrea, Cristina, Sree, Julia, Perrine, Naila, Earnst, and all the rest.

And a few words for the real discoveries I made in MBI. I am not talking about a protein or a cellular mechanism, but a couple of persons: Akila, it has been great to meet you, my beloved friend. Thanks for the many hours we spent together talking about the PhD project, PhD life, PhD in general, and life in general. Thanks for your friendship, I still hear you laugh, and I hope to hear it lively again soon. Maruxa, mis gracias no caben en cuatro líneas. Hiciste inolvidable mi última estancia en Singapur, y este manuscrito no estaría escrito sin tu apoyo, tu cariño, tus consejos. Cuando me acuerdo de cómo preparabas tus membranas de stretch y tus immunos, me viene a la memoria tambien los Kings of Leon, la neutral buoyancy, y los cereales de chocolate. Y esto es solo el principio! I must say: thanks Benoit for bringing us together!

A brief thank to the people who scientifically contributed, sometimes minorly, sometimes without knowing, to my PhD. Thanks to the people in the doctorate school FdV, with whom I shared stimulating scientific meetings especially in the first year, thanks Samuel and François. Thanks to Julien Collombeli, who trained me in the use of the laser ablation set-up, and was always there to solve my technical problems and to advise me scientifically. Thanks also to Sebastien, for his Fiji plugins and patience to teach me macro-writing. Gràcies al Jordi Alcaraz per discussions científiques i consells.

Gràcies a la gent que, tot i no estar relacionada directament amb el doctorat, ha estat important en aquest període. Gràcies a la meva nina Laura, amb qui he passat hores i hores parlant del doctorat, i en part culpable que m'embarqués en aquesta aventura, com també jo soc en part culpable que ella sigui thésarde. Gràcies als meus pares i a l'Eduard, que sempre han estat al meu costat, s'han preocupat per la meva tesi, i m'han animat a tirar endavant.

Por último, gracias a mi compañero de viaje, sin el cual este proyecto no estaría aqui. Gracias por darme la mano durante el trayecto, por ayudarme a levantar cuando tropezaba, por compartir mis ilusiones cuando avanzaba, por hacerlo todo más fácil. Gracias por tu cariño y por tu comprensión. Gracias por subirte a la montaña rusa conmigo y sentarte en la primera fila.

Wow, that was long. But give me this. It's been 4 years, 3 countries, many experiences, many people. Forgive me if I missed someone, I will surely have a thought for you sometime. I hope many of you will also stop by in my future way. I will keep you posted about it!

Résumé (Français)

Les cellules peuvent migrer sous différentes conditions qui dépendent de l'environnement biochimique ou mécanique. Connaître les mécanismes de la migration, les protéines impliquées et leur régulation est essentiel pour comprendre les processus de morphogénèse ou certaines situations pathologiques. Dans ce contexte, la migration collective des cellules est un processus clé qui intervient pendant le développement ainsi que dans la vie adulte. Elle joue un rôle très important pour la formation et l'entretien des couches épithéliales, notamment au cours du développement embryonnaire et pendant la cicatrisation des trous épithéliaux résultant, par exemple, d'une blessure. Lorsque l'épithélium présente une discontinuité, des mécanismes actifs qui impliquent une migration coordonnée des cellules sont nécessaires pour préserver l'intégrité des tissus. Dans ce travail, nous avons étudié les mécanismes impliqués dans la fermeture des trous dans un épithélium. Pour des blessures de faible taille, le mode de fermeture dit de *purse string* est souvent évoqué, impliquant la contraction d'un anneau contractile d'acto-myosine qui ferme la blessure. Pour des blessures de tailles plus importantes, il est courant d'observer un mécanisme différent conduisant à la migration active des cellules du bord qui couvrent la surface "libre".

Pour étudier ces aspects de manière quantitative et reproductible, nous avons développé une nouvelle méthode basée sur des techniques de microfabrication et de lithographie dite « molle » qui permet de faire une étude quantitative de la fermeture des trous épithéliaux. Nous avons fabriqué des substrats de micropiliers de diamètre et de forme variés dans les quels les cellules sont libres de pousser entre les microstructures. Lorsqu'elles sont parvenues à confluence, on retire le substrat qui laisse apparaître des trous contrôlés.

De cette manière, nous avons observé que les cellules épithéliales forment des lamellipodes pour la fermeture de ces trous. Le mécanisme de fermeture dépend de la taille des trous et nous avons pu observer différents régimes en fonction de diamètre des piliers. Les trous petits (de la taille d'une seule cellule) sont fermés par un mécanisme passif alors que la fermeture de trous plus larges nécessite un mécanisme actif de migration conduisant à la formation de lamellipodes et à des modes de migration collective.

Par la suite, nous nous sommes intéressés à l'aspect mécanique de la fermeture des trous épithéliaux. Pour cela, nous avons utilisé un système d'ablation laser pour rompre quelques cellules dans une monocouche épithéliale. Nous avons alors mesuré les forces de traction que les cellules exercent au substrat

et leur évolution temporelle et spatiale. Nous avons pu mettre en évidence différents modes de traction: au début, les cellules exercent des forces de traction importantes sur leur substrat pour laisser place à des contraintes mécaniques qui sont davantage issues d'un processus collectif au travers de la formation d'un câble multicellulaire qui les relie les cellules de bord entre elles.

En conclusion, ce travail nous a permis d'obtenir des informations sur les mécanismes dynamiques de fermeture des tissus épithéliaux qui sont évidemment impliqués dans la cicatrisation des blessures mais aussi dans certains problèmes de malformations congénitales lors l'embryogenèse.

Abstract (English)

Most cells migrate under the appropriate conditions or stimuli; understanding the mechanisms of migration, the players involved, and their regulation, is pivotal to tackle the pathological situations where migration becomes an undesired effect. While largely overshadowed by the study of single cell migration, collective cell migration is a very relevant process that takes place during development as well as in adult life. Collective migration is very relevant for the formation and maintenance of epithelial layers: extensive migratory processes occur during the shape of the embryo, as well as during the healing of a skin incision in the adult. When openings or discontinuities appear in the epithelia, it is crucial that the appropriate mechanisms are activated.

In the present work we attempt at deciphering what are the mechanisms involved in gap closure. Until now, most of the literature concerning the subject has reported contradictory results, mainly arising from the complexity of the process and the lack of systematic analysis. We have designed a novel approach to address epithelial gap closure under well-defined and controlled conditions. By using our gap patterning method, we have observed that epithelial cells extend lamellipodia when exposed to a newly available space. Interestingly, we found that the closure of such gap depends on the size: small gaps are closed by a passive physical mechanism, while large gaps are closed through a Rac-dependent cell crawling mechanism, in a collective migration-like manner.

Next, we also addressed the mechanical component of epithelial gap closure. In this study, we took advantage of a laser-ablation system to disrupt some cells within an epithelial monolayer, and study how the remaining cells sealed that gap. By measuring the traction forces that cells exert on the substrate along the closure, we observed that cells first pulled on the substrate to propel themselves. By the last steps of closure, there is a transition in the direction of the force, so that cells are pulled to the center of the gap due to the assembly of a supracellular actin cable. Altogether, this work provides valuable knowledge on the current understanding of the mechanisms accounting for epithelial gap closure. We believe that a better comprehension of these mechanisms can help to shed light in clinically relevant situations where epithelial gap closure is impaired.

Thesis context

Motion is an inherent feature of cells, and most cells can migrate under the appropriate conditions or stimuli. Researchers have been plating cells in Petri dishes and studying their movement for many decades now. Deciphering the fundamental mechanisms of cell migration has important clinical applications. For example, tumor spreading results as a de-regulation of the migratory capacity of cells. Understanding the mechanisms of migration, the players involved, and their regulation, is thus pivotal to tackle the pathological situations where migration becomes an undesired effect.

Indeed, cell migration is essential both during development and in postnatal life, and both under physiologic and pathologic conditions. While the migration of isolated cells has been widely studied, it is only applicable in few examples, such as in immune cells migration, some cases of metastating tumour cells, and several examples during development. Nevertheless, studies in single cell migration have provided insightful achievements on the mechanism of migration leading to a well-established model. Research is intense in this field in trying to reconcile the concepts (mostly arising from 2D migration) with more sophisticated *in vivo* migration mechanisms, such as amoeboid or mesenchymal-like 3D migration.

Furthermore, a rather new but promising field of study is the collective movement of cells. In collective cell migration, many features of single cell migration apply, but a level of complexity is added by the fact that groups of cells move coordinately and coherently as a collective. Such mode of migration is very relevant in most of the first stages of development: during gastrulation, there is extensive migration of the ectoderm (together with cell proliferation, intercalation and other processes). Often, such migratory movements have to be tightly coordinated with other morphogenetic events. In addition, collective migration takes place during adult life, with relevant clinical impact: tumors spread by migrating collectively outside the primary site, and wounds have been shown to heal through collective migration processes.

We have focused in the study of a particular case of collective migration, which is the closure of gaps within epithelia. Early morphogenetic stages are based on extensive cell movements involving sealing of gaps. If cell sheets do not seal these gaps properly, malformations or even lethal effects can occur. Also, in such a common situation as a cut in the skin, epidermic cells are activated to migrate into the created discontinuity. Understanding the sealing of epithelial gaps can provide valuable insights into the sealing of a naturally occurring openings (such as

Drosophila dorsal closure, *Caenorhabditis elegans* ventral enclosure, last stages of neurulation, trachea tube closure, eyelid closure, etc.) and the sealing of artificially produced openings during injury events. Moreover, such situation can also be paralleled with the extrusion of cells from an epithelial sheet, as occurs with apoptotic cells in developing tissues or in homeostasis of adult tissues.

Up to now there is rather extensive literature on epithelial gap closure, coming mainly from studies of embryonic healing, embryonic movements involving gap closure, and epidermic wound healing. Furthermore, epithelial gap closure has been traditionally addressed in the scratch-wound assays, and these studies have provided instrumental information in the basic mechanisms of collective cell migration. However, the intricacy of the process, its complex regulation by the family of RhoGTPases, and the experimental variability between such studies has led to opposing results and divergent conclusions. Thus, we attempted to address the question of epithelial gap closure from two flanks: on one hand, we present an approach where the experimental conditions are well defined and tightly controlled. In such set-up, we can thoroughly investigate the mechanism of closure of undamaged gaps within an epithelial sheet in an *in vitro* model. On the other hand, we provide the mechanical analysis of epithelial wound closure, since the forces exerted during wound healing have remained unknown until now.

Altogether, we believe that studying *in vitro* epithelial gap closure can provide insightful mechanistic understanding of both specific gap closure situations and general features for improving the current knowledge of collective cell migration.

Thesis outline

The thesis manuscript is structured as follows:

In the **<u>first chapter</u>**, we start presenting the ultimate cellular structure responsible for migration (as well as for numerous cellular processes): the acto-myosin cytoskeleton. Then, we explain how the acto-myosin is structured at the leading edge of cells as a lamellipodia, and how it is connected to the substrate through focal adhesions. After, we discuss a second protrusive structure, filopodia, which is complementary to lamellipodia. Having introduced the modular cellular elements required for migration, we put these parts together to present an integrative mechanistic view of cell migration. We first focus on single cell migration, and its regulation by the Rho family of GTPases. We continue by addressing cell collectives, in the specific case of epithelia, and how cells are connected between each other through specific cell adhesions. We highlight the basic characteristics of collective cell migration and the rationale behind collectivity, while framing the situations where collective migration occurs. Then, we present the different mechanisms proposed to explain collective migration in different situations. After, we address the main stages involving collective migration during the closure of an epithelial discontinuity: during development and in wound healing. We also address a particular wound healing-like case, which is the extrusion of apoptotic cells. Finally, we present the two mechanisms that have been proposed to explain the closure of epithelial gaps: purse-string contraction and cell crawling. We provide the evidences for the presence of one or the other mechanism, to what extent both mechanisms have been proven to occur concomitantly, and where the literature shows controversy or disagreement. This will lead us to proposing the objectives of the present thesis in order to shed some light in the unresolved topic of epithelial gap closure.

After, we present our results based on the studies that have been carried out during this PhD. The **<u>second chapter</u>** presents a novel set-up where epithelial gap closure can be systematically studied under well-controlled conditions. First, we introduce the set-up we have designed for this study, as a methodology-like section. A characterization of the gap-producing method is also provided. By using our approach, we can directly tackle the question of size-dependent mechanism. We expose the results obtained: a quantitative analysis of the dynamics of closure and the concomitant cell rearrangements, and the regulation of the process by the Rho family of GTPases. Overall, we show how small gaps close by a different more passive mechanism, which is not controlled by the classical closure regulators, while large gaps are highly dependent on the extension of lamellipodia to be

closed. We frame our results in the existing literature and finalize the chapter with the conclusions of the work and possible future directions that can be pursued. The **third chapter** addresses a more physical part of epithelial gap closure. We start by motivating why the mechanics of the process can help to better understand epithelial gap closure. Then, we present the methodology we have used in this study. After, we provide and discuss the results obtained. In this work, we have (for the first time) measured the traction forces exerted by epithelial cells that move inwards to seal a laser-induced wound. We show a local response of the wound-margin cells to the presence of a wound. Then, we analyse the temporal evolution of traction forces as closure progresses. We end the chapter by elaborating our current working hypothesis and presenting the implications of such study. This project has been carried out in the Integrative Cell and Tissue Dynamics lab, at the Institute of Bioengineering of Catalonia (Spain), under the supervision of Xavi Trepat.

Finally, the **fourth chapter** presents a general discussion of the thesis project, and the conclusions derived from the work. We define how the presented work has contributed to the better understanding of the topic of epithelial gap closure, and point out some questions that remain to be addressed.

Table of contents

CHAPTER 1:

Mechanisms of cell migration

I. Cellular machinery

In this section, we will introduce the eukaryotic cell and the cellular components more related to the cellular movement from a molecular and functional point of view.

1. The eukaryotic cell

The cell has been long considered as the building block of multicellular systems, i.e. the basic unit of life. Eukaryotic cells are very complex systems highly anisotropic and extremely variable in shape and size. They are composed of different organelles, such as the endoplasmic reticulum, Golgi apparatus, mitochondria, lysosomes, etc., each one in charge of a specific and indispensable function (Figure 1. 1). One the most important component of eukaryotic cells is the nucleus, which stores the genetic information required for cellular activities and in particular for cell division. All these organelles are confined by a lipid bilayer, a selective barrier that isolates the organelles from the cytoplasm and allows for a different soluble protein content, ionic strength, pH, among other features. Alongside, the cell itself is enclosed in a lipid bilayer or plasma membrane. This membrane acts as a barrier between the cytoplasm and the exterior, but also enables external communication thanks to its permeability, transmembrane channels, and transmembrane or membrane-associated proteins. The organelles are embedded in the cytoplasm, a gel-like component (70-90% composed of water) that fills the cells (Alberts et al., 2008). The cytoplasm also contains the cytoskeleton, which is the cell scaffold. The cytoskeleton is a conglomerate of different types of filaments, which from the engineering standpoint may be seen as structural elements of a biopolymer network defining the architecture of the cell. Cells interestingly show material properties characteristic of both solids and liquids; they are able to elasticly mantain their shape and yet plastically adapt it to the changing environment. Furthermore cell response to external deformations may be highly non-linear (Trepat et al., 2007; Kollmannsberger et al., 2011). The cytoskeleton and plasma membrane together are thought to define the viscoelastic properties of cells (Kumar et al., 2006; Kasza et al., 2007), which may also depend on the degree of internal stresses as well as on the mechanical properties of the extracellular milieu (Tee et al., 2009).

Inside the cell, there are certain structures particularly relevant for cell migration. These include: the acto-myosin cytoskeleton, which constitutes the

basic structural and functional integrative unit; the lamellipodium, a sheet-like extension of the membrane at the front of cells; and the focal adhesions, the sites of cytoskeleton-substrate anchoring. Filopodia also play an accessory role in certain migration processes as environment-sensing structures. All these structures are highly dynamic and adapt to changes in both the intracellular state of the cell as well as variations of the surrounding matrix. Therefore, we will hereafter focus on these structures that have an active role in migration. We will describe them from a structural and functional point-of-view and discuss how they are related to the extracellular environment.
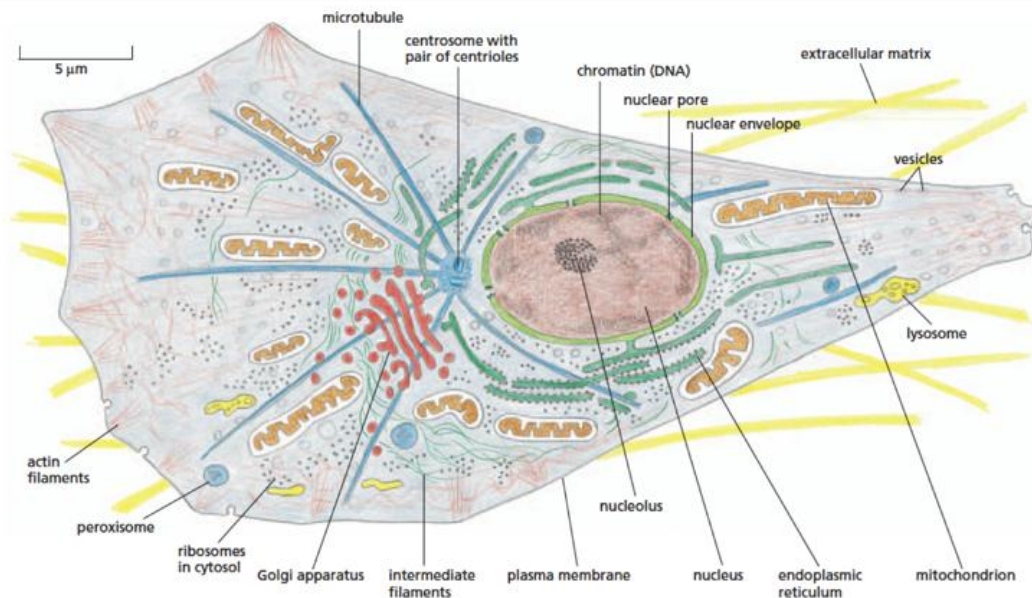
Figure 1. 1. Classical scheme of the major features of a eukaryotic animal cell. From (Alberts et al., 2008).

2. Acto-myosin cytoskeleton

The basic cellular module related to migration is the cytoskeleton. The cytoskeleton is the functional and structural scaffold of the cell; it is involved in most, if not all, of the cellular processes: migration, division, endo/exocytosis, signalling, environmental sensing, etc. (Pollard and Cooper, 2009). The cytoskeleton includes the acto-myosin cytoskeleton, and the microtubules and intermediate filaments network. Although microtubules and intermediate filaments are in charge of very relevant cellular functions, such as providing coherence, maintaining cell shape, promoting intracellular vesicular transport, among others, we will not thoroughly address them in the present work. We will focus on the structure more relevant to cell migration, which is the acto-myosin

cytoskeleton. However, microtubules and intermediate filaments will also be mentioned when their implication is notable.

2.1. Actin

Actin is one of the most abundant and ancient proteins in the cell, highly conserved in eukaryotic cells and with prokaryotic ancestors (present at intracellular concentrations of 10-100 μM). Monomers of globular actin (G-actin, 375 AA, 42 KDa) polymerize to form helicoidal actin filaments (F-actin) of 8 nm in diameter. Because the G-actin protein itself is polar, such filaments are also polar, where one of the ends is called (+) or barbed, and the other is called (-) or pointed end (Figure 1. 2. A) (Didry et al., 1998).

The polymerization process is triggered by the energy released in the hydrolysis of ATP to ADP+Pi and can be divided in 3 steps:
- *Nucleation*: three actinG monomers are stable enough to act as a nucleation core for the subsequent addition of new monomers.
- *Growth:* new actinG monomers are added to the core, more rapidly at the (+) or barbed end than at the slow polymerizing (-) or pointed end. At this moment, ATP is hydrolysed to ADP (Korn et al., 1987).
- *Depolymerization:* actinG bound to ADP favours the release of monomers from the actinF, which occurs faster at pointed ends.

Such polymerization process is described as *actin treadmilling*: the barbed end elongation balances the pointed end depolymerization, resulting on net forward movement maintaining filament length ((Figure 1. 2. A) (Bugyi and Carlier, 2010). Created either by *de novo* assembly of nucleation cores or by severing or uncapping of existing filaments, free barbed ends act as the template where new actin monomers are added. The process, which *in vitro* is thermodynamically slow (0.3 s^{-1}) and some of steps are kinetically unfavourable, must be regulated (namely sped up) by actin binding proteins in the cellular context, so that rates of treadmilling are up to 100 times faster *in vivo* (Pantaloni, 2001; Bugyi et al., 2008).

Actin can be found in many cellular structures: in the acto-myosin cytoskeleton itself, in lamellipodia and filopodia, in cilia and microvilli, in the cytokinetic ring, in podosomes and phagocytic cups, among others. Actin is thus indispensable for a considerable number of processes. Needless to say, it is essential for migration: cells treated with drugs that disassemble the actin cytoskeleton present altered motility, protrusivity, and polarization, among other aspects (Cooper, 1987). However, for most of its functions, actin is typically associated with its partner myosin, which provides the F-actin scaffold with the capacity to contract and bear tension (Parsons et al., 2010).

2.2. Myosin

Myosin is a complex family of proteins, containing many different cell type-, cell compartment- specific family members and isoforms (from myosin I to myosin XIV) (Cheney et al., 1993). It is a key protein in many aspects such as scaffolding, polarity, adhesion, migration, etc. Altogether, myosin can be considered as a master integrator of many biomechanical cellular processes. The most abundant myosin type is myosin II, which is the only one capable of forming polymeric assemblies (bipolar filaments, described below). We will hereafter focus in myosin II.
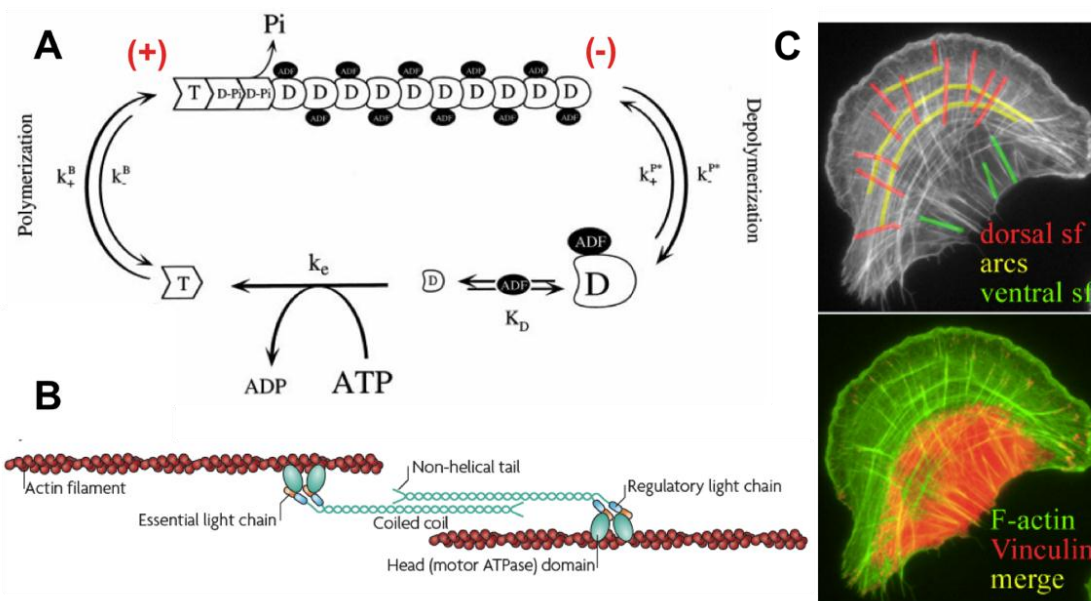
Figure 1. 2. Structure of acto-myosin cytoskeleton. (A) Actin treadmilling. The sizes of the complexes are indicative of their relative abundance in steady state. Treadmilling concept refers to the constant depolymerization from pointed (-) ends and the growth on the barbed (+) ends. In *in vitro* conditions, the process is slow. Inside the living cell, the associating/dissociating constants (Kx) are modulated by actin binding proteins. Adapted from (Carlier et al., 1997). (B) Scheme depicting how myosin cross-links actin filaments forming a bipolar filament. Note how myosin interacts with actin through its head domain, where it possesses its ATPase activity, so it can walk along actin filaments and contract the bipolar filament in an anti-parallel manner. From (Parsons et al., 2010). (C) Stress fibres are classified into ventral stress fibres (when both ends are docked at focal adhesions, in green), dorsal fibres (one end attached, in red) and transversal fibres or arcs (both ends free, in yellow). In the bottom image, focal adhesions are seen as small red dots (vinculin). From (Naumanen et al., 2008).

2.1.1.   Myosin structure

Myosin II is composed of 2 heavy chains (MHC), 2 essential light chains (MLC), and 2 regulatory chains (MRC). The N-terminal globular domain (the "head") contains the actin and ATP-binding sites (and concomitantly the ATPase catalytic domain), while the C-terminal are α-helices coiled-coil domains that form

homodimers. Myosin units assemble into bipolar filaments composed of several tail-to-tail associated units (Siddique et al., 2005). Now, these bipolar filaments can assemble with antiparallel actin filaments to form the acto-myosin cytoskeleton (Figure 1. 2. B). There are three main myosin II isoforms that differ in their biochemical specifications, including their ATPase activity (Kelley et al., 1996). They are spatially and functionally segregated and generally one isoform cannot account for another one (Bao et al., 2007), although some functions could be redundant by different isoforms. **Myosin IIA** has a fast ATPase activity and thus constitutes a rapid motor, being efficient for the regulation of cytoskeletal dynamic remodelling and actin retrograde flow (Conti and Adelstein, 2008). It is thus more related to protrusion and to exerting traction forces (both actions being finely balanced to maintain cytoskeletal integrity), and is typically localized at the cell front and rear (Cai et al., 2006; Cai and Sheetz, 2009). **Myosin IIB**, on the other hand, is slower and more stably cross-linked with actin (Lo et al., 2004), present predominantly at centre and back of the cell, and it is presumably more implicated in tail retraction (Kolega, 2003; Vicente-Manzanares et al., 2007; Smutny et al., 2010; Saitoh et al., 2001). Myosin IIB is also implicated in providing directionality to migration (Lo et al., 2004). **Myosin IIC** is present at lower degree and less well characterized (Golomb et al., 2004).

2.1.2. Myosin regulation

Myosin activity is regulated *via* reversible phosphorylation at Ser19 and Thr18 of MRC (Adelstein et al., 1975) by multiple kinases, which affects the ATPase activity of myosin (when bound to actin) but does not act in the affinity of myosin for actin. Such phosphorylations have also been shown to regulate the assembly of myosin II filaments *in vitro* (but not verified *in vivo*), unfolding head-head interactions and allowing it to assemble with actin (Jung et al., 2008).

Many kinases can phosphorylate and thus activate myosin II MRC via distinct activation signals. Myosin light chain kinase (MLCK) acts downstream of Ca^{2+}-calmodulin pathway, while Rho-associated kinase (ROCK) and citron kinase respond to RhoA signalling and can also activate myosin II by inhibiting its dephosphorylation (by acting on myosin phosphatase MYPT) (Matsumura, 2005). Protein Kinase C (PKC) inhibits MRC in an alternative pathway, by phosphorylating MRC on different residues, thus rendering it a poorer substrate for the MLCK activation. Other regulating kinases include leucine-zipper interacting kinase (ZIPK), myotonic dystrophy kinase related cdc42-binding kinase (MRCK), among others. Due to the existence of multiple kinases phosphorylating myosin, if one kinase is not activated (for instance due to external manipulations) other kinases can overcome the absence. As a consequence, such intricate regulation has relevant implications when studying possible roles of myosin during cell

migration, as the inhibition or depletion of one kinase can produce no final effects if other kinases are at play.

Actin and myosin have a tight structural and mechanical connection, constituting the acto-myosin cytoskeleton, the basic architectural and functional scaffold of the cell. **Stress fibres** are one of the best examples of the close collaboration of actin and myosin. Stress fibres are bundles of actin filaments decorated with myosin and α-actinin distributed periodically (Cramer, 1997). Actin filaments extend between two substrate attachment points (ventral stress fibres) or grow from one attachment point (dorsal stress fibres), and myosin conveys the contractile capability to such filaments ((Figure 1. 2. C) (Hotulainen and Lappalainen, 2006).

Acto-myosin cytoskeleton is relevant for most of the cellular routines (cohesivity, migration, polarization, division, etc.) and must be especially highlighted in the present work since it is the structure ultimately responsible for cell movement. Acto-myosin cytoskeleton drives the extension of cellular protrusions (lamellipodia and filopodia) in the direction of migration and accounts for the cellular contractility needed to translate the cell forward. Moreover, it is also implicated in the relation of the cell with its environment through cell-substrate and cell-cell adhesions.

3. Lamellipodia

Lamellipodia are largely involved in the migration of cells and their directionality, specifically for the mesenchymal-like mode of migration, on which we will focus (will be further explained in Chapter 1 section I. 7). Even lamellar fragments (excised from a migrating keratocytes), without other cellular components, retain their migratory capability and even the directionality (Verkhovsky et al., 1999). Lamellipodia were first described in fibroblasts in 1970 by Abercrombie et al. (Abercrombie et al., 1970) from electron micrographs as flat-membrane structures rich in microfilaments. Indeed, lamellipodia are thin sheet-like membrane extensions (0,1-0,2 μm high, 10 μm wide) containing a dense mesh of crosslinked actin filaments (average of 100 per μm of leading edge, actin density linearly decaying form very edge inward) (Abraham et al., 1999; Watanabe and Mitchison, 2002; Small et al., 1995). Lamellipodial movement is based on the pushing of growing actin filaments onto the membrane to propel it forward. As such, plasma membrane plays a very relevant role in the extension of lamellipodia (Keren, 2011). During lamellipodial protrusion, plasma membrane unfolds

allowing for extra membrane surface to extend due to the pushing of F-actin, and thus membrane tension increases (Gauthier et al., 2011). Interestingly, a certain degree of basal membrane tension is required for efficient propulsion of lamellipodia, since membrane tension helps in directing actin filament thrust to the direction of migration, preventing lateral lamellipodia (Batchelder et al., 2011).

Actin filaments in the lamellipodium are organized in a branched or dendritic array to cover wide areas at the front of the cell. Despite the features of the actin cytoskeleton explained in Section 2.1 hold true *in vivo*, in migrating cells many other factors are involved in regulating the dynamics of actin cytoskeleton. Very importantly, there are numerous regulatory proteins that boost treadmilling rates so that cells can adapt to different requirements of motility speed. In the context of migrating single cells, the actin treadmilling concept is translated into the larger framework that is the lamellipodial actin array. Early observations showed that a photo-activated fluorescent actin particle within the actin array did not absolutely displace inside a moving cell, indicating that the cell movement occurred at the same rate of actin treadmilling. Thus treadmilling is actually understood for the whole processive actin array (Wang, 1985; Webb et al., 2002). Such process is described in the dendritic nucleation/treadmilling model (Figure 1. 3):
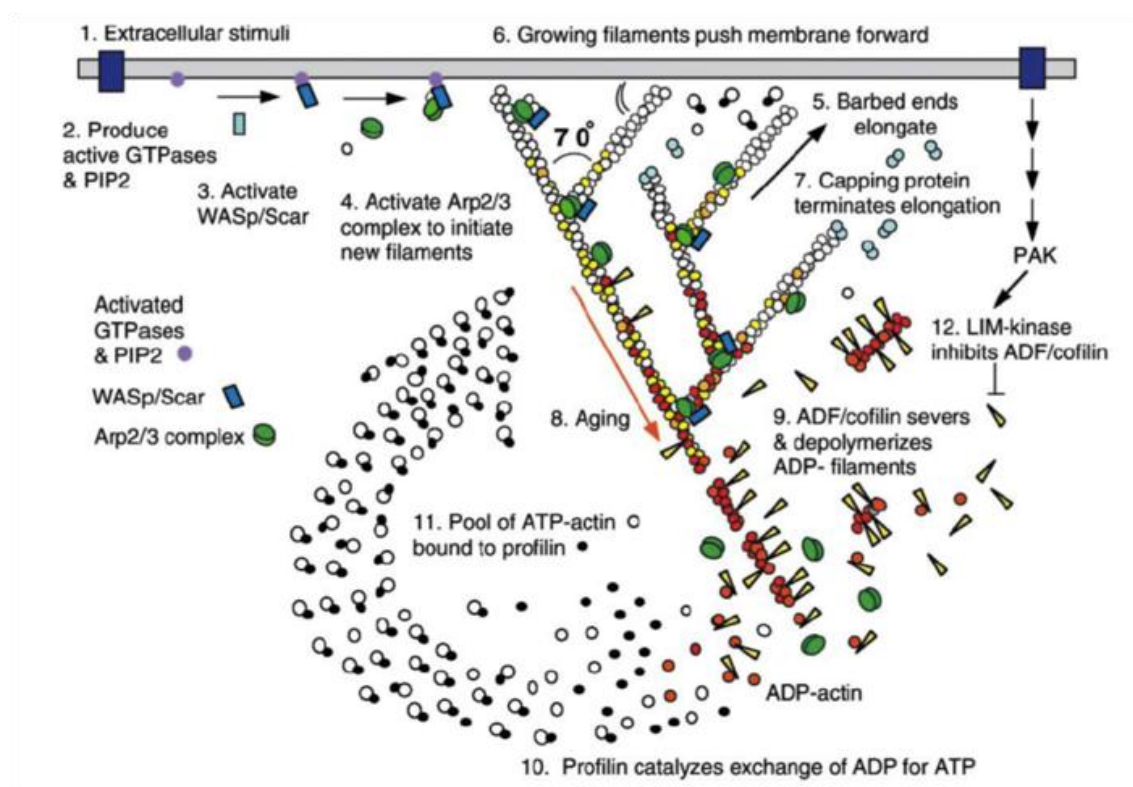
Figure 1. 3. Actin dendritic array model. Treadmilling occurs at a larger scale: the array grows at the front and disassembles further from the leading edge. From (Pollard and Borisy, 2003).

1. **Extracellular signals**, such as growth factors, chemoattractants, etc. trigger an intracellular signalling cascade, which typically results in the clustering of membrane proteins such as Rho family of GTPases, SH3 adaptor proteins, or PIP2. These intermediaries activate **nucleation-promoting factors** (NPFs), typically those belonging to WASP/Scar family.

2. NPFs stimulate **Arp2/3** to trigger the growth of a new actin filament from the side of a pre-existing filament typically close to its barbed end, at an angle of 70° (Amann and Pollard, 2001) (Figure 1. 4). However, a recent study reported that there could exist a wider distribution of insertion angles (Koestler et al., 2008). Arp2/3 is thus the key player in lamellipodial branched actin, as proved by suppression of lamellipodia in absence of Arp2/3 itself or its cofactors (Machesky and Insall; Suraneni et al., 2012). Arp2/3 must be tightly regulated in both its activity, important for maintaining high rates of actin treadmilling, and its localization, to control the sites of protrusion.

3. **Globular actin** from the pool of actin monomers sequestered by profilin and thymosin, is incorporated by Arp2/3 at the barbed end of the new filament. **Profilin** is a key actin-binding regulatory protein that by binding actin monomers accelerates treadmilling rate by 125-fold (Didry et al., 1998). Such assembly implies hydrolysis of ATP to ADP.

4. The incorporation of actin monomers has been proposed to produce the advancement of the membrane, according to the **elastic Brownian ratchet model** (Mogilner and Oster, 1996). In this model, the actin filament in physical contact with the membrane bends due to thermal fluctuations, leaving some minimal space for an actin monomer to attach at the barbed end. When bending is restored, and since the filament behaves like a Hooke's spring (according to the model), the recovering load force pushes the membrane forward. However, this model presents some limitations: it considers pushing actin filaments individually so it does not account for a possible crosslinking of the filaments (by α-actinin for example), it does not consider the contribution of the motor protein myosin, and it does not acknowledge the reported attachments of the actin filaments with the membrane. The elastic Brownian ratchet model predicts the force generated per individual filament to be on the order of few picoNewtons, which estimated across several hundred of actin filaments present in the lamellipodia would render a force capable of counteracting membrane resistance (Abraham et al., 1999). However, studies in the intracellular propulsion of Listeria by actin-rich tails have reported higher propulsive forces by crosslinked actin filaments (Dickinson et al., 2004; Gerbal et al., 2000; Marcy et al., 2004). Along this line, theoretical models have proposed an **active gel theory** to explain the pushing forward of the actin at the

membrane. In this approach, the lamellipodial actin is assumed to behave as an active gel composed of filaments and crosslinked by molecular motors (myosin). Such approach is used to explain how the treadmilling of actin is transformed into net forward membrane movement (Joanny and Prost, 2009). These latter works tackle actin-driven propulsive force from a mesoscopic point of view that can improve the understanding of actin filament pushing.

5. The growth of branched filament is terminated by **capping proteins** (such as heterodymeric capping protein, gelsolin, tensin, Eps8, among others). Stopping actin filament growth is important to control very precisely the areas of actin filament pushing against the membrane. Moreover, because the branched filaments are kept short, they are stiffer and thus more effective to push on the membrane. Interestingly, such capping activity can also be inhibited when permanence of the pushing is required by PIP2 signalling via Cdc42 or VASP effectors, displacing gelsolin and other capping proteins. Very importantly, by capping the existing filament, the available pool of actin monomers is kept high, so that such monomers can be used in other non-capped filaments to foster their growth, in a mechanism known as funnelling treadmilling.

6. As branching continues along direction of movement, actin filaments far from the membrane age. Such older filaments dissociate γPi, promoted by **ADF/cofilin**. Upon detachment of Pi, the binding of Arp2/3 with the actin filament is weaker, and ultimately the actin filament is detached. Then, this filament can be subsequently annealed with other actin filaments to produce a longer filament back in the lamellar region. Severed filaments can also be disassembled into actin monomers by ADF/cofilin.

7. ADP-actin monomers are recycled to ATP-actin monomers by **profilin** and added to the intracellular pool of actin as an ATP-actin monomer bound to profilin-form. Maintaining a high pool of ready-to-use actin monomers is key to ensure the adaptability of the cell to a changing environment, setting the conditions for a sudden burst of migration or reorientation.

As it has been highlighted, the main factor responsible for inducing the branching of actin filaments at the edge of the cell (i.e. structural induction of lamellipodia) is Arp2/3 (Figure 1. 4). Thus, its regulation is pivotal for controlling the extension of lamellipodia.
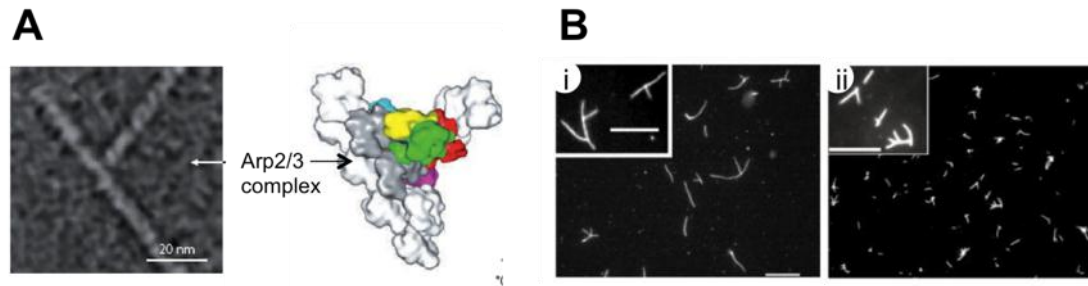
Figure 1. 4. Actin branching. (A) Arp2/3 complex induces the branching at 78° from the "mother" actin filament. From (Campellone and Welch, 2010). (B) In vitro, within a mixture of fluorescently labelled actin monomers, actin filaments can spontaneously polymerize and branch if WASP/Scar and Arp2/3 are present. Such branching only occurs concomitantly with the nucleation phase, and is dependant of the concentration of Arp2/3 (15 nM in i, 50 nM in ii, branching increases with Arp2/3 addition). From (Blanchoin et al., 2000).

Regulation of Arp2/3

Arp2/3 regulators are nucleation-promoting factors, namely **WASP family of proteins** (responsible for dendritic branching), and **formins** and **WH2 domain-containing proteins** (responsible for actin filament elongation, more related with filopodia). The main members of WASP family are N-WASP and WAVE/Scar subfamily of proteins (Pollard, 2007). Traditionally, N-WASP was thought to be in charge of filopodia dynamics, while WAVE/Scar proteins were related to lamellipodia (Higgs and Pollard, 2001). However, studies challenged this view in experiments where N-WASP was found in lamellipodia and its suppression did not compromise filopodia formation, pointing towards a more synergistic role of both regulators (Campellone and Welch, 2010). Interestingly, a novel regulator has been identified, IQGAP1, which can bind as well microtubules binding proteins, adherens junctions proteins, RhoGTPases, and could be the integrative link of Arp2/3-mediated response to growth factor stimulation (Benseñor et al., 2007).

Interestingly, the Arp2/3-mediated dendritic actin model of Pollard and Borisy has recently started to be challenged by new observations not reporting dendritic actin structures at the very edge of cells. The branching model had been precisely characterized mainly from *in vitro* measurements, although also supported by electron micrographs of actin networks on the cell periphery (Blanchoin et al., 2000; Svitkina and Borisy, 1999) (Figure 1. 4 and Figure 1. 5. A). However, by using a different electron microscopy technique (tomography of vitreously frozen samples), the group of Small et al. have reported 3D reconstructed images where the branched structure is very infrequent (Urban et al., 2010) (Figure 1. 5. B). Such observations, although have generated important controversies (Insall and Higgs, 2011; Small, 2010), do not necessarily rule out a role for Arp2/3 in lamellipodium, which is quite well-established thanks to numerous studies showing abrogation of

lamellipodia in absence of Arp2/3 (Nicholson-Dykstra and Higgs, 2008; Hartwig et al., 2005). Instead, these studies may indicate an even more dynamic process of branching that cannot be captured in static electron microscopy analysis. Also, the degree of branching of the actin network can depend on the balance of Arp2/3 versus formins and WH2 domain-containing proteins, which can vary according to environmental conditions (Yang et al., 2007). Nevertheless, other actin nucleators are arising as candidates for actin filament formation factors, alternatively or in conjunction with Arp2/3.
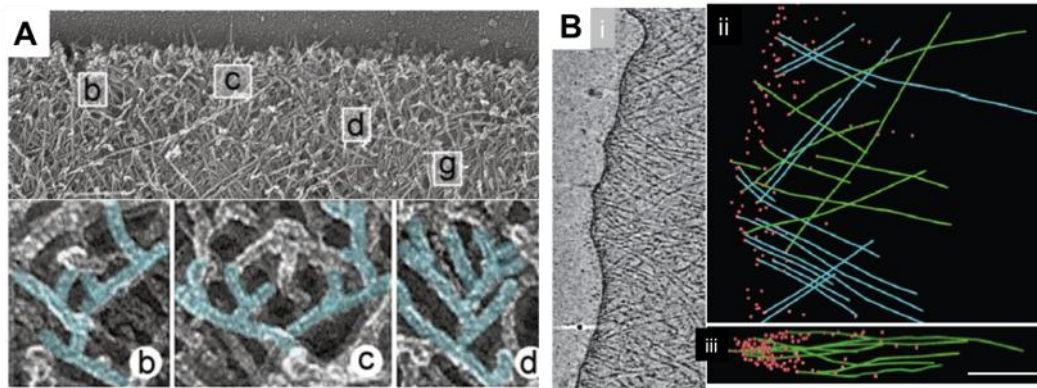
Figure 1. 5. Actin structure at the leading edge. (A) Electron micrographs of lamellipodia of *Xenopus* keratocytes. Note the presence of branched filaments and Y-junctions. Equivalent structures have been found for mouse fibroblasts. From (Svitkina and Borisy, 1999). (B) (i) Tomographic slice from an electron microscopy image of lamellipodia of fibroblasts. (ii) Projection of the reconstructed 3D model of tracked actin filaments, where only few of these filaments are depicted for clarity. Note that the filaments show little interconnection or branching, but most often present parallel trajectories (highlighted in blue). (iii) Side view of (ii). From (Urban et al., 2010).

Following up on the actin architecture at the leading edge of a migrating single cell, a distinction is typically established between lamellipodium and the part right before it, the lamellum (Heath and Holifield, 1991) (Figure 1. 6. A). Lamellum is considered to be the region right after the highly cross-linked, dendritic actin meshwork finishes (from 3 to 15 μm away from the edge). Such area presents thicker actin bundles associated with myosin II (and hence contractile) and tropomyosin, like stress fibres. These fibres grow from the focal complexes at the interface between the lamellipodium and lamellum and extend to the inner part of the cell (Koestler et al., 2008). Advancements in the lamellum study by the groups of Waterman-Storer and Danuser are rising controversy by questioning the well-established notion that lamellipodium is the responsible part for migration (Ridley et al., 2003). First, Ponti et al. suggested a model where the lamellum extended until the very edge of the cell and the lamellipodium was on top of it, based on observation of high number of long-lived slow-moving actin speckles in the lamellipodial region (Ponti et al., 2004). Such view is also supported by findings from the Sheetz group, where they propose a model to account for periodic

contraction of the cell's leading edge (lamellipodial protrusion-retraction cycles) (Giannone et al., 2007), (Figure 1. 6. B). Furthermore, Gupton et al. reported that when microinjecting tropomyosin in cells, Arp2/3 was displaced and lamellipodial extension abrogated, but surprisingly leading edge protrusion persistence and migration rates were increased (Gupton et al., 2005). These findings lead to the speculation that the lamellum is the main responsible for motility by linking edge protrusion with acto-myosin cytoskeleton, and the lamellipodium would have a minor role, more related to environmental sensing. However, such hypothesis is not widely accepted in the scientific community and requires further evaluation by means of different techniques (Vallotton and Small, 2009; Koestler et al., 2008).
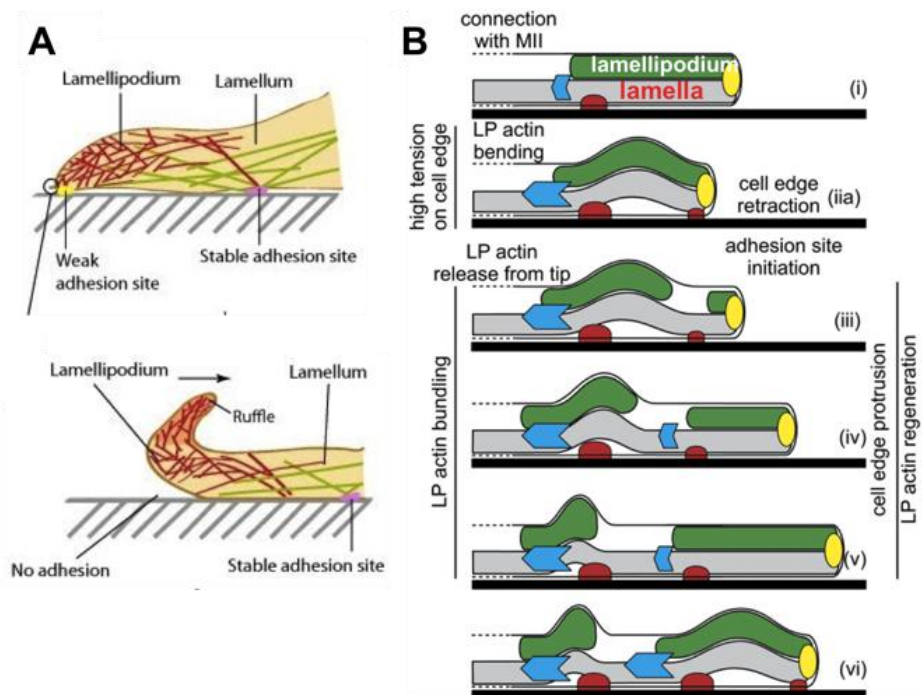
Figure 1. 6. Differentiation between lamellipodium and lamellum. (A) Scheme depicting the classical view of the lamellipodium (dense in F-actin) at the front and the lamellum (less F-actin) right after the lamellipodium. When the lamellipodium is not attached at the substrate, it can bend dorsally and form a so-called ruffle. From MBI website. (B) Proposed model describing a predominant role of the lamellum in the protrusion of the leading edge. From (Giannone et al., 2004).

One of the major differences between lamellipodium and lamellum is their rate of actin retrograde flow. Actin retrograde flow describes the movement of filament-contained actin speckles from the edge of the cell inwards. Retrograde flow results from both the growth of actin filaments at the cell distal-most end (Watanabe and Mitchison, 2002) and myosin contractility nearer to the cell centre (Lin et al., 1997). In the lamellipodium, actin retrograde flow is fast (1-5 μm/min), while in the lamellum retrograde flow rates are lower (0.1-0.3 μm/min), containing long-lived speckles (Vallotton et al., 2004; Ponti et al., 2004; Gardel et

al., 2008; Alexandrova et al., 2008). Such differences may arise from the coupling of actin dynamics with the substrate through cell-substrate adhesions. These adhesions could act as barriers for the actin retrograde flow and are mainly located at the interface between lamellipodium and lamellum. In this manner, cell-substrate adhesions would stop or slow down the actin retrograde flow moving inwards from the lamellipodium. One of the models proposed that the connection between acto-myosin cytoskeleton and substrate would occur through a **molecular clutch** (Giannone et al., 2009)**.** Such molecular clutch would link the actin array with the substrate, being critical to ensure the net propulsion of the lamelliupodium. In other words, the pushing of dendritic actin filaments against the membrane to protrude would only result in net movement if the leading edge-actin array is coupled both to the contractile cytoskeleton and to the substrate (Mitchison and Kirsch, 1988) (*gripping mode*) (Figure 1. 7. A). If the actin filaments were not mechanically linked to the substrate, actin network treadmilling would dissipate in actin retrograde flow (*slipping mode*) (Figure 1. 7. B) (LeClainche and Carlier, 2008). However, this binary model must exist in a more dynamic state *in vivo*, in order to accommodate F-actin motion while maintaining attachment to the substrate, so that a continuous transition between on and off clutch engagement should exist (Jurado et al., 2005; Gardel et al., 2008). Such molecular clutch would be mainly composed of adhesive proteins like talin, vinculin, etc., that link integrins in the ECM with F-actin. These adhesive proteins are grouped under the family of focal adhesion proteins. Thus, to understand cell movement it is important to take into account focal adhesions, which are the biological and mechanical links between the cytoskeleton and the matrix.
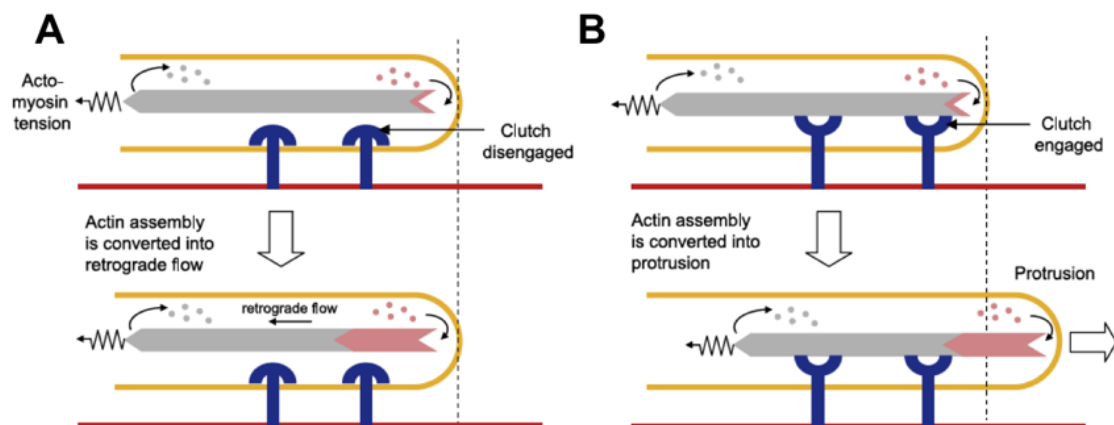
Figure 1. 7. Proposed model where cell-substrate adhesions act as molecular clutches to effectively convert the force from protruding actin filaments to net forward membrane movement. From (LeClainche and Carlier, 2008). (A) If the actin cytoskeleton is not coupled to the ECM (clutch disengaged), actin treadmilling is vanished into retrograde flow and there is no protrusion. (B) If there is mechanical link between actin filaments and substrate (clutch engaged), the protrusion of the growing actin filament is converted into net movement of the membrane.

4. Focal adhesions

Focal adhesions are protein complexes [grouped under the concept of **adhesome** –(Zaidel-Bar and Geiger, 2010)] that link the extracellular matrix with the acto-myosin cytoskeleton. These complexes undergo a specific process of maturation, which is highly dependent on mechanical forces (Balaban et al., 2001). They can be classified in different structures depending on their maturation state, protein composition, size, lifetime, etc. (Zamir and Geiger, 2001).

The adhesion of the cell with the ECM starts in the **nascent adhesions** that form at the very edge of the cell, in the lamellipodial region (Figure 1. 8. A, left panel). These are very small, dot-like structures, which can either fade rapidly (within 60 sec) or progress to focal complexes. Such transition depends on the activation of integrins by binding to their correspondent ECM partners (fibronectin, collagen, etc). Once integrins are activated, the cytoplasmic tails of integrins can open and bind actin filaments together with their intracellular partners (vinculin, talin, etc.). These complexes can exert significant traction forces (in the nanoNewton range), as they enable the forward propulsion of the leading edge (Beningo et al., 2001; Tan et al., 2003). **Focal complexes** (FC) are highly dynamic adhesions located at the interface between lamellipodium and lamellum of ~1 μm diameter that can persist for several minutes. These complexes contain $\alpha_5\beta_3$ integrin, talin, paxilin (and later recruiting vinculin, α-actinin, VASP, FAK). Focal complexes later develop into **focal adhesions** (FA), which are more stable and with slower turnover. Focal adhesions contain talin, paxilin, vinculin, α-actinin, VASP, FAK, as well as $\alpha_5\beta_3$ integrin, zyxin. FAs are located more to the cell centre and typically associated with stress fibres, bearing forces of tens of nanoNewtons (Tan et al., 2003; Balaban et al., 2001; Saez et al., 2005) (Figure 1. 8. A, right panel). These mature focal adhesions are responsible for stabilizing the cell. Somewhat more specific adhesions are fibrillar complexes, traditionally observed in fibronectin-coated stiff substrates, more stable, larger, and highly elongated.

Although it is well accepted that focal adhesions are highly affected by traction forces and vice-versa, the exact relationship between both is not fully understood. Clear evidence showed many years ago that focal adhesions grow under application of force (Figure 1. 8. B) (Riveline et al., 2001). Along this line, it has been repeatedly shown that large focal adhesions can exert high traction forces (Balaban et al., 2001) (Figure 1. 8. D and E). However, in some cases an inverse relationship is established, as small focal adhesions can exert high traction forces (Figure 1. 8. C and D, shaded area) (Tan et al., 2003). Recently, some studies showed that the dependence of focal adhesions on force transmission is not straightforward and is highly dependant on the distance of the adhesion from the

leading edge, i.e. the maturation state of the adhesion (Figure 1. 8. A), and can also depend on the attachment of such adhesions to stress fibres (Stricker et al., 2011; Prager-Khoutorsky et al., 2011; Trichet et al., 2012).
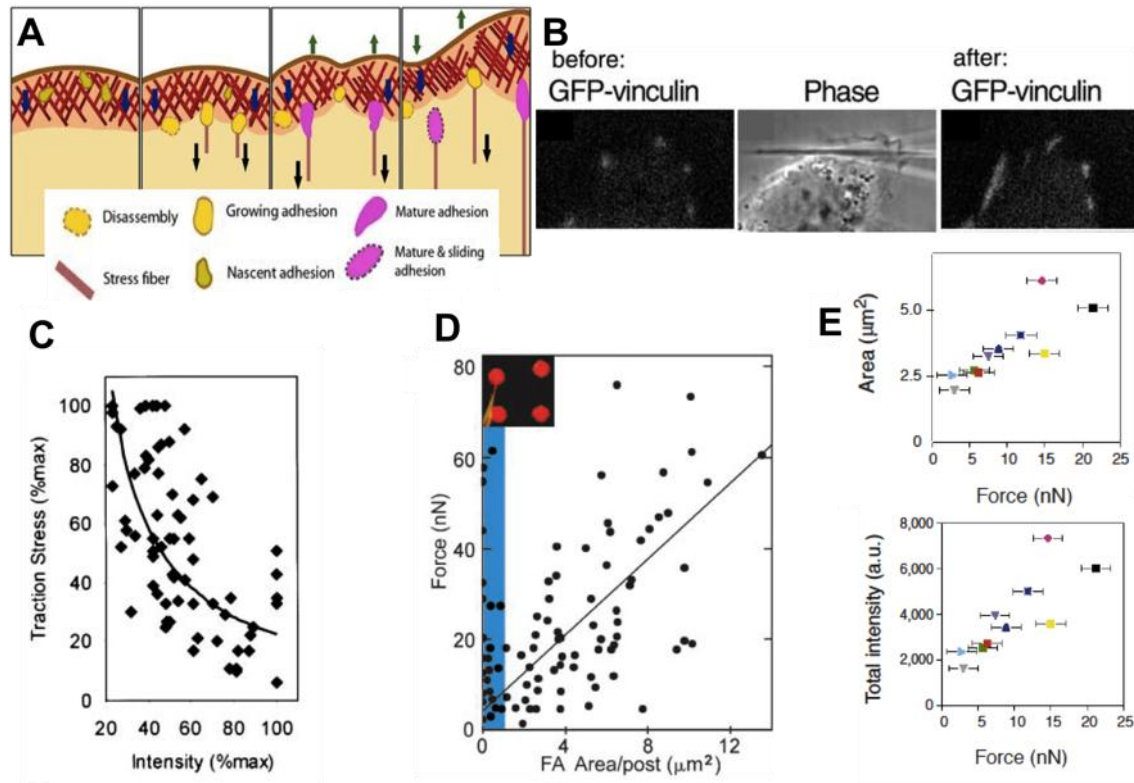
Figure 1. 8. Relationship between focal adhesions and traction forces. (A) Scheme depicting the maturation of focal adhesions, from nascent adhesions (left panel) to mature adhesions (right panel) upon application of force by stress fibres. From MBI website. (B) Focal adhesions grow upon application of an external mechanical stimuli. From (Riveline et al., 2001). (C) Relationship of focal adhesion fluorescence intensity (from zyxinGFP) and traction stress sustained by the adhesion, only for adhesions at the leading edge. The stress supported by the adhesions is inversely related to the intensity, and the intensity of adhesions increases from the leading edge inwards to the lamellar region. From (Beningo et al., 2001). (D) Force generated by cells plated on a micropillar force sensor array as a function of the area of vinculin per post; the shaded area represents focal adhesions <1 μm^2. Small adhesions can exert a wide range of forces, but support also notably high traction forces. From (Tan et al., 2003). (E) Relationship between force and area (top) or force and fluorescence intensity (bottom) of a focal adhesion. The higher the applied force, the larger and more elongated the adhesions develop. The force applied through focal adhesions depends, in turn, of the stiffness of the substrate. From (Balaban et al., 2001)

As it has been pointed out, the evolution of focal complexes to focal adhesions is highly dependent on myosin II, although it is dispensable for the formation of the first nascent contacts (Choi et al., 2008) (Figure 1. 8. A and Figure 1. 9. A). However, there is no direct link between the adhesion complex and myosin II, but they are coupled through actin and many actin-binding proteins, such as vinculin, talin, and α-actinin (Figure 1. 9. B). Myosin II-dependent maturation of focal

adhesions can be explained by two hypotheses: clustering of focal adhesion proteins or force-dependent maturation.

4.1. Clustering hypothesis

In this model, the actin filament crosslinking action of myosin II brings actin filaments together along with their accessory proteins (Chrzanowska-Wodnicka and Burridge, 1996; Saarikangas et al., 2010; Oakes et al., 2012; Choi et al., 2008). In this manner, the concentration of focal adhesion proteins increases locally, which will increase the global avidity of the focal complex for its extracellular protein partner (Paszek et al., 2009). At the same time that myosin II affects adhesion maturation via clustering or conformational changes, adhesion molecules can also signal back to acto-myosin cytoskeleton. Integrin activation results in paxilin and FAK phosphorylation, which can stimulate an upper revel of regulators (RhoGTPases) and trigger changes in the acto-myosin cytoskeleton, like Arp2/3-dependent actin polymerization on the focal adhesion site or increased actin filament bundling (Figure 1. 9. B) (Burridge and Chrzanowska-Wodnicka, 1996).

4.2. Force-dependent maturation

Another hypothesis accounts for the maturation of focal adhesions through the dorsal stress fibres-mediated application of force. Upon tension, cryptic binding sites of focal complexes proteins are exposed, and new adhesion molecules are recruited (Figure 1. 9. B) [reviewed in (Vicente-Manzanares et al., 2009; Parsons et al., 2010)]. This last hypothesis is now under intense research, providing interesting studies on the mechanotransduction capabilities of some proteins. p130cas was the first protein described to be mechanosensitive, when Sawada and coworkers showed that p130cas was activated under stretch (Sawada et al., 2006). Similarly, talin has been shown to bind vinculin upon force-induced conformational changes (del Rio et al., 2009). Moreover, myosin II itself can change conformation when subjected to stretch (Schwaiger et al., 2002).

These above-mentioned mechanosensitive proteins, together with mechanosensitive ion channels (Martinac, 2004; Kobayashi and Sokabe, 2010), are key in integrating mechanical stimuli from the surrounding environment to trigger intracellular (biochemical or purely mechanical) responses. Since cells probe the surrounding environment by applying traction forces through focal adhesions, local changes in environmental stiffness can affect focal adhesions proteins. Recent experiments show that focal adhesions of the same size could support different values of traction forces when the stiffness is varied (Trichet et al., 2012). While focal adhesions area does not vary, stress fibres reorganize according to the applied force, pointing out a prominent role of the acto-myosin cytoskeleton itself

in sensing the substrate stiffness. Along this line, other experiments show that cells apply increasing traction forces upon increasing-stiffness substrates. Interestingly, the adaptation of the traction forces to the stiffness of the substrate is instantaneous and could not be explained by force-dependent mechanochemical transduction processes, but a purely physical response (Mitrossilis et al., 2010). Moreover, such response is sensitive to impairment of acto-myosin contractility, further supporting a pivotal role of the acto-myosin cytoskeleton as a global mechanosensor (Mitrossilis et al., 2009; Fouchard et al., 2011). Altogether, these experiments regarding the mechanosensitive properties of focal adhesions prove that cells can respond to mechanical stimuli either at the local scale (by changes in the activation state of single proteins within the focal adhesion complex itself) and at the global scale (by adaptations at the whole-cell level) (Solon et al., 2007). As it has been highlighted, many factors could account for rigidity sensing, so the relationship between focal adhesions and substrate stiffness remains an open question driving intense research efforts (Schwarz, 2007; Ghibaudo et al., 2008; Walcott and Sun, 2010).

Given the high sensitivity of focal adhesions to substrate stiffness, the morphology and composition of focal adhesions will strongly depend on the compliance of the substrate and on the contractile state of the cell. Typically, cells grown on plastic or glass substrates (which are infinitely stiff for the cells) develop larger and mature adhesions, while in soft substrates their adhesions will be smaller and dynamic, more difficult to capture under the microscope (Pelham and Wang, 1997; Discher et al., 2005).
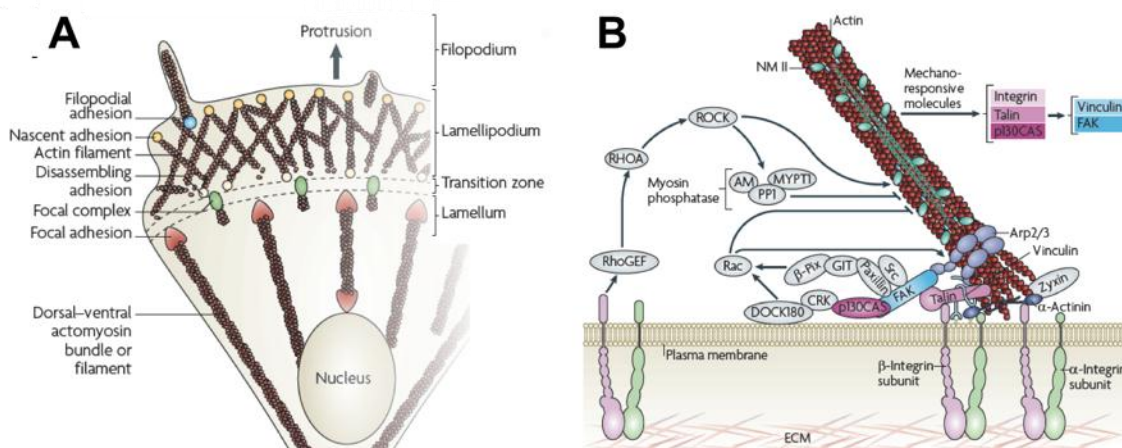
Figure 1. 9. Substrate adhesions location and composition. (A) Scheme depicting the maturation of substrate adhesions in the cellular context, from nascent adhesions at the leading edge, to focal adhesions more located towards the cell centre, typically at the transition zone. From (Vicente-Manzanares et al., 2009) (B) Focal adhesion scheme where focal adhesion proteins (talin, zyxin, FAK, vinculin, etc.) are attached to a stress fibre (acto-myosin filaments). The application of force through the stress fibre to the focal adhesion complex induces many biological signalling, both

recruitment of new proteins to the adhesion site and regulatory feedback loops involving RhoGTPases. From (Vicente-Manzanares et al., 2009).

Another critical parameter defining the nature of focal adhesions is the motile state of the cell. Adhesions have a two-faced role in the motility process: anchor and transmit traction forces from the cytoskeleton to the substrate as well as permitting cell movement, and thus they must be tightly regulated (Ridley et al., 2003) (see section 7). Thus, generally, fast moving cells have highly dynamic and small focal adhesions, while quiescent or slow cells exhibit well-developed adhesions (Palecek et al., 1997).

A last cellular module by which cells relate to their environment is filopodia. Filopodia can be understood as a lamellipodia-related structure, and share some features with them. However, the role of filopodia in driving migration is somewhat different to lamellipodia: filopodia are more related to environment sensing rather than actual forward cell movement (Chan and Odde, 2008).

5. Filopodia

Filopodia are finger-like membrane protrusions rich in actin filaments (0.6-1.2 μm in diameter, few to tens μm in length), very variable among cell types (Ahmed et al., 2010) (Figure 1. 10). They are highly dynamic (lifetime of tens of seconds) and contractile, thus capable of exerting forces (Kress et al., 2007; Bridgman et al., 2001). Filopodia extend and retract rapidly while sensing the environment, which is their main role: to explore the extracellular matrix and detect directional cues (Chan and Odde, 2008). Such extension and retraction result from actin polymerization at the barbed end and actin retrograde flow of the filament, respectively (Mallavarapu and Mitchison, 1999).

Filopodia contain 15-30 actin filaments aligned in parallel, always with their barbed end at the distal tip of the filopodia (Medalia et al., 2007) (Figure 1. 10. A). The free end accommodates the tip complex, an electron-dense structure formed by numerous proteins (VASP, Ena, Mena), and it is the site of new actin monomers addition. Filaments are tightly attached by bundling proteins, like fascin, α-actinin, fimbrin and filamin, being fascin the more abundant one. Such cross-linking is crucial to ensure the mechanical stability of the filopodia to resist the buckling forces associated to its small aspect ratio when pushing the membrane. Moreover, the actin filament shaft is anchored at the plasma membrane through the ERM complex (ezrin, radixin, moesin) (Fievet et al., 2007).
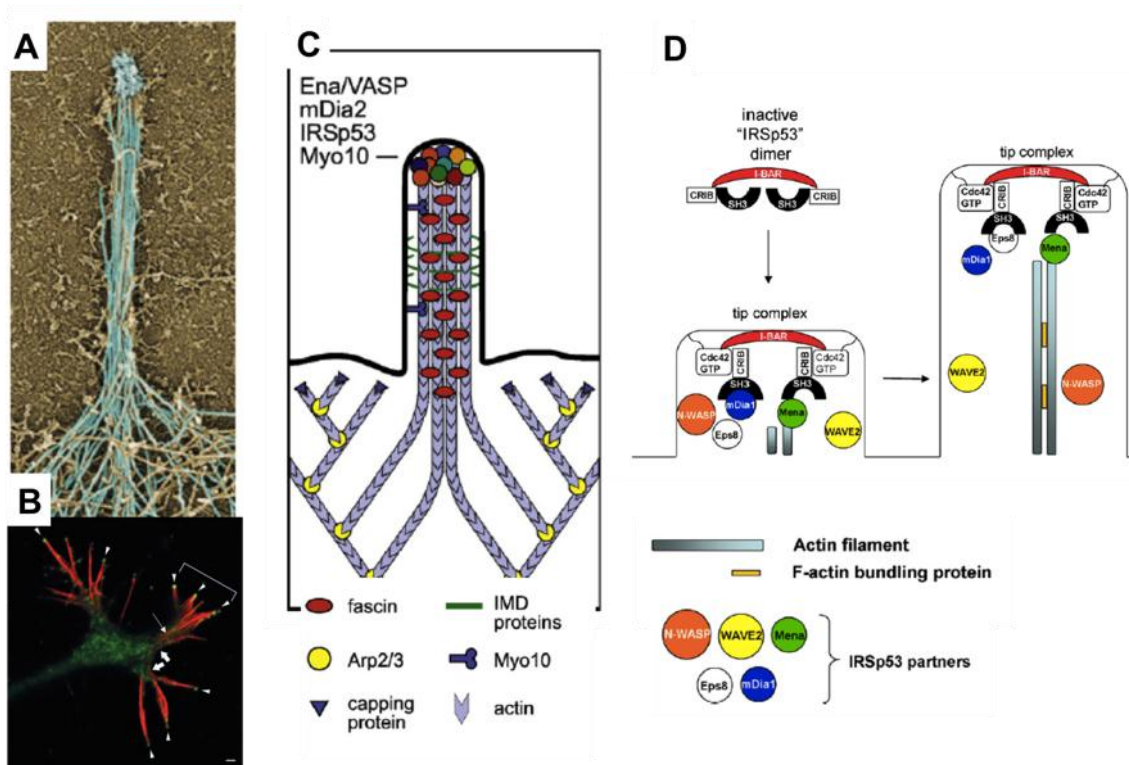
Figure 1. 10. Filopodia structure and proposed formation models. (A) Electron micrograph of a filopodium, false coloured in blue are actin filaments. From (Mellor, 2010). (B) Fluorescent micrograph of filopodia in the growth cone. In green, WAVE protein, clearly localized at the very tips of filopodia; in red, actin. Scale bar is 1 μm. From (Nozumi, 2002). (C) Model for convergent growth of filopodia: emergence from lateral fusion of lamellipodia-contained actin branched filaments, which would be the stem for further filament elongation without branching. From (Mellor, 2010). (D) Model for *de novo* nucleation of filopodia, thanks to the actin polymerization activity of formins, independently of Arp2/3-mediated actin filament polymerization. From (Ahmed et al., 2010).

Filopodia formation is regulated mainly by Cdc42, which via WASP activation can trigger Arp2/3-dependent actin filament polymerization (Rohatgi et al., 1999). Another plausible pathway involves the protein IRSp53, which can interact both with Cdc42, WAVE2 and Mena protein. Additionally, IRSp53 contains an IM or I-BAR domain that induces membrane deformation, facilitating actin filament driven protrusion. However, the observation that cells devoided of Cdc42 could still protrude filopodia (Czuchra et al., 2005) led to the identification of another Rho GTPase regulator: Rif (Rho in filopodia) (Ellis and Mellor, 2000), which can regulate the formation of fillopodia via formin mDia2 (Pellegrini and Mellor, 2005).

It is interesting to note how filopodia and lamellipodia are crossregulated and spatially coordinated at the membrane, given that both structures share most of their components but differ very much in structure. But because most of the proteins are present in both filopodia and lamellipodia, it is understandable that they will coexist in the cell. However, there is no clear agreement on how filopodia

are formed, and two main different models are contemplated [convergence-extension model (Svitkina et al., 2003), and *de novo* formin-driven filopodial growth (Steffen et al., 2006); Figure 1. 10].

The high surface area to volume ratio and the clustering of receptors at filopodia membranes are key features for their sensory ability, as they can act as antennae or signal amplifiers. Filopodia are important in neuritogenesis (Dent et al., 2007), axonal guidance in neuronal growth cones (Zheng et al., 1996; Bridgman et al., 2001), endocytosis (Lidke et al., 2005), pathogen phagocytosis (Niedergang and Chavrier, 2004), cell-cell adhesion formation (Vasioukhin et al., 2000), and embryonic gap closure (Millard and Martin, 2008; Raich et al., 1999), among others. These last two functions are somehow related and based on one particular feature of filopodia: they can accumulate cadherin at their tips (Vasioukhin et al., 2000). Thus, filopodia of closely positioned cells can interact and thanks to cadherin interactions interdigitate and bring cells together. This function of filopodia is particularly important in processes involving the sealing of gaps, since it has been observed that filopodia are extended by confronting cells to mediate the fusion of opposed epithelial sheets, exerting a zippering activity (as will be further discussed later in the context of epithelial gap closure) (Vasioukhin and Fuchs, 2001; Martín-Blanco and Knust, 2001).

All the presented cellular structures are key players of cell migration. They are finely spatially and temporally regulated to produce cellular movement. The most important level of regulation is accomplished through RhoGTPases, which are master regulators of most cellular responses.

6. Regulation of cellular structures and behaviour: the pivotal role of RhoGTPases

Cells receive a myriad of stimuli that affect cell behaviour typically through activation of intracellular signalling cascades involving multitude of proteins. Rho family of small GTPases participate in the integration of many of these intracellular cascades and in the regulation of cell responses. Thus, Rho GTPases are key regulators in many cellular processes, mostly famous for the regulation of actin cytoskeleton, but also important in microtubules dynamics, cell division, polarity, membrane transport, gene expression, and a variety of enzymatic activities (Hall, 1998; Buchsbaum, 2007; Etienne-manneville, 2002; Heasman and Ridley, 2008).

RhoGTPases belong to the Ras superfamily of GTPases, the master regulators of cell biology. There are more than 20 members of the Rho GTPases family

identified, being RhoA, Rac1, and Cdc42 the classical canonical proteins. Most Rho proteins act as switches by alternating and active GTP bound state and an inactive or GDP bound state. The regulators of this cycle are guanine nucleotide exchange factors (GEFs), which activate Rho proteins by promoting exchange of GDP for GTP; GTPase activating factors (GAPs), which enhance the intrinsic GTPase activity thus resulting in hydrolysis of GTP to GDP; and guanine nucleotide dissociation inhibitors (GDIs), which halts the cycle by binding and sequestering RhoGDP (Figure 1. 11. A) (Etienne-manneville, 2002).

Due to the complex regulation of the RhoGTPases themselves (there are 60 known human GEFs and 70 GAPs), the complex regulation of the many processes they control (RhoA, Rac1, and Cdc42 have more than 60 protein targets), and the complex interplay between different Rho-regulated pathways, such network is intriguing, often unclear, and far to be understood as a whole (Figure 1. 11. B) (Etienne-manneville, 2002; Pertz, 2010).
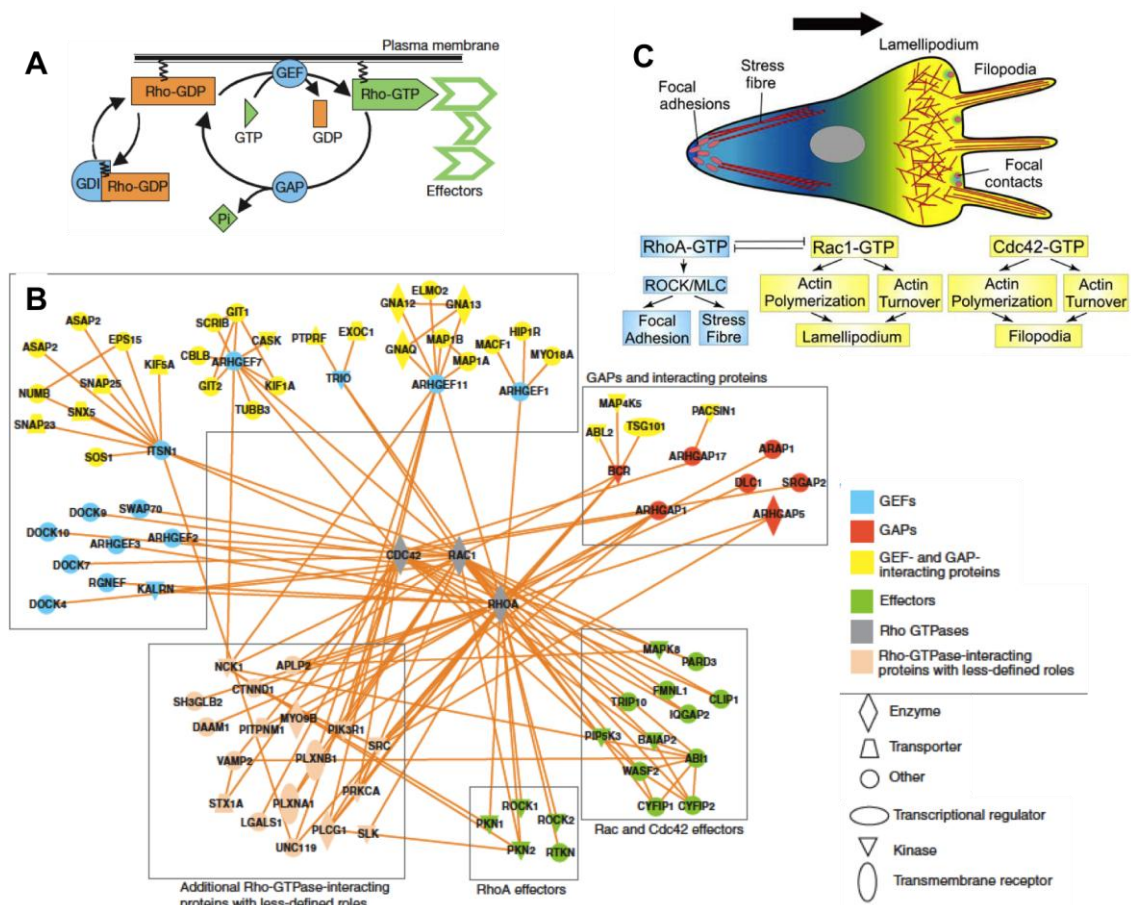
Figure 1. 11. RhoGTPases regulation. (A) RhoGTPases cycle between GTP (active form) and GDP (inactive form), and are directly regulated by GAPs, GEFs and GDIs (in blue). From (Etienne-manneville, 2002). (B) Interaction network of RhoGTPases in neurons shows the complexity of the RhoGTPases network and their numerous interactions with effector proteins. From (Pertz, 2010).

(C) Rho GTPases affect actin-based structures within a migrating cell. From (Mayor and Carmona-Fontaine, 2010).

The general approach, *a grosso modo* and mostly valid for single cells, is that RhoA regulates actomyosin cytoskeleton and stress fibres, Rac1 controls actin-rich protrusions (mainly lamellipodia), and Cdc42 controls filopodia, as observed from many experiments of RhoGTPases suppression or overexpression (Ridley et al., 1992; Ridley and Hall, 1992; Nobes and Hall, 1995) (Figure 1. 11. C). We will briefly describe how the main RhoGTPases affect cellular structures. The roles of RhoGTPases in cell migration will be presented later on.

6.1. Rac1

Rac1 regulates actin polymerization during protrusion in many different ways: by activating actin nucleating proteins (WAVE-Arp2/3 complex), formins (mDia1), by removing capping proteins to free actin filament barbed ends, and by increasing the availability of actin monomers by interacting with cofilin (Kraynov, 2000; Small et al., 2002; Yang et al., 1998) (Figure 1. 12. A). Moreover, Rac1 also interacts with other regulators of leading-edge actin dynamics, such as IRSp53, PI3K, LIMK, p65Pak (Connolly et al., 2005) (Figure 1. 12. A). Dominant negative Rac1 has been reported to inhibit lamellipodium extension, membrane ruffling and cell migration in numerous cell types, although to different extents (Ridley, 2001). The precise localization of Rac1 activity at the leading edge to promote protrusion is not fully understood, but could presumably be due to recruitment by the scaffolding complex DOCK180-CrkII. Rac1 can also regulate lamellipodial width by decreasing cofilin activity (at the rear of the lamellipodial actin array), which would account for the localization of Rac1 slightly before the leading edge (Machacek et al., 2009).

6.2. Cdc42

Cdc42 is the main regulator of planar polarity establishment, i.e. it defines a front edge where lamellipodia and filopodia will extend, and a rear part (Etienne-manneville, 2002; Palazzo et al., 2001). Cdc42 acts mainly by: 1) docking Rac1 to the leading front membrane, where it will promote membrane ruffling (Figure 1. 12. A); 2) positioning the microtubule organizing centre (MTOC) along the front-rear axis via PAR6-PAR3-αPKC complex, and the Golgi apparatus via non-canonical Wnt signalling pathway (Etienne-manneville, 2002; Schlessinger et al., 2007); and 3) stabilizing microtubules, which have recently been proposed to account for lamellipodia stabilization during the protrusive phase, and act as railways for anterograde transport of Golgi vesicles for membrane supplies during lamellipodial extension (Siegrist and Doe, 2007). Cdc42 is also important in the

formation and regulation of filopodia, as it has been explained in section I. 5 (Figure 1. 12. A).

6.3. RhoA

RhoA plays a central role in the contractile state of the cell, through many different targets, especially kinases such as MLCK, ROCK, LIMK, etc. (Sit and Manser, 2011) (Figure 1. 12. A). As it has been explained in section I. 2. 1. 2, these kinases phosphorylate MLC and thus they regulate the activation state of myosin. Hence, RhoA is mainly responsible for the assembly and contraction of stress fibres (Pellegrin and Mellor, 2007). Likewise, it also regulates the maturation of focal adhesions by controlling the tension applied to focal adhesions, as it has been explained in section I. 4. 2. Since RhoA has a prominent role in the structure and function of acto-myosin filaments, it also regulates any specific structures containing acto-myosin bundles, such as the cytokinetic ring, the cortical acto-myosin cortexes, and the supracellular acto-myosin cable that forms in wound closure processes, as will be later discussed (Matsumura, 2005; Lecuit and Lenne, 2007; Kiehart, 1999).
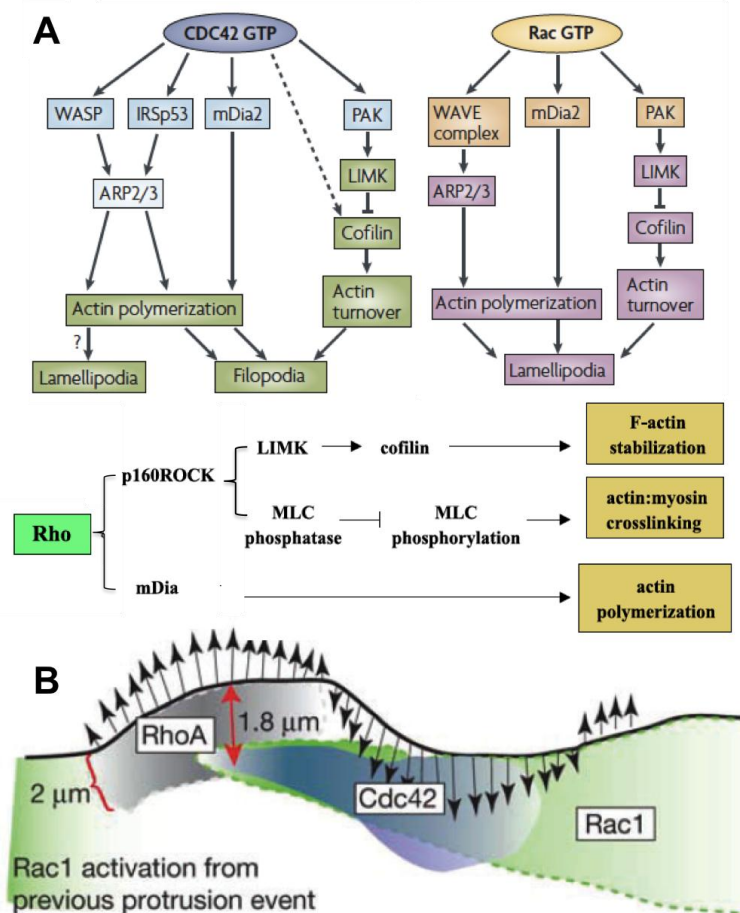
Figure 1. 12. RhoGTPases pathways and localization. (A) Cdc42 and Rac1 have multiple effectors that have independent or combined actions. Cdc42 and Rac1 ultimately regulate acto-myosin dynamics, thus affecting mainly actin structure at the leading edge, i.e. at lamellipodia and filopodia. RhoA controls many kinases affecting myosin phosphorylation.From (Heasman and Ridley, 2008; Raftopoulou and Hall, 2004). (B) Recently proposed model of the dynamic spatio-temporal activation of the RhoGTPases main members at the protruding leading edge. Black line indicates the cell edge that protrudes outwards and inwards according to the arrows. Note differential areas of RhoA (black), Cdc42 (violet) and Rac1 (green) activation within a small region of the leading edge. From (Machacek et al., 2009).

The advancement on imaging technology has shed new light into the intricate topic of RhoGTPases regulation in single cells and some of the dogmas of RhoGTPase biology are being revisited. Most of the work done until now is based on dominant-positive or –negative mutants of the three canonical GTPases (Rac1, Cdc42 and RhoA). While very informative, such experiments can be masking or overseeing some minor effects of those proteins. By using fine techniques with precise spatio-temporal resolution, mostly based on FRET biosensors, different groups have been able to provide detailed information on the circuitries of RhoGTPases in migrating single cells (Pertz, 2010). Surprising results showed that the bulk of RhoA activation occurs at the leading edge of protruding lamella in fibroblasts, despite the intuitive location of RhoA at the back where it would control RhoA-mediated cytoskeletal contractility (Pertz et al., 2006). Simultaneously, bursts of RhoA activation are observed at the cell rear, as well as in peripheral ruffles. Such observation points out the fact that RhoGTPases can be activated simultaneously at different locations and exert different functions, presumably depending on their downstream effectors, which would be different depending on the cell area. This leads to the concept of modularity or compartmentalization of RhoGTPases functions. Direct evidence has been shown for Cdc42, which interacts with PAK effector in cell protrusions and with N-WASP in endosomal compartments in breast cancer cells (Parsons et al., 2005). Similar complex binding–dependant functions have been also described for Rac1 (Connolly et al., 2005). Another anti-intuitive yet very relevant result was presented by the group of Klaus Hahn, showing a tight spatial and temporal regulation of the three canonical GTPases located close together in the lamellipodium. They demonstrated that the three proteins are highly confined in few microns at the leading edge, with activation/inactivation cycles of 90 sec periodicity. Despite the confinement, there is a clear temporal (lag phase between RhoA activation and Rac1 and Cdc42) and spatial antagonism (zones of mutual exclusion of Rac1 and Cdc42) between the three GTPases (Figure 1. 12. B). A similar tight regulation has been reported in embryonic wound healing on *Xenopus* oocytes, where concentric circles of RhoA and Cdc42 activation are observed upon wounding, clearly dynamic and mutually exclusive (Benink and Bement, 2005) (further discussed in Chapter 1 section II. 8. 1).

While there is extensive literature reporting many different RhoGTPases regulatory networks for a myriad of cell types and conditions, some reported contradictory functions remain to be explained. On the one hand, it is not clear if some of their functions could be cell-type specific. For example, while Rac1 and Cdc42 suppression typically results in loss of motility due to lack of lamellipodia and filopodia extension, some cells can still produce lamellipodia and filopodia and are only mildly affected in their migration (Wheeler et al., 2006; Czuchra et al.,

2005). On the other hand, the fine spatial regulation or the physical compartmentalization of RhoGTPases and their regulators (GAPs and GEFs) are not clear yet. Also, contradictory roles of RhoGTPases in epithelial gap closure have been proposed, as will be later explained.

In summary, these studies emphasize the intricacy of RhoGTPase regulation, which include synergies and counteracting effects between them (Figure 1. 11. B). Due to its complexity, some contradictory results have been published regarding RhoGTPases functions in specific contexts. Moreover, they have been widely investigated in single cells, but less is known about their role in cell collectives. Very likely, RhoGTPases also regulate polarization and protrusion in migrating collectives while coordinating these activities across cells. We will focus again on RhoGTPases in the context of collective migration when describing the regulation of epithelial gap closure events and highlight the proposed role for the different RhoGTPases in that context.

Up to now, we have presented the structure, function, and regulation of the cellular modules that are important for cell migration. We will hereafter integrate all these modules to present how cell migration results from an orchestrated coordination of the different cellular structures to result in effective movement.

7. Single cell migration: an integrated process

Single cell migration has been intensively studied for the last decades and nowadays there is a comprehensive understanding of the process, despite many questions remain open and under careful investigation. Hereafter, we will focus on the prevalent mode of migration, which is the mesenchymal-like. Note, however, alternatives modes of migration exist, as is the ameboidal migration by blebbing. Blebbing is restricted to highly motile cells like neutrophils or lymphocytes, and to some cases of 3D migration in particularly dense matrices, thus it will not be addressed since it is not of relevance for the present work.

Single cell migration is described in a canonical 5-step process, which include front-rear polarity establishment, cell protrusion, leading edge attachment, cell contraction, and rear detachment (Figure 1. 13) (Sheetz et al., 1998; Ridley et al., 2003). Such cycles are recurrent *ad infinitum* while the appropriate migratory signal (intrinsic or extrinsic) is present. On basal conditions cells develop a persistent random walk, which can be altered by various external cues, such as

presence of chemoattractants, topographical cues, substrate compliance gradients, etc.

It is assumed that a sessile cell can detect a motogenic or migration-promoting agent (not necessarily a chemoattractant) and respond to it by entering the migrating cycle (this issue will be further discussed in Chapter 1 section II. 3) (Binamé et al., 2010).

The first requirement for motility is the acquisition of intracellular polarity or asymmetry, reflected in a differentiation between the leading edge (at the front) and the trailing edge (at the rear). Such **polarization** will define the areas of protrusion, the differential adhesiveness of focal adhesions as a function of their position, and the gradient in myosin contractility.
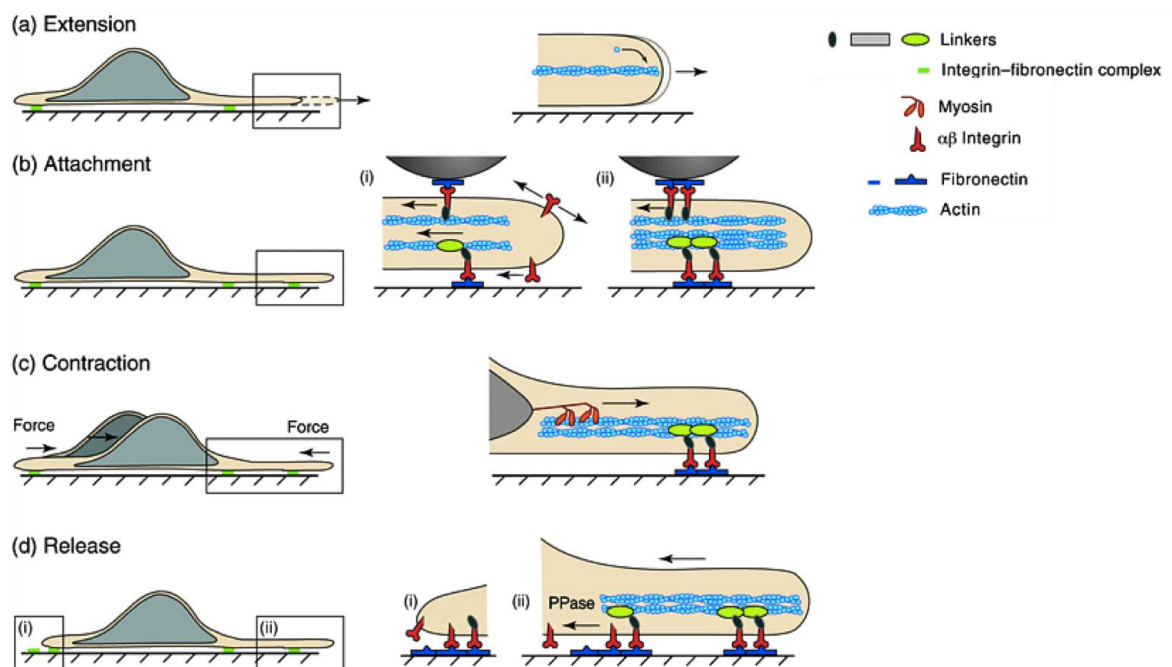
Figure 1. 13. Cycle of single cell migration. The first step, not depicted in the scheme, is the polarization of the cell to form differentiated front and a trailing edge. (A) Lamellipodia protrude at the leading front, then attaches to the substrate (B) and through application of traction forces the cell body is translated forward (C), with disassembly of the focal adhesions at the back (D). On the right, a more detailed scheme of the boxed region is shown, where the engagement of the molecular clutch is depicted. From (Sheetz et al., 1998)

Once the leading front is defined, branched actin polymerization can push on the membrane to protrude forward (in the fashion reported in section I.3) (**extension** of the leading edge, Figure 1. 13. A) (Sheetz et al., 1998; Ananthakrishnan and Ehrlicher, 2007). To translate the protruding filament force

into membrane advancement, cell front must be anchored to the substrate, first through focal contacts that can mature to focal adhesions (see section I.3, molecular clutch; section I.4 focal adhesions) (**attachment** at the leading edge, Figure 1. 13. B).

For the cell to advance in the migration path, cell body must be translocated inwards to match the newly formed protrusion, and it is accomplished by a myosin II-dependent **contraction** of the cytoskeleton. Such contraction is due to the tensile force that is related to the substrate through the focal adhesions and represents thus the traction force. This traction force follows a biphasic relation with the adhesiveness of the traction sites, which depends on the density of cellular receptors, on the density of ECM molecules and on the avidity of their interaction (Lauffenburger and Horwitz, 1996; Huttenlocher and Horwitz, 2011; Schwartz and Horwitz, 2006; Gupton and Waterman-Storer, 2006). This implies that there is an intermediate optimal density of these components that enables the most convenient migration, while lower and higher densities unfavor migration (de Rooij et al., 2005). Thus, the resulting migration will depend on a finely-tuned balance between the consistency of focal adhesions to bear traction forces, and the necessity to disassemble such adhesions when cell body translates forward (Figure 1. 13. C and D) (Chen, 2008). This step is regulated by the degree of myosin II phosphorylation, directly controlled by MLCK and ROCK by either direct phosphorylation or by inhibition of MLC phosphate MYPT1.

The disassembly of focal adhesions and thus the **release** of the cell rear can be mediated by different mechanisms: 1) actin assembly at the front contributes to the disassembly of lamellum-positioned focal adhesions; 2) severing of the adhesions due to the tension of stress fibres, as has been verified in studies reporting trails of extracellular domains of adhesion receptors behind the migrating cell (Palecek et al., 1997; Regen and Horwitz, 1992); 3) proteases activity, as seen for Ca^{2+}-activated calpain, that can cleave talin and integrin β_3 for example (Franco and Huttenlocher, 2005); 4) kinases that can phosphorylate certain proteins that render focal adhesions protein complexes more loose and prone to disassembly under actin retrograde flow (Webb et al., 2002); and 5) degradation of ECM molecules, for example by matrix metalloproteinases (MMPs), which plays a more important role in 3D migration and cancer invasion (Nabeshima et al., 2002). The microtubule network can also be relevant for the recycling of focal adhesion proteins, which can be enclosed in vesicles at the trailing edge for example and transported up to the front to be reused.

Overall, the migration cycle is ulteriorly controlled by RhoGTPases, which control each step of the cycle (as has been explained in section I. 4) as well as the

integration of all the different steps in order to produce a coherent migratory cycle. However, besides the intracellular regulation, cell migration is highly determined by environmental conditions.

8. Regulation of cell migration by external cues: the importance of the cells niche

As cells migrate, they interact with their environment by probing the biochemical composition: ECM specificity, adhesive ligand density, gradients, etc. A very well-studied phenomenon of biochemical extracellular regulation of cell migration is *chemotaxis*: cells migrate in a directed manner along a soluble chemical gradient (will be further discussed in Chapter 1 section II. 3. 3). Similarly, cells also respond to gradients in ECM receptors and thus migrate towards increasing ECM proteins density (*haptotaxis*).

On the other hand, migrating cells also detect and respond to physical cues of the surrounding matrix. The biomechanical environment refers to the topography, roughness, anisotropy, and rigidity of the substrate (Geiger et al., 2009). As such, cells can be embedded in a myriad of different physical contexts, ranging from 3D soft matrices to 2D aligned fibrils. Thus, cell behaviour can be modified by differences in the mechanical properties of the environment (Paszek et al., 2005). Relevant work has shown that stem cells could be lineage-specified only by varying the stiffness of the substrate (Engler et al., 2005). Interestingly, cell migration also results affected when varying physical parameters. Matrix rigidity, for instance, influences the migration of cells in a biphasic manner (Peyton and Putnam, 2005; Dokukina and Gracheva, 2010). In soft substrates focal adhesions poorly develop, so they are typically small and very dynamic. In stiffer substrates, cells develop typically large focal adhesions that can sustain high traction forces, thus allowing for a fast migration. However, too stiff substrates promote very stable adhesions not adequate for fast migration. The dynamics of focal adhesions and migration speeds are also tightly correlated to the traction forces applied to the substrate. When cells tug the ECM through application of traction forces, the focal adhesions are modified and mechanosensitive proteins can result activated and trigger intracellular signalling responses. However, purely physical mechanisms can also apply, such as the build-up of intracellular tension, which can guide the disassembly of rear-edge focal adhesions and determine the formation of new adhesions at the leading edge. Along this line, a preferential migration of cells to stiffer areas has been reported, which is referred to as *durotaxis*, albeit not all cells durotax (Georges and Janmey, 2005). During durotaxis, cells migrate from

soft to stiff areas, clearly showing how substrate compliance can modulate cell migration (Lo et al., 2000; Isenberg et al., 2009). Recent experiments provide evidences that the rationale behind durotaxis is a preferential alignment of cells along the stiffness gradient, rather than an effect on the motility rates. One possible explanation for rigidity sensing mechanism would be via cytoskeleton rearrangements, as it has been shown that stress fibres and focal adhesions polarize according to stiffness variation (Saez et al., 2007; Trichet et al., 2012; Zemel et al., 2010; Prager-Khoutorsky et al., 2011).

As it has been discussed, cell migration is a complex process that is regulated intracellularly by many factors. At the same time, extracellular cues, both biochemical and biomechanical, can also affect cell migration. Thus, it is important to take into account the niche where cells are located in order to fully understand cell behaviour. Importantly, such cell niche is typically the extracellular matrix, but interaction with other cells must also be taken into account. We will hereafter focus on the structure, function of migration of the most widespread cell type: epithelial cells.

II. COLLECTIVE CELL ADHESION AND MIGRATION

While there are many examples of cells living as single entities (cells embedded in connective tissues, fibroblasts, osteocytes, neurons, etc.) and migrating isolatedly (mobilized stem cells, immune system cells, etc.), cells often group together to form cell collectives. The paradigmatic case of cell collectives is the epithelium, where cells are tightly connected to each other forming a continuous multicellular 2D layer.

1. Building epithelia: Cell-cell adhesion

Epithelia are central to the construction of the body, representing more than 60% of the vertebrate body cells (Alberts et al., 2008). Epithelial tissues cover the entire body surface, line internal cavities, and compartmentalize organs. Depending on their *in vivo* body location, epithelial cells can be greatly specialized: blood vessel-lining endothelial cells, highly-absorptive enterocytes, etc. However, the basic and common feature of epithelia is its function as a barrier, protecting from extracellular milieu and creating boundaries between differentiated spaces. As such, the hallmark of epithelia is the presence of cellular adhesions. Cells are hold together by cell-cell adhesion complexes that connect the cells in different ways (Figure 1. 14): 1) Structurally, to ensure a physical stability of the epithelial barrier, by linking the cytoskeleton and membranes of contiguous cells. 2) Communication-wise, by means of metabolites that traverse between cells through adhesion complexes to trigger signals in the neighboring cells. 3) Mechanically, by the transmission of intracellular stress to nearby cells.

In order to satisfy all the functions that cell-cell adhesions convey to the epithelium, there are different cell adhesion complexes that are in charge of different aspects. Although the traditional picture described in Figure 1. 14 can apply for most of the cells, some of them might form predominantly one type of adhesion that would suit better their functions.
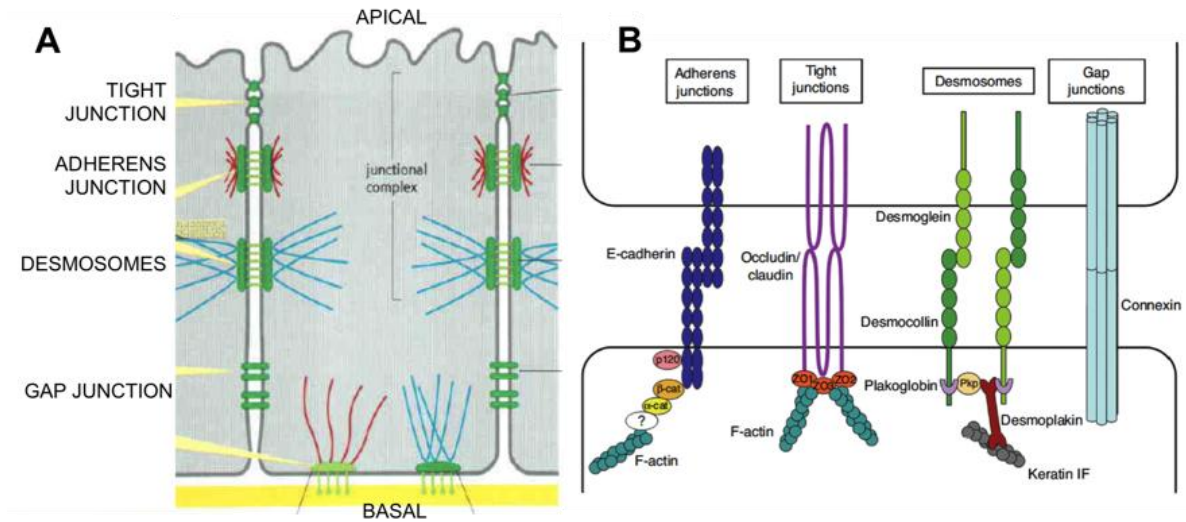
Figure 1. 14. Epithelia structure. (A) Scheme depicting the cellular localization of cell-cell adhesion compelxes. Modified from (Alberts et al., 2008). (B) Proteins involved in each type of cell adhesions. From (Trepat et al., 2012).

1.1. Adherens junctions

Adherens junctions are the best well-studied and usually claimed responsible for maintaining the cohesivity. Adherens junctions are based on the Ca^{2+}-dependent homophylic interaction of cadherin extracellular domains. There are many members of the cadherin family, among which E-,N-, and VE-cadherin are the most widely reported (Hulpiau and van Roy, 2009). The presence of many different types of cadherins hints towards the high specificity of adherens junctions depending on cell type, which is key for boundary formation and cell populations sorting (Halbleib and Nelson, 2006; Solanas et al., 2011). The intracellular domain JMD interacts with p120-catenin that strengthens the junction and signals to RhoGTPases. Such complex then interacts with α-catenin and β-catenin to be linked to the actin cytoskeleton, in a sequence not fully understood that is currently being revisited (Yamada et al., 2005; Drees et al., 2005; Cavey et al., 2008) (Figure 1. 14. B). Eplin has emerged as a connector candidate (Abe and Takeichi, 2007). Since adherens junctions connect neighbouring cells via the acto-myosin cytoskeleton (conforming the zonula adherens), forces supported by the cytoskeleton are also transmitted between cells (Mège et al., 2006; Lecuit and Le Goff, 2007). As such, it is tempting to speculate about the mechanosensitive capability of the proteins involved in adherens junctions. In this regard, recent works have pointed out a mechanosensitive reponse of adherens junctions similar to mechanosensing mechanisms at focal adhesions (Ganz et al., 2006; Ladoux et al., 2010). Alike tension-modulated vinculin recruitment to focal adhesions (del Rio et al., 2009; Pasapera et al., 2010), vinculin also localizes to tension-bearing cell-cell adhesion sites (le Duc et al., 2010). α-catenin has been proposed to mediate such force-dependent recruitment of vinculin (Yonemura et al., 2010). Thus, although α-

catenin might not be the direct link between cadherin and actin cytoskeleton, it plays an important role in the mechanosensitive response of adherens junctions as well as in regulating actin dynamics via Arp2/3 modulation, independtly of cadherins (Benjamin et al., 2010).

1.2. Desmosomes

Since in many stages, despite loosening the adherens junctions, cells still remain connected, other junctional proteins must be playing a role. Desmosomes are the main contributors to the mechanical stability of tissues. They have a similar structure to cadherin adhesions and include desmosomal cadherins from the desmocollin and desmoglein family (Figure 1. 14. B). The intracellular partners are armadillo proteins, plakoglobin, desmoplakin, and plakophilin, which connect to intermediate filaments. Interestingly, a closely related structure, the hemidesmosomes (that can connect epithelial cells to other cell types through the ECM) has been proposed to be capable of transmitting tension. These adhesive structures would transmit the stress generated by contractile muscles all along the epithelial cells, triggering a biological signal to coordinate extension of such epithelial layer, representing another example of the mechanosensitive capability of adhesion complexes (Zhang et al., 2011).

1.3. Gap junctions

Gap junctions are another adhesive complex, that serve both for the mechanical and the signalling connectivity, given that their structure (6 connexins Cx forming a hollow cylinder) allows the transit of different small metabolites between neighbouring cells (Mese et al., 2007) (Figure 1. 14. B). Gap junctions have been proven to be implicated in cancer progression (tumor cells exhibiting low expression of Cx), possibly acting as tumor suppressors, since their overexpression can reverse malignant phenotype. However, Cx26 has been found to re-express at some stages of the metastatic process, further suggesting the implication of collective migration in cancer spreading (Czyz, 2008).

1.4. Tight junctions

Tight junction (Smalley et al., 2005) proteins include claudins, occludins and IgG-like family of junctional adhesion molecules (JAMs), plus scaffolding proteins ZO1-3 (Figure 1. 14. B). Tight junctions are typically located at the apical cellular domain and are key for maintaining the apico-basal polarity (Figure 1. 14. A). These proteins represent the barrier for proteins to traverse the epithelia, so they confer the epithelia its characteristic impermeability [although it has been shown that epithelial cells defective for occludins still preserve the barrier function,

(Nusrat et al., 2005)]. As such, tight junctions seal together apposing membranes while regulating the apico-basal metabolite trafficking.

1.5. Cell-cell adhesions maintain apico-basal polarity

Essentially all epithelia are polarized, with their basal side anchored to ECM or basal lamina, their apical side free of attachments, and laterally linked to the neighbouring cells (Figure 1. 14. A). Asymmetry is key for the establishment of apico-basal polarity, which is maintained by a differential distribution of cell-cell junctions, namely tight and adherens junctions being located at the apical part of lateral membranes. The establishment of apico-basal polarity is regulated by RhoGTPases. Since nascent adherens junctions occur from interdigitating filopodia and lamelipodia from neighbouring cells, Rac1 is activated at these areas and help the formation of the first adherens contacts (Yamada et al., 2007; Takaishi et al., 1997; Braga et al., 1999). Then, Rac1 also helps in the maintenance of such junctions via IQGAP (Kaibuchi et al., 1999). For tight junctions establishment, Cdc42 drives the formation of Par6- αPKC complex, that then phosphorylates Par3 which binds to junctional proteins such as JAM (Rojas et al., 2001; Yamanaka et al., 2002). Tight junction formation and stabilization is also dependant on RhoA, probably via ROCK (Walsh et al., 2001). Finally, Rac1 also helps in the correct assembly of extracellular lamina, which was shown to be critical for the orientation of apico-basal axis in 3D cysts forming epithelial cells that face lumen on the upper part and basal lamina on the bottom (O Brien et al., 2001; Masuda-Hirata et al., 2009).

Apico-basal polarity is typically associated with highly specialized epithelial tissues, and is essential in absorptive/secretive epithelia, such as the intestinal or kidney epithelia. These cells are dedicated to engulfing metabolites from the apical part and in ion exchange. As such, they have a clearly differentiated apical side with highly specialized structures such as the microvilli. However, under the appropriate conditions epithelia can loose their apico-basal polarity and acquire a planar (or front-rear) polarity. Such transition occurs in the context of epithelial to mesenchymal transition and is accompanied by changes in cell-cell adhesions.

2. Moving epithelia: the Epithelial to Mesenchymal transition paradigm

Epithelial tissues have also important roles in shaping tissues and organs during embryonic development, as well as in certain pathological conditions during wound healing events or in cancer. In all these situations, stable epithelia transition to a motile state, in a process termed as epithelial to mesenchymal

transition (EMT) whereby tightly packed and polarized epithelial cells become migratory isolated mesenchymal cells. Rather than an on-off switch, with extreme cases being the exception [[observed for neural crests emigration and primordial germ cell gonad-targeting (Coles et al., 2007; Blaser et al., 2005) respectively], increasing body of evidence suggests that such process is finely tuned to accommodate an intermediate state (Christiansen and Rajasekaran, 2006; Revenu and Gilmour, 2009). In this manner epithelial tissue becomes motile while cells remain physically linked, thus tissue coherence is preserved. The hallmark of EMT is a down-regulation of cadherin, the magnitude of which will depend on the degree of EMT advancement (Figure 1. 15).
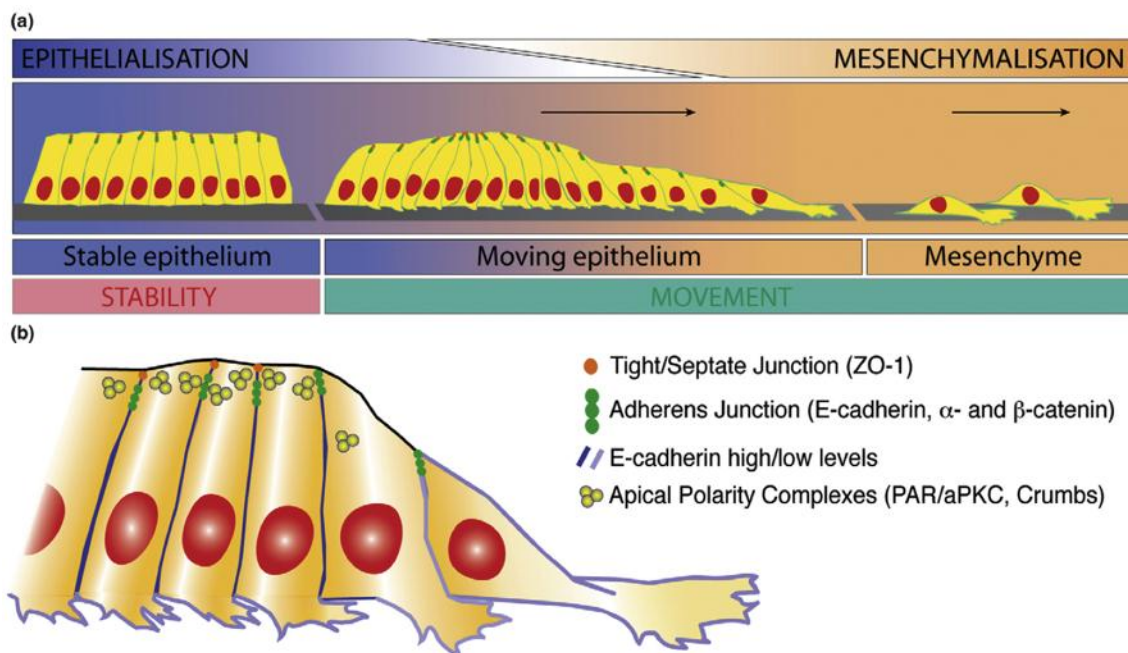
Figure 1. 15. Epithelial to Mesenchymal transition. In a stable epithelium (left panel), cells are polarized with the junctional complexes at the apical part. An intermediate state of EMT renders a migrating epithelium, with conserved junctional complexes and acquired front-rear polarity. If adhesions are down-regulated, mesenchymal cells dissociate from the epithelium and migrate as single cells (right part). From (Revenu and Gilmour, 2009).

Thus, the adhesive state between cells is critical for epithelial migration and must be very carefully regulated. High cohesiveness is frequently associated with decrease of speed, as it has been shown that knocking down adhesive proteins leads to an acceleration of migration (Simpson et al., 2008). Moreover, it is recurrently observed that epithelial cells can slide and change neighbours while moving collectively and cohesively, suggesting that cadherins might flow and reorganize to accommodate such movements (Kametani and Takeichi, 2007). This "softening" of adherens junctions is mediated by different kinases in response to growth factors (such as scattering by HGF, EGF, etc.), Eph receptors, Src and Abl (Gumbiner, 2005). Together with changes in cadherin, other junctional proteins of

adherens junction complex, as well as tight junctions, desmosomes, and apical polarity complexes are affected (Chidgey and Dawson, 2007). In addition to a down-regulation of adhesive proteins, mesenchymal-associated proteins are up-regulated, as for example vimentin, an intermediate filament component, smooth muscle actin, fibronectin, among others (Thiery and Sleeman, 2006).

Several growth factors have proved to induce EMT, being TGFβ the most well-studied due to its implication in cancer progression (Zavadil and Böttinger, 2005). Also, FGF, SDF1, TNFα, NF-kβ can induce epithelia towards a motile state (Grutnert et al., 2003; Huber et al., 2005). Motility-inducing extracellular factors typically trigger intracellular cascades associated with tyrosine kinase receptors. Ras, Src, Phosphatidylinositol-3-kinase (PI3K) and Mitogen-activated protein kinase (MAPK) are kinases typically implicated in promoting epithelial-mesenchymal transition (Christiansen and Rajasekaran, 2006). Interestingly, many of these kinases are found activated in development processes rich in epithelial movements. Likewise, mesenchymally-migrating cells can revert back to a stable epithelia following the mesenchymal to epithelial transition (MET) by re-expressing adhesion and apico-basal polarity complexes (Chaffer et al., 2007; Thiery et al., 2009).

3. Collective migration: mechanisms

As it has been pointed out in the context of EMT, cells migrate collectively when they move together with other cells, not only physically coupled but also functionally related. The number of migrating cells during collective cell migration is highly variable: it ranges from ten cells (as in border-cell migration during *Drosophila* development), to several hundreds of thousands of cells (as in Dyctiostelium slug development) (Weijer, 2009). The overall migratory cohort can be structured in many ways, as chains, sheets, branches, etc., depending on the *in vivo* situation (Figure 1. 16. A). In some scenarios during cancer progression or morphogenesis, migrating cell collectives also interact with migrating single fibroblasts or specialised isolated cells that help in determining the directionality or invasive capacity of the collectives (Gaggioli et al., 2007; Caussinus et al., 2008).

Why collective movement? By belonging to a group, cells can double-sense extracellular signals in two fashions: globally (or macro), at the level of the cell cohort; and locally (or micro), at the level of a single cell. Even more, by further integration of the cell response to the local signal, another response can emerge. At the same time, such multi-faced sensing strategy permits that, thanks to the average signal output, the cell cohort can disregard local fluctuations if necessary.

Another interesting strategy is the compartmentalization of tasks within the cohort, where an immobile set of cells could be carried along by the surrounding migratory cells. Similarly, the migrating group could transport cells irresponsive to extracellular cues (Ghabrial and Krasnow, 2006). Likewise, an encapsulation mechanism could protect the inner cells from external assaults (as in the case of immune system protection during tumor spreading). And last, note that the migrating process itself can be the driving force of intra and intercellular rearrangements required for morphogenesis (Zhang et al., 2010). For instance, it was elegantly shown that the pulling force of the migration of the tip cell is condition *sine qua non* for adhesion junction remodelling and cell intercalation to form lumen during tracheal branch growth (Caussinus et al., 2008) (Figure 1. 16. B).
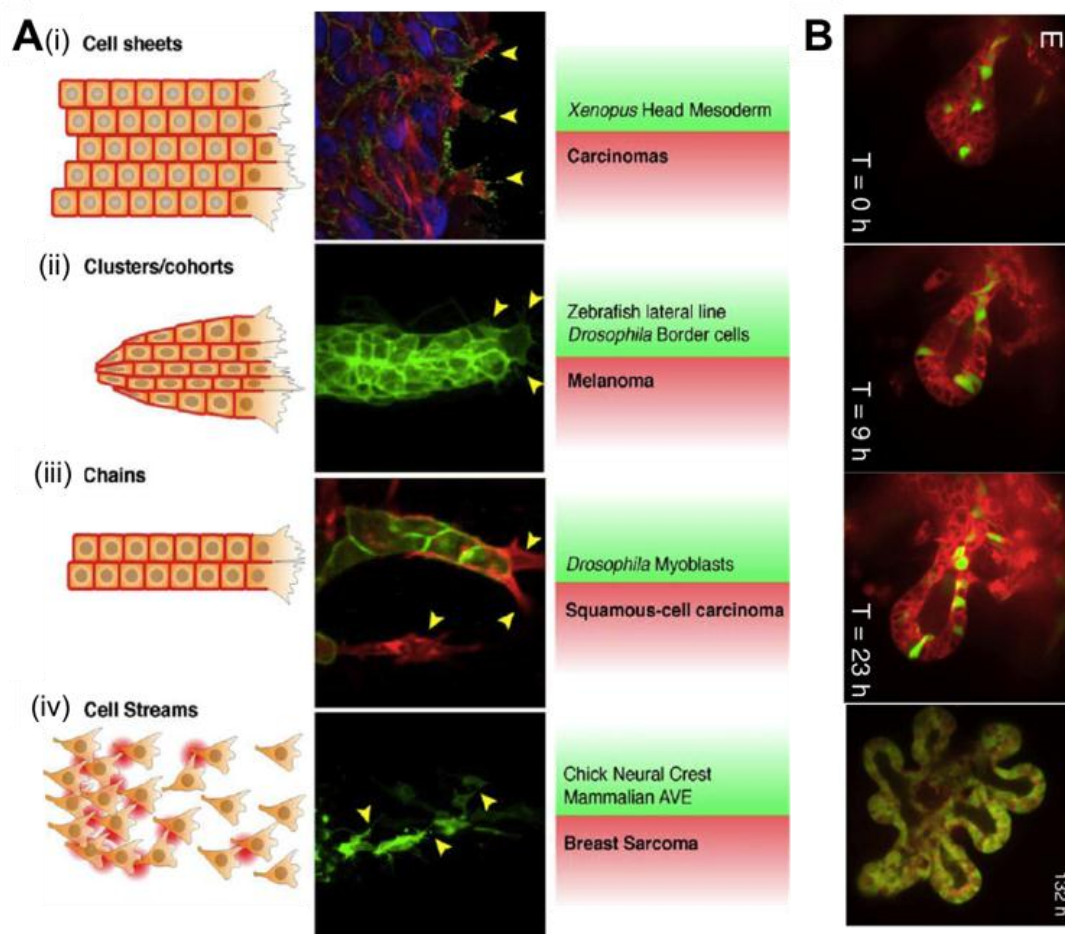
Figure 1. 16. Examples of collective cell migration. (A) Left column is a schematic representation of the different modes of collective migration, central panels are confocal images of collective migration in different organisms, right panel are examples of such collective migration modes in physiological (green) and pathological (red) conditions. (i) *In vitro* migration of epithelial cells from the intestine. (ii) Zebrafish lateral line. (iii) Squamous cell carcinoma invasion, lead by the protruding cell (highly stained for actin in red). (iv) Migrating avian neural crest cells. From (Mayor and Carmona-Fontaine, 2010). (B) Collective migration plays an important role is shaping tissues and organs in 3D as well. See the evolution of a mammary gland from a primordium to a complex lumen-containing structure. From (Ewald et al., 2008; Andrew and Ewald, 2010).

Cells migrate collectively also through the 5-step migration cycle described for single cell migration, i.e. mesenchymal migration (in most of the cases) (see section I. 7). But in addition, cell migration must be coordinated at the multicellular level to produce a coherent migratory output. Such coordination can vary among cell types and be influenced by the environment and thus different mechanisms of collective migration emerge. These mechanisms have been widely explored from a biological point of view and give rise to different models to explain collective migration according to different *in vivo* events (

Figure 1. 16).

3.1. Tumor progression

There is increasing evidence showing that tumor invasion and even metastasis are driven by collective cell migration, challenging the classical dogma that cells abandon the primary tumor as single isolated cells (Alexander et al., 2008). Nevertheless, collective cell invasion is predominant especially in highly differentiated tumors, as in breast, prostate, lung, and all epithelial cancers (Bell and Waizbard, 1986; Friedl and Wolf, 2003; Friedl and Alexander, 2011). Histological sections of primary tumors show clusters, chains, and sheets surrounding the tumoral mass and staining positive for adherens junctions proteins, and groups of tumor cells have been found in the blood and lymph in their journey to colonize new tissues (Nabeshima et al., 1999; Byers et al., 1995; Brandt et al., 1996; Alexander et al., 2008).

In the context of tumor invasion, Smad4 and TGFβ have been recurrently proposed to trigger EMT so that tumor cells become motile. The migration of tumor cells is highly influenced by the environment, which undergoes drastic changes along tumor progression (Levental et al., 2009). Moreover, tumor cells typically exit the primary tumor site and enter stromal tissues in their way to colonize new sites. As such, the main feature of tumor cell migration is the remodelling of the surrounding matrix via specificity in integrin engagement, degradation of the matrix, and secretion of modified ECM. The migrating front is characterized by a differential expression of integrins, with $\alpha_v\beta_3$, $\alpha_v\beta_6$, $\alpha_6\beta_4$, and β_1 being upregulated (although the specific integrins can vary among situations) (Guo and Giancotti, 2004; Hegerfeldt et al., 2002) (Figure 1. 17. A). The engagement of these integrins triggers intracellular cascades involving FAK, Src kinase, Ras pathways, and other MAPKs, highly related to migratory phenotype (Reddy et al., 2003). Alongside, the front presents notable activation of MMPs, in order to actively degrade the surrounding matrix and deposit and crosslink new ECM components, typically collagen (Nabeshima et al., 2002; Levental et al., 2009). This causes a stiffening of the underlying substrate that will constitute the migration

track for the rear cells. The stiffnening of the substrate acts as a positive feedback signal further promoting the migration of tumor cells, as discussed in section I. 8.

The described activation of integrins and MMPs is a hallmark of migrating tumor cells. However, there is not only one mechanism responsible for tumor cells migration, but rather cancer cells present relevant plasticity and ability to shift their migration mode. Tumor cells can compensate for the loss of a particular motility feature (for example inhibition of MMPs by therapeutic agents) by developing another migratory mode. Thus, depending on many features of the environment and the cellular state itself (expression of adhesion receptors, cell contractility, cytoskeletal regulation, substrate adhesiveness, matrix composition and structure, etc.) cells can switch from highly adhesive to less adhesive motility strategy (mesenchymal or collective to amoeboid transition, mesenchymal to collective or viceversa transition, all of them partial or total transitions) (Figure 1. 17. B) (Friedl and Wolf, 2003). Such adaptation can be natural, due to the evolution in time of the tumor microenvironment (increase of stromal stiffness, loss of cell contractility, etc.) or due to therapeutic treatments (drug-induced plasticity). Moreover, because most of the migration modes are based on redundant mechanisms, the inactivation of one of them can be surpassed and tumor invasion progresses. This plasticity and reciprocity is one of the main reasons why there is no effective cancer treatment targeting adhesion receptors or proteases (Friedl, 2004; Sahai and Marshall, 2003; Friedl and Wolf, 2010; Friedl and Alexander, 2011). Another interesting consideration is the similarity of the cancer invasion patterns with morphogenetic movement, which is giving raise to the theory that collective invasion in cancer mimics morphogenetic movements, albeit in a disorganized manner (Figure 1. 17. C).
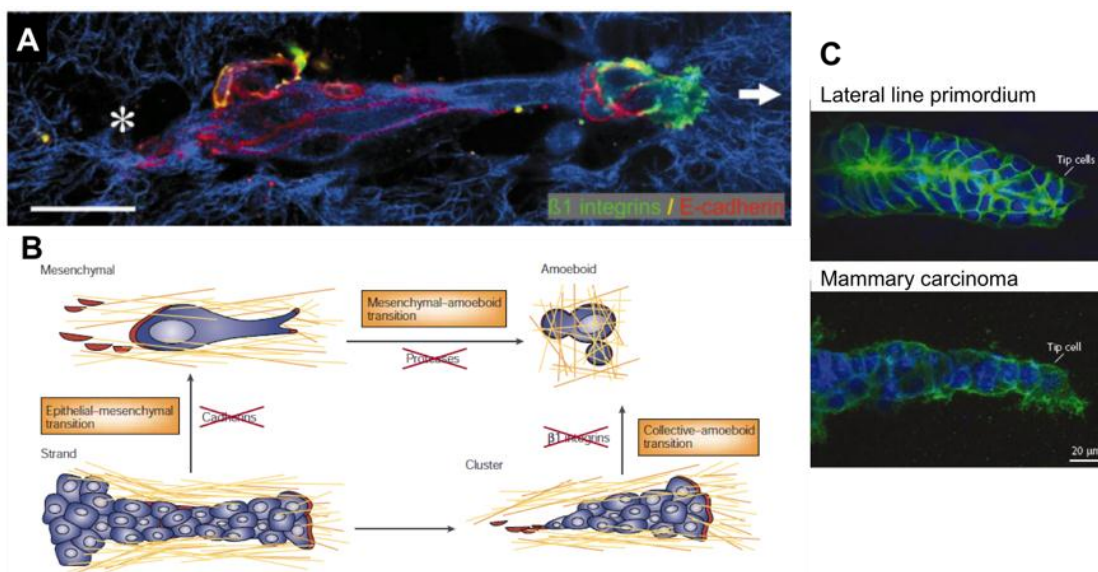
Figure 1. 17. Cancer invasion mechanisms. (A) Melanoma tumor cells invade an artificial 3D matrix by migrating collectively. Note the polarization of the cluster and the differential expression of integrins at the leading front, while cadherin are expressed in all the cells of the cluster. Asterisk denotes area of active matrix degradation, namely the trailing edge. Scale bar is 50 um. From (Friedl et al., 2004). (B) Tumor escape mechanisms. Migrating cells can alternate their migration mode to better suit the environment. Such plasticity enables tumor cells to switch their migration strategy to escape the surrounding stroma and metastasize. This mechanism shifting includes cell detachment from a cohort by down-regulation of cadherin (EMT), and transition form mesenchymal-like migration to amoeboid, when the matrix is denser. From (Friedl and Wolf, 2003). (C) Migration of cancerous cells resembles patterns of developing epithelia. From (Friedl and Gilmour, 2009).

3.2. Migration by cell proliferation and pressure

In the context of tumor progression, another possibility to explain the movement of tumor clusters is increased cell proliferation. Given that one hallmark of cancer cells is their disregulated proliferation, the multiplication of tumor cells would produce an increasing compressive pressure or stress on the surrounding ECM that would promote the migration outside the tumor site and posterior colonization of stromal tissues (Butcher et al., 2009; Tracqui, 2009). Migration by cell proliferation has also been described in certain cases of tubulogenesis, like in the mammary glands. In this case, the proliferation of cells in the protruding gland bud causes an increase in volume that would induce the elongation of the pushing bud (Ewald et al., 2008)

However, the two above-mentioned mechanisms (migration of tumor cells and cell proliferation-induced migration) apply mostly to the cancer context, since the mechanisms are based on features prominent in tumor cells (differential secretion of ECM components and MMPs, and disregulated cell proliferation). Thus, in the case of migration of non-tumorous cells, other mechanisms must exist.

3.3. Chemotactic migration

One of the widest-studied mechanisms for collective migration is chemotaxis, which occurs extensively during developments. In this situation, cell collectives migrate thanks to biochemical signalling and in response to gradients of motility-promoting factors. Much evidence of chemotactic migration comes from studies of Dictyostelium slugs, where thousands of cells migrate collectively in response to shallow gradients of cAMP (Lecaudey and Gilmour, 2006). During development, there are many examples of cell collectives migrating along gradients of growth factors and signalling proteins. For instance, border cells migrate towards the oocyte during *Drosophila* oogenesis in response to EGF and PVF (PDGF/VEGF-related factor) signalling (Rørth, 2009). Border cells are clusters of 6-8 migratory cells that follow a gradient of EGF and PVF emanating from the oocyte (Montell,

2003). Such signalling induces protrusive activity on the migrating cells, and surprisingly such cells exchange positions often within the migrating cluster, all being able to chemotax adequately toward the oocyte (Bianco et al., 2007).

Primordium lateral line migration during zebrafish developments is another well-studied example of how biochemical signal drives the concerted migration of a cohort of ≈100 epithelial-like cells (Rørth, 2009) (Figure 1. 18). These cells migrate from the anterior part to the posterior while depositing small clusters that will later develop to mechanosensory organs (neuromasts) for a period of about 2 days (Weijer, 2009) (Figure 1. 18. A). The migration of the primordium follows a line of the chemokine stromal-derived factor 1 (SDF1) and crucially depends on the expression of SDF1 receptor, chemokine receptor 4 and 7 (CXCR4 and CXCR7) (Haas and Gilmour, 2006) (Figure 1. 18. C). In this situation, SDF1 is not present in a graded fashion but rather as a continuous signal, only indicating the migration path. The directionality and motility arises from the regulated integration through CXCR4 and CXCR7 of SDF1 ligand. Such directional migration is strengthened by primordium polarizing signals from antagonistic FGF and Wnt signalling activities: Wnt promotes migration at the advancing front of the primordium while FGF represses movement at the back, allowing for neuromasts to be deposited along the way (Rørth, 2009). Thus, the combination of both promigratory and directional biochemical cues drives the orchestrated migration of the lateral line.
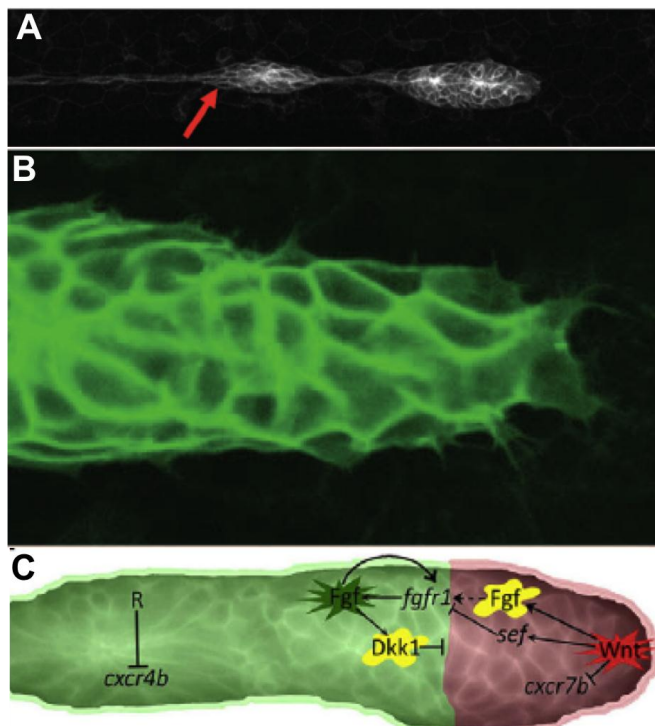
Figure 1. 18. Migration of the lateral line in Zebrafish. (A) General view of the migration of the primordium, and how clusters of cells are deposited along the way, which will later develop into neuromasts. From (Trepat et al., 2012). (B) Close-up of the tip of the primordium, where lamellipodia anb filopodia protrude. From (Lecaudey and Gilmour, 2006). (C) Scheme of the signalling events regulating the directional migration of the primordium. From (Aman and Piotrowski, 2010).

Thus, chemotactic migration requires a differential or graded expression of either ligand or receptor. In cases of homogeneous signalling, other mechanisms of collective migration have been described.

3.4. Contact inhibition of locomotion

Another plausible hypothesis to explain movement of cell cohorts is contact inhibition of locomotion (CIL) (Figure 1. 19). CIL describes the observed behaviour of cells changing direction after contacting each other, and is based on the inhibition of the cellular protrusions at the site of contact [(first described for single migrating fibroblasts by (Abercrombie and Heaysman, 1953)]. The sensing of other cells can be either by filopodia and lamellipodia, and both can result inhibited after contact (Mayor and Carmona-Fontaine, 2010). CIL has been described for the migration of neural crest cells, which are cells that emanate from the neural tube and migrate. This is a classical example of cells undergoing EMT, since epithelial cells from the neural tube loosen their adhesions and disperse as small clusters and migrate as streams, eventually becoming mesenchymal migratory cells that travel to different body locations (central nervous system, skeletal and connective tissue, etc.) (Labonne and Bronner-Fraser, 1999). Neural crest cells migrate by extending protrusions (lamellipodia and filopodia) (Teddy and Kulesa, 2004). When these protrusions contact other cells, planar cell polarity/non-canonical Wnt pathway is activated, which leads to RhoA activation. RhoA antagonizes with Rac1 and thus inhibits protrusion at the site of contact, so that protrusion at other regions of the cell will be extended and cell will change the direction of migration (Carmona-Fontaine et al., 2008) (Figure 1. 19. B).

In a more general context of collective migration, CIL would explain how cells at a leading edge extend lamellipodia into the free space, while cells behind could not protrude due to inhibition of lamellipodia by contact with the neighboring cells (Figure 1. 19. A). When first-row cells move forward, the contact inhibition of cells at second row would be released and thus these cells could also protrude and advance, and thus by progressive movement of the cell rows the collective would move forward. The movement in a graded fashion as well as the necessity of free space for lamellipodia to protrude implies that sheets migrating by CIL are not very cohesive. Indeed CIL mostly accounts for migration of neural crest cells, which are cells with advanced EMT. Thus, CIL could not explain movement of tightly packed epithelia.
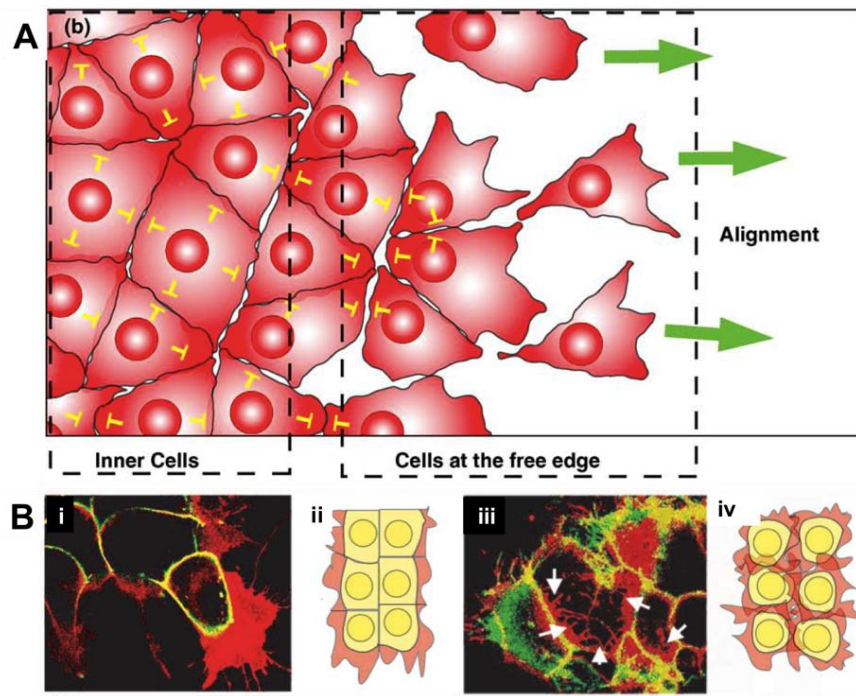
Figure 1. 19. Contact inhibition of locomotion. (A) Scheme depicting the model of how cell-cell contacts inhibit the protrusion of lamellipodia and filopodia, while cells at the edge can extend protrusions in the absence of neighbours. From (Mayor and Carmona-Fontaine, 2010). (B) CIL is mediated by the planar cell polarity pathway. In wild type conditions (i and ii), protrusions (in red) are only extended at the free borders and not at cell-cell contact regions, while when the planar cell polarity pathway is inhibited (iii and iv), cells extend protrusion in all directions, regardless of cell-cell contacts. From (Carmona-Fontaine et al., 2008).

Related to CIL, there is another proposed mechanism of collective migration based on the primordial role of first-row cells in extending lamellipodia: leader cells-driven collective migration.

3.5. Migration driven by leader cells

Migration driven by leader cells can occur during development, where cell sheets migrate over other tissues during embryogenesis, and in adult life, when epidermal cells are activated in response to an injury-induced available space. Such case has been widely studied in *in vitro* systems by exposing cells to a free surface, and much knowledge is now available about such mechanism of migration.

As described for CIL, the cohort acquires a constitutive asymmetry dictated by the front cells detecting neighbours only at their back and sides while having an empty space with respect to inner cells, which detect neighbouring cells in all directions. This translates into a strong polarization of the cohort and a specialization and differentiation of margin-located cells in terms of phenotype, function, and mechanical state. Traditionally, these cells at the leading edge are

called *leader cells* or pathfinders (as opposed to *follower cells*), because they are supposed to explore and guide the rest of the cohort. Leader cells can be variable in number (one cell in tracheal branching, few cells during tumor invasion, or many more cells during sheet expansion or epidermal wound closure) and are typically transient. They are intrinsically physically bipolar (one side attached to neighbours, the other side free), and their asymmetry is maintained by differential adhesion proteins distribution (integrins at the front due to membrane protrusions, and cell-cell adhesion proteins at the laterals and rear). Such physical bipolarity also determines differential extracellular factors sensing. By being the first(s) in the advancing front, they are in charge of modifying the ECM. Leader cells are sometimes referred to as mesenchymal-like cells and show changes in cell polarity: they loose apico-basal polarity and acquire planar polarity. Rho-dependent cytoskeletal reorganizations result in characteristic phenotypical features such as a large fan-like lamellipodia, disassembly of cortical actin, and increase of stress fibres (typically perpendicular to the advancing front) (Omelchenko et al., 2003) (Figure 1. 20. A). They can be relatively constant in their leading position (up to hours during sheet migration) (Aman and Piotrowski, 2010).

Follower cells retain the classical characteristics of restant epithelia, such as defined apico-basal polarity, tight and adherens junctions, and express low levels of guidance receptors. Interestingly, follower cells exhibit radial cell-cell adhesions with the leader cells, instead of the classical tangential adhesions, indicative of the tensional degree of leader cells (Omelchenko et al., 2003; Poujade et al., 2007) (Figure 1. 20. A. iv). During migration all cells move cohesively, thus this feature differentiates leader cells-driven migration from CIL.

According to the leader-follower model, the mechanical aspect of the migration should be dominated by the leader cells, which intuitively would be pulling the rest of the epithelia forward and follower cells would be passively dragged. This had been the working model for some time, supported by all the studies advocating for a differential form and function of the first-row cells (Poujade et al., 2007; Gov, 2007; Mark et al., 2010).

However, studies have reported the presence of cryptic lamellipodia in cells located many rows away from the leading edge (Farooqui and Fenteany, 2005; Tambe et al., 2011) (Figure 1. 20. B). The existence of cryptic lamellipodia challenges the notion of only leader extending protrusions. The fact that many cells well inside the cell collective can also protrude has prompted studies proposing a migration model where each cell is self-propulsed by the extension of lamellipodia, promoting its own migration.
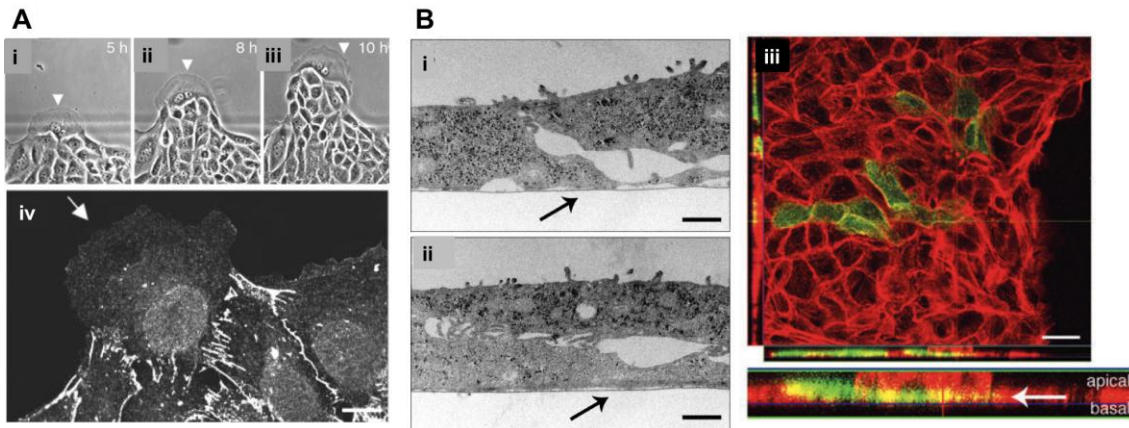
Figure 1. 20. Leader and follower cells. (A) At the migrating front of an epithelial intestinal sheet, some cells appear more prominent, with a large fan-like lamellipodia (i-iii). (iv) Cadherin adhesions between leader cell and followers appear typically radially emanating from the leader cell. From (Omelchenko et al., 2003). (B) Cryptic lamellipodia. (i-ii) electron micrographs showing the interdigitation of a cryptic lamellipodia beneath another cell, in a row far from the leading edge. (iii) By mixing a population of actinGFP and actinRFP transfected cell, it can be appreciated the presence of actinGFP-positive lamellipodia beneath actinRFP cells in an orthogonal view. From (Farooqui and Fenteany, 2005).

3.6. Self-propelled cells

Given the possibility that each cell can extend lamellipodia independently of their position and the presence or not of neighboring cells makes the hypothesis of self-propelled cells plausible. In this case, the collective motion would only result from the individual propulsion of each cell *per se*, with lack of supracellular coordination. Computational models accounting for such mechanism (i.e. not taking into account cell-cell contacts, multicellular coordination, or biochemical signalling) provided output data fitting adequately experimental observations (Bindschadler and McGrath, 2007). Along these lines, physical approaches to the study of collective migration are supporting a prominent role of cell density in determining emergent multicellular behaviours, independently of other biochemical variables. In this model, cells grown at increasing confluence start displaying coordinated motions (Szabó et al., 2006). This behaviour is recurrently observed in colloidal systems where an increase in the density of particles causes glass-transitions to ordered states. The analogy between colloids and cells in increasing densities is attracting the attention of many theorists trying to model collective migration from a soft-matter physics point of view (Angelini et al., 2011).

From the proposed models, some of them have mutually-exclusive features, while some aspects could overlap and occur simultaneously. It is reasonable to speculate that the progression of tumor cells by mesenchymal migration ressembles the leader cells-driven motility, as in both situations there is a

significant modification of the firsts cells. Likewise, in contact inhibition of locomotion the first-row cells also protrude lamellipodia, although they have not been described (up to date) to be as specialized as the classical leader cells or the guiding tumor cells. On the other hand, the self-propulsion model seems to be in contradiction with the leader-cells driven migration, where only leader cells pull for the advancement of the monolayer and follower cells are passively dragged. However, an intermediate model could emerge from an overlap between the two models when taking into account the evidence for cryptic lamllipodia. In this synergy, leader cells could be guiding in terms of biochemical sensing and transmitting information to inner cells, which could also contribute to migration by the protrusion of lamellipodia.

Since migration is ultimately a mechanical process, a key parameter to decipher the mechanism of migration is to take into account mechanical component of the movement. By measuring the traction forces of a migrating epithelia and correlating them to the cells position within the epithelia, the contribution of each cells row would appear clearer. In this manner, the mapping of traction forces could discriminate between leader cells-driven, self-propelled, or pressure-driven migration. Indeed, direct measurements of the traction forces within a migrating monolayer has helped clarifying the mechanisms of migration and unveiled interesting phenomena.

4. Mechanics of a migrating monolayer

In order to shed some light into the mechanics of migration, recent works have provided direct measurements of the traction forces of a migrating epithelium (by both micropillar force sensor array and traction force microscopy) (du Roure et al., 2005; Trepat et al., 2009) and surprising results emerged, challenging the established models (Figure 1. 21). Tractions measurements unveiled that, indeed, leader cells exert high traction forces at the advancing rim, but follower cells also exhibit significant traction forces, even at long distances far away from the leading edge (Figure 1. 21. B and D). Evidence shows that a growing epithelial sheet is subjected to tensional stress (computed from the measured traction forces), and such stress propagates and accumulates within the sheet, suggesting long-range transmission of forces to the interior of the sheet. Moreover, by computing traction maps of migrating monolayers it can be observed that all cells display a similar mechanical behaviour, which would rule out the existence of two separate cell group, leader versus followers (Trepat et al., 2009). Hence, migration of a monolayer would result from cooperative and long-range integrated self-propulsion of each cell (leaders and followers, at the front and well inside the

sheet), in a tug-of war manner (Figure 1. 21. C). Moreover, this proven requirement for force propagation and cooperativity points out the importance of cell-cell adhesion in collective migration. The overall migration-driving force would then result from the integration of multiple force vectors arising from each of the cells locally, and contributing to the build-up of a tensile stress state (Figure 1. 21. C). Such tensile stress state had been already previously inferred by laser ablation experiments in *Drosophila* epithelia, where the initial tissue recoil right after hole drilling was indicative of the epithelium being subjected to tensile stress (Kiehart et al., 2000; Hutson et al., 2003; Ma et al., 2009).
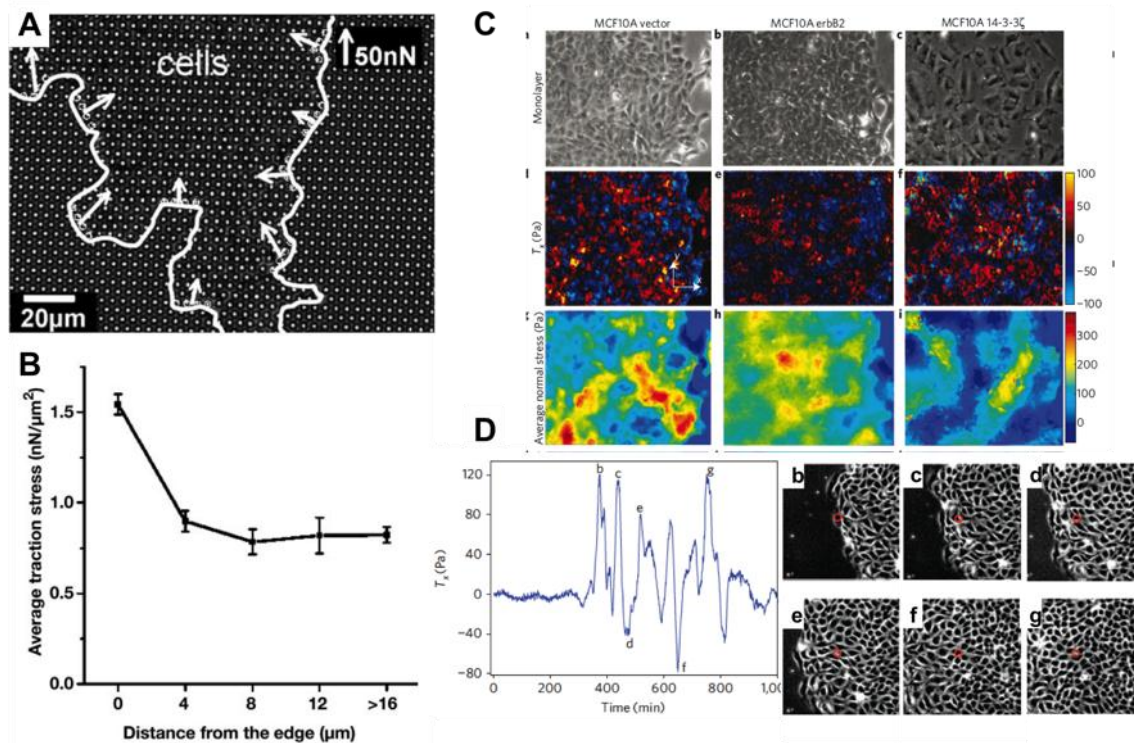
Figure 1. 21. Physical forces during collective cell migration. (A) By using the micropillars force sensor array, the group of Ladoux and Silberzan measured for the first time the traction forces of a migrating group of cells, outlined in white. White arrows are the resulting traction force vectors (du Roure et al., 2005). (B) Analysis of the traction forces as a function of the distance from the leading edge showed that, despite tractions are higher at the edge, significant forces are being exerted well behind the leading edge. From (du Roure et al., 2005). (C) Similarly, Trepat et al. have measured the traction forces of migrating monolayers by using the method of traction force microscopy. They also calculate the stresses that migrating cells experience, and both traction and stresses provide very heterogeneous landscapes. From (Trepat et al., 2009). (D) Analysis of traction forces of an advancing monolayer shows many peaks of high traction forces. The distance between peaks does not correspond to a cell size, but might be caused by 3rd or 4th-row cells. From (Trepat et al., 2009). Details on the technical aspects of force measurements can be found in Chapter 3 section 1.

This new hypothesis is supported by the fact that despite abrogating leader cell motility, epithelial migration is not impaired, and thus inner cells can compensate for such motility loss (Fenteany et al., 2000). Even more, this model is in good agreement with the finding of submarginal (or follower) cells extending "cryptic" lamellipodia beneath other cells, further suggesting the notion of self-propulsion (Farooqui and Fenteany, 2005) (Figure 1. 20. B). Nevertheless, the concept of leader cells can still be valid for the reported works, given that leader cells probably play a relevant role in directing and guiding the monolayer (Khalil and Friedl, 2010).

It still remains to be seen how general such tug-of-war model is. Possibly, the mode of migration (from both a biochemical and biomechanical point of view) is determined by many factors, including monolayer size and density, strength of cell-cell adhesions, matrix nature, presence of soluble factors, among others.

Interestingly, unravelling the mechanics of collective cell migration has also led to the emergence of a new feature of collective cell migration, which is how cells move according to a gradient of stress. Stress maps can be calculated from the measured traction forces of cells on the substrate by advanced algorithms, using a model described in (Tambe et al., 2011) (Figure 1. 22). Then, by overlapping measurements of stress and velocity within a migrating monolayer, Tambe et al. showed that cells move along the direction of principal maximum stress. This behaviour has been termed as *plithotaxis*, referring to how crowds move, in analogy to the well-described phenomena of chemotaxis, durotaxis or haptotaxis.

A MDCK / RPME
Stress ellipses and velocity vectors

B
Lowest 20%
Shear stress quintiles (RPME)

Middle 20%
Shear stress quintiles (RPME)

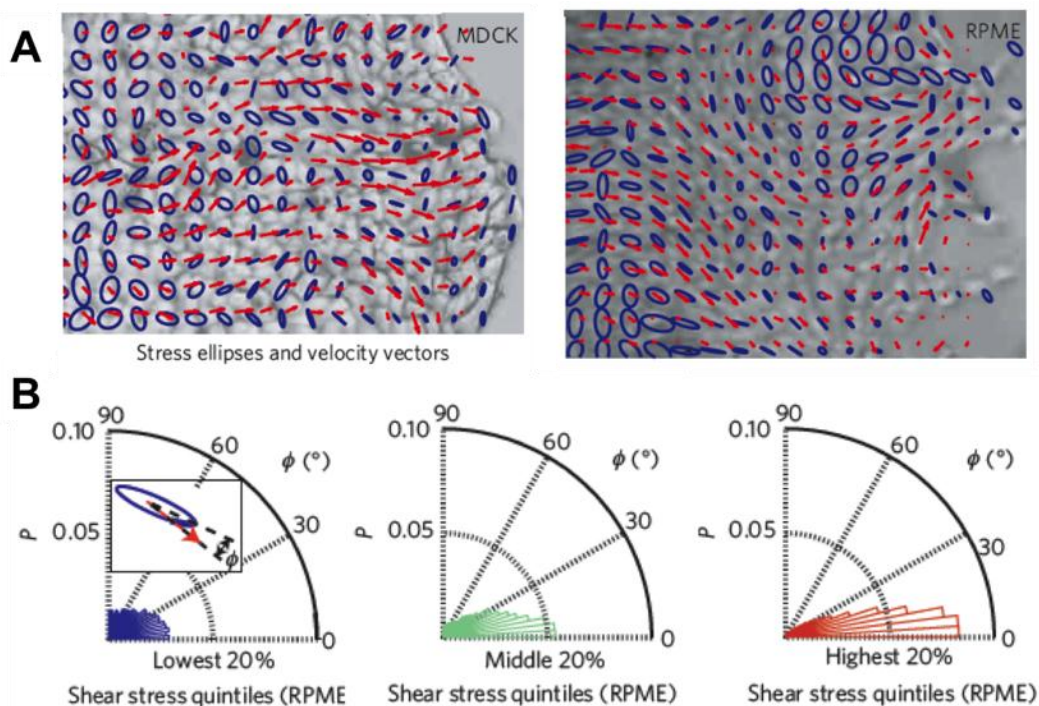Highest 20%
Shear stress quintiles (RPME)

Figure 1. 22. Plithotaxis. (A) Overlap of velocity field (in blue ellipses) with stress maps (in red arrows) on a bright field image of a migrating monolayer of epithelial cells (MDCK cells on the left, RPME cells on the right). (B) Cumulative probability distribution (*P*) of a given alignment (Φ) between the major axis of the principal stress ellipse and the direction of motion. From (Tambe et al., 2011).

Although very insightful, the presented works tackling the mechanical component of collective migration are restricted to a specific scenario, which is the expansion of an epithelial monolayer. Other cases of collective migration, such as the invasive migration of tumor cells strands, the advancement of the primordium while leaving cell clusters behind during lateral line migration, among many others, are far from being understood from a mechanical point of view.

While the discussed modes of migration apply in some cases to very specific situations of collective migration, extensive processes of collective migration take place recurrently during development and in adult life. Certain situations are associated with specific events where opposing sheets are drawn together. This process is known as **epithelial gap closure** and has pivotal importance for a correct embryogenesis and for maintaining epithelial barrier integrity. We will hereafter focus on epithelial gap closure situations, as they will provide relevant information for our understanding of epithelial gap closure.

5. Epithelial closure in development

It is clear that during the process of embryo shaping and tissue organization, extensive migration events occur, together with other morphogenetic routines like cell proliferation, sorting, intercalation, etc. Some collective migration steps occur during tissue remodelling or extension, for example in the case of hystoblasts nests expansion. Here, histoblasts cells migrate centrifugally to colonize the surrounding tissue and form the adult abdomen of insects (Ninov et al., 2007). On the other hand, some morphogenetic events consist on the migration of epithelial layers into an opening to finally zip the two advancing edges together, resulting in a continuous monolayer. These events typically occur after epibolic stages or during tubulogenesis, being the more prominent examples *Drosophila* dorsal closure, *C elegans* ventral enclosure, eyelid closure, neural tube closure, palatogenesis, and trachea invagination. These cases, especially dorsal closure in *Drosophila*, are under intense research since they represent an *in vivo* model where basic mechanisms of collective migration can be tackled, and also thanks to the ease of genetic manipulation of those embryos (with a wide repertoire of *Drosophila* mutants readily available). Moreover, such gap sealing events can also provide

valuable information to a presumably-similar clinically-relevant event, which is re-epithelialization during wound healing (Wood et al., 2002; Martin and Parkhurst, 2004). Thus, we will focus on these cases of epithelial sheet fusion events, since they are of relevance to the topic of this thesis.

5.1. *Drosophila* dorsal closure

Drosophila dorsal closure is a widely studied morphogenetic movement, adopted as the paradigmatic example of epithelial sheet fusion. It is also the most thoroughly characterized thanks to the great myriad of available mutants, the ease of producing genetic modifications at researcher's will, and reasonably good imaging techniques.

Dorsal closure is one of the latest morphogenetic movements in the shaping of *Drosophila* embryo. It consists on the sealing of an eye-shaped opening at the dorsal part resulting from germband extension. Such closure is accomplished by the drawn up of the two lateral epithelial sheets over the internal amnioserosa tissue and lasts 2-3 hours (Figure 1.23. A). The closure process is a combination of different overlapping steps and requires the combined effort of both epithelium and amniosera.
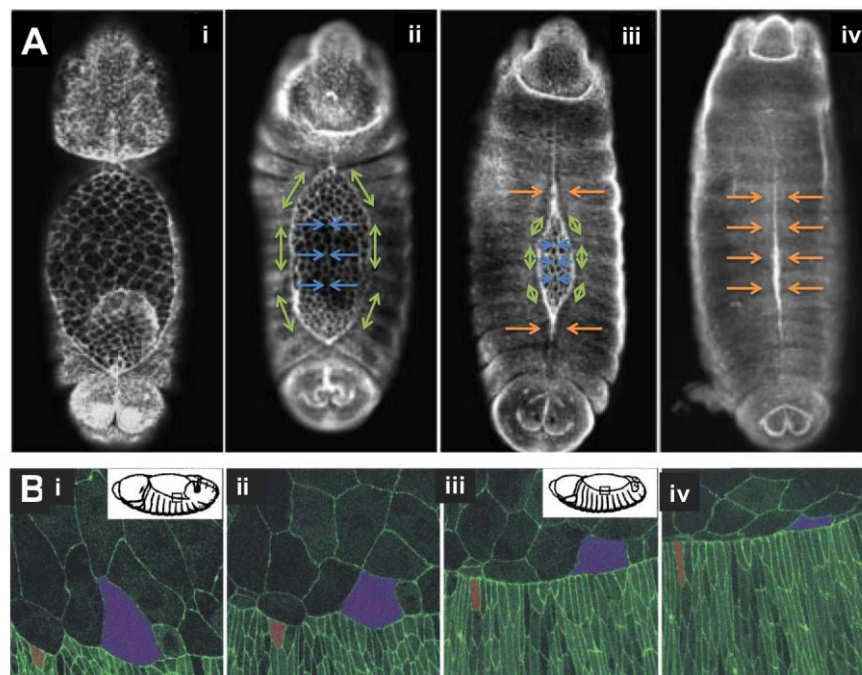
Figure 1. 23. *Drosophila* dorsal closure. (A) Fluorescent micrographs of the progression of the closure. Overlapped, a schematic representation of the forces that presumably would be acting at each step. Green arrows represent the tension accumulated at the actin cable, blue arrows are the force induced by the contraction of the underlying amnioserosa cells, and orange arrows depict the zippering forces. Modified from (Harden, 2002). (B) Snapshots of the initiation phase of dorsal closure, where cell-cell junctions are labelled in green. Note that in (i) and (ii) there is mainly

contraction of the amnioserosa cells, while in (iii) and (iv) the leading edge of the epithelium starts to elongate and the "epithelial sweeping" commences. By (iv), it is obvious that the epithelium is moving over the amnioserosa cells. Note the changes in area of amnioserosa cells. From (Jacinto et al., 2002).

At the beginning, the opening is filled with large, flat polygonal amnioserosa cells, surrounded laterally by smaller and cuboidal epithelial cells (which are covering all the embryo surface) (Figure 1. 23. B i). Dorsal closure starts right after full retraction of the germband. It is not fully understood what is the start signal: it could be related to a pre-established dorso-ventral patterning, or a mechanical result of germ band extension. It is clear though that this initiation is related to a differential activation of c-Jun N-terminal kinase (JNK) pathway. JNK, also known as stress-activated protein kinase, belongs to the family of MAPKs, and is increasingly recognized as a regulator of morphogenesis and motility (Xia and Karin, 2004). In the context of initiation of dorsal closure, JNK is up-regulated in the leading cells of the epithelium and down-regulated in amnioserosa cells (Homsy et al., 2006) (Figure 1. 24). The expression of JNK in leading cells locally activates the transcription of Dpp and Puc via AP1 expression (Reed et al., 2001; Stronach and Perrimon, 2002). Mutants for JNK pathway fail to seal the gap (Homsy et al., 2006; Ricos et al., 1999; Riesgo-Escovar, 1997), but it is still not understood the reason of such fatal effect. The requirement for JNK pathway activation has also been reported in similar situations of gap closure, such as in neural tube fusion and in vertebrate palatogenesis (Colas and Schoenwolf, 2001), and also in adult wound healing (Rämet et al., 2002; Li et al., 2003). During this initiation phase, epithelial cells are somewhat disorganized, show no actin accumulation and no regular shape. Amnioserosa cells reduce their apical size during this initiation step. Overall, although there is slight advancement in closure, there is no net migration of epithelial cells along amniosera, suggesting the closure here is mostly due to amnioserosa contraction (Figure 1. 23. B i-ii).
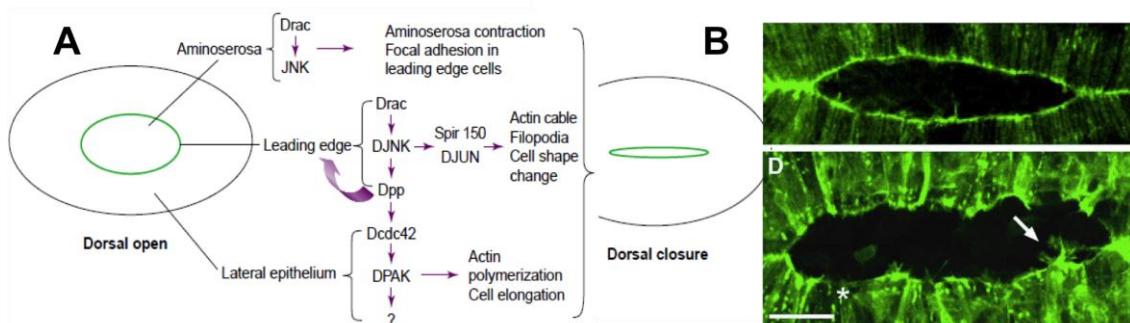

Figure 1. 24. Regulation of *Drosophila* dorsal closure. (A) JNK implication in dorsal closure. JNK is activated at amnioserosa cells and helps driving their contraction. At the leading edge, JNK activates the formation of the marginal actin cable and the extension of filopodia and membrane protrusions.

From (Xia and Karin, 2004). (B) Effect of Rac depletion on dorsal closure. Rac mutants (bottom) fail to assemble a proper actin cable compared to wild type (top). From (Woolner et al., 2005).

Later on, actin starts to assemble at the apical edge of epithelial sheets to form a thick actin cable. Such assembly is presumably responsible for the elongation of epithelial cells, resulting in a regular array of elongated cells (Figure 1. 23. B iii-iv). The planar polarity of these epithelial cells is reinforced by the dorso-ventral alignment of microtubules, which can also help in orienting the actin accumulation (Jankovics and Brunner, 2006). The accumulation of actin is reported to occur through Rac-mediated cytoskeletal reorganizations (Harden et al., 1996) (Figure 1. 24). Rac could also regulate the expression and paracrine secretion of Dpp by leading edge cells by acting upstream of the JNK pathway (Harden et al., 1999). By either pathway, Rac mutants fail to complete dorsal closure when Rac is depleted before the initiation phase (Harden et al., 1999). The actin cable also contains Zipper (the myosin II homolog), and its assembly is dependent of Rho1 activity (RhoA homolog) (Young et al., 1993). Rho1 also regulates anchorage of the acto-myosin cable at adherens junctions, similar to what described for purse-string mediated wound healing (Danjo and Gipson, 1998). Interestingly, RhoGTPases regulate acto-myosin cable assembly and contraction differentially at different anterior-posterior segments, given that dominant-negative mutants for Rac and Cdc42 cause cable disassembly in different degrees depending on the region (Harden et al., 1999; Woolner et al., 2005). This phase accounts for the major closure of the opening, which at this step occurs due to both contraction of the actin cable and size-reduction of amnioserosa cells (Figure 1. 23. ii to iii). Now filopodia, and to a lesser extent lamellipodia, start to protrude from opposing epithelial edges.

The zippering phase starts once the facing leaflets are close enough so that opposing filopodia entangle (Figure 1. 25. A). These actin protrusions zip the two epithelia together, from the canthi to the centre, and ensure correct matching of the embryonic segments. Mutants that do not extend filopodia (Cdc42 dominant negatives) fail in this zippering phase. Even more, stripped Cdc42-dominant negative leads to mismatching of such stripes on the embryo midline (Jacinto et al. 2000). Despite the requirement of filopodia for the matching, the contribution of the zipping force to the closure is dispensable. Laser cutting experiments showed that abrogating zipping at the canthis only introduced small delays in the sealing but did not prevent it. Once the hole is sealed, the break signals that prevent cells from overshooting are not fully understood. It could be just contact inhibition, as described in many other situations, and it could also be related to the maturation of the interdigitated filopodia to mature junctions (Mayor and Carmona-Fontaine,

2010). At the end of the process, a neat, and subsequently invisible seam is formed where the two epithelial edges have met one another.
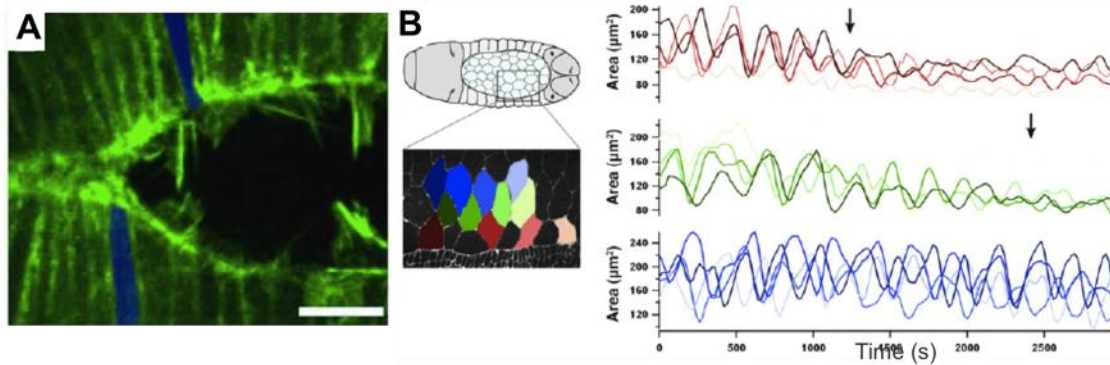

Figure 1. 25. Contribution to closure of zippering and amnioserosa cells contractility. (A) Zippering at the final stages of dorsal closure. Note the filopodial extensions. From (Woolner et al., 2005). (B) Pulsatile behaviour of amnioserosa cells. The area of cells highlighted in the left is measured along the progression of closure. See how the area varies, in a pulsed manner, until cells closer to the epithelial sheet decrease in area and stop varying their size. From (Solon et al., 2009).

The JNK-mediated assembly of the actin cable is a condition *sine qua non* for dorsal closure completion (Homsy et al., 2006; Ricos et al., 1999; Riesgo-Escovar, 1997). Although the contraction of the acto-myosin was thought to be the major driving force (similar to what observed in embryonic wound healing by Bement and Martin (Bement et al., 1993; Martin and Lewis, 1992), some experiments have hinted that the contractility of the cable is not the principal, for sure not the only, closing force. Laser cutting the cable fail to halt the advancement of the epithelial front (Kiehart et al., 2000). Alongside, Rho1 mutants, in which acto-myosin contraction is mildly disrupted, are still able to accomplish dorsal closure (Magie et al., 1999). Even if not the major driving force for the closure, the cable is most surely responsible to maintain the tension in the leading edge during the sweeping of the leaflets. Thus, the cable can act in ensuring a uniform advancement of the leading front. Indeed, striped Rho1 mutants show that Rho1-negative cells escape cable restraint, spill out and migrate over their *wild-type* neighbours (Bloor and Kiehart, 2002; Jacinto et al., 2002). Also, the cable is important for the phenotypic reorganization of epithelial cells, from a somewhat flat organization in the initiation phase to a rectangular and oriented shape most suited for the sweeping phase. Hence, the function of the actin cable is double-sided: contract to help in the closure process and maintain uniform epithelia edge advancement.

Besides the participation of the actin cable in the sealing, there is increasing evidence for a crucial role of amniosera in drawing the epithelium forward. Elegant laser cutting experiments proved few years ago that amniosera is under tension, which is required for the proper closure. Drilling holes in the amniosera,

thus releasing the tension of the tissue, lead to gaping of the adjacent epithelial sheets (Kiehart et al., 2000). Likewise, affecting the contractility of amnioserosa cells by Rac mutants (either dominant-negative or over-expression) (but not any other RhoGTPase) disrupted the progression of closure, further supporting a role of Rac-controlled Crumbs-mediated amnioseroa contractility in dorsal closure (Harden, 2002; Wodarz et al., 1995). Depleting amnioserosa cells also impaired dorsal closure (Scuderi and Letsou, 2005).

The current working model is that both the contractility of the amniosera cells and the contractility of the actin cable are responsible for the closure (i.e. the forces would be as schematized in Figure 1. 23. A). Both processes could result in additive forces, given that abrogating one causes a delay but not necessarily prevent from closing, thus one can be compensated by the other mechanism (Franke et al., 2005; Kiehart et al., 2000). A recent study evidenced how these two forces (from the amnioserosa and from the actin cable) contribute and are coordinated during dorsal closure (Solon et al., 2009). Solon and coworkers showed that an intrinsic pulsatility of the amniosera cells can drive the epidermal flanks dorsally. When the amniosera cells pulse and diminish their apical area, the epidermis advances forward. Such displacement is maintained by the tension of the actin cable, which acts as a ratchet by preventing the ventral-ward epidermis relaxation after the pulse of the amniosera cells (Figure 1. 25. B). With time, the amniosera cells become more compressed and their pulsing amplitude decreases. In the same work it was hypothesized that the actin cable does not act as a pure purse-string, i.e. it does not drive an inward force, at least not for most of the process. Instead, it would act as re-opening preventer cable which slowly builds-up tension [as shown by cable retraction after laser cutting (Hutson et al., 2003)]. Only at the later stages of closure would the actin cable be a purse-string by itself, but then its minor force contribution would be hampered by the zippering of the canthis.

It is interesting to note that this model explains dorsal closure from mechanical point of view, which can account for the different behaviours of actin cable and amniosera cells. For that, it challenges well-established purely biological-based dorsal closure models (Xia and Karin, 2004; Martin and Parkhurst, 2004). It will be interesting to see how the two viewpoints can be reconciled to provide a broader framework where the biological signals (that very likely must play a role in the process) control, modulate, or somehow interact with the mechanics. For example, it remains to be understood what drives the pulsatility of the amniosera cells, or how the migration of epithelial cells is stopped.

5.2. *C. elegans* ventral enclosure

Similar to *Drosophila* dorsal closure, during *C. elegans* morphogenesis, the closure of a ventral oval opening by the laterally surrounding hypodermis (epidermis) occurs (Figure 1. 26. A). This process occurs simultaneously with dorsal intercalation and partly overlaps with the subsequent body elongation. Ventral enclosure is defined as a two-step process carried out by two functionally and morphologically distinct groups of cells. First the two pairs of anterior-most cells elongate towards the midline, becoming 'leader cells'. The elongation and migration of such leading cells is indispensable for closure to occur, as disrupting them by laser ablation halts the closure (Williams-Masson et al., 1997). These leading cells extend actin-rich filopodia that contain HMP-1 (α-catenin homolog) and AJM-1 (adherens junction marker homolog), which are crucial for the establishment of the first adhesive contacts between opposing filopodia. In a second step, posterior cells acquire a wedged-shape morphology and also progress towards the midline. These cells show the same requirement for adhesive proteins to form stable junctions with their facing cells. The remaining opening, or ventral pocket, is surrounded by an actin cable (similar to the actin cable in dorsal closure). The closure of such pocket has been proposed to happen thanks to this actin cable, following the purse-string mechanism (Williams-Masson et al., 1997; Bement et al., 1993; Martin and Lewis, 1992). It has been proven that the actin cable is anchored at adherens junctions, and hmp-1 (α-catenin homolog) mutants display an actin cable detached from the junctions, proposing the catenin complex as the link between the cable and the junctions (Costa et al., 1998). In hmp-1 mutants, since the mechanical force that would be originated in the purse-string cannot be translated to the epithelial cells, subsequent movements are abrogated. Along this line, a recent paper proposes a more prominent role of the attachment of the acto-myosin cable to the cell-cell junctions in driving constriction of *C. elegans* cells during gastrulation rather than on the contraction itself (Roh-Johnson et al., 2012). The authors claim that acto-myosin pulsatility is present well before apical contraction, as it has also been observed in other situations (Kasza and Zallen, 2011; Martin et al., 2010). In this case, only when coupled to the cell-cell contact areas would the constriction be effective. Such *slip or stick* mechanism could be analogous to the molecular clutch defined in the section I.3 accounting for the connection of the actin cytoskeleton to the substrate via focal adhesions. Although the article focuses on the apical intracellular actomyosin belt promoting cell shape changes, it is tempting to speculate that such mechanism could also apply to the intercellular acto-myosin cable driving ventral pocket closure.
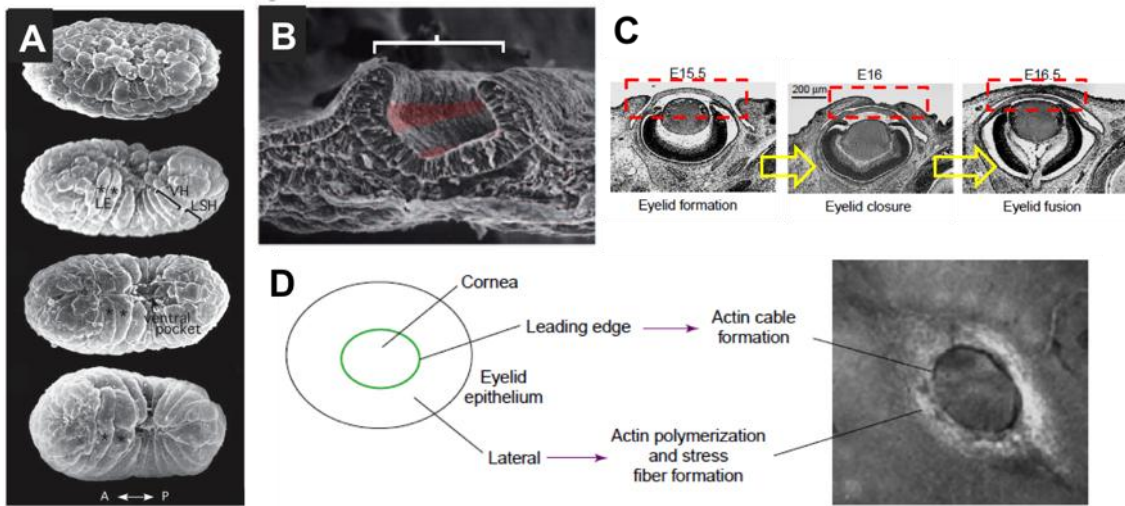
Figure 1. 26. Other epithelial closure scenarios. (A) *C. elegans* ventral enclosure. Leading edge cells migrate towards the centre, surrounding the opening or ventral pocket, until they fuse. The process is alike *Drosophila* dorsal closure. (B) Neural tube closure. Note how the neuro-epithelium (in brackets) bends and will then migrate so that the two opposing flanks will fuse and internalize as a tube. From (Lecuit and Lenne, 2007). (C) Eyelid closure progression, note how two opposing advancing sheets migrate and fuse in the midline (in red dashed box). From (Xia and Karin, 2004). (D) The process of eyelid closure resembles *Drosophila* dorsal closure. From (Xia and Karin, 2004).

5.3. Neural tube closure

Neural tube closure is the last step in neurulation, when two dorsolateral neuroepithelial sheets bend laterally, are somehow brought together, and fuse, all occurring in three dimensions (Figure 1. 26. B) (Davidson and Keller, 1999). Proper closure of the neural tube is critical for the correct development. Aberrant processes result in spina bifida, exencephaly, or even anencephaly, which prevents the neurological control of vital functions such as respiration, and is thus lethal (Copp, 2005; Copp and Greene, 2010). Acto-myosin contraction also appears as a prominent mediator of cell shape changes associated to apical constriction. In this context, planar cell polarity regulators have been proposed to account for an assymetric contraction of adherens junctions, that would result in a polarized bending of the neuroepithelium (Nishimura et al., 2012). However, a conclusive mechanism to explain tube closure has not yet been proposed, given that research is mostly focused on the actomyosin contraction–mediated apical constriction that promotes tube invagination, which cannot explain by itself the final closure of the neural tube.

5.4. Other fusion events

Many situations during development involve the sealing of gaps, typically by epithelial sheets that migrate while shaping the embryo. Eyelid closure is another remarkable example, as well as palatogenesis. All these processes follow the described mechanisms, where epithelial cells migrate to the midline and then fuse in a filopodia-dependent manner, but they have been far less studied (Figure 1. 26. C and D).

6. Epithelial closure during wound healing

Wound healing can occur at any moment in any tissue during both development and postnatal life, as for instance after a skin cut, in the airway system during asthma or acute lung injury, in spinal-cord injury, in the intestine, during heart infarction, etc. Independently of the tissue, the healing process is similar in all the cases (Gurtner et al., 2008). Due to its prevalence, cutaneous wound healing is the most well studied case. It is a critical, complex, multi-step process involving many players. Injury to the skin initiates a cascade of events that include inflammation, tissue remodelling and new tissue formation, finally leading to an almost perfect reconstruction of the wounded area (Figure 1. 27).

6.1. Adult wound healing

With the damaging of the skin, superficial disrupted blood vessels leak many growth factors, cytokines, and platelets at the wound site. From this very first moment, the inflammatory cascade is activated and self-sustained in time all throughout the healing process. Such accumulation of blood components leads to the formation of the blood clot, composed of platelets, cross-linked fibrin, fibronectin, vitronectin and thrombospondin. The blood clot acts both as a protection from invading microorganisms and as a wound bed for inflammatory cells to colonize and for neighbouring tissues to migrate over. Neutrophils, monocytes and lymphocytes arrive at the injury site to produce reactive oxygen species (ROS) as a defence mechanism, phagocyte cell debris, and secrete growth factors and cytokines required for the proliferative and resolving phase. From the myriad of factors secreted, TGFβ and PDGF play a major role in stimulating and activating fibroblasts and keratinocytes, and in sustaining inflammation for clot maintenance (Martin and Leibovich, 2005). Then, fibroblasts migrate into the provisional matrix and deposit large amounts of ECM molecules, preparing the wound bed for its sealing by migrating epithelial cells. Concomitantly, fibroblasts acquire a contractile phenotype and transform to myofibroblasts that will drive wound contraction (Gabbiani, 2003) (Figure 1. 27). There is also massive angiogenesis. The resulting healed tissue is somewhat granular and by further

deposition of collagen, it develops into a scar. Such interposition of fibrotic tissue prevents further regeneration, impairing a perfect healing (Gurtner et al., 2008). Scar tissue is different: it is more fibrotic and it lacks hair follicles and glands (Werner and Grose, 2003; Martin, 1997). Such result is opposed to embryonic wound healing that resolves perfectly, leaving no trace of injury, pointing out fundamental differences between embryonic and postnatal healing process.
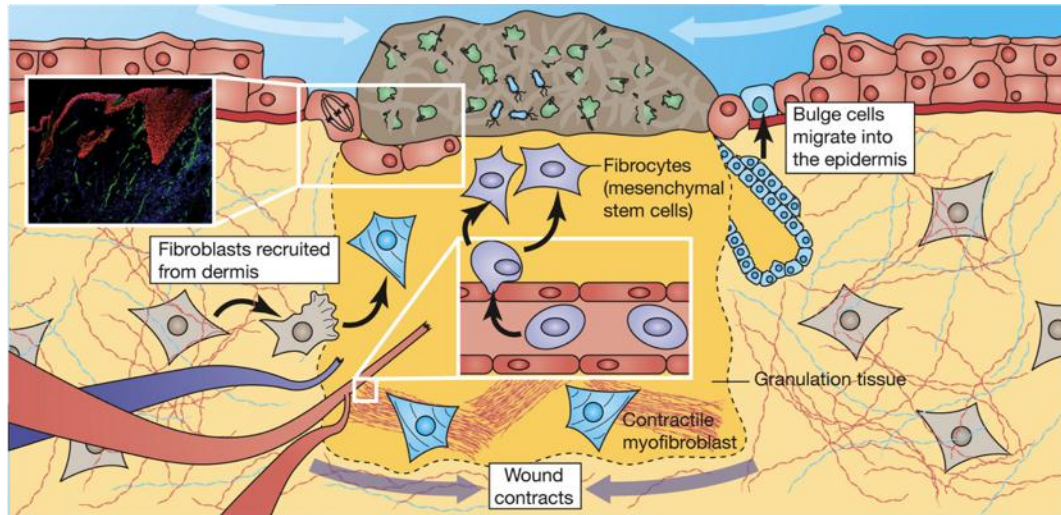

Figure 1. 27. Wound healing after a skin injury. The scheme depicts how the wound is closed by contraction of the wound bed by activated myofibroblasts together with migration of the outer layer of epithelial cells. From (Shaw and Martin, 2009).

In adult skin injuries, several hours after the injury event, the re-epithelization step starts and can last up to days. At this stage, activated keratinocytes migrate actively and collectively over the wound matrix, dragging forward their own basal lamina as they move forward (Grinnel et al., 1992) (Figure 1. 27). Simultaneously, leading front cells remodel their underlying ECM: they secrete proteolitic enzymes and matrix metalloproteinases and deposit new integrins (Hertle et al., 1992; Toriseva and Kähäri, 2009). Thus, there is a distinction between the initial rows-cells and the cells inner back in respect to the integrins they attach to the ECM through (Grose et al., 2002; Cowin et al., 2006). These leading front cells are often categorized as leader cells as well, since they typically extend broad lamellipodia and show precise cytoskeletal reorganizations (Omelchenko et al., 2003) (see section II. 3. 5).

Already many years back, tracking migrating keratynocytes in wound healing showed profound cell rearrangements during this process (Garlick and Taichman, 1994). Such tissue fluidity must be associated with junctional liability at the advancing front, with TGFβ being one possible candidate, as well as other growth factors present at the wound site, like FGF (Werner and Grose, 2003). These factors activate MAPK signalling pathways that sustain fluid migration (Nikolić et

82

al., 2006; Matsubayashi et al., 2004). Such cell jostling and interchanging is also related to the presence of motility stimulating-integrins, observed up to 10 rows deep from the leading edge (Hertle et al., 1992).

6.2. Embryonic wound healing

Wound healing in embryos, on the other hand, shows relevant distinctions. Embryonic wound healing has concentrated many research efforts thanks to the perfect resolution of the healing process, leaving no scar or trace behind, resulting in an unaltered epithelia (Martin, 1997). The neat healing is reminiscent of gap closing events during morphogenesis that also result in invisible sealing seams. Another difference is the presence of stratified epithelium in embryos, which is two-layered, while it is a single monolayer in adults. Typically, embryonic wound healing occurs through a purse-string mechanism, by rapid recruitment of actin and myosin and assembly into a thick cable at the edges of the marginal cells encompassing the wound (Martin and Lewis, 1992; Abreu-Blanco et al., 2011) (Figure 1. 28). Such purse-string mediated wound closure has been found to be regulated by RhoA (Brock et al., 1996). Hence, in this case cells do not actively crawl over the substrate, but are drawn together by the contraction of the actin cable, remaining totally adherent to the substrate and dragging the basal lamina forward along with them at their pace (McCluskey et al., 1993; McCluskey and Martin, 1995). Also, filopodia extended by the wound margin cells are typically observed, and occasionally contacting the substrate beneath (Figure 1. 28. A). However, there is no indication of active adhesion of these filopodia or any evidence that they contribute to the advancement of the leading wound border. Filopodia would only be necessary for the last stages, since Cdc42 blocking prevents the final knitting of the wound edges (as in the case of dorsal closure in *Drosophila*) (Wood et al., 2002). The initiation cues are still not known, but one hypothesis is that the mechanical signal resulting from the stretching of cells during the production of the wound could trigger intracellular regulators and thus initiate the closure, as it has been reported for Twist activation in *Drosophila* embryos upon mechanical stimulation (Farge, 2003). In embryonic wound healing, there is also contraction of the underlying connective tissue mediated by TGF1, but it does not require conversion of wound-site fibroblasts to myofibroblasts (McCluskey and Martin, 1995). Nevertheless, it is noteworthy that in the absence of acto-myosin cable assembly in Rho mutants, exuberant filopodia and lamellipodia can compensate and account for the closure, although in a delayed fashion (Wood et al., 2002).
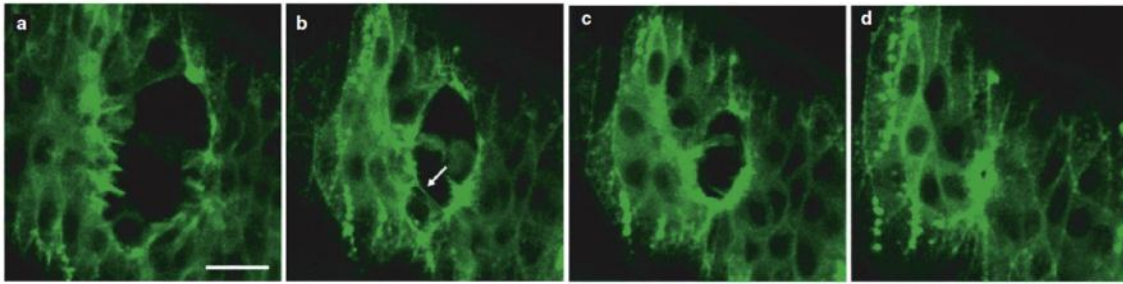
Figure 1. 28. Embryonic wound healing. Time-lapse progression of an embryo healing a laser-induced wound. Total time is around 60 min, scale bar is 10 μm. From (Wood et al., 2002).

Importantly, one of the main differences between embryonic and adult wound healing is the lack of (or minimal) inflammatory cascade activation. In early embryos there are no platelets, and differentiation of inflammatory and hematopoietic lineages occur during mid late embryogenesis (Rugh, 1990; Morris et al., 1991). Also, even at later stages when macrophages are already functional, they are not recruited at the wound site. Because macrophages and generally all inflammation-mediating cells are responsible for growth factors and cytokines production, the absence of such factors is tightly linked to the lack of scar. Many studies are suggestive of the fact that abolishing growth factors and cytokines in adult wound healing could benefit repair and render scar-free tissues. Early studies already hinted that depleting the neutrophile-mediated inflammatory response resulted in normal wound healing (under sterile conditions) (Simpson and Ross, 1972). Indeed, experiments with reduced TGFβ signalling proved successful in reducing the scarring at the wound site of adult tissues (Shah et al., 1992). Similarly, when platelets or neutrophils are abolished healing is unaffected (Szpaderska et al., 2003). Very interesting experiments in PU.1 null mouse, which lack several hematopoietic lineages and cannot thus raise inflammatory response, display an enhanced repair process. In these cases, healing is more rapid thanks to increased vascularity at the wound site, and results in a scar-free intact epithelium (Martin et al., 2003). Thus, at the crudest level, inflammation is not an essential pre-requisite for wound healing. However, it is of course required for the protection of the wounded area against microbial infection (Martin and Leibovich, 2005).

A particular case of wound healing is the extrusion of apoptotic cells from an epithelial barrier. In this case, the "wound" is the cell or cells that have been determined to enter the apoptotic death and will thus be eliminated.

7. Apoptotic cell extrusion

Apoptotic cell extrusion is the process by which cells that have entered the apoptotic cascade (and are thus determined to die) are expulsed from an epithelial monolayer. Such process occurs widely in development, where cells dispersed among germ layers are established to die and be replaced by new differentiated cells. Apoptotic extrusion also occurs recurrently in adulthood during tissue turnover and homeostatic processes. Intestine, for example, is a very dynamic tissue whose cells are completely renewed every 60 days in humans (Hunter et al., 2003*)*. Since epithelial barrier should not be compromised, cells preset for clearance undergo apoptotic extrusion (Eisenhoffer et al., 2012). As such, apopototic extrusion is an adequate mechanism to control tissue homeostasis in terms of numbers of cells, and it has been shown to kick in when cell overcrowding occurs (Eisenhoffer et al., 2012). Apoptotic or necrotic cells may also appear because of cytokines, pathogens, or other forms of stress (Villar and Zhao, 2010). Apoptosis can affect a single cell (such as during gut epithelia renewal) or up to large number of cells. In the process of extrusion, the epithelium presents no empty space *per se*, but there is a physical discontinuity in the viability and thus functionality of the epithelial barrier. In case the apoptotic events are not resolved, epithelium becomes leaky and phagocytic cells are activated to clear the dying cells, which would result in open gaps within the epithelia.

Traditionally, the clearance of apoptotic cells had been proposed to occur by phagocytosis (Hall et al., 1994; Hall, 1999). However, when apoptotic cells are phagocytosed, a decrease in the electric resistance of epithelial barrier is observed, which is an undesired effect because it alters the impermeability of the epithelial barrier (Peralta Soler et al., 1996). Intense efforts from Rosenblatt's lab points that the main driver of apoptotic clearance is extrusion of the apoptotic cell(s) upwards of the epithelia. Only when the dying cell has been removed from the epithelia can it be phagocyted, in a process that has been termed as apoptotic cell extrusion [(Rosenblatt et al., 2001), but also hinted before by (Madara, 1990; Abrams et al., 1993; Corfe et al., 2000)].
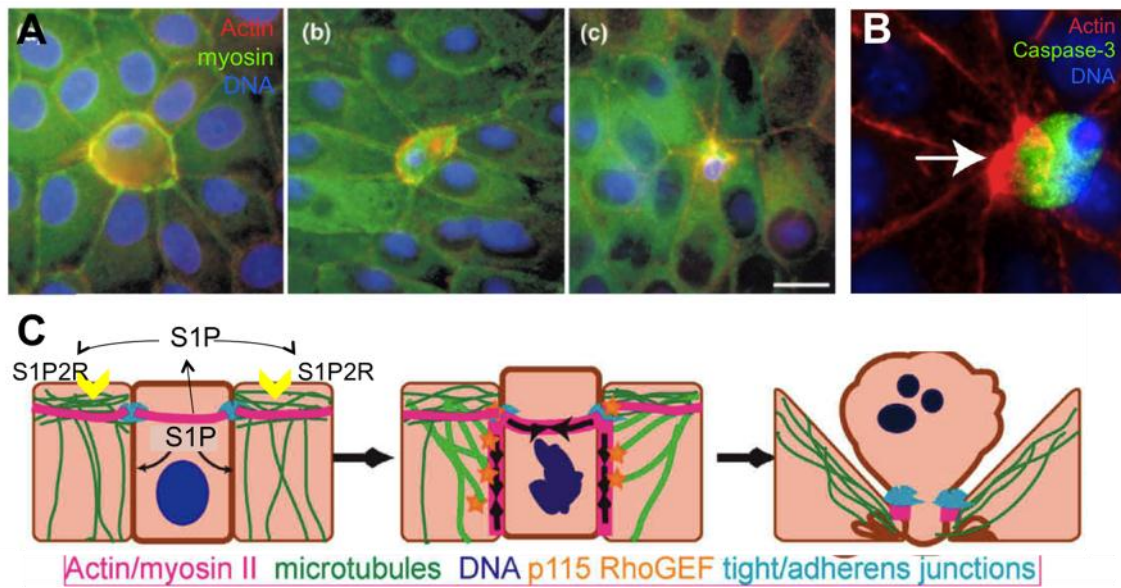
Figure 1. 29. Apototic cell extrusion. (A) Time-lapse showing an acto-myosin ring forming around the apoptotic cell, at the centre. From (Rosenblatt et al., 2001). (B) The extruded cell shows positive for caspase-3, an apoptotic marker. Note that DNA in the nucleus is disorganized. Actin is denser in the apoptotic cell. From (Rosenblatt et al., 2001). (C) Model proposed to explain how the apoptotic cell signals its neighbours to trigger the accumulation of acto-myosin in a contractile cable. Modified from (Andrade and Rosenblatt, 2011).

Typically, the extrusion of such cell(s) is triggered by apoptotic signals from the dying cell(s) to the neighbouring healthy cells (Rosenblatt et al., 2001). Induction of extrusion is found both in response to extrinsic apoptotic signals (activation of TRAIL – tumor necrosis factor-related apoptosis inducing ligand, for example) and intrinsic signals (excess of double-stranded DNA breaks) (Andrade and Rosenblatt, 2011). The two pathways converge in the activation of caspase routes, which somehow induce the expression and secretion of sphingosine-1-phosphate (S1P) (Gu et al., 2011) (Figure 1. 29. C). S1P can then bind to S1PR2 receptor present in the neighbouring cells and activate p115RhoGEF (Slattum et al., 2009), which mediates the assembly of a basolateral actomyosin ring (Figure 1. 29. C). The contraction of the ring squeezes the apoptotic cell out of the epithelium (Figure 1. 29. A). Although some actin accumulation has also been observed in the dying cell itself, the process mostly relies on the actomyosin cable assembled by the neighbouring cells (Mills et al., 1998; Rosenblatt et al., 2001) (Figure 1. 29. B). At the same time, caspases also control the remodelling of tight and adherens junctions (Gregorc et al., 2007), in order to promote the extrusion of the apopotic cells itself but also to ensure the integrity of the epithelium once the dying cell has been removed (as extrusion ensures correct levels of transepithelial resistance) (Suzanne and Steller, 2009). Such extrusion process typically results in a rosette-like distribution of the remanent epithelial cells, seen recurrently at end of gap

closing events (Wood et al., 2002; Rosenblatt et al., 2001) (Figure 1. 29. A, Figure 2. 18. C, Figure 3. 6).

Noteworthy, the extrusion machinery (i. e. the contractile acto-myosin ring) is activated by rather downstream effectors of the apoptotic pathway. This is important because many apoptotic and even necrotic inputs can be integrated along the caspase pathway to produce an effect in a no-return step of the pathway, ensuring a robust but free of false-positives response. Nevertheless, because inhibiting caspase pathway can also lead to partial formation of acto-myosin ring, the ring could also form in response to other factors.

However, a mechanical signal from the interface dying cell/healthy neighbouring cells cannot still be ruled out (Kolega, 1986). Such mechanical signal relies on the tension that is accumulated on every cell membrane, due to the action/reaction forces of each cell on its neighbours (Kasza and Zallen, 2011). When one or more cells undergo apoptosis, their membrane tension decreases, and that could signal their neighbours to assemble an acto-myosin ring.

Process	Mechanism	Time frame	Comments	References
Drosophila dorsal closure	Amnioserosa cell contraction Actin cable ratchet Filopodia	3-4 hours	JNK regulated	Kiehart et al. 2000
C elegans ventral enclosure	Elongation and migration of epithelial cells Actin cable sealing	90 min		Williams-Masson et al. 1997
Tubulogenesis	Epithelial sheets bending and migration	Hours-days		Davidson et al. 1997
Adult wound healing	Cell crawling	Days	Inflammation Scar	Werner et al. 2003
Embryonic wound healing	Purse-string	Hours	Perfect healing	Redd et al. 2004
Apoptotic extrusion	Acto-myosin cable	Min (up to 2h)	Perfect healing Caspase dependent	Andrade et al. 2011

Table 1. 1. Summary of the different situations involving epithelial gap closure events. References only show one relevant citation for each example. For more details, see main text.

8. Purse-string versus lamellipodial crawling: evidence and controversies

As it has been exposed, the presence of openings is a recurrent situation during development and throughout adult life, which can arise as a result of fusion of embryonic epidermic sheets or during processes of cell monolayer disruption, as during wound healing or in expulsion of altered cells from an epithelium (Table 1. 1). Naturally occurring gaps closure has been studied in a large diversity of *in vivo* animal models, for example in the well-studied case of *Drosophila* dorsal closure, or ventral enclosure in *C elegans*. Animal models, like chicken, frog or fly embryos, have also been used to study embryonic wound healing or the response to excised epidermic patches. With the goal of having a more controlled environment where genetics can be applied, numerous studies of epithelial gap closure in 2D *in vitro* cell cultures have also been carried out in diverse cell lines.

All these numerous studies have been pursued in the sake of clarifying the response of epithelial cells to the presence of an opening (Table 1. 1). It is worth noticing that the currently available literature has repeatedly disregarded cell proliferation as a candidate mechanism to drive the closure, at least for gaps that are sealed in few hours. Many studies addressed the question of cell division rates during closure, and found that proliferation is not significant for a long period after initiation of closure (Poujade et al., 2007; Matsubayashi et al., 2004; Grasso et al., 2007). Only at later stages of closure, many hours after initiation (then of course only applicable to very large openings), cell division is relevant, and it acts in helping in the restitution of average cell density within the tissue. Thus, cell proliferation can be ruled out as the driver of the closure.

Instead, two mechanisms are predominantly found to account for closure processes: purse-string and cell crawling (Table 1. 2, Table 1. 3, and Table 1. 4). We will hereafter expose the evidences and confront the mechanisms.

8. 1. Purse-string closure

The mechanism of purse-string is based on the accumulation of actin and myosin in the form of a cable surrounding the wound or gap margin. Purse-string was first identified by Paul Martin as a supracellular structure at the wound margin composed of filamentous actin and motor protein myosin II (Martin and Lewis, 1992). Also, Bement et al. ascertained the accumulation of actin and myosin at wound margins (enrichment of 10 and 3-fold respectively compared to cell borders not belonging to the wound edge), together with villin and tropomyosin (Bement et al., 1993). The purse-string structure is believed to maintain the apico-basal polarity of the contained cells, as shown by strong accumulation of cadherin,

tight junction proteins, and vinculin at sites of cell-cell adhesion (Bement et al., 1993; Grasso et al., 2007; Petroll et al., 2001). Actin and myosin are linked between neighbouring cells through cell-cell adhesions, presumably through adherens junctions (Danjo and Gipson, 1998; Brock et al., 1996; Campos et al., 2010) or tight junctions (Florian et al., 2002; Tamada et al., 2007). There is evidence suggesting that acto-myosin accumulation in cables can build-up and maintain tension, which could be transferred to all wound/gap bordering cells implicated in the supracellular cable. In this manner, the contraction of the acto-myosin cable can progressively bring the marginal cells close up to the final sealing (Tamada et al., 2007) (Figure 1. 30). Regarding the regulation, some studies propose opposing roles of RhoGTPases in controlling the closure. Russo et al. suggested that ROCK was indispensable for the assembly of the cable, but the contraction was dependent on MLCK (Russo et al., 2005). Tamada et al. showed that myosin could accumulate when ROCK was inhibited, but the cable could not contract (Tamada et al., 2007) (Figure 1. 30). Alongside, Desai et al. pointed out a more complicated regulation of the process, where all players must be present for the cable contraction to be effective. In their study it was shown that RhoA is necessary at the right concentration, and that also Rac1 was implicated in the process (Desai et al., 2004). Thus, although the most plausible conclusion is the implication of RhoA in the purse-string functioning (Brock et al., 1996), there is no agreement on the exact regulation.
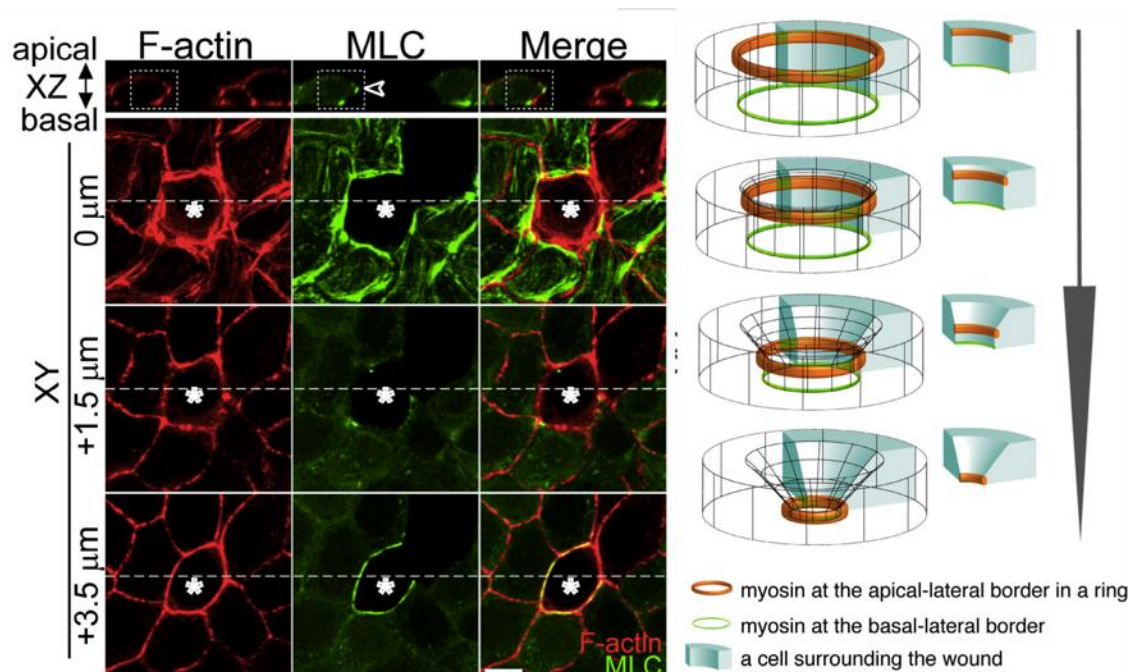

Figure 1. 30. Multicellular purse-string during wound closure in an *in vitro* epithelial culture. Note how actin and myosin accumulate at the margin of the wounded cell (with white star) forming a supracellular cable. The cable contracts from the apical part to the basal side to seal the opening, as shown in the model (right side). From (Tamada et al., 2007).

Purse-string closure is recurrently described in single cell wound repair (Bement et al., 2007) (Figure 1. 31). Single cell wounding is a critical event that must be quickly addressed to avoid leakage of intracellular components and posterior cell death. During single-cell healing, two processes occur concomitantly: 1) plasma membrane restitution by fusion of intracellular vesicles and membrane patches, which occurs in a Ca^{2+}-dependent manner (McNeil and Steinhardt, 2003). This process is exclusive of single cell repair. 2) Cytoskeletal remodelling, which is required for guiding vesicles and membrane patches to the site of wounding, but also for restoration of the actin cortex. In single cell wound repair, the temporal evolution of cytoskeletal restructuration has been precisely defined: actin and myosin accumulate at the injury site within the first min post-injury, and then progressively segregate to form two circumferential spatially segregated rings (Bement et al., 1999; Mandato and Bement, 2001). Myosin II is localized interiorly, right bordering the wound, and actin accumulates externally to the first ring (Figure 1. 31. B). Such precise distribution has been found to be regulated by concomitant circumferentially-sorted rings of activated RhoA and Cdc42 (Benink and Bement, 2005). Recently, Abr has been proposed as the candidate protein that spatially sorts RhoA and Cdc42 activation: Abr localizes at the site of RhoA activation and locally inhibits Cdc42 through its GAP activity (Vaughan et al., 2011) (Figure 1. 31. C). During the healing process, acto-myosin rings contract while pulling the membrane inwards. The acto-myosin rings are associated to the membrane through E-cadherin (Abreu-Blanco et al., 2011). In this situation, microtubules play an important role in organizing the acto-myosin rings (Mandato and Bement, 2003; Togo, 2006; Abreu-Blanco et al., 2011) and in guiding vesicles to be fused with the membrane. Single-cell wound healing by purse-string mechanism appears to be a conserved mechanism, it has been found in embryos (Bement et al., 1999; Mandato and Bement, 2001, 2003) as well as in adult cells of mammalian and non-mammalian origin (Miyake et al., 2001; Togo, 2006; Togo and Steinhardt, 2004; Godin et al., 2011). Single cell wound rehabilitation occurs typically within minutes.

A similar purse-string closure mechanism occurs in the healing of a cellular defect in a multicellular context. In this situation, acto-myosin accumulates at the wound margins, but interestingly neighbouring junctional acto-myosin also participates in the healing process (Clark et al., 2009). The resulting purse-string is a hybrid of local acto-myosin and junctional acto-myosin. Surprisingly, a recent paper in healing small wounds in adult nematodes showed also strong actin accumulation at the wound edge, but claimed a negative regulation of myosin in the process, which would be actually due to Ca^{2+}-dependent actin polymerization (Xu and Chisholm, 2011).
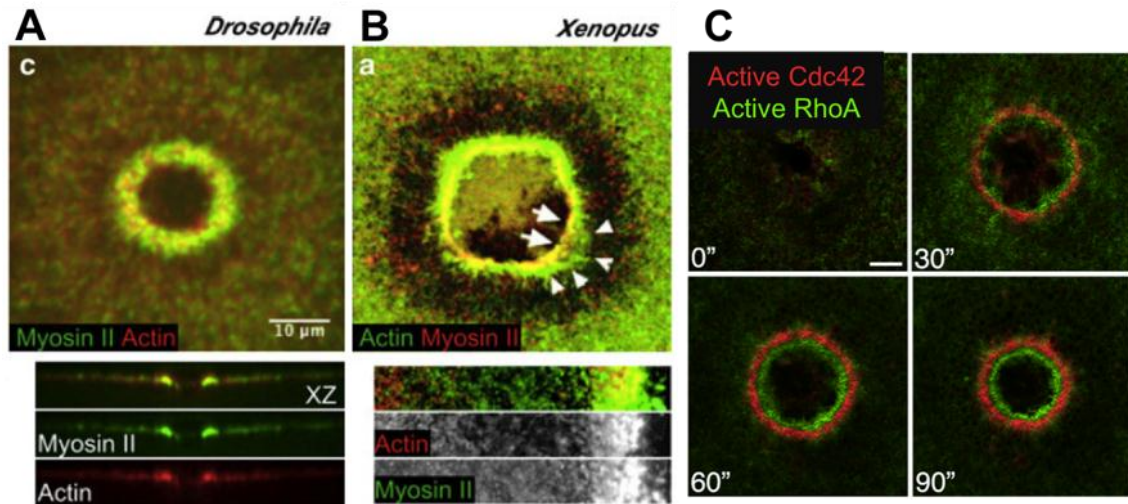
Figure 1. 31. Single-cell wound healing in response to a laser-induced wound. (A) Single-cell wound healing in a *Drosophila* embryo. Note how myosin and actin accumulate in a ring around the wound site. From (Abreu-Blanco et al., 2012). (B) In *Xenopus* embryo, the differential activity of myosin (innermost) and actin (outer) is more evident. From (Abreu-Blanco et al., 2012). (C) In *Xenopus* embryo, concentric areas of RhoA and Cdc42 activation have been reported. From (Benink and Bement, 2005).

In the case of gaps closure events involving multiple cells, a purse-string has been reported to form in all the cells directly in contact with the gap or wound, being connected through cell-cell adhesions. In this situation, purse-string has been mainly found in the closure of small defects, typically of one or few cell sizes (Tamada et al., 2007; Rosenblatt et al., 2001) (Figure 1. 30).

mechanism of closure	cell line	method for gap production	size of gap	time/speed of closure	comments	reference
purse-string	Epithelial-like cells in chick embryo	needle	0.5 mm diameter, ~circular	10-15 µm/h		Martin et al. 1992
purse-string	Chick embryo	needle	500 µm long, 70 µm wide	6h	Rho dependent Rac independent	Brock et al. 1996
purse-string	*Xenopus* oocyte	laser ablation	?	?	regulation by concentric exclusive rings of Cdc42/Rhoa	Benink et al. 2005
purse-string	*Xenopus* oocyte	laser ablation	?	?	integration of single and multicellular wound responses by fusion of actomyosin cables, adherens junctions role	Clark et al. 2009
purse-string	early *Drosophila* embryo	laser ablation	hundreds µm^2	4 µm^2/s	E-cadherin anchors actomyosin at membrane	Abreu-blanco et al. 2011
purse-string	MDCK cells	laser ablation	1-3 cells size	30 min-1h	MLCK ROCK dependent, actin cable anchored at tight junctions	Tamada et al. 2007
purse-string	Caco2	needle	few cells size, tens of µm in diam	30-45 min	MLCK and ROCK dependent	Russo et al. 2006

Table 1. 2. Summary of different works in epithelial gap or wound closure proposing purse-string as the closure mechanism. Red fading indicates that the method of gap production is associated to cell damage.

8. 2. Lamellipodial crawling

The mechanism of lamellipodial crawling is based on the extension of lamellipodia into the wound or gap space by the cells bordering the wound or gap. In this situation, cells, especially the ones at the free border, loose their apico-basal polarity, but instead acquire a strong front-rear polarity, more related to actual migration. This mechanism is reminiscent of the classical described collective migration. Indeed, many mechanistic insights related to collective cell migration come from scratch-wound assay studies (Figure 1. 32. A). Scratch-wound assay is based on the mechanical removal of a strip of cells by manually scraping a monolayer with a pipette tip or a razor blade. Such assay typically results in the creation of an opening that cells must then reoccupy. In this case, it has been recurrently observed that the closure occurs by lamellipodial crawling, independently of the width of the stripe created (Figure 1. 32. C). During the closure, cells at the wound or gap margin polarize due to the presence of a differential edge, which is the interface cell-wound/gap. These first-row cells extend lamellipodia and crawl into the opening, in a Rac1-dependent manner (Fenteany et al., 2000). Noteworthy, not only the cells contacting the gap or wound protrude, but also cells positioned many rows behind the leading edge also extend cryptic lamellipodia (Farooqui and Fenteany, 2005). Thus the closure must not necessarily be lead by the first-row cells, as shown by the mechanical characterization of a migrating monolayer (du Roure et al., 2005; Trepat et al., 2009; Vedula et al., 2012). Interestingly it has been shown that when only the first row of cells are subjected to Rac1 depletion, closure proceeds normally; cells behind the leading edge, with normal levels of Rac1 activity, can jostle through the first row of cells and become leader cells. Instead, closure is abrogated when Rac1 is inhibited in 3 rows of cells from the gap edge. (Figure 1. 32. B). This evidences the implication of outer-more cells in the closure. Indeed, advanced image analysis of cells response to a rather large opening showed that cells well back to the inner epithelial monolayer also mobilise. The extent of cell mobilization depends on the initial size of the gap up to a point where no more cells can entangle to move and the opening remains unclosed (Matsubayashi et al., 2011). Along this line, computational simulations relying solely on the migratory capacity of cells have shown that the cell crawling behaviour (either as individual migrating entities or collective migrating cells connected through cell-cell adhesions) is sufficient to account for gap closure in *in silico* models (Vitorino and Meyer, 2008; Lee and Wolgemuth, 2011). These models claim that purse-string would have a minor role (if any) in the closure.
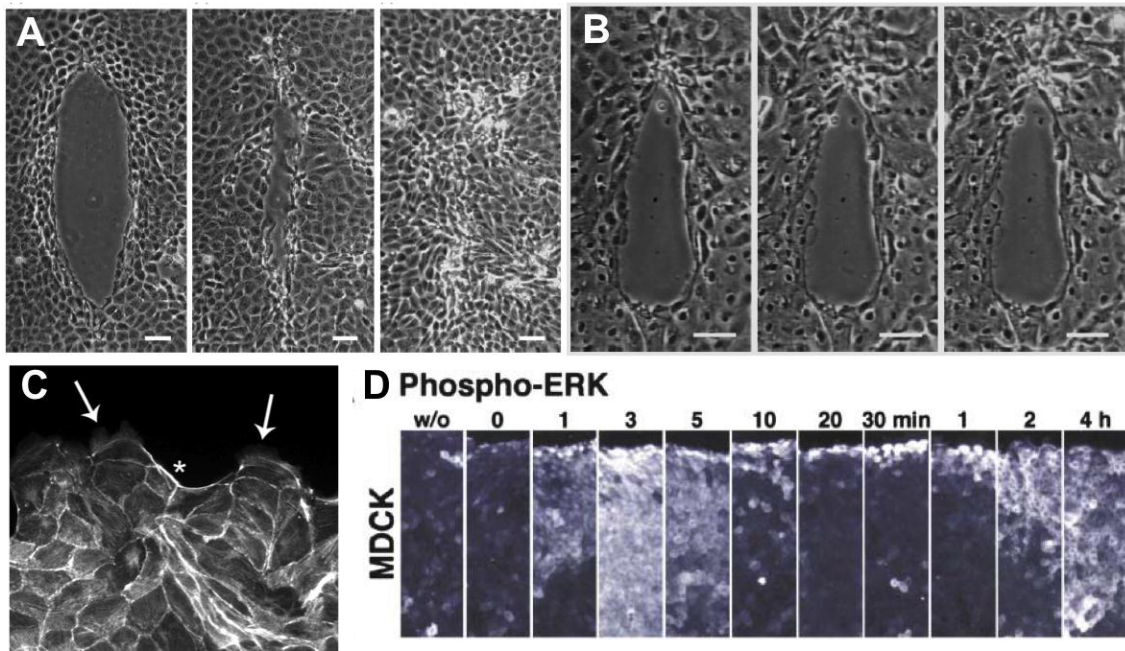
Figure 1. 32. Cell crawling response to a gap. (A) MDCK cells migrate in response to a scratch by extending lamellipodia. From (Fenteany et al., 2000). (B) When Rac1 is inhibited in the first rows, gap is not closed. From (Fenteany et al., 2000). (C) Extension of lamellipodia during closure of a scratch, as shown by actin staining. From (Altan and Fenteany, 2004). (D) 2 waves of ERK activation during gap closure of a scratched epithelia. From (Matsubayashi et al., 2004).

Regarding the initiation cues, it is still controversial what triggers the activation of the protrusive machinery. In studies where cell death occurs during the closure process (i.e. studies of wound healing, typically scratch-wound assays or modifications of such assay), damage-induced factors have been proposed to be instrumental in initiating the response. At the onset of wound closure, a complex and poorly characterized mix of cell debris, reactive oxygen species (ROS) and various other factors are released from the wounded cells (McNeil et al., 1989).

The presence of cell damage can induce the closure mechanisms from two proposed ways: 1) among the numerous death factors released there is extensive ATP liberation. ATP can directly induce transactivation of EGFR, which in turn trigger PI3K and ERK cascades, ultimately leading to activation of wound closure machinery (Yin et al., 2007). However, EGFR has been proven to activate also in absence of cell damage (Block et al., 2004). On the other hand, ATP can also a Ca^{2+} wave that advances from the damaged leading edge inwards (Sammak et al., 1997; Klepeis et al., 2001, 2004; Matsubayashi et al., 2004). Ca^{2+} waves can then trigger other signalling cascades, as the activation of classical MAPK/ERK (LaBonne et al., 1995; Matsubayashi et al., 2004). MAPK/ERK signalling pathway will ultimately result in the activation of the protrusion-based migration machinery (Figure 1. 32. D). 2) Damage-induced cellular stress and ROS can activate JNK, which shows a peak of activation within min after wounding (Altan and Fenteany, 2004). JNK has

been recurrently related to collective cell migration, although in a cell type-specific manner (Xia and Karin, 2004). JNK can stimulate membrane protrusive activity through Spir protein, which in turn can modulate RhoGTPase function but can also directly interact with WASP, a regulator of Arp2/3-mediated actin polymerization at lamellipodia (Otto et al., 2000). Activation of JNK also occurs in *Drosophila* dorsal closure during the migration of the lateral epidermic sheets, in a situation where cell damage is not prevalent (Rämet et al., 2002; Galko and Krasnow, 2004; Homsy et al., 2006; Ricos et al., 1999; Riesgo-Escovar, 1997) (see section II. 5. 1). Similarly, JNK is required for proper eyelid closure, a similar process of epithelial sheets sealing (Zenz et al., 2003). However, in these morphogenetic processes the role of JNK is tightly related to phosphorylation of c-Jun, which has been found to be irrelevant for wounded epithelia migration (Altan and Fenteany, 2004). Altogether, strong evidence suggest that MAPK family (which includes classical MAPK/ERK and JNK) may have a prominent role in driving the sealing of epithelial sheets, although the exact mechanism remains to be elucidated (Altan and Fenteany, 2004; Matsubayashi et al., 2004; Nikolic et al., 2006; Mine et al., 2005; Xia and Kao, 2004).

On the other hand, many studies have showed that gap closure can be triggered by the mere presence of free space, without death factors signalling (Poujade et al., 2007; Nikolic et al., 2006; Block et al., 2004). By using surface masking strategies, these studies show how, upon releasing a spatial constraint or blocking agent, cells readily start to migrate and close the available area by the cell crawling mechanism.

8.3. Controversies

As it has just been exposed, there is vast literature addressing the question of epithelial gap closure in numerous different *in vivo* and *in vitro* situations. While it is reasonable to study epithelial closure in all the possible scenarios where it can take place, the intrinsic variability associated to different experimental conditions complicates extracting a global conclusion on the mechanism of closure. Thus, given the diversity in experiments and conclusions, we will hereafter confront the different works and try to outline what possible parameters can determine the mechanism of closure. For comparison purposes, we will focus on the experiments reported in Table 1. 2, Table 1. 3, and Table 1. 4, and mention evidences from epithelial gap closure of developmental processes, mainly from *Drosophila* dorsal closure.

mechanism of closure	cell line	method for gap production	size of gap	time/speed of closure	comments	reference
cell crawling	MDCK	PDMS membranes masking surface	~400 μm wide, cm long	~30h		Poujade et al. 2007
cell crawling	MDCK	needle scratching	100-200 μm wide, 500 to 1000 μm long	~18h	Rac dependent	Fenteany et al. 2000
cell crawling	MDCK	scratching	250 μm wide	6h	Src and ERK activation (2 waves)	Matsubayashi et al. 2004
cell crawling	MDCK	PDMS slab =clean gap	infinite	10 μm/h	1 MAPK wave	Nikolic et al. 2006
		ripping =damaged borders		30 μm/h leader cells, <10μm/h followers	2 MAPK waves	
cell crawling	primary culture of corneal cells	scratching	~1 mm wide	~15h	activation of EGFR activation of JNK	Block et al. 2004
		agarose slab	~1 mm wide	~15h	activation of EGFR no activation of JNK	
cell crawling	corneal epithelium (in vivo)	scratching	2-2.5 mm	~18h	notable cell jostling	Danjo & Gipson 2002
cell crawling +actin accumulation	airway epithelial cells 16HBE	pipette tip scratching	700 μm wide	15-20h	Rho and Rac dependent at appropiate concentrations	Desai et al. 2004
cell migration	human esophaegal epithelial cells Het1A	cell squeezing with PDMS stamps	squares of 250 μm side	15h		Lee et al. 2011

Table 1. 3. Summary of works proposing cell crawling as the closure mechanism. Green fading indicates processes in absence of cell damage, red fading processes with cell damage associated.

Embryonic versus adult gap closure

First, we acknowledge that indeed the mechanism of closure must be highly affected by the *in vivo* situation where it takes place. Most evidence indicates that embryonic wound healing, for instance, occurs through the purse-string mechanism, while in adult wound healing there would be cell crawling (Table 1. 1). Note, nevertheless, that embryonic wound healing in *Drosophila* displays also protrusive activity from wound-margin cells at the same time as purse-string. Moreover, epithelial closure of naturally occurring gaps during development also display protrusions and actin accumulation, and note that actin cable would not be the driver of the closure but act like a ratchet (as we mentioned in section II. 5. 2).

In vivo versus in vitro gap closure

Along this line, another reasonable parameter to take into account is the experimental conditions of the study, i.e. if it has been carried out *in vivo* or *in vitro*.

Numerous works have shown that wounded embryos (i.e. *in vivo* epithelial closure) heal by a purse-string mechanism. On the other hand, most of the works carried out *in vitro* point towards cell crawling as the mechanism of closure. *A priori*, one could conclude that *in vivo* purse-string dominates, while *in vitro* gaps show more of active migration. Note, however, that most of the *in vivo* experiments are done in embryos, and not in adults, fact that could bias the conclusion that *in vivo* the closure occurs surely by the purse-string mechanism. Interestingly, one study reported that after a first lapse of purse-string formation, cell crawling was the closure mechanism of an excised area in *Xenopus* embryo (Davidson et al., 2002). And in turn, one of the few studies reporting wound healing *in vivo* (from adult mice corneas) pointed cell crawling as the mechanism of closure (Danjo and Gipson, 2002). Thus, why in these studies cell crawling was associated to *in vivo* gap closure? The difference in these *in vivo* experiments with respect to the classical purse-string-mediated embryonic closure was the size of the gap.

mechanism of closure	cell line	method for gap production	size of gap	time/speed of closure	comments	reference
1st purse-string, 2nd cell crawling	T84 colon carcinoma cells	aspiration	0,018 mm2, 400 cells size	120-150 min	hihly dependent on integrin activation	Lotz et al. 2000
1st purse-string, 2nd cell crawling	Epithelial-like cells in *Xenopus* embryo	microsurgery	~200 µm^2, squared	60-90 min	Small wounds close at faster rate than large wounds	Davidson et al. 2002
purse-string +lamellipodia	mouse cornea	needle	4 mm^2	24 h	actin cable anchored at adherens junctions	Danjo et al. 1998
purse-string +lamellipodia +filopodia	Ventral epithelial cells of *Drosophila* embryo	Laser ablation or needle	10 cell diam, ~800 µm^2, ~15 µm diam, ~circular	120 min, 7 µm^2/min	-/- RhoA x2 slower but closes / Rac independent / Cdc42 no final zipping / adherens junctions	Wood et al. 2002
purse-string +cell crawling	Caco-2	gauge	1-8 cell diameter (<100 µm)	2-6 h	Size dependent: / <8 cell diam= purse-string, / >8 cell diam= crawling	Bement et al. 1993
cell crawling OR purse-string	Bovine corneal endothelial cells	Razor blade for ECM removal / Silicone tip for ECM maintenance	Large 2 mm / Med 150 µm / Small <10 cell d	W/ ECM: 15 µm/h / W/o ECM: 6.25um/h	With ECM, cell crawling / Without ECM, purse-string / Irrespective of size	Grasso et al. 2007
sincitium formation +lamellipodia	*Drosophila* larvae	needle	6 cells size	24 h	JNK dependent	Galko et al. 2004
actin polymerization	adult *C. elegans*	laser ablation or microneedle	20 and 40 µm diamater	~2 h	negatively regulated by myosin	Xu et al. 2011

Table 1. 4. Summary of works proposing cell crawling and purse-string to explain closure. Green fading indicates processes in absence of cell damage, red fading processes with cell damage associated.

Gap size

The experiment of the excised area in *Xenopus* provided insightful evidences. Davidson et al. showed how, upon removing a rather large cell area, bordering cells developed a supracellular actin cable that proved to be not contractile. After 10 min, bordering cells developed protrusion that together with underlying cells drove the closure of the gap. Similarly, other studies showed a sequential activation of first purse-string and then cell crawling response in large gap closure (see Table 1. 4).

Indeed, most of the studies studying the closure of large gaps report a cell migration-mediated response (Table 1. 3). On the other hand, small wounds are typically closed by purse-string (Table 1. 2). However, in some small gaps there is also presence of lamellipodial protrusions (Bement et al., 1993; Grasso et al., 2007). This latter work proposed the presence of ECM in the gap as a determinant for cell crawling mechanism induction, while in the absence of ECM a purse-string would form, independently of the gap size.

Noteworthy, purse-string has also been associated to closure of large wounds (Table 1. 2). In what conditions purse-string would close large gaps? Purse-string closes large gaps when they happen in embryos. Thus, again embryonic tissue appears as a strong inducer of a purse-string mediated closure.

While it is tempting to associate small gaps with a purse-string and large gaps with cell crawling response, there are exceptions to the rule, and no systematic analysis of the mechanism of closure as a function of gap size has been reported.

Presence of death factors

Importantly, all the reported cases of purse-string mediated gap closure are associated to wound healing events, i.e. processes where the gap to be closed results from needle puncture, laser ablation, or other aggressive methods (Table 1. 2). Similarly, the extrusion of apoptotic cells, a process clearly related to death factor signalling, also occurs through a purse-string. Interestingly, in situations where gap closure occurs in the absence of cell damage, cell crawling is proposed as the closure mechanism (Poujade et al., 2007; Nikolic et al., 2006; Block et al., 2004). However, in these studies the gaps generated are large in size, and thus one could argue that the cell-crawling response is determined by the size of the gap rather than by the absence of death factors. Thus, the logical question to ask is:

would small gaps close by purse-string or by lamellipodial crawling in the absence of cell damage?

Geometry of the gap

Another key parameter that emerges when comparing the experimental conditions of the reported studies is the shape of the gap. Intuitively, it is reasonable to associate a tension-bearing purse-string located at circular gap margins. Due to the contractile nature of the acto-myosin cable, when developed at the gap margins it would always tend to drive the closure in a circular-like fashion. Indeed, purse-string is typically assigned to gaps produced by laser ablation and needle puncture, which recurrently result in circle-like gaps and close while maintaining a strong circularity (Table 1. 2). On the other hand, scratch-resulting gaps are typically removed stripes of cells, thus large aspect ratio rectangular-like areas. Actually, they can be considered as straight migrating edges of a given width. These gaps are recurrently closed by cell crawling (Table 1. 3). Thus, it seems that gap shape can also have an influence on determining the closure mechanism. However, since the rectangular-like gaps are typically large in size, and given the dependence of the closure mechanism on the size of the gap, these assumptions beg the question: would small non-circular gaps be closed by purse-string or by cell crawling?

Can both mechanisms coexist?

Despite in the last section we have been just confronting the two mechanisms as being present or absent in a specific gap closure situation, both mechanisms need not to be mutually exclusive. Indeed some studies report the presence of cellular protrusion and actin accumulation [(Wood et al., 2002; Bement et al., 1993), Table 1. 4]. Similarly, in gap closure processes during development, actin cable and protrusions coexist, and are both required for efficient closure. Interestingly, protrusions have been shown to compensate the induced-absence of purse-string, while purse-string alone is not sufficient for the sealing when protrusions are abrogated.

Thus, it is not yet clear to what extent both mechanisms coexist and what is the relative contribution of each mechanism to the closure of wounds or gaps. The complex relationship between acto-myosin cable formation and cellular protrusions remains unclear, and the activation of one or the other mechanism could be context-dependent.

How to solve the controversies?: A systematic study of epithelial gap closure and insights from the mechanics of the process.

All the raised questions appear as key parameters for the better understanding of epithelial gap closure, and must thus be tackled. In the present work, we will address such questions as an approach to shed light on the intricate process of gap closure. For this purpose, we have undertaken two approaches:

1) To perform a systematic study under controlled experimental conditions, where different candidate parameters in determining the mechanism of closure can be analysed. In our approach, we will study the effect of gap size, shape, and death factors in the closure of well-defined gaps. In this context, we will also address also address the concomitant actin accumulation and lamellipodial protrusion. This work is presented in Chapter 2.

2) To analyse the mechanics of the closure, which can help us dissect the contribution of each mechanism to the closure and provide valuable information that has remained (to our knowledge) unaddressed until now. This work is presented in Chapter 3.

CHAPTER 2:

Size and shape dependence of undamaged epithelial gap closure

1. Background

Epithelial tissues comprise sheets of adherent cells that cover the outside of the organism to protect it from the external environment, line the internal organs of the body, and carpet the cavities and tubes that transport gases and liquids throughout the body. For all these reasons, it is of pivotal importance to maintain the integrity of the epithelial layers. Whenever a discontinuity appears in the epithelia (either naturally or injury-induced), it must be correctly addressed to ensure the proper functionality of the epithelial barrier. Because of its relevance, the maintenance of epithelial integrity has been the focus of intensive research. Moreover, many developmental events include also a step of sealing of an opening by epithelial sheets, as described in Chapter 1 section II. 5.

We refer to epithelial gap closure as the process by which epithelial cells close an opening. Such process may include: closure of gaps resulting from injury events, such as in the re-epithelialization step during wound healing response; closure of naturally occurring openings during morphogenetic processes, such as *Drosophila* dorsal closure; closure of the discontinuity resulting from the extrusion of apoptotic cells, such as during homeostatic tissue renewal in the gut epithelia; closure of gaps in the lung epithelia, resulting from insults in pulmonary tissue, etc. These situations occur in very distinct environmental, genetic, and developmental scenarios, but addressing the question in well-defined conditions will provide valuable information that can be then extrapolated to the different in vivo cases, always bearing in mind the differences.

There are some *in vivo* models to study the phenomenon of epithelial gap closure, being *Drosophila* dorsal closure the most paradigmatic example. While very informative and close-to-nature, *in vivo* experiments are usually technically challenging, and limited information can be extracted. Despite extensive studies carried out in *Drosophila* dorsal closure and meaningful information on the mechanism of closure has been extracted, it has yet to be explored to what extent these evidences can be generalized across organisms. On the other hand, *in vitro* 2D sheet migration has emerged as a very appropriate model to study collective migration and epithelial fusion events in a more controlled and systematic manner with regards to the in vivo situation. Studies on *in vitro* models have provided key clues on the mechanism and mechanics of migration, proposing models that can be further tested in *in silico* and *in vivo* models.

1.1. Techniques to study epithelial gap closure: the scratch assay

Traditionally, gap closure has been addressed using the classical scratch wound assay, where a strip of cells is removed from a monolayer of cells by mechanical means (scratching with a pipette tip or a razor blade) (Figure 2. 1. A) (Todaro et al., 1965; Yarrow et al., 2004). Such simple technique has produced huge amount of data on collective migration through high-throughput screenings, and some very relevant discoveries on the nature of migration (Simpson et al., 2008; Soderholm and Heald, 2005; Vitorino and Meyer, 2008). However, it also presents many drawbacks: 1) when manually scratching the monolayer, the size and shape of the resultant gap is difficult to control, and thus the technique is hardly reproducible; 2) it either disrupts the ECM of the scratched area or leaves cells fragments behind at the removed-cells stripe, depending on the pressure of scratching; 3) the scratching process releases a complex and not fully understood mixture of death factors and small compounds that can mask the gap closure response; 4) the resulting gaps are typically large in size. More precise techniques to produce gaps or wounds of better-defined size are laser ablation, micromanipulated needle puncture, and electrical wound assays (Tamada et al., 2007; Keese et al., 2004; Gorshkova et al., 2008). However, these approaches require specific instrumentation and produce wounds with associated debris, resulting in injured or destroyed cells at the wound border, which can potentially result in confounding measurements.
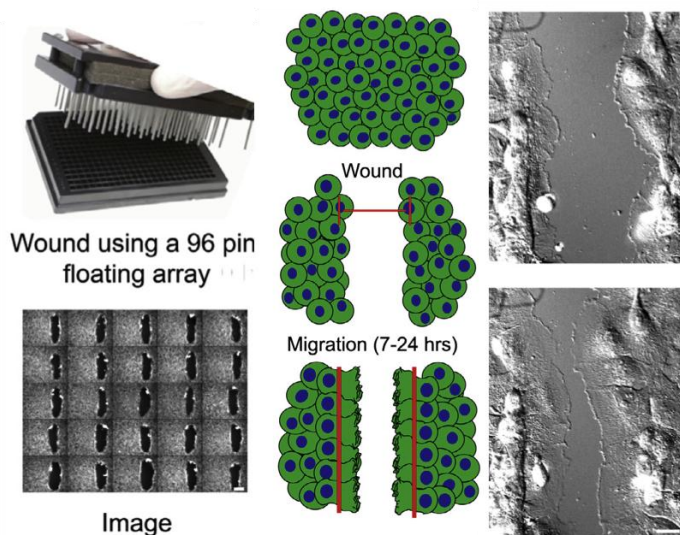

Figure 2. 1. Classical scratch wound assay. Typically, a wound is created in a monolayer by removing a strip of cells. The wound can be created by scratching with a pipette tip (as shown), a razor blade, a needle, etc. From (Yarrow et al., 2004).

1.2. Surface masking techniques

In the sake of more standardizable techniques, more recent studies have taken advantage of surface masking techniques to precisely control the space available

for cells to migrate. Surface masking approaches rely on the use of physical constraints and barriers that create cell exclusion zones. These barriers can be made of PDMS, agarose, or any other elastomeric material, which can be easily patterned to create the appropriate blocking object.

Poujade et al. used microfabricated PDMS membranes with a rectangular opening. Epithelial cells were allowed to grow in these openings and form a monolayer. Then, the PDMS membrane was released, allowing free space for cells to migrate (Figure 2.2.A). This proved to be a very appropriate method to study the migration of epithelial cells in well-defined starting conditions (Poujade et al., 2007; Serra-Picamal et al., 2012). In a similar manner, PDMS slabs placed within a monolayer can be used to create clean gaps and damage-associated gaps depending on the treatment of the PDMS surface (Nikolic et al., 2006). Similarly, Block et al. used agarose slabs as the blocking object, to which cells cannot attach (Block et al., 2004). By using such surface masking techniques, the resulting gap is similar is in the classical scratch assay but with better-defined initial wound or gap conditions which produce more reproducible and robust results (Gough et al., 2011). Varying the size and shape of the blocking object allows creation of various wound or gap geometries in a reproducible manner, which is hardly attainable in the classical scratch assay (Eileen Fong, PhD thesis). Surface masking techniques have proven very effective for high throughput assays, since the reproducibility of gap patterning is considerably higher than classical scratch assays. Moreover, these platforms allow kinetic as well as endpoint measurements. As such, surface masking approaches to study collective cell migration have recently started to be commercialized (Oris technology™-Platypus technology) (Figure 2. 2. B).
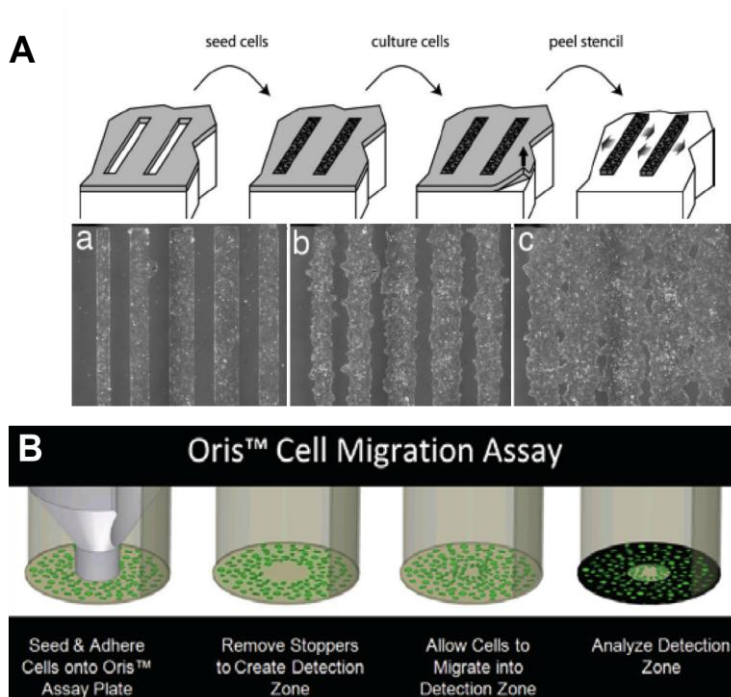

Figure 2. 2. Surface masking approaches. (A) Wound closure model using surface masking strategies. Here, an elastomeric membrane with apertures is placed on the substrate and cells are seeded on the openings. When cells are confluent, the blocking membrane is removed and cells are allowed to migrate, similar as in the scratch-wound assay. From (Poujade et al., 2007). (B) Surface masking approaches to study collective migration are commercialized by Oris™, Platypus technology. They offer easy-to-perform assays in high

throughput formats (96 and 384-wells plates). Their technique is based on the use of stoppers to create cell exclusion areas. From Platyplus website.

1.3. The relevance of surface masking approaches: a key role for cell damage

The removal of the masking objects in a clean manner (without damaging the surrounding cells) is an important issue since the initiation of the migratory response has been long associated with the presence of death or damage factors (Jacinto et al., 2001). In this context, growth factors and other compounds released to the extracellular medium from dead or damaged cells during the production of the gap could initiate the closure response by activating the migration of the remaining uninjured cells (Matsubayashi et al., 2011, 2004; Sammak et al., 1997). From both *in vivo* and *in vitro* studies, FGF, EGF, TGFα, and KGF have been recurrently related to damage-induced response (Rämet et al., 2002). Such growth factors typically act through activation of the three members of the MAPK family (ERK, p38 MAPK, and JNK) (Sharma et al., 2003). Recurrently, an upregulation of JNK is observed especially at the damaged front, thus JNK could be the intracellular transducer candidate for the transmission of the signal (Altan and Fenteany, 2004). Interestingly enough, MAPK family also play an important role in regulating epithelial migration during other closure processes not involving damage, such as *Drosophila* dorsal closure and eyelid closure (Xia and Kao, 2004). Regarding other compounds, Ca^{2+} is a very likely candidate to mediate the closure response. Ca^{2+} has been shown to be transiently elevated within seconds after wounding, and a Ca^{2+} wave-like transmitted in a graded-fashion from the edge (from the first row of uninjured cells after the bordering dead cells) up to 10-12 rows inwards (Sammak et al., 1997). Such long-range transmitted signal could be the activator of the migratory machinery of cells, engaging a wide front of the monolayer in the closure (Klepeis et al., 2001). Similarly, ATP has also been proposed as the messenger of the activation in a similar manner, diffusing from the front of damaged cells inwards (Block and Klarlund, 2008). ATP has been proved to stimulate EGFR, which would then transduce intracellularly the presence of cell damage and thus the necessity for the cells to migrate. Noteworthy, such EGF activation has also been shown to occur in the absence of cell damage (Block et al., 2004).

On the other hand, the fact that epithelia tend to move when edges are present (thus in response to an interface cells-free space) was hinted long ago (by Rand et al. in 1915). More detailed studies have shown that migration can be triggered by the mere exposal to free space, after the release of a given spatial constraint or blocking object, in the absence of cell damage (Block et al., 2004; Nikolic et al., 2006; Poujade et al., 2007; Klarlund and Block, 2011). In such cases, many of the

motility-promoting factors are also upregulated (for example growth factor receptors) independently of damage-induced compounds such as ATP (Block and Klarlund, 2008).

An interesting work points towards reconciling both approaches (migration triggered by death factors or by free space) by showing 2 activation waves of ERK1/2 (a MAPK family member widely accepted to be related to migration). The first wave was shown to be fast, acute, and transient, quite ressembling the Ca^{2+} wave; the second wave was slow, mild, and sustained (Matsubayashi et al., 2004). Such second wave showed a great correlation between phospho-ERK1/2 signal and cell motility. A more thorough study demonstrated that the first wave would be due to the damage, and the second wave occurs in the absence of damage and would be the real driver of migration (Nikolić et al., 2006).

technique	advantatges	disadvantatges	reference	specification
scratch assay	compatible for high throughput screening	possible disruption of underlying ECM	Todaro et al., 1965	pipette tip scratching
	easy to produce	difficult to standardize	Yarrow et al., 2005	automated scratching
	cheap	uncontrolled initial conditions	Matsubayashi et al., 2004 and 2011	pipette tip scratching
	widely used	mostly for large wounds	Simpson et al., 2010	automated scratching
	commercially available	damage and death factors release		
laser ablation	controlled wound size	damage and death factors release	Tamada et al., 2007	1-3 cells laser ablated
	possibility to perform small wounds	advanced instrumentation		
surface masking techniques	controlled initial conditions	materials chemistry required for optimization of protocol	Nikolic et al., 2006	PDMS slabs
	preserved ECM substrate coating		Poujade et al., 2007	PDMS membranes
	no damage factors associated		Block et al., 2004 and 2008	agarose slabs or drops
	commercially available			

Table 2. 1. Comparison of the different techniques to study collective cell migration in the context of epithelial gap/wound closure.

1.4. Proposed approach

Hence, it remains elusive to what extent the mechanisms thought to initiate motility in the presence of cell damage can also be activated without the presence of cell damage (Table 2. 1). In this context, assays to uncouple the effect of cell damage on the closure response seem very appealing to better understand the response to newly available surface. However, the current techniques do not allow for a proper analysis of the size-dependence gap closure mechanism. And moreover, no approach can tackle at the same time the different questions that remain unsolved about epithelial closure, raised in Chapter 1 Section II. 5. 3.

To address these questions, we propose a novel experimental model to shed some light in the intrincated and far from standardized process of gap closure. Inspired by these latter masking strategies, we designed an array of PDMS pillars that are used to block a circular space to the cells. Upon removal of these PDMS pillars, the pillar-surrounding cells are now exposed to a newly available area. In this manner, an array of gaps is created within a confluent epithelial monolayer in a very clean and controlled manner.

2. Methodology: Gap patterning method

The gap patterning method consists briefly on sticking a stencil of microfabricated pillars of a given and tunable diameter to a glass substrate (Figure 2. 3). The surfaces of both the substrate and the pillars must be chemically modified. Then, cells are cultured in between the grid of pillars until confluence, at which point the stencil is carefully removed and an array of gaps is created. We will hereafter explain the processes used for producing the microfabricated pillars and the gap patterning protocol. A detailed description with the exact protocol is provided in the Annex C.
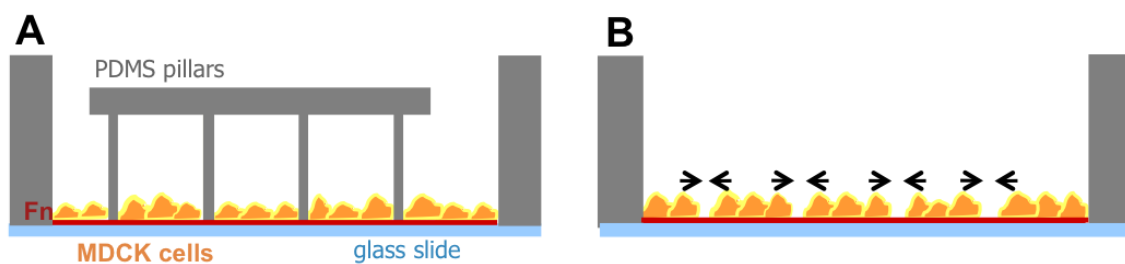
Figure 2. 3. Scheme of the gap patterning protocol. (A) A microfabricated stencil of pillars is stuck to a fibronectin-coated glass and cells are cultured between the pillars. (B) Upon removal of the stencil, gaps are produced in areas previously covered by pillars.

2.1. Microfabrication

In order to microfabricate such pillars, we take advantage of photolithographic techniques together with molding approaches. Photolithography consists of transferring a motif printed on a photolithographic mask to a photoresist on a substrate. Masks are typically constituted of quartz and chrome, although when working with rather large motifs, high-quality printed-transparency paper can also be used. The photoresists lie on top of a substrate (a silicone wafer or a glass slide, for example) as a layer of controlled thickness. The resist is deposited by spin coating the viscous product at a certain speed, time and acceleration. By taking into account the viscosity of the resist, the speed of spinning will determine the thickness of the layer. Then the mask and resist-coated wafer are placed together

in the photolithographic mask aligner, which will control the power and time of UV exposition. The mask allows UV light to pass through certain areas and modify the underlying photosensible resist, either by crosslinking the resist (for negative photoresists) or by rendering the exposed area soluble to posterior treatments (positive photoresists). It is important to have the mask in very close contact with the resist-coated substrate to avoid diffraction effects of the UV light. After UV exposure there is typically a baking step to further crosslink and cure the areas that have or have not been exposed (depending on the nature of the resist). The resist-coated substrate undergoes now a developing step, which means that the substrates are immersed in a product than can dissolve the non-crosslinked resist. This developing step is highly dependent on the nature of the resist itself and also on the size of the features.

In the present work, we have followed two microfabrication approaches depending on the size of the features: etched Si wafers and SU8 masters.

2.1.1. Etched Si wafers

For pillars of ≤60 μm, we used a protocol described previously in Alexandre Saez and Marion Ghibaudo PhD manuscripts. In this case, circular motifs of varying diameter (15, 20, 30, 40, 50 and 60 μm in diameter) are designed and printed on a quartz-chrome mask, where circles are in black (chrome) and the rest is transparent (quartz), being thus a negative mask. Then the motifs are transferred to a positive resist-coated (AZ9260, Electronic Materials) silicon wafer by photolithography. After, there is a deep reactive ion etching process (DRIE) (Figure 2. 4. A). The DRIE step is based on the chemical etching of silicon areas non-covered by the photoresist, by using a highly reactive gas (SF_6 and C_4F_8). This allows the creation of deep holes (up to few hundreds of μm, up to 1:20 aspect ratio), where the depth depends on the time of etching. The rests of photoresist are eliminated with acetone. The DRIE step has represented a relevant advancement in the microfabrication of pillars for cell traction force measurements [(du Roure et al., 2005) *versus* (Tan et al., 2003)] (Figure 2. 4. B *versus* C). Thus, we obtain a silicon wafer with different grids containing arrays with holes of different diameters and depth of 20 μm in the first produced wafers and 100 μm for the actual employed wafers. In regards the present work, these processes were performed by technicians in a clean room in either Institut d'Electronique de Microelectronique et de Nanotechnologie (Villeneuve d'Ascq, France) or in Mechanobiology Institut (Singapore). We acknowledge the technicians in IEMN and Mohammed Ashraf in MBI.
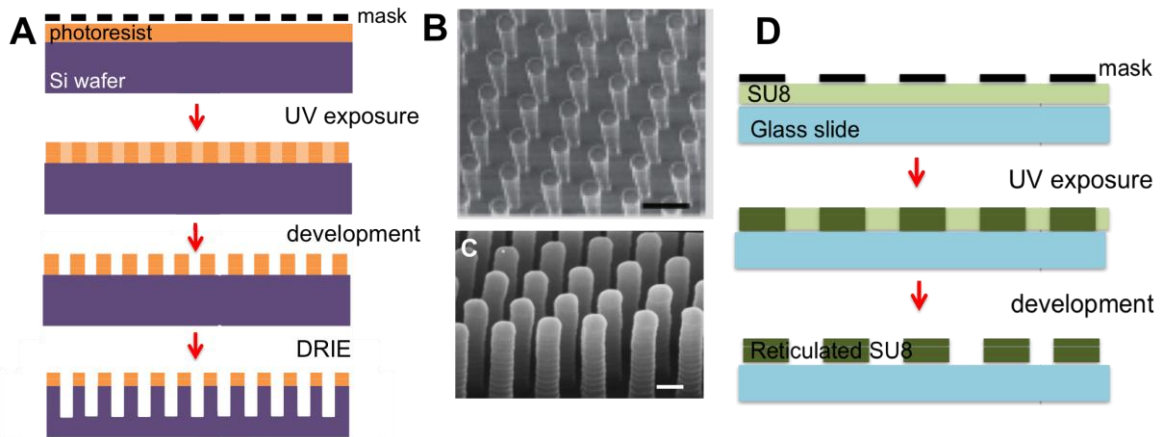
Figure 2. 4. Microfabrication of the masters. (A) Scheme of the processes used. (B) PDMS pillars obtained without the DRIE step. Note that they are sparce and rather large. Scale bar is µm. From (Tan et al., 2003)(C) PDMS pillars obtained when adding a DRIE step. Note that they are smaller and thus more dense. Scale bar is 1 µm. From Alexandre Saez PhD manuscript. (D) Scheme showing the microfabrication for large features in SU8.

2.1.2. SU8 masters

On the other hand, the microfabrication of pillars ≥80 µm was carried out by ourselves in the facilities of Plataforma Nanotecnologia in PCB, Barcelona (Spain). In this case, since the features are larger, the mask could be a common transparency paper with high-quality printed black circular motifs of different diameters. The photoresist employed is SU8-50 (MicroChem). SU8 is a negative photoresist widely used in microfabrication processes with good mechanical properties and well-known chemical characteristics (the commercial vendor MicroChem provides thorough protocols and detailed information). Since our goal was to obtain features of close to 100 µm in height, we performed two rounds of spin coating, thus obtaining two stacked layers of aprox 50 µm. In this case the substrates were impeccably clean glass slides (pretreated with piranha to favor resist attachment), which for the given feature size the bonding of SU8 features on the glass slide proved to be a long-lasting bond. Upon 345 nm UV light exposure, the resist areas beneath transparent circles are crosslinked. After a baking step, the master is developed with a SU8 developer (Figure 2. 4. D). Because almost all the glass slide, except for the circular motifs, is covered with uncured resist that must be dissolved, the developing step can be longer than normal. We have experimentally adapted the developing time at our convenience. Such developing step is strongly influenced by the shaking of the SU8 master on the developer, so it is always recommended to assess with isopropanol the presence of uncured SU8 remaining. A detailed protocol is provided as Annex A. Note that the resulting master consists of SU8 pillars, not holes as described before for the silicon wafer, since we found experimentally that the photolithography works better for producing pillars for such SU8 layer thickness (100 µm). This issue will be

afterwards resolved by 2-step PDMS molding (later explained). Note that this latter microfabrication approach is a much affordable process: the use of transparency paper as a mask instead of quartz-chrome mask, the use of regular glass slides instead of silicon wafer as substrate, and skipping the DRIE process, reduces the fabrication price. Moreover, it requires of the most basic elements of a clean room and can be typically carried out by the user.

This silicon or SU8 master is silanized to enable the release of the elastomer and allow reuse of the master (Figure 2. 5). Such silanization is performed in vapor phase with a hydrophobic fluorosilane [(Tridecafluoro-1,1,2,2-tetrahydrooctyl) trichlorosilane; 97%, ABCR]. The silicon-based elastomer poly-dimethylsiloxane (PDMS) (Sylgard 184, Dow-Corning) is prepared by through mixing base and reticulant agent at 10:1, degassed, poured over the master, degassed again, and cured at 65°C for around 12h. After, it can be easily peeled off from the master (Figure 2. 5) (for detailed protocol see Annex B). From the silicon wafers (which contain holes), we will obtain stencils with PDMS pillars. However, note that for the SU8 masters, the first PDMS mold contains holes (given that SU8 masters have pillars), so that a second molding step is required. Thus, the first PDMS mold must be silanized as before, and PDMS is poured again and cured over this first mold. Now, this second mold contains PDMS pillars.
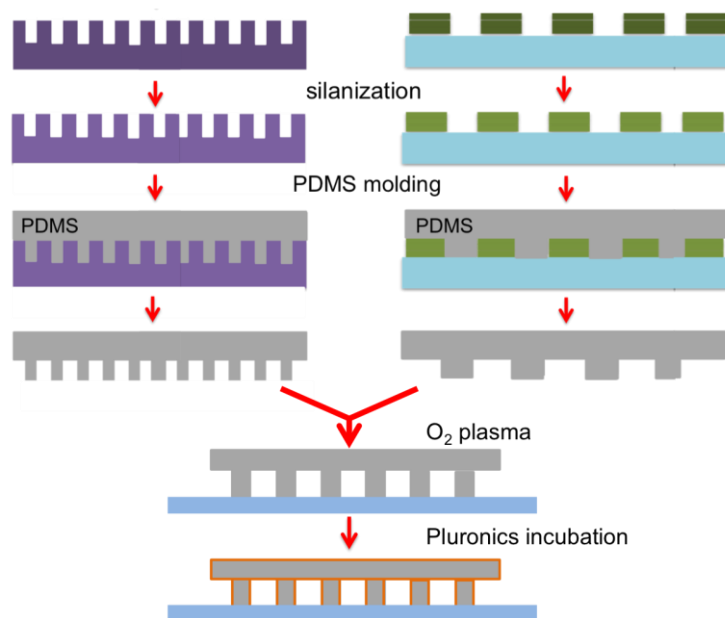

Figure 2. 5. Scheme of the soft lithography steps. Silicon (left) and SU8 (right) masters are silanized and PDMS is cured on the masters. PDMS pillar stencil is stuch to a glass slide and incubated with Pluronics.

2.2. Surface treatment

The pillar stencil is then stuck to a fibronectin pre-treated glass substrate (Mattek® Petri dishes are coated with 20 µg/ml of fibronectin and then let dry) by mild plasma treatment. Oxygen plasma ionizes both surfaces and enables the PDMS to subtly attach to the glass substrate (Figure 2. 5). It is important that the PDMS stencil is mildly attached (so that it will not lift off when liquid is added) but not too strong (so it can be easily removed). Note that this is a critical step of the process and highly dependent on the characteristics of the oxygen plasma, so additional adjusting parameters must be required for a different plasma machine. Plasma treatment renders PDMS hydrophilic for aprox 30 min. After the plasma effect has fade out, PDMS recovers its hydrophobicity. Such hydrophobicity is a key feature that enables the differential surface treatment of PDMS stencil with respect to the substrate when they are already attached.

At this moment, there is a crucial step of PDMS pillar passivation to avoid attachment of cells at the pillar walls. While PDMS is an inert polymer for cells, serum-contained fibronectin and other ECM molecules usually present in the cell media could deposit inespecifically (by physical adsorption) on the PDMS pillar walls and enable the attachment of cells to the pillars. Should that happen, cells would be ripped off or teared when peeling off the PDMS stencil. In our aim for not damaging the pillar bordering cells, it is critical to coat the PDMS pillars with a compound that will prevent the binding of any kind of cell adhesive peptides to the pillars walls.

Typically, PDMS is passivated by immersion in BSA solutions, a well-known protein that prevents cell attachment and is commonly used in patterning methods and in PDMS-based surface blocking strategies (Chiu et al., 2000; Wong and Ho, 2009). In such cases, PDMS slabs or membranes are immersed in BSA and then placed in the substrate. However, in our approach, dipping the PDMS pillar stencil in BSA prevents the binding of PDMS pillars to the glass, and BSA incubation of the PDMS pillars after attachment to the glass substrate did not completely abolish cell attachment to the pillars walls. We then tried the compound Pluronics (BASF), which is also used as a passivating agent during surface patterning protocols. Interestingly, Pluronics is a non-adhesive polymer that only binds to hydrophobic surfaces, thus it covers PDMS pillars but not the substrate (Figure 2. 5). Moreover, Pluronics proved very effective in preventing cell attachment to PDMS. Thus, when the effect of plasma on PDMS is no longer present (i.e. PDMS pillars are hydrophobic again) we incubate the sandwich PDMS stencil-glass substrate with Pluronics. Such incubation is a critical parameter that must last exactly one hour: shorter incubation times can result in cells attaching to the PDMS and longer times

will prevent cell attachment even in the glass substrate. With the proper Pluronics passivation, there are no adhesions between the pillars and the bordering cells, being the pillar a mere blocking object. An additional step of fibronectin coating is performed to ensure proper presence of fibronectin in the substrate, by incubation with 20 µg/ml of fibronectin, for 20 min at the incubator. Thorough rinsing before and after fibronectin coating is also important to ensure complete absence of Pluronics in the substrate.

2.3. Cell culture

The cells used in the present study are Madin-Darby Canine Kidney (MDCK) cells strain II, which derive from the kidney distal tubule of *Canis familiaris* (CCL-34 in ATCC). This epithelial cell line is widely used in *in vitro* studies of epithelial migration, and has been reported in wound closure studies (Tamada et al., 2007; Fenteany et al., 2000b; Nikolić et al., 2006; Poujade et al., 2007). MDCK cells are at an intermediate state of EMT: they form migratory monolayers. When plated at low density, MDCK form clusters of well-spread, flat cells with notable ruffling activity. As cells grow and increase in density, they become taller and less spread. When highly packed, MDCK cells form a monolayer of cuboidal polarized cells, with well-defined adherens and tight junctions (Hartsock and Nelson, 2009). Cell-cell adhesion proteins are linked to the actin cytoskeleton, and thus all cells belonging to the monolayer result mechanically and functionally coupled. As previously discussed in Chapter 1 section II.1, these junctions also help to define a different apical and basolateral domain.

MDCK cells are maintained at 37^0C and in a humidified atmosphere with 5% of CO_2, supplemented with 10% fetal calf serum, 100 U/ml of penicillin, 100 µg/ml of streptomycin. Cells are used up to 15 passages, to avoid aging of the cultures and to use relatively similar number of passages on the experiments. For quantitative experiments, MDCK cells stably transfected with actin-GFP, lifeact-GFP, and lifeact-Ruby are used, with medium supplemented with geneticin. Stably expressing actin-GFP cells were kindly provided by James W. Nelson. Stably expressing lifeact-GFP and lifeact-Ruby cell lines were established in the lab by Elsa Bazellieres (lifeact-GFP MDCK) and me (lifeact-Ruby MDCK).

MDCK cells are seeded by adding a highly concentrated drop of cells at the side of the PDMS stencil, which will enter the stencil by capillarity and cells will be evenly distributed. After 20 min of sitting, the petri dish is filled with 2 ml of medium. MDCK cells are cultured in between the pillars overnight until when

confluency is reached. Then, the PDMS stencil is carefully removed with tweezers, and an array of gaps is created within the monolayer (Figure 2. 3).

It is important to note that we started the project by using PDMS pillars of 20 µm in height. However, given that the stencil is composed of the pillars and a roof, such pillars proved to be too short so cells were growing slower than usual inside the pillars grid and cultures presented increased dying cells (Figure 2. 3). Presumably, fluid flow was reduced inside the grid and there was not enough medium renewal. We then decided to use pillars of 100 µm in height, which are the ones we have been using all throughout the presented project (Figure 2. 3).

Thus, by using a stencil with microfabricated pillars we can obtain many gaps of well-defined size and shape, in a highly reproducible manner. The size and shape of the pillars were varied to obtain circular pillars of different diameters, ranging from 15 to 150 µm, and squared and ellipsoidal pillars of two different sizes. Most of the study has been carried out with circular pillars. Squared and ellipsoidal pillars are addressed at the end of this chapter under the section 4.

2.4. Experimental measurements and analysis

Experiments were typically conducted in an automated inverted microscope (Olympus or Nikon), equipped with a weather chamber maintaining the temperature at 37°C and a 5% of CO_2. Images were acquired at 1 frame/30 sec or 1 min, unless otherwise stated. For confocal measurements, Nikon A1R confocal microscope was used. For quantitative analysis, actin-GFP, lifeact-GFP or lifeact-Ruby stably transfected MDCK cells were used, and in such cases experiments were performed with phenol red-free medium for a better fluorescence visualization. The analysis was carried out in Fiji. For gap area calculations, a routine in Fiji was created to obtain a mask of the gap for the different experiments. Specifically, we: 1) adjusted the fluorescence intensity so that all the videos displayed the same intensity; 2) set the proper contrast intensity that optimizes the detection of the gap edges; 3) automatically thresholded the fluorescence images to detect the cell-denuded area; 4) created a binary image or mask; 5) calculated the area of the mask at each time point; and 6) exported the values for posterior analysis. Since the gap area was analyzed Time of closure is determined when the gap area is inexistent, as detected in the binary mask of the thresholded videos. The automatic detection of gap area across different experiments by using such Fiji macro avoids the user-induced errors and prevents any possible bias in the measurements.

2.5. Protocol characterization

Note that in our method the PDMS pillars only act as passive objects blocking the surface available for the cells (Figure 2. 6. A). By treating the pillars walls with Pluronics, cells do not recognize the pillars as cells. In order to confirm that cells do not establish specific junctions with the pillars, we checked for the presence of adherens and tight junctions between the surrounding cells and the pillars. Indeed, staining for E-cadherin (an adherens junction protein) and ZO-1 (a tight junction protein) proved negative at the interface cells-pillar (Figure 2. 6. D and E).

Moreover, since we have an array of pillars in the stencil, we can obtain many gaps in parallel within the same sample and thus increase the statistical power of the methodology (Figure 2. 6. B and C).
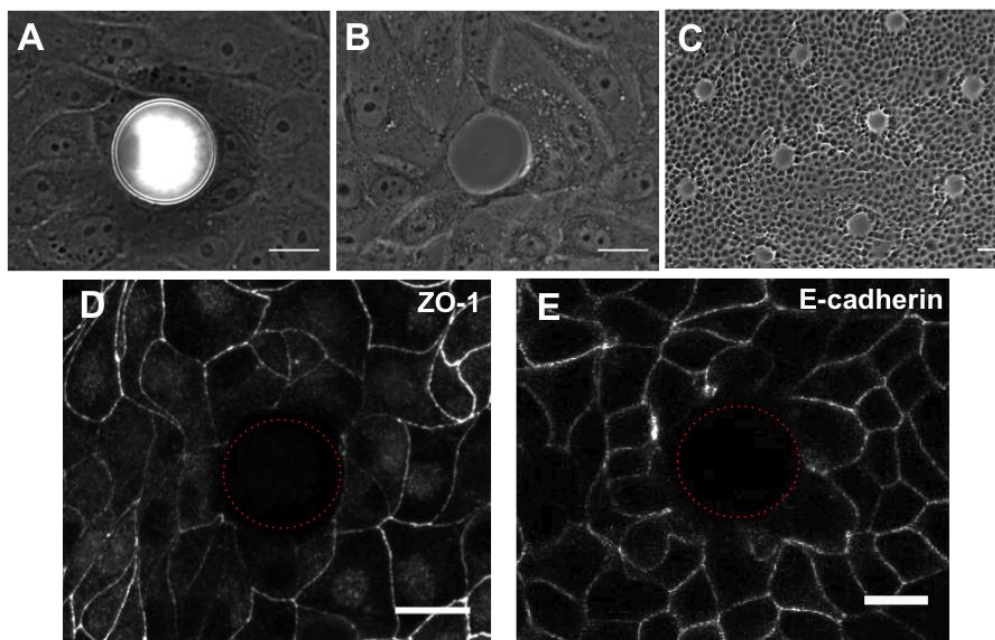
Figure 2. 6. PDMS pillars act as passive blocking objects. Surrounding cells do not form specific adhesions with the PDMS pillars thanks to their Pluronics coating. (A) PDMS pillars are used as blocking agents to pattern circular free-of-cells areas. (B) After pillar removal, gaps are created within the monolayer. (C) By using a stencil containing numerous PDMS pillars, an array of gaps can be obtained. Scale bars are 10 μm. (D) Immunostaining for ZO-1, a tight junction protein. Dotted red line denotes the presence of the PDMS pillar, and has been slightly located inside of the pillar to allow better visualization of the pillar-cells interface. Note that there is no signal at the cells-gap interface. Scale bar is 20 μm. (E) Immunostaining for E-cadherin, an adherens junction protein. There is no specific adherens junction signal at the pillar-cells interface. Scale bar is 20 μm.

As a proof of quality, we analyzed the capability of the designed experimental approach to retrieve systematically well-defined gaps without cell damage. We have characterized the gaps obtained by PDMS pillars in terms of their size and shape. Regarding the size, gaps are of almost the same area as the pillars used for

their patterning (Figure 2. 7. F and Figure 2. 6. A-B). Moreover, there is not much variability between gaps, as the initial size is rather constant for all gaps analyzed (Figure 2. 7. F). On the other hand, by image analysis tools we determined the resulting shape of circular gaps by calculating how close to a circle they are. The sphericity of the present analyzed gaps is 0.89±0.09 (mean±SE) (n=24, 12 different samples), being 1 a perfect circle (Figure 2. 7. A-E).
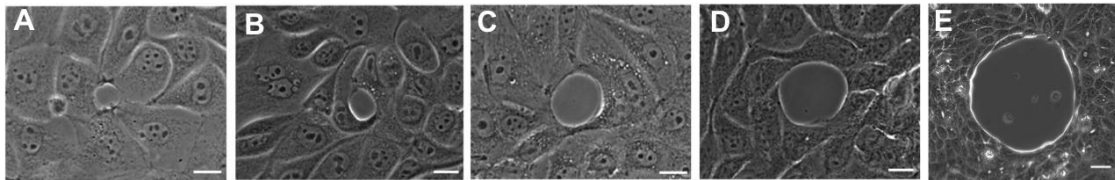
Pillar diameter (μm)	**Pillar area (μm²)**	**Mean gap area (μm²)**	**SD of gap area (μm²)**
15	177	163	33
20	314	327	15
30	707	727	30
40	1257	1311	58
50	1963	1965	14
60	2827	2826	11

Figure 2. 7. Characterization of the gaps produced with the pillar stencil. Phase contrast images of gaps right after peeling off the pillar stencil, produced with pillars of 15 μm (A), 20 μm (B), 30 μm (C), 40 μm (D), and 150 μm (E). Note the regularity in the gap shape. Scale bars are 20 μm. (F) Summary of the quantification of the area of the produced gaps. Comparison of the calculated area of the pillar used for the patterning with respect to the measured gap area right after pillar removal. Experimental data shown is means and standard deviation of a pool of experiments performed in different days, containing at least 15 gaps analyzed per pillar size.

Also, it is important to note that cells are distributed randomly along the gap perimeter, with no preferential alignment or shape of cells contacting the pillar with respect to inner positioned cells (Figure 2. 8). Neither are there differences in their organization as a function of gap size or cell density. However, we do acknowledge the possibility that cells contacting a small gap can be set to a different mechanical state with regards to cells contacting larger gaps, due to their line tension at the cell-pillar interface, which is higher for small gaps (since these gaps present have higher curvature).
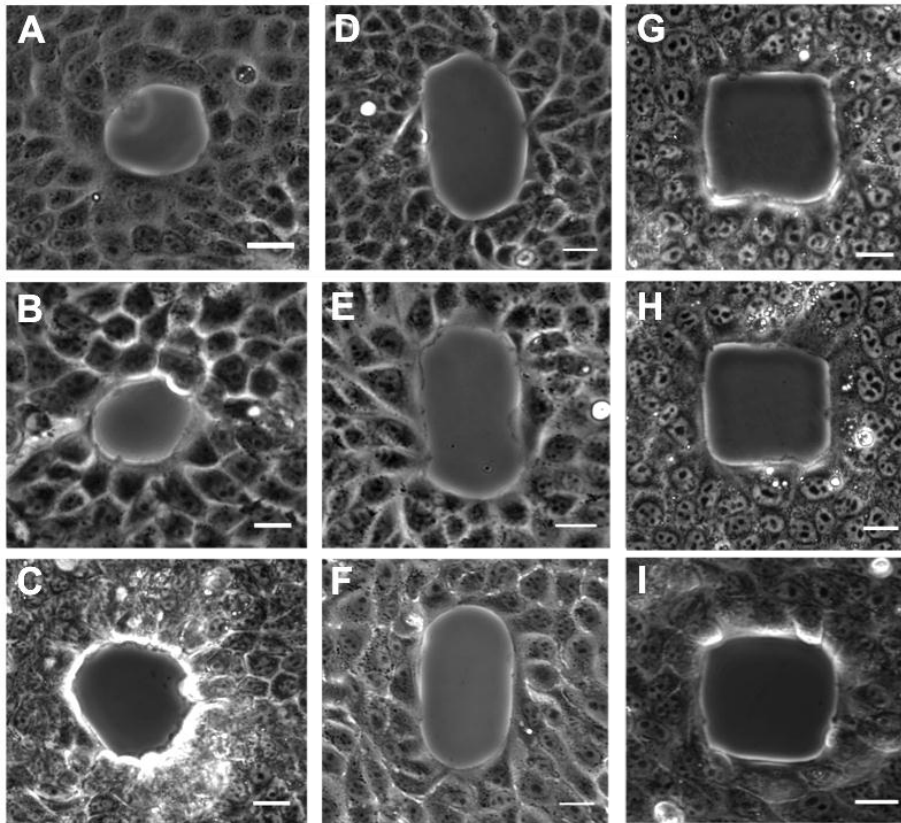
Figure 2. 8. Initial conditions of cells surrounding the pillars. (A-C) Cells around circular pillar under increasing degree of confluency, from fairly spread (A) to highly dense cells (C). (D-F) Cells are randomly distributed around ellipsoidal gaps. The differential convexity of the gap perimeter does not determine the positioning or alignment of cells at its poles. (G-I) Again, the squared shape has causes no cornering effect on the cells distribution, that are evenly positioned. Scale bars are 20 μm.

2.6. Assessment of extracellular matrix presence

To ascertain that our gap patterning protocol has no undesired effect on the assembly of ECM, we verified the presence of ECM in the substrate during our protocol. First, we assessed the coating of the substrate with fibronectin by using labeled fibronectin (home-made prepared Cy3-conjugated fibronectin, see Annex E). By using this fluorescent fibronectin, we observed that fibronectin was roughly deposited everywhere, although in a somewhat heterogeneous manner (Figure 2. 9. A and B). Importantly, after removing the PDMS pillar fibronectin was present in the gap area and cells migrated over this fibronectin substrate (Figure 2. 9. C). Next, we also checked fibronectin deposition by the cells by doing immunostaining for fibronectin detection. We did not observed any specific pattern of fibronectin deposition, but it could be appreciated that fibronectin was secreted and reorganized by cells (Figure 2. 9. D and E). Note that we analyzed as well fibronectin deposition in a different susbtrate used, namely PDMS substrate, as

will be later on explained. For this PDMS substrate, fibronectin deposition presented no differences with respect to glass substrate (Figure 2. 9. F). We also checked for another ECM protein, laminin, and reported that laminin is not present at the gap area (because the substrate is not coated with laminin but only with fibronectin). However, we could note that laminin was being secreted by cells in their way to produce a basal lamina, as seen by the positive laminin staining in the area covered by cells (Figure 2. 9. G).

As we have shown that a fibronectin-based ECM is present in the gap area throughout the experiment, and no specific features in fibronectin deposition can be observed, we can rule out a possible effect of ECM presence in determining the ulterior closure mechanism.
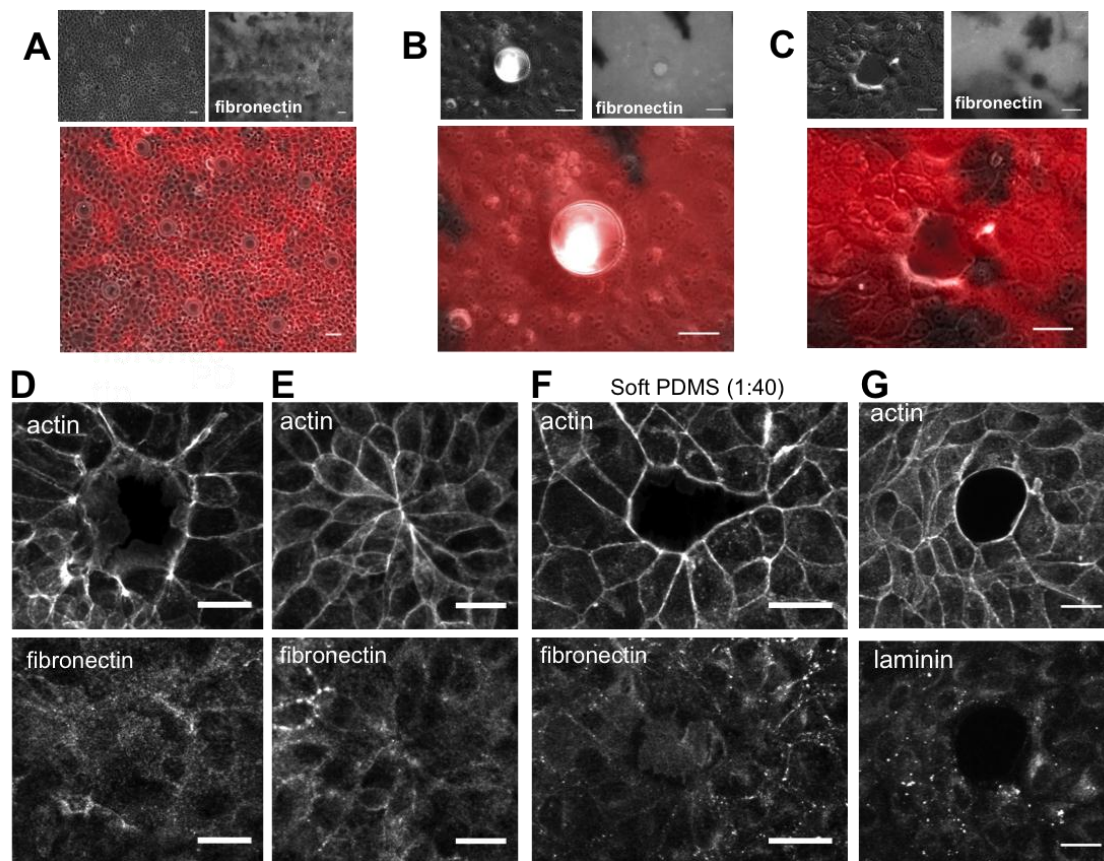

Figure 2. 9. Extracellular matrix assembly beneath cell culture. We have tested fibronectin location by two approaches: using fluorescently labelled fibronectin to coat the substrate (A-C) and immunostaining fibronectin to observe fibronectin secretion and reorganization by cells (D-F). (A) Pillar stencil between the epithelial culture on glass at low magnification, and fibronectin assembly. Bottom image shows the merged images. (B) In a close-up view it can be appreciated that fibronectin is present beneath PDMS pillar. (C) Removal of the stencil does not tear the fibronectin beneath. (D) Fibronectin and actin staining after 30 min of pillar removal and (E) at the closure time (65 min after pillar removal). (F) Fibronectin deposition on soft PDMS substrates at 1:40 crosslinking ratio is not altered. (G) Laminin assembly: laminin is not present in the gap area, while it is in the area covered by cells. All scale bars are 20 μm.

2.7. Gap patterning method: cell damage-associated gaps

As it has been previously discussed, it is not clear yet what is the contribution of death and damage factors to the closure response. Migration can be triggered in both damage-associated and damage-free situations, and no study (to our knowledge) has focused on the effect of the presence or absence of damage under the same experimental conditions in a gap closure assay. For this reason, we aimed at creating gaps in a similar protocol as described, but under the presence of cell damage produced during the gap patterning protocol. In this case, since the gaps would present dead or damaged cells, gaps could be called proper wounds. For that purpose, we also took advantage of the PDMS pillar stencil to inflict wounds in an epithelial monolayer, thus obtaining an array of wounds, similar to the array of clean gaps presented before.

We followed two distinct experimental strategies (Figure 2. 10): 1) holding the PDMS stencil with a needle at the top, we approached the array of pillars to the cell culture and placed in slight contact, always with medium filling the dish. It is important not to exert too much pressure or not to slide the stencil when contacting the cells to avoid ripping out a too large part of the cell monolayer. In this way, the cells beneath the pillar are killed. We termed this approach "*crushed gaps*". 2) running the same pillar removal assay described before, but without the Pluronics incubation step. In this manner, cells attach to the PDMS pillar walls, and when the stencil is removed, some cells are ripped off and teared, thus resulting damaged and/or dead. We refer to the resulting gaps as "*ripped gaps*". For a detailed protocol see Annex D.
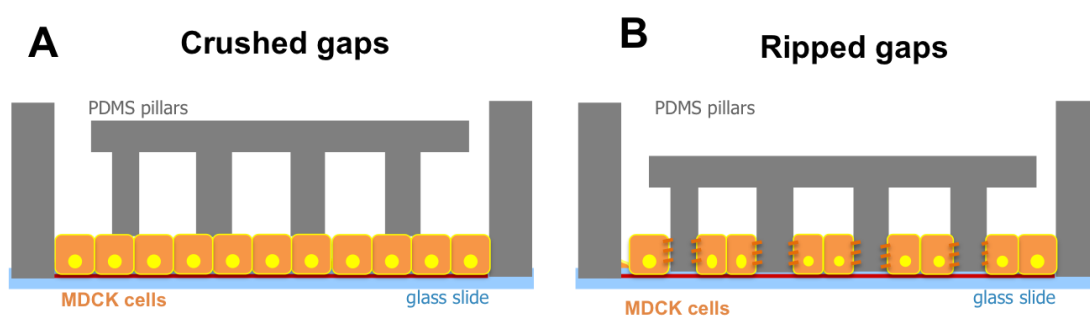

Figure 2. 10. Methods for producing damage-associated gaps. (A) Crushed gaps are produced by squeezing the cells with the PDMS pillar stencil. (B) Ripped gaps are created by not incubating the PDMS pillar stencil with Pluronics, so that cells will attach to PDMS pillar walls.

2.8. Damage assessment

Our set-up has been devised to ensure gap production in a clean manner, i.e. without killing or damaging any cells, and putting special care in not tearing the bordering cells. To ensure that gaps are created in a free of cell damage manner, we doubled-checked for damaged cells by using FITC-dextran and propidium iodide (SIGMA). FITC-dextrans are low molecular weight compounds (40KDa in our experiments) that can penetrate porous, permeabilized or damaged membranes. Such compounds are typically used in permeability assays (for example for quantifying the porosity of a 3D collagen gel) or in diffusion assessment assays, but are also employed to check membrane damage (Trappmann et al., 2012; Brock et al., 1996). By using this FITC-dextran incorporation assay, we have not detected cell damage in our system (Figure 2. 11. A). Moreover, we double-checked the absence of cell damage by also using propidium iodide (PI). PI is a non-permeable dye that labels dead or membrane-damaged cells (Unal-Cevik et al., 2004). Again, no cells showed positive for PI in our pillar removal assay (Figure 2. 11. B).
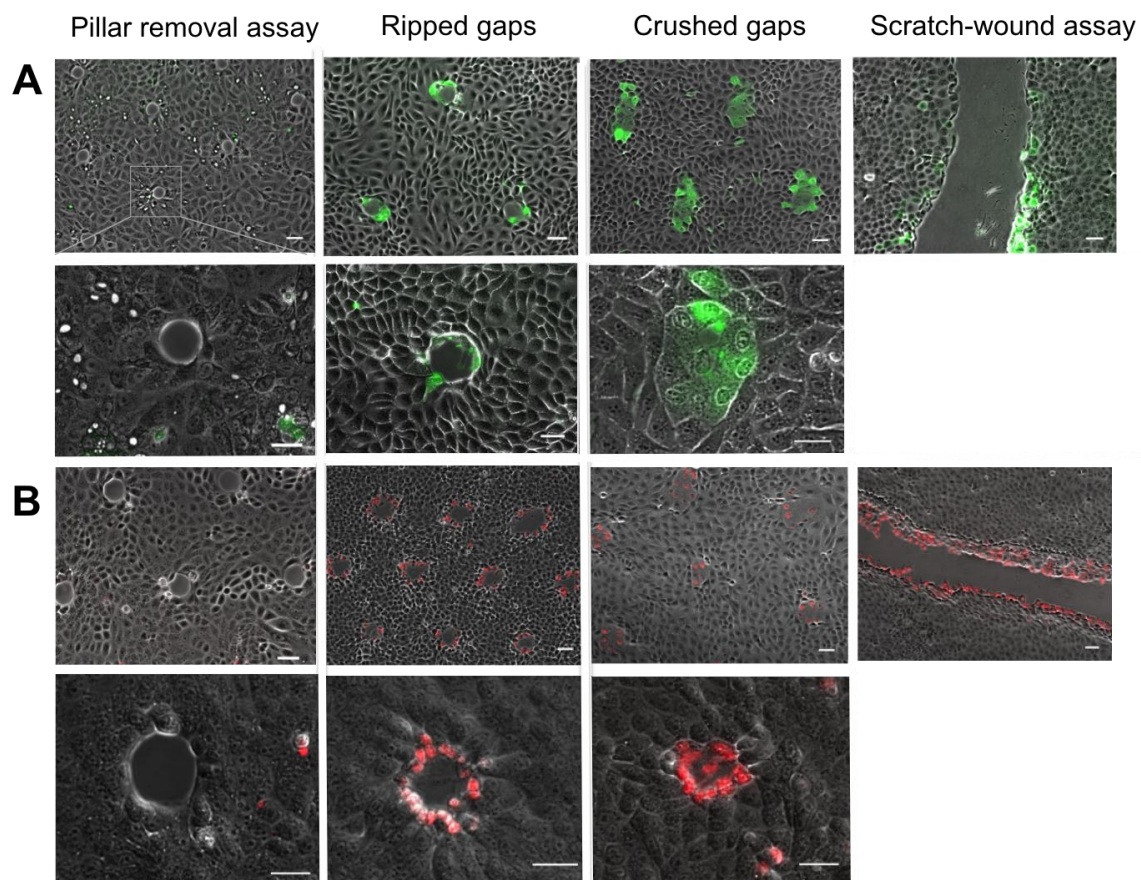

Figure 2. 11. Cell damage assessment for the different gap (pillar removal assay) or wound (ripped and crushed gaps) patterning methods used. We also compared with the classical scratch-wound assay. (A) FITC-dextran uptake. (B) Propidium iodide internalization. All scale bars are 20 μm.

121

On the other hand, we also assessed the cell damage produced in the on-purpose damage-associated gaps. We performed the two assays, FITC-dextran incorporation and Propidium Iodide internalization, on "Crushed gaps", "Ripped gaps", and in the classical scratch wound assay. In the case of "Crushed gaps", all cells beneath the pillar result squeezed so they are positive for damaged cells staining. Thus, we obtain patches of dead cells. For "Ripped gaps", gaps are created, but surrounded by dead cells, as ascertained by both FITC-dextran and Propidium iodide labeling. As expected for the classical scratch-wound assay, all the cells at the first-row of the leading edge, and probably also cells in second and third row, result severely damaged (Figure 2. 11)

As we have shown, in our gap patterning approach there is no damage of cells surrounding the pillar after removal (Figure 2. 11, *pillar removal assay*). And yet, right upon removal of the blocking object, cells start moving in to fill the newly available space. Thus, we also show here that death factors are dispensable for the induction of motility, as it has been previously discussed in Chapter 1 section II. 3 and II. 8. 2. What we cannot rule out here, though, is the possibility that mechanically-activated signals are responsible for inducing motility. While we have proven that there is no specific interaction between cells and pillars (as shown in Figure 2. 6. D and E), and thus there is no breakage of junctions, it could well be that stretchable proteins at the interface cells-pillars are activated and signal intracellularly upon release of the constraint. In conclusion, our methodology prevents the damage of cells surrounding the pillar after removal, as opposed to what is observed during classical scratch assays.

3. Gap closure dynamics

3.1. Lamellipodial extension during closure

In order to analyze the dynamics of the closure process, we have typically performed time-lapse measurements right after removal of the pillar stencil. The beginning of the presented experiments represents 1-2 min after removal of the pillars, the minimum time to remove the stencil and set-up the microscopy acquisition.

By monitoring the closure we have observed that upon removal of the pillar stencil cells lining the gap extend lamellipodia throughout the process of closure (Figure 2. 12). The formation of lamellipodia starts shortly after the release of the PDMS pillar (during the first 10 min) and they are present until there is no more available space, at which point opposing or contiguous lamellipodia contact and fuse (Figure 2. 12, red arrowheads indicate the extension of lamellipodia).
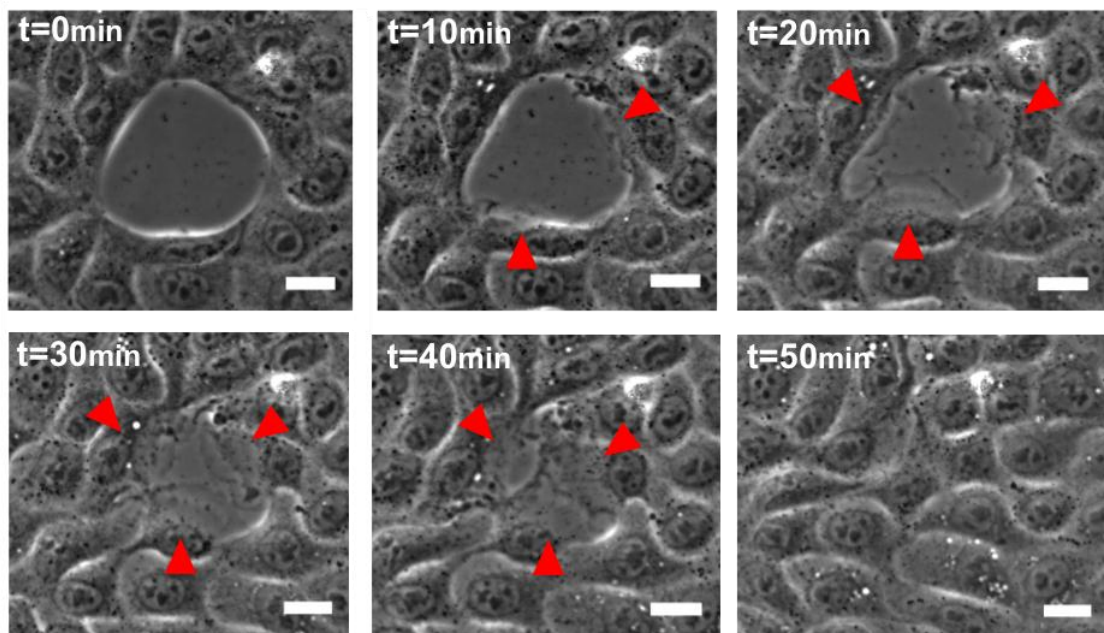

Figure 2. 12. Snapshot phase contrast images of a gap closing. Red arrowheads indicate protrusion of lamellipodia. Scale bars are 15 μm.

The extension of lamellipodia is independent of the size of the gap: from the smallest gaps (15 μm in diameter) to the largest gaps (150 μm), lamellipodia protrud during the closure (Figure 2 .13). In small gaps (15 to 30 μm diameter), all

cells contacting the gap extend lamellipodia (Figure 2 .13. A). For larger gaps, the number of cells at the gap border increases, and not all of these cells extend lamellipodia (Figure 2 .13. B). According to previous studies, it was suggested that purse-string contraction repaired small epithelial wounds (Bement et al., 1999; Tamada et al., 2007) whereas larger wounds induced cell crawling with formation of lamellipodia (Fenteany et al., 2000; Garcia-Fernandez et al., 2009; Poujade et al., 2007). Our experiments provide evidence that even for gaps of a single cell size (15 μm in diameter), lamellipodia are present during the closure.
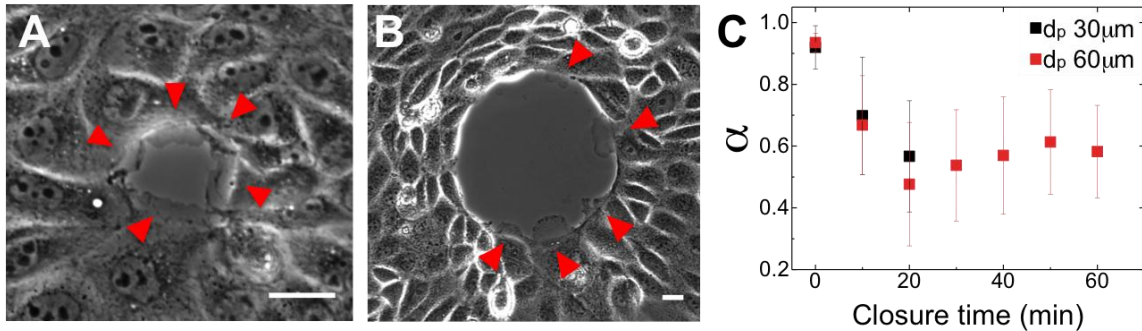

Figure 2. 13. Extension of lamellipodia by gap-bordering cells. (A) Even for small gaps, cells extend lamellipodia during closure. Snapshot at 8 min after pillar removal. Scale bar is 10 μm. (B) In the case of large gaps, cells also extend lamellipodia during closure, but not all cells at the periphery do. Snapshot at 30 min after pillar removal. Scale bar is 10 μm. (C) Evolution of roughness (α) of the cell-gap interface. Experiments were analyzed for two pillar sizes, 30 and 60 μm in diameter.

Due to the extension of cellular protrusions into the available free space, the borders of the gap roughen considerably after the removal of the pillar. In order to quantitatively characterize lamellipodial extension, we have analyzed the variations of the contour length by measuring the shape factor, $a = \dfrac{2}{R}\dfrac{A}{p}$, which is the ratio of the area A over the contour length of the interface p, normalized by half the instantaneous radius R. For a very rough interface, the perimeter is larger for a given area, so that $a \gg 0$, whereas $a \gg 1$ would indicate a circular hole. We indeed observe a decrease of this parameter α with time from 0.96 at the onset of gap closure down to around 0.5. The decrease in the shape factor α indicates how the boundary becomes irregular due to the emergence of lamellipodia surrounding the gap.

3.2. Closure rate

In order to obtain quantitative information about the closure of the gap, we have analyzed the time evolution of the gap area, *A(t)* for different gap sizes. We have used pillars of 15, 20, 30, 40, 50, 60, 80 and 150 μm in diameter. For all the

gap diameters tested, the decrease of the area with time is strikingly linear with time down to a complete closure (Figure 2. 14. A), showing very similar trends of closure. However, a closer look in the closure dynamics of small gaps shows that gaps of 15 and 20 μm in diameter present different trends. (Figure 2. 14. B). Likewise, the closure time varies linearly with the size of the gap above a gap diameter of 20 μm (Figure 2. 14. C).
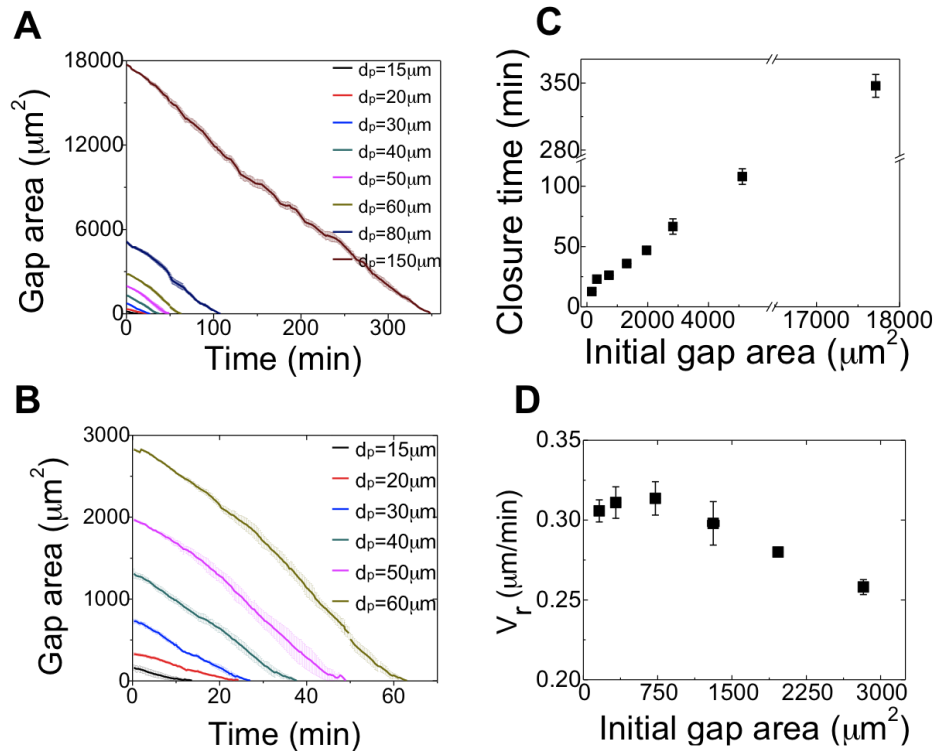

Figure 2. 14. Closure of gaps by surrounding cells. (A) Decrease of gap area over time, for all the gaps analyzed, from 15 to 150 μm in diameter (dp in the legend stands for diameter of the pillar used for patterning the gaps). (B) Close up of the previous graph, where only the gaps from 15 to 60 μm in diameter have been plotted. Two different trends of closure can be appreciated. (C) Closure time as a function of the initial gap area (for gaps of 15 to 150 μm in diameter). (D) Initital radial velocity as a function of gap area. Note there are two different regimes, for small and large gaps. Data are means and standard deviation for at least 8 gaps analyzed per condition, pooled from different experiments.

From the slope of *A(t)*, we have computed the initial radial velocity (which represents the velocity at the onset of closure) as a function of the gap size (by computing the derivative of the decrease in *A(t)* and normalizing by the gap perimeter). This velocity is roughly constant (0.3 μm/min) for areas up to 750 μm^2 and then slightly decreases for larger gaps (Figure 2. 14. D). Consistently, the advancement velocities of the protruding lamellipodia are around 0.3 μm/min during the initial stage of lamellipodia formation (computed from the kymographs of gap closure) (Figure 2. 15). Similarly, the cell body advancement displays at the same velocity at the onset of gap closure.
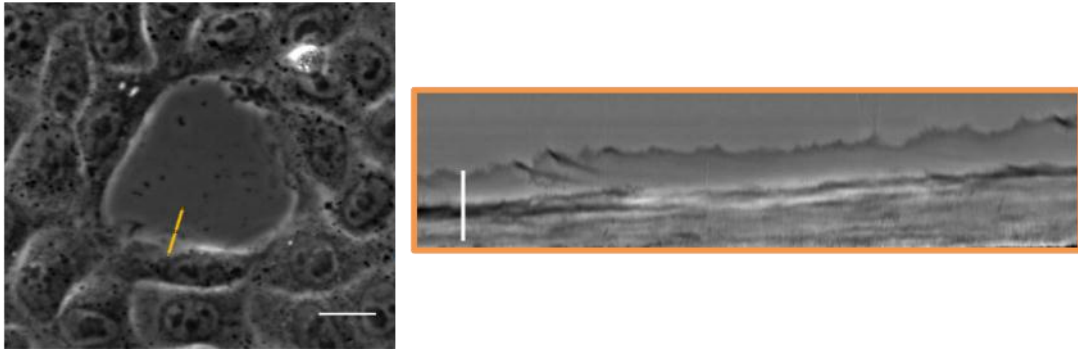
Figure 2. 15. Kymograph showing the advancement of the lamellipodia and cell body at the onset of closure, corresponding to the orange line indicated in the right snapshot. In the kymograph, the time acquisition was 1 frame/2 sec, scale bar is 3 μm.

These first experiments have revealed that: despite lamellipodia are present during the closure of all the gaps sizes tested, the dynamics of the closure differ depending on the size. Small gaps (≤20 μm) show a different behavior with respect to large gaps. These differences hint towards a size-dependent mechanism driving the closure of these gaps.

Since one of our aims is to uncouple the mechanism of closure from the presence or absence of death factors during the closure process, we have investigated if the observed dynamics of closure are universal for the closure of gaps independently of the presence of death factors. In order to do this, we have analyzed the decrease of area as a function of time for damage-associated gaps, i.e. ripped and crushed gaps. First, we have determined that both methods used for damage-associated gap patterning produce gaps with similar closure trends (Figure 2. 16. A). Because of the wound patterning protocol, the obtained wounds are more variable in their initial size, so for statistical purposes we pooled together wounds of similar initial areas ($\pm$ 500 μm^2) coming from different experiments. Interestingly, the dynamics of the closure of such wounds exhibit broader distributions due to variable initial conditions and the closure is not as regular as for clean gaps (Figure 2. 16. B). The trends of closure follow exponential decay laws as a function of time, different than the linear trend of closure observed for clean gaps closure (Figure 2. 16. C). This indicates that the presence of damaged cells or debris strongly alters the dynamics of epithelial gap closure. Importantly, the role of damage factors is more relevant in determining the trend of closure than availability of denuded space. Note that ripped gaps present free area as well as death factors, while crushed gaps do not present free space per se, but a wounded area of dead cells, and yet both damage-associated gaps close in a similar fashion. Interestingly, the closure dynamics of these "wounds" are consistent with reported data on embryonic wound healing and adult epithelial wound closure (Figure 2. 16. D) (Danjo and Gipson, 2002; Abreu-Blanco et al., 2011).
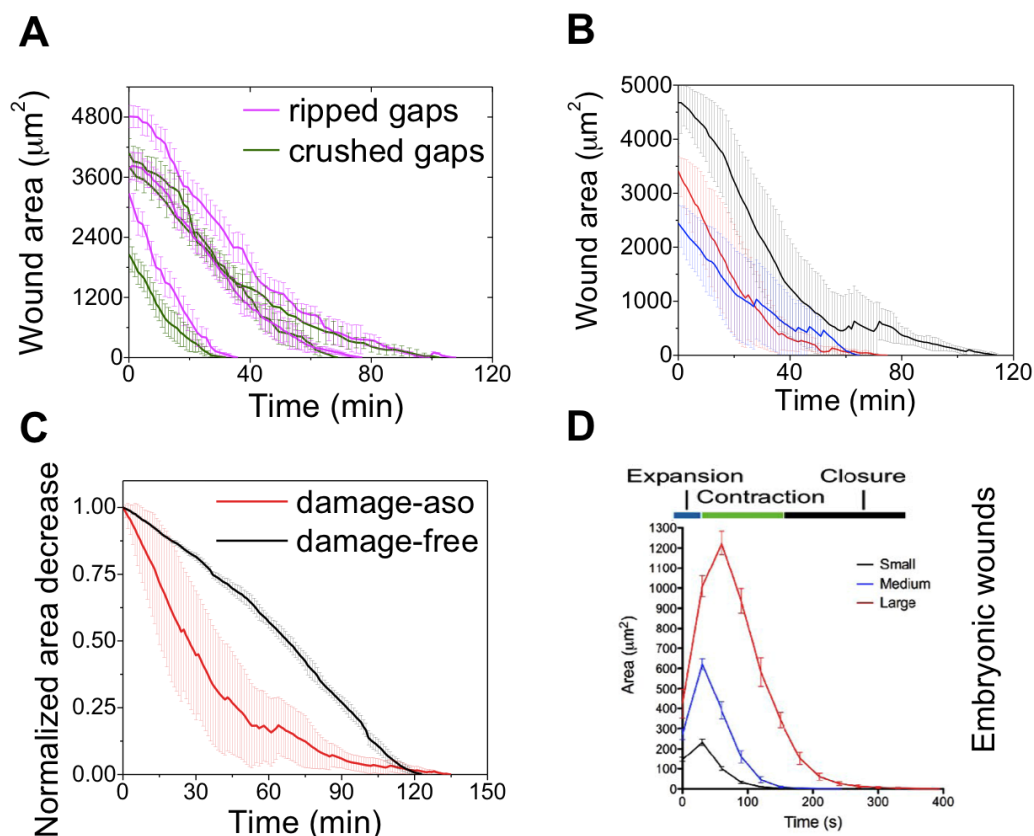
Figure 2. 16. Decrease of area in "wounds" within epithelial monolayer. (A) Decrease of wound area over time for damage-associated gaps, comparing the two methods used for patterning the wounds (ripped versus crushed gaps). Each line shows 3 gaps analyzed in the same sample. (B) Area of the wound as a function of time. Many experiments (>8 for each condition) have been pooled according to the initial area of the wound, i.e. blue line corresponds to wounds initially ranging from 2000 to 3000 µm², red line are 3000 to 4000 µm² initial area wounds, and black are 4000 to 5000 µm². Crushed and ripped gaps have been pooled together. Note that they present a very broad distribution. (B) Comparison of the area decrease for damage-associated gaps (crushed and ripped gaps) with respect to damage-free gaps (performed with the pillar removal assay). (D) Closure rates for wound in embryos, from (Abreu-Blanco et al. 2011).

3.3. Cell movements during gap closure

Time-lapse monitoring during closure also reveals significant fluidity in the cell culture. This fluidity is more obvious for larger gaps, where cells are allowed to migrate into larger spaces and thus for longer times. Cells can be observed moving relative to one another and changing neighbors. These cell rearrangements have been observed as well in other *in vitro* experiments, and can be explained by a decrease in cadherin and desmosome adhesiveness (Wood et al., 2002).

127

In order to better characterize cellular reorganizations and movements, we have analyzed the cell shapes and dynamics along the process. First, we have tracked the trajectories of cells during closure by automated tracking of labeled nuclei (for a detailed protocol on nuclei tracking see Annex F) (Figure 2. 17. A and B). The trajectories show that cells at the first row experience directed motion towards the center of the gap and moved 98%±20% of the gap initial radius (Figure 2. 17. A-C). Cells behind the leading edge show progressively smaller and less persistent displacements (55% for the second row, 16% for outer cells). Cells far from the gap (tracked in the corners of the field of view) move randomly and result in short effective displacements. This indicates that the migration of cells is coordinated and regulated in a graded fashion from the gap bordering cells towards inner cells in the monolayer. Such model could resemble the movement described for contact inhibition of locomotion in the context of collective cell migration, which accounts for the extension of lamellipodia at areas where there are no neighboring cells (the cell-gap interface) (Carmona-Fontaine et al., 2008; Mayor and Carmona-Fontaine, 2010). When these first cells would displace, the following row would be released of the inhibition induced by the neighboring front cell and move as well, and so forth. However, MDCK cells have been reported to extend cryptic lamellipodia far inside the monolayer, independently of the presence of neighbors around all cell perimeter, proving the absence of an inhibitory signal of contacting cells (Farooqui and Fenteany, 2005).
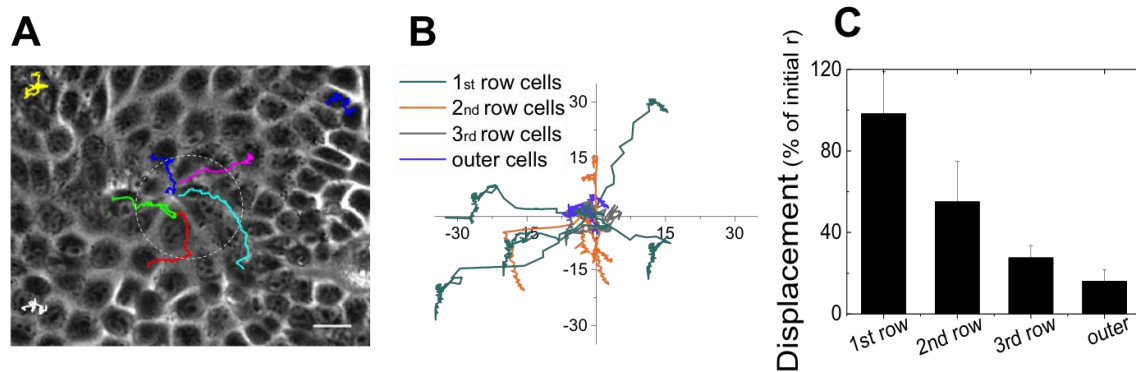

Figure 2. 17. Cell rearrangements during gap closure. (A) Tracking of cells during the closure process. The tracks are shown after closure is completed. The dotted line in the phase-contrast image represents the original gap margin. Scale bar is 20 μm. (B) Cell trajectories of the tracked cells. Graph shows the trajectories (axis in μm) as a function of the cells' position with respect to the gap edge (i.e. 1st row correspond to cells contacting the gap, 2nd row refer to those behind, and consecutively). Trajectories are shown for one experiment, trends being representative of 3 more experiments analyzed. (C) Displacement of cells at the end of closure with respect to the beginning of the experiment, depending on their position with respect to the gap.

Together with cell migration, cells experience shape rearrangements and polarization. By analyzing the changes in nuclei circularity, we could observe how nuclei elongate in the direction of migration for the cells at the first row (Figure 2.

18. A). This elongation is more prominent in cells extending lamellipodia, hinting towards a relationship of nuclei elongation, cell polarization, and lamellipodial extension. Alongside, cells also change shape and elongate along the direction of migration, acquiring a wedge-like morphology (Figure 2. 18. B). At the closure time point, cells typically form a rosette-like structure that would be later dissolved through epithelial remodeling (Figure 2. 18. C). Interestingly, this rosette-like structure has been observed in various situations related to the closure of circular or small gaps (Bement et al., 1993), apoptotic cell extrusion (Rosenblatt et al., 2001), cell delamination (Muliyil et al., 2011), embryonic healing (Meghana et al., 2011), and *in vitro* wound healing (Tamada et al., 2007).
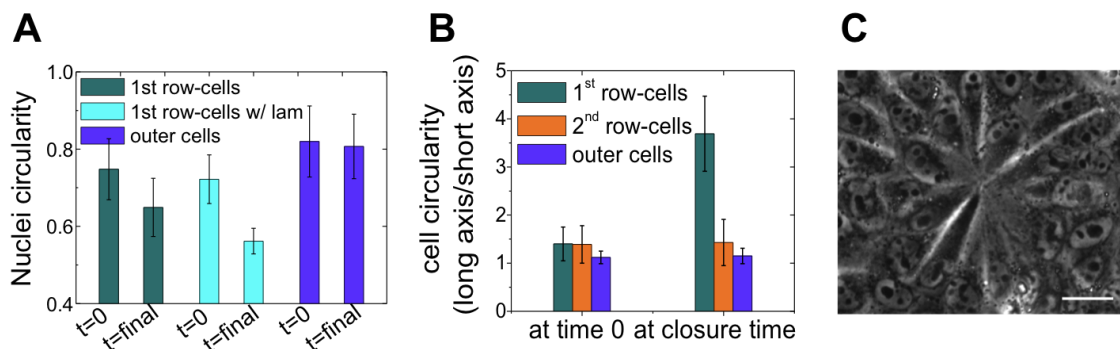

Figure 2. 18. Cell shape reorganizations during gap closure. (A) Changes in nuclei circularity during closure. Cells analyzed correspond to those contacting the gap (border cells), cells at the edge of the gap that extend lamellipodia during the closure, and cells far from the gap (outer cells) (typically taken at the four corners of the field of view). Data are means and standard errors from at least 8 analyzed gaps. (B) Changes in cell circularity (long axis/short axis) from the onset to a complete closure, as a function of cell's position with respect to the gap. (C) At the end of closure, cells have acquired a rosette-like structure. Scale bar is 20 μm.

Altogether, these results indicate that first-row cells detect the presence of free space, extend lamellipodia, and also polarize in the direction of the gap. These changes indicate that the closure response is an active and directed process governed by cells at the leading edge. The fact that free space is enough to trigger cell migration has also been hinted in previous experiments of exposure of cells to a free space (Nikolic et al., 2006; Poujade et al., 2007). During the closure of large gaps cells at the leading edge have been proposed to have a prominent role in the colonization of new space, as suggested in many studies characterizing the appearance of leader cells (see Chapter 1 section II. 3. 5) (Poujade et al., 2007; Omelchenko et al., 2003; Mark et al., 2010). As occurs in our experiments, these first-row cells extend lamellipodia to protrude into the denued area. Moreover, these studies report fingering structures that emerge from a migrating flat front as columns of few to dozen cells, with a leader cell at the tip (Omelchenko et al., 2003; Poujade et al., 2007). According to Poujade et al. fingering starts to appear after 1 h of migration into the gap, while Omelchenko et al. reported 4-6 cell-containing

finger-like structures emerging after 4-6 h. In our experiments, no finger-like structures appear. This can be due to a lack of space in the analyzed gaps (for the ones <60 μm, since fingering structures take time to appear). Even in the case of the larger gaps analyzed, i.e. 150 μm in diameter, which take around 6 hours to close, we did not observe fingers of cells preferentially protruding on the gap edge. This can be explained by either the absence of cell damage or the line tension accumulated at the gap-cells interface (given the circularity of the closing gap), which would prevent the preferential protrusion of few cells above the others.

3.4. Influence of substrate stiffness

Given the relevance of lamellipodial protrusion in our gap closure experiments, it is reasonable to wonder how these lamellipodia interact with the substrate. The interaction of lamellipodia with the substrate has been reported to be highly affected by substrate stiffness (Pelham and Wang, 1997; Lo et al., 2000; Jiang et al., 2006; Giannone et al., 2004). In order to assess the effect of substrate stiffness in our gap closure model, we carried out gap closure experiments in substrates of varying stiffnesses. Due to technical limitations, we chose PDMS as a substrate of tunable stiffness. By varying the crosslinking ratio of reticulant agent:base, PDMS of different stiffnesses can be obtained, down to 3-8 KPa for 1:60 crosslinker:base ratio [Mirjam Ochsner PhD manuscript, (Ochsner et al., 2007; Murrell et al., 2011)]. For PDMS substrates, we also verified that ECM coating was not affected by the PDMS material properties. Indeed, fibronectin is present beneath the cells and in the gap area, similar to the control conditions (in glass substrates) (Figure 2. 9. F).

Regarding the dynamics of closure, we have first analyzed gap closure in substrates of similar stiffness as glass, i.e. using PDMS substrates at 1:10 crosslinking ratio that render a Young's modulus of 0.5-2 MPa, which is sensed as an infinite stiffness by cells [above a certain stiffness threshold of tens to hundreds of KPa, cells cannot discriminate higher stiffnesses (Tee et al., 2011)]. Gap closure in 1:10 PDMS substrates show no differences either in dynamics or in closure time with respect to control experiments (in glass). We have analyzed two different gap sizes (20 and 50 μm in diameter, a so-considered small and large gap respectively) to discriminate if there are differences in the closure as a function of substrate stiffness depending on the gap size. As the stiffness decreases, we observe a drastic decrease of the migration speed of the cells into the gap (a 2.7 increase in closure time of 20 μm gaps and 1.9 in 50 μm gaps) (Figure 2. 19. B). Furthermore, softer substrates (1:40 and 1:60) prevent the final closure of the gap even after 300 min as well as the formation of lamellipodial protrusions (Figure 2. 19). In such soft

substrates (1:60), cells are not migrating in a directed manner towards the center of the gap, but acquire varied trajectories so that no closure is attained (Figure 2. 19. A). Since the dynamics of lamellipodia is closely related to the application of tension to cell-substrate adhesions by acto-myosin contraction, it is likely that cells on such soft substrates cannot sustain a maintained extension of lamellipodia (Giannone et al., 2004; Vogel and Sheetz, 2009). Therefore, stiff substrates are needed to generate the activation of the lamellipodium around the gap and stabilize it. Since cells are probing substrate stiffness by applying contractile forces (Pelham and Wang, 1998; du Roure et al., 2005; Saez et al., 2005), it appears that the pulling force induced by leading cells that exhibit lamellipodial protrusions can be a key player in our experimental model of epithelial closure.

Besides the extension of lamellipodia, substrate stiffness can also affect cell polarization through a differential distribution and dynamics of focal adhesion formation, maturation and maintenance (Prager-Khoutorsky et al., 2011). As such, in soft substrates cells could not polarize properly and thus migration is not directed, resulting in a failure of gap sealing.
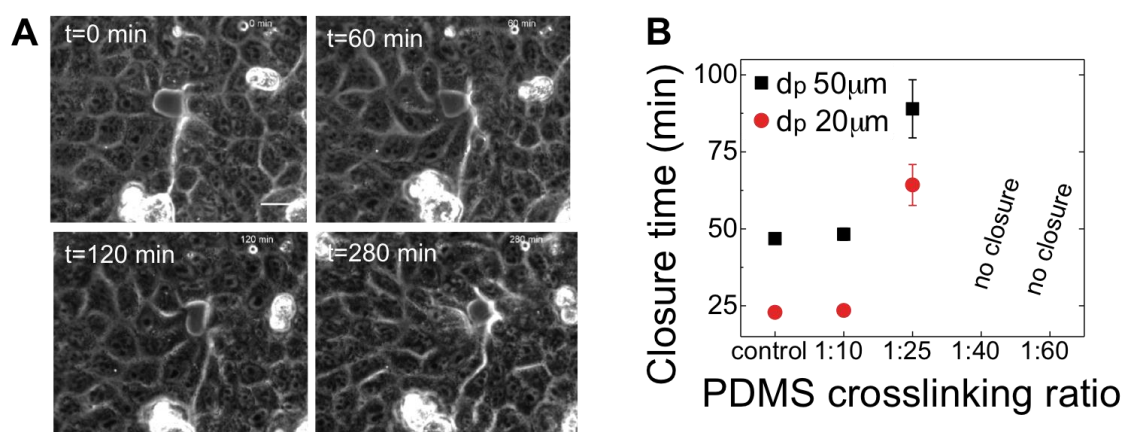

Figure 2. 19. Effect of substrate stiffness on the closure of gaps. (A) Micrographs from a time-lapse experiment of the closure of a 20 μm –diameter gap in 1:60 PDMS crosslinking ratio. Note that the gap changes shape but does not complete closure for at least 300 min recorded. (B) Quantification of the closure time of two different gap diameters, 20 and 50 μm. X-axis indicates the PDMS ratio used to attain different stiffnesses. *No closure* stands for gaps that were not closed after 300 min.

Nevertheless, we do acknowledge a possible effect of the PDMS material properties on the cell response. Although PDMS has been recurrently used as a substrate of tunable rigidity for cell behavior and migration studies, its vosco-elastic properties can also affect cells (Trappmann et al., 2012; Douezan et al., 2012; Murrell et al., 2011). For instance, it has been proven that the pore size of the material can determine the density and architecture of ECM coating and impact on the differentiation of stem cells (Trappmann et al., 2012).

Experiments in tuned substrates stiffness are interesting for their biological implications. *In vivo*, cells migrate in a variety of different substrates or even over other cells. Epithelial cells migrating over a basal lamina typically detect stiffnesses in the range of several to dozen KPa. On the other hand, during wound healing, the wound bed is rich in fibrin, fibrinogen, and collagen, rendering this provisional matrix stiff for cells to migrate over (Tomasek et al., 2002). In other gap closure events, such as *Drosophila* dorsal closure, it is not clear what stiffness might epithelial migrating cells sense beneath them, as they migrate over a layer of amnioserosa cells. Thus, the stiffness that epithelial cells detect while migrating can be stiff or soft, since it varies depending on the *in vivo* niche. More data on the mechanical aspect of the matrix or underlying cells *in vivo* is required to better address the dependence of migration on the stiffness.

3.5. Influence of cell density

MDCK cells are epithelial cells which can undergo epithelial-to-mesenchymal transition (Nicolas et al., 2003). When a confluent monolayer is at low density, MDCK cells are typically highly spread and flat, while in higher densities they become taller, cuboidal cells (Figure 2. 20. C). One could argue, therefore, that cells at low packing degrees are already in a pro-migratory mesenchymal-like state, thus the protrusion of lamellipodia and active cell migration observed would not be a *de novo* response triggered by the sudden availability of free space. We have thus investigated how could the cell density influence gap closure in our set-up. We have tested different cell packing densities, ranging from highly spread and flattened cells to the maximal density of cells within the culture, always after confluence is reached (Figure 2. 20. B). In all densities analyzed, lamellipodia are extended by gap surrounding cells. For large gaps (30 and 60 μm diameters), cell density has no impact either on the closure time or on protrusive activity (Figure 2. 20. A). In addition, this result confirms that the closure mechanism is not triggered by a possible release of the internal pressure within the epithelial cell sheet after the removal of the pillar but instead by the lamellipodium extension. However, for the smallest gaps, there is a decrease in the closure time as packing density increases, further suggesting that distinct mechanisms govern the closure of small versus large gaps (Figure 2. 20. A).
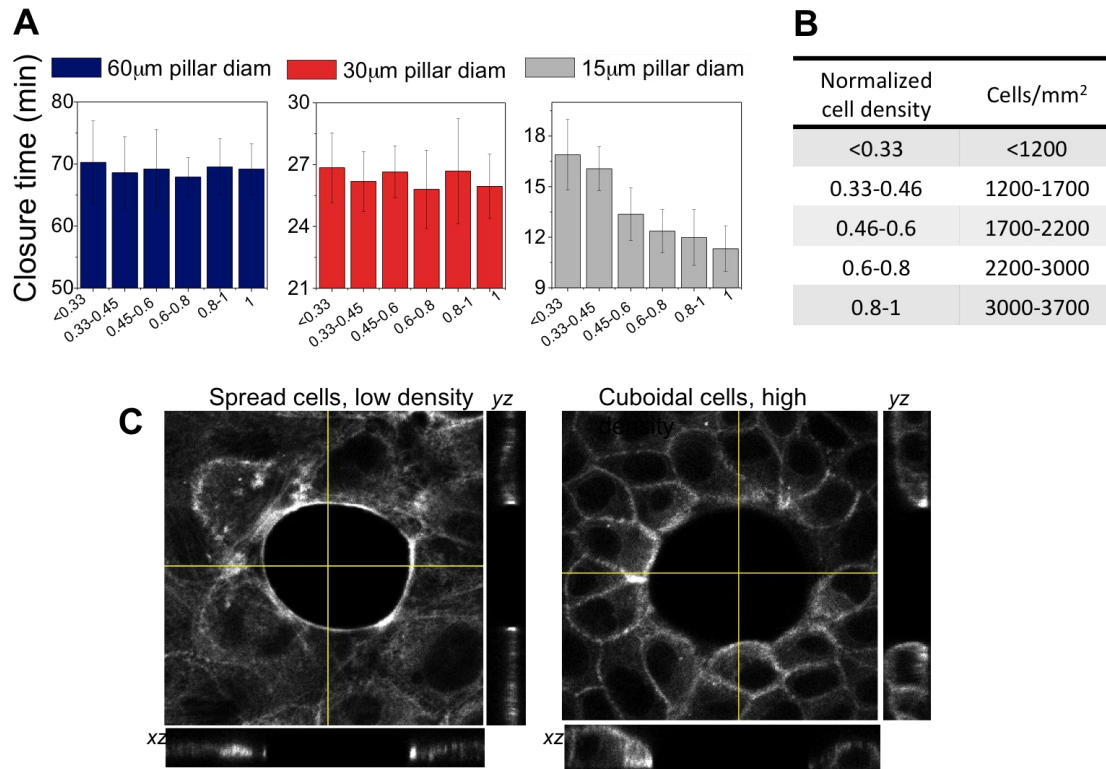
Figure 2. 20. Effect of cell density on closure. (A) Closure time as a function of cell density, examined for 3 different gap diameters (60, 30 and 15 μm gap diameter). Cell density is indicated in the x axis, and is calculated from (B). Each graph shows the experiments from a different pillar diameter. (B) Number of cells considered for the grouping on different degrees of cell density, always after reaching confluence. Normalized cell density is obtained by dividing the number of cells per mm2 by the maximal number of cells per mm2. The bin labeled as <0,33 depicts low density and the bin 1 is the mean of the 3 experiments at highest density (>3700). (C) Effect of cell density on cell monolayer thickness. Central images are the mid plane of a z-stack, and bottom and right images are orthogonal projections of the stacks on the yellow lines. In the left image is shown how right upon reaching confluency, cells are highly spread and thus flat. As cell density under the pillar stencil increases, cells become smaller and taller, as shown in the right image. In highly packed cultures, the thickness of the layer is greater than in sparse epithelia. As can be observed in the xz and yz orthogonal projections, the lateral membrane in dense cultures is larger. Details on confocal data acquisition can be found in Annex F.

3.6. Inhibition of gap closure regulators

Regarding the regulation of epithelial gap closure, two main regulatory pathways have been proposed to control the closure, according to the two mechanisms of closure (purse-string and cell crawling). Rac1 has been reported to drive the closure by controlling the extension of lamellipodia (Fenteany et al., 2000), and MLCK and ROCK have been proposed to regulate the assembly and contraction of the acto-myosin cable (Tamada et al., 2007; Russo et al., 2005; Desai et al., 2004) (Figure 2. 21. A). However, as it has been previously described, it is not

clear to what extent both regulatory pathways could be active simultaneously or at different stages [see Chapter 1 section II. 8. 1. and (Bement et al., 1993; Garcia-Fernandez et al., 2009)]. In order to gain some insight into the regulation of the closure mechanism, we have performed different inhibitory treatments of these regulators, analyzed the phenotypical changes during closure, and measured the effect in the closure time. We have used the different inhibitors:

- Rac1 inhibitor NSC23766 (Calbiochem) to deplete lamellipodial activity. Rac1 inhibitor is a cell-permeable pyrimidine compound that specifically inhibits Rac1 GDP/GTP exchange activity by interfering with the interaction between Rac1 and Rac- specific GEFs Trio and Tiam1, rendering Rac inactive.
- ML-7 (Calbiochem) to inhibit MLCK. ML-7 is a cell permeable compound that inhibits Ca^{2+}-calmodulin-dependent and -independent smooth muscle myosin light chain kinases by competing for the binding site of ATP (Saitoh et al., 2001).
- Y27632 (Calbiochem) to inhibit ROCK. Y27632 inhibits all types of ROCK by competing with ATP for the catalytic binding site (Narumiya et al., 2000).
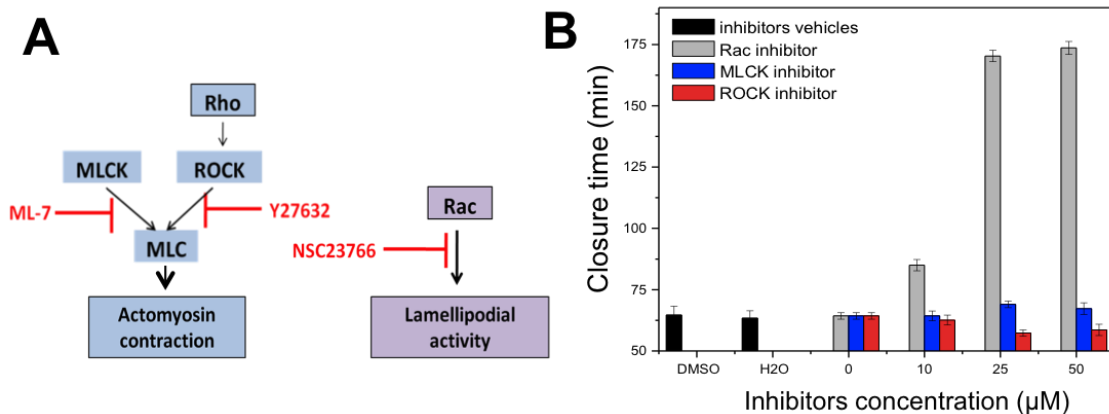

Figure 2. 21. Inhibitory treatments performed in the gap closure model. (A) Scheme of the mechanism of action of the pharmacological inhibitors used. (B) Dose-inhibition response curve for the different inhibitors used (NSC23766, Y-27632 and ML-7) and their vehicles (either DMSO or water). The three concentrations tested are the most recurrently found in literature. 25 μM proved to be an adequate inhibitory concentration in our set-up.

We have performed a dose-inhibition response curve and can conclude that 25 μM is an appropriate concentration for an optimal inhibition (Figure 2. 21. B).

Phenotypically, we observe that inhibition of MLCK and ROCK does not prevent the extension of lamellipodia. Rac1 inhibition, however, precludes the appearance of lamellipodia (Figure 2. 22).
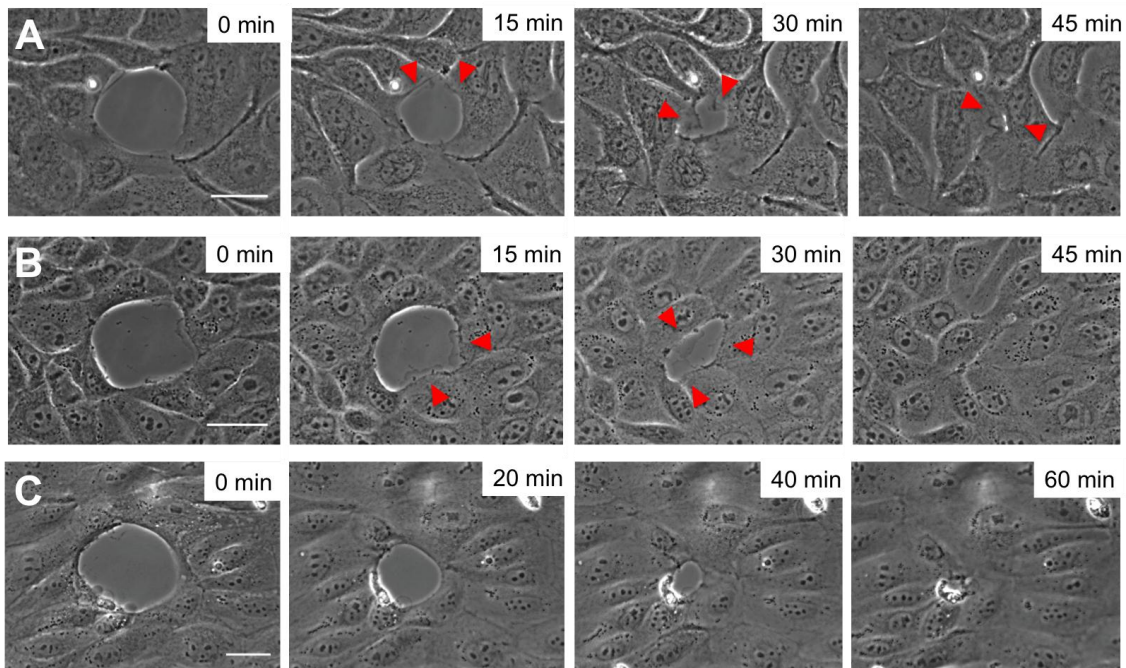
Figure 2. 22. Snapshots of a time-lapse movie of gap closure under different inhibitory treatments. Red arrowheads indicate where lamellipodia protrude. Scale bars are 20 μm. (A) MLCK Inhibition. (B) ROCK inhibition. The closure of the gap is more irregular, less isotropic. (C) Rac1 inhibition. Note there are no lamellipodia protruding. Gap is closed in a very isotropic manner.

Regarding the closure time under the different inhibitory treatments, we do not observe an effect of the inhibition of MLCK and ROCK on the closure for any of the gap size tested (Figure 2. 23. A). On the other hand, the inhibition of Rac1 drastically slows down the closure process of large gaps, while does not affect closure of small gaps (≤20 μm). The larger the gaps, the more affected the closure is by Rac1 inhibition (Figure 2. 23. B). As it can be observed in Figure 2. 22. C, Rac1 inhibition precludes the extension of lamellipodia and maintained a strong circularity of the gaps throughout closure, as shown by the maintenance of the shape factor a close to 1 (Figure 2. 23. C).

It is interesting to note that small gaps are insensitive to any of the pharmacological treatments. Such small gaps also present a different trend of closure, as well a dependency of their closure time on the density of the monolayer. This strikingly universal behavior in the closure of small gaps is suggestive of a mechanism of purely physical origin. One such mechanism could be cell spreading based on an unspecific mechanical balance between cell-substrate adhesion and cortical tension (Cuvelier et al., 2007), similar to how a drop spreads on a surface. This mechanism has been shown to produce a linear dependence of spreading area with time. Moreover, it is consistent with the reported decrease of closure time with higher cell densities only in the case of small gaps. When cells are highly packed, they become more columnar and thus offer larger lateral area

for cell spreading (Figure 2. 20. C). Larger gaps, however, even if undergoing the same process of passive spreading, present a too large area for the gap to be closed only by cell spreading. In this case, "active" mechanisms of closure would be required, which appear to be the closure by Rac-regulated cell crawling.
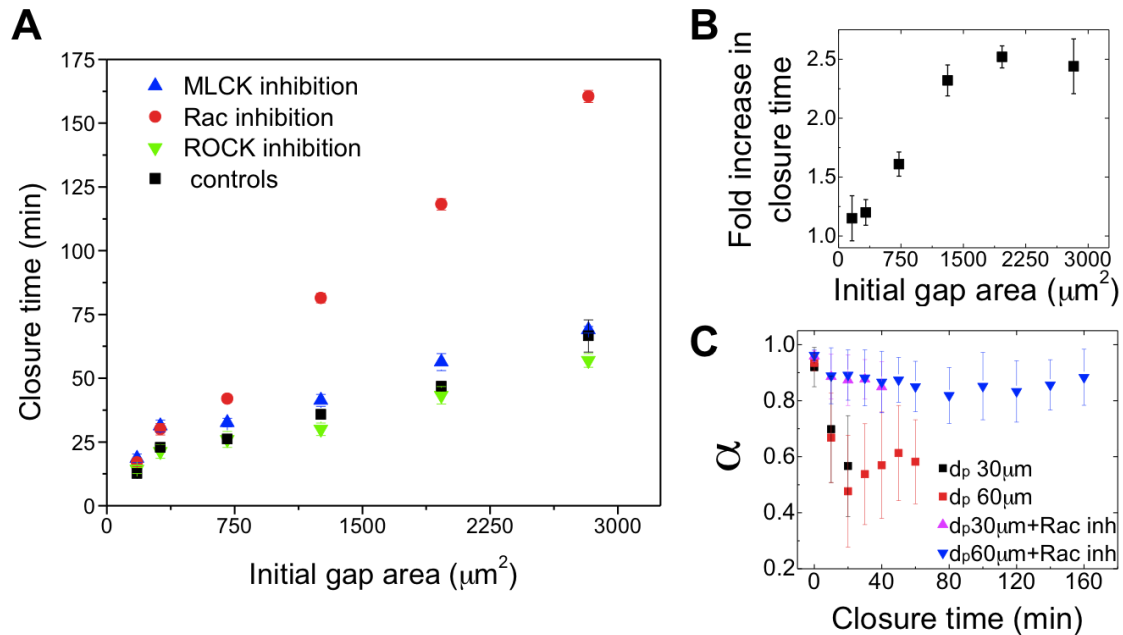

Figure 2. 23. Inhibitors effect on the gap closure process. (A) Closure times of the different gap sizes in control conditions and subjected to drug treatments of the regulators (MLCK, ROCK and Rac1 inhibition, for 6 gap sizes). Data points represent means and error bars are standard errors of seven analyzed gaps. (B) Fold-increase in the closure time of Rac1-inhibited cells with respect to control conditions for the 6 different gap sizes. (C) Evolution of roughness α at the cell-gap interface. Experiments performed with two pillar sizes, 30 and 60 μm in diameter. Controls are also showed for a comparison. Data points represent means and error bars are standard errors of five analyzed gaps.

Interestingly, Rac1 inhibition does not have such a slowing down effect in damage-associated gaps, which progress similarly to non-inhibited damaged-gaps (Figure 2. 24). This is further suggesting that damage-free gaps follow a different and specific mechanism of closure, which we show here to be highly dependent on the Rac1-regulated lamellipodial extension.
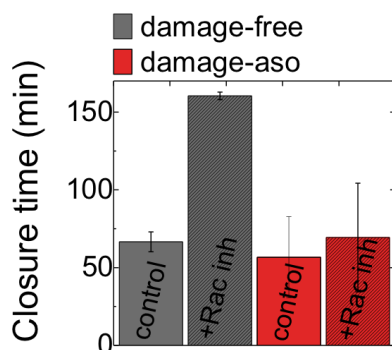

Figure 2. 24. Closure time of damage-free gaps (from pillar removal assay gap patterning) versus closure time of damage-associated gaps (ripped and crushed gaps), and the effect of Rac1 inhibition in their closure time. Data are means and standard errors of at least 8 analyzed gaps or wounds.

3.7. Acto-myosin distribution during gap closure

To further analyze the possible contribution of the purse-string mechanism in our closure model, we have investigated acto-myosin distribution at the gap edge.

First, we have wondered whether the presence *per se* of PDMS pillars for the gap patterning triggers actin accumulation at the pillar periphery. Actin does not majorly accumulate at the cells-pillar interface, as shown by phalloidin staining in micropillar-present fixed samples (Figure 2. 25. A). However, phalloidin staining immediately after pillar removal shows that actin accumulates in a continuous supracellular cable-like structure at the margins of the gap (Figure 2. 25. B). We have quantified the intensity of actin signal from a pool of different pillar-containing samples and from gap-containing samples (since we have used pillars and gaps of 50 μm in diameter that are very close to a perfect circle, they can be easily averaged). The profile of actin intensity in the gaps after removal of the pillar shows a sharper peak of actin accumulation at the gap-cells interface when compared to the pillar-cells interface. Thus it appears that the pillars do not induce clustering of actin at their walls.
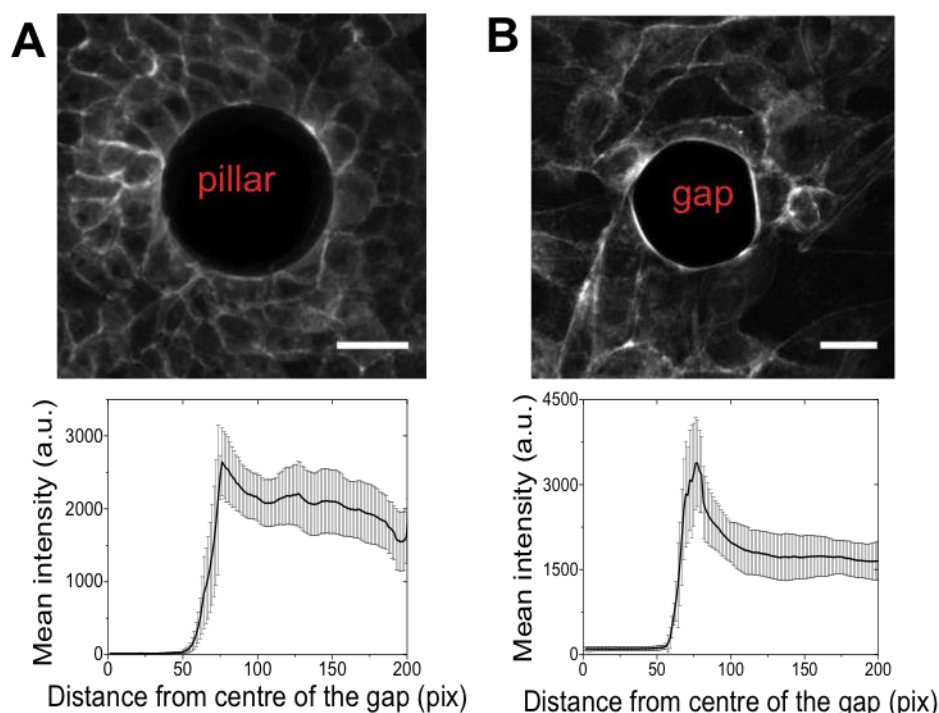

Figure 2. 25. Actin accumulation at the pillar-cells and gap-cells interface. (A) The presence of the pillar does not promote accumulation of actin surrounding the pillar. The graph shows the quantification in radial profiles of the actin signal (from phalloidin staining) by plotting the fluorescence intensity at a given distance from the center of the gap (average intensity of concentric circles of increasing diameter starting from the center). At least 8 different pillars of 50 μm have been pooled together for the quantification. (B) 2 min after releasing the pillar stencil, there is some

actin clustering at the cells-gap interface. The quantification of the actin signal shows a higher peak of actin fluorescence at the cells-gap interface with respect to the cells-pillar interface.

However, actin assembles into a supracellular cable right after removing the pillar stencil. This surrounding actin cable is then disrupted as closure proceeded: the discontinuity of the actin cable is concomitant to the formation of cell protrusions such as the extension of multiple lamellipodia into the gaps (Figure 2. 26), as also shown by the values of the roughness α (Figure 2. 13. C). Moreover, based on confocal images in the *x-z* and *y-z* planes, it appears that areas of actin accumulation localize at the lateral surface of cuboidal cells whereas lamellipodial extension induces a flattening of the monolayer with a more diffuse and homogeneous actin distribution (Figure 2. 26. B). While one could argue that actin cable could be more prevalent in densely packed cultures and less prevalent in highly spread monolayers, we have verified that this is not the case. Both in dense cultures (Figure 2. 26. A) and in sparse cultures (Figure 2. 26. B), there are regions of actin accumulation in cuboidal-like cells and regions lacking actin clustering while extending lamellipodia. Note also that, in the presented experimental conditions, actin typically accumulates at medial-basal level, and not apically as previously reported (Tamada et al., 2007).
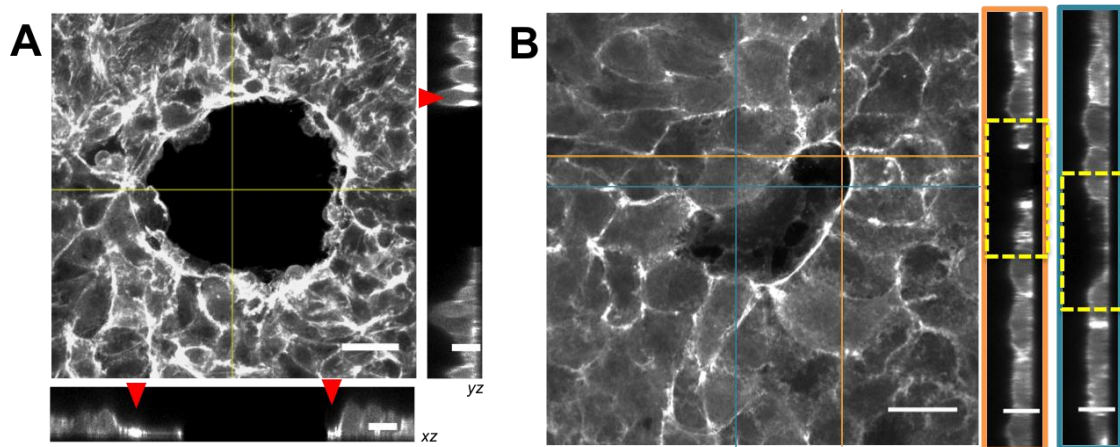

Figure 2. 26. Actin distribution along the z-axis: z-stack projections and xz and yz orthogonal projections. (A) Dense monolayer after 30 min of closure progression. Note how actin accumulates preferentially where lamellipodia do not extend and/or medial-basally. Orthogonal xz and yz projections correspond to the yellow lines. Scale bar is 25 μm in the z-projection and 5 μm in the orthogonal projections. (B) Sparse monolayer after 60 min of progression. As closure progresses, actin is still accumulated at the gap border where there are no lamellipodia (orange-boxed yz projection), while where the actin protrudes into the lamellipodia there is no actin clustering (blue boxed projection). Scale bars are 20 μm in z-projection and 5 μm in the orthogonal projections.

We have also stained for the presence of phospho-MLC (pp-MLC) as a marker for contractile myosin. We have chosen phospho-MLC as opposed to myosin or MLC to focus on the activation of myosin, since closure by purse-string has been

proposed to be based on the contraction of myosin (thus active, phosphor-myosin) and not only on the structural contribution of myosin as member of the cytoskeleton (Salbreux et al., 2009; Tamada et al., 2007). Staining of phospho-MLC shows that active myosin co-localizes with the actin cable immediately after pillar removal (Figure 2. 27). It is noteworthy that phospho-MLC signal is located only at the cells border in contact with the gap, thus it is a specific response to the presence of space. Junctional actin does not colocalize with phospho-MLC. And only the areas of major actin accumulation at the cells-gap interface colocalize with phospho-MLC (see for example how cell-cell junctions at the gap margin lack phospho-MLC staining). This lack of connectivity of the myosin cable among cells at the gap border suggests that it is not a functional purse-string, in the sense that it cannot account for the contraction of the belt inwards driving the closure.
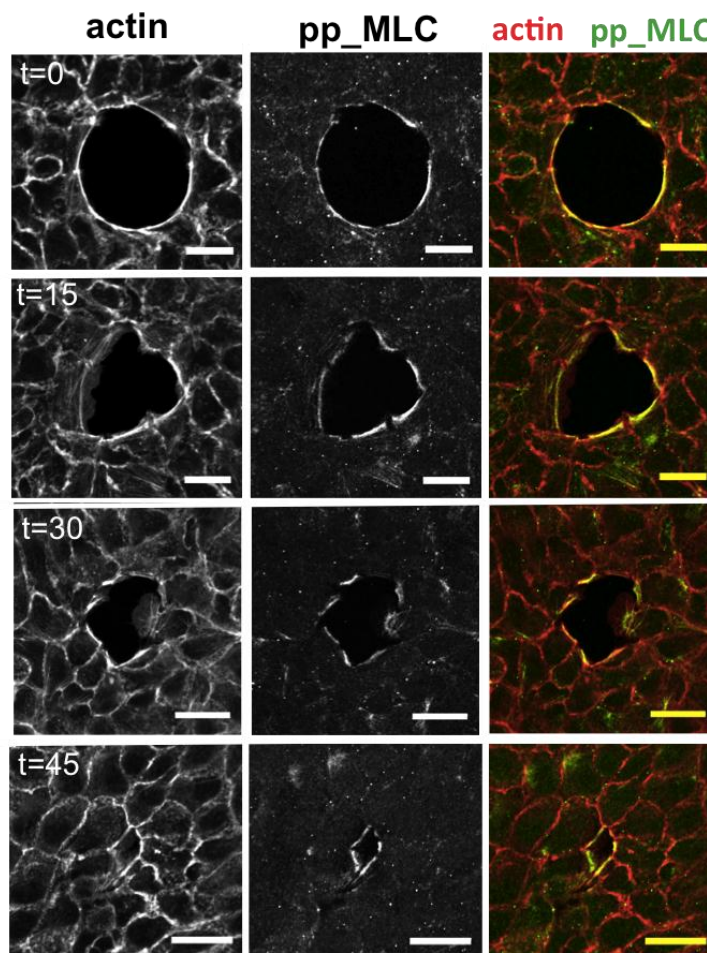

Figure 2. 27. Actin and phospho-MLC (pp-MLC) distribution during gap closure. Confocal images of immunostained actin and phospho-MLC. Note that actin and phospho-MLC accumulate at the gap margin at t=0 min, but do not progress as a continuous ring as closure proceeds (t=15, 30 and 45 min after pillar removal). All scale bars are 20 μm.

A similar picture of actin distribution was reported in Bement et al., 1993; where they supported implication of both mechanisms during the closure of a laser-induced wound in an embryo. In this study, they showed how actin accumulated preferentially at areas where lamellipodia do not protrude, while actin belt is disassembled when lamellipodia are extended. In the literature, previous results typically associated strong acto-myosin recruitment in wound

closure or laser ablation induced gaps. Moreover, it has been reported that apoptotic cells release signals that favor the assembly of a continuous actomyosin cable all around the dying cell to promote the extrusion of the cell from the monolayer (Rosenblatt et al., 2001). Our findings show that only an incomplete acto-myosin ring could form in the absence of cell injury, which strengthens the concept that death factors are required to develop a functional multicellular acto-myosin cable.

3.8. Coordination of cell movements by cell-cell junctions and myosin action

To further understand the role of cell-cell communications in the gap closure process, we have used an α-catenin knock-down MDCK cell line. As it has been previously explained in Chapter 1 section II. 1. 1, α-catenin is a member of the adherens junction complex, necessary for establishing cell-cell adhesions (Hartsock and Nelson, 2009). As shown by Benjamin *et al.,* α-catenin knock-down MDCK cells display increased membrane dynamics together with higher migration rates but exhibit a lack of cadherin-mediated cell-cell adhesion (Benjamin et al., 2010),. We have also observed an increased protrusivity in α-catenin cells. Since these cells do not form proper adherens junctions, they cannot support the formation of continuous multicellular cable surrounding the gap (Abreu-Blanco et al., 2011; Danjo and Gipson, 1998) as well as a collective behavior mediated by cell-cell interactions. In our experimental model, α-catenin cells do not migrate in a graded manner depending on their position with respect to the gap as the wild type cells, but instead move in an uncoordinated manner towards the gap center (Figure 2. 28. C and D). Thus, they displaced greater distances than *wild-type* MDCK cells due to their lack of coordination (Figure 2. 28. E). As we mentioned in Chapter 2 section 2.4, we define closure time as the time where no more available space can be measured. In this case, α-catenin cells close the gaps at a rate comparable to the *wild-type* MDCK cells (Figure 2. 28. F). However, the most appropriate term here would be that α-catenin cells fill the available space, since they do not establish cell-cell junctions among opposing cells at the final sealing step of the closure. These findings have been ascertained by using a Ca^{2+} chelation treatment. In this case, by adding EGTA to the medium, Ca^{2+} is sequestered and thus adherens junctions, who are Ca^{2+} dependent, are no longer present. These experiments suggest that such gaps can be filled by migrating cells independently of adherens junctions. In this situation, we observe filling of the denuded area, although we cannot ascertain the complete sealing of the gap. We acknowledge the possibility that other mechanisms might be at play in this situation, since these α-catenin cells do not migrate collectively in a strict sense, given that they lack a supracellular

coordination by cell-cell junctions. In this situation, gaps are closed because of the tendency of cells to migrate towards an empty space, which prompts cells to migrate inwards.
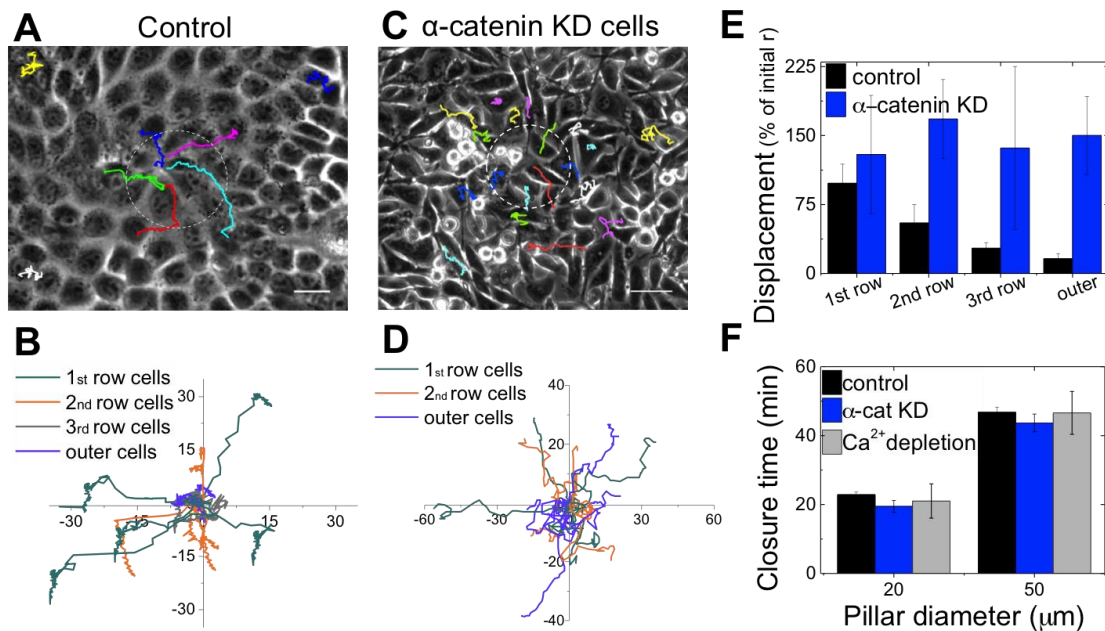

Figure 2. 28. Effect of cell-cell junctions in the coordination of the closure. (A and B) Trajectories of control experiments are included for comparison, from Figure 2.17. (C) Tracked α-catenin knock-down MDCK cells during closure, overlapped in the phase contrast image at the end of the closure. Scale bar is 20 μm. (D) Trajectories of the tracked cells as a function of their distance with respect to the gap. (E) Displacement of cells indicated as a percentage of the initial radius of the gap, for control and α-catenin knock-down MDCK cells, indicating the effective net movement of cells. Data represents means and standard errors of at least 3 experiments. (F) Closure time of 20 and 50 μm diameter-gaps of α-catenin knock-down MDCK cells with respect to control conditions. Data are means and standard errors from at least 12 analyzed gaps from different experiments.

We have also performed experiments of direct inhibition of myosin by blebbistatin treatment. Such blebbistatin inhibition, since it directly inhibits myosin independently of its regulators (MLCK, ROCK, LIMK or any other upstream kinases, as explained in Chapter 1 section I. 2. 1. 2) should directly interfere with purse-string contraction. Cells treated with blebbistatin extend very broad lamellipodia with considerable ruffling activity. When we track the cells trajectories, we find that cells move in an uncoordinated manner, displace longer distances, but their paths are not directed towards the center of the gap (Figure 2. 29. C and D). Moreover, the displacement magnitude is greater (aprox. 150% displacement of the initial radius) and independent of the distance from the gap edge (Figure 2. 29. E). Thus, the closure under blebbistatin treatment is achieved in an uncoordinated manner, resulting in a delay in the time of closure (Figure 2. 29. F). However, this delay in closure only affects the larger gaps (50 μm in diameter) (1,7-fold increase in the closure time), since there is more space to fill in this case.

Small gaps (≤20 μm) are not affected by the discoordinative effect of blebbistatin and thus their closure time is similar to control.
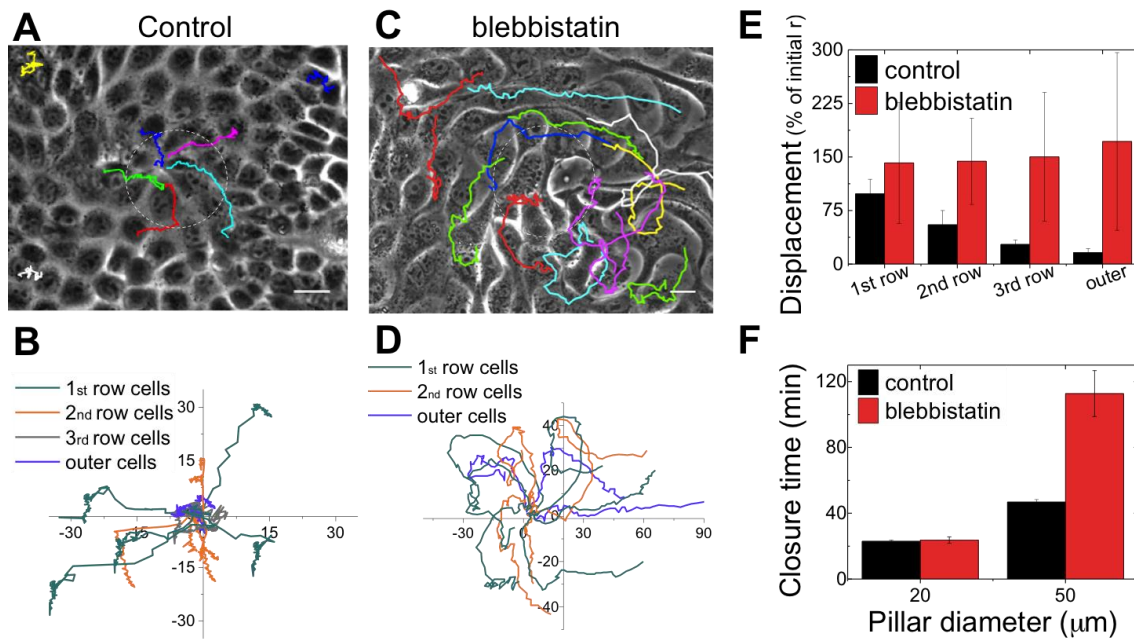

Figure 2. 29. Effect of myosin in the coordination of the closure. (A and B) Trajectories of control experiments are included for comparison, from Figure 2.17. (C) Tracked cells under myosin inhibition by blebbistatin, overlapped in the phase contrast image at the end of the closure. Scale bar is 10 μm. (D) Trajectories of the tracked cells as a function of their distance with respect to the gap. (E) Displacement of cells indicated as a percentage of the initial radius of the gap, for control and blebbistatin-treated cells, indicating the effective net movement of cells. Data represents means and standard errors of at least 3 experiments. (F) Closure time of 20 and 50 μm diameter-gaps of cells treated with blebbistatin with respect to control conditions. Data are means and standard errors from at least 12 analyzed gaps from different experiments.

This observation suggests that myosin may contribute to gap closure through a mechanism that is independent of purse-string contraction. Myosin IIA silencing or inhibition has previously been shown to cause increased membrane ruffling and migration speed in numerous cell types (Even-Ram et al., 2007), mostly analyzed for single cells. Indeed, in our blebbistatin experiments gap-contacting cells extend broad lamellipodia, and generally all cells migrate longer distances in the same time frame. Furthermore, myosin has recently been proposed to play an important role also in the coordination of migrating epithelial sheets (Vedula et al., 2012). In this context, blebbistatin treatment would cause a decrease in the acto-myosin mediated connectivity between cells (Lecuit and Lenne, 2007), increasing the length scale of the cooperative migration, which results in a loss of supracellular coordination of movements. In that line, our findings suggest that the role of myosin II is not to drive collective cell motion but to guide it, acting in the

coordination between cells at the gap edge but also inner-positioned cells to direct their migration towards the center of the gap.

In gap closure, the position of cells with respect to the gap can provide positional information for their collective behavior to close the gap, similarly to how spatial pre-patterning coordinates epithelial sheet migration during development (Galko and Krasnow, 2004; Martin and Parkhurst, 2004). For example, it has been proposed that the Ca^{2+} and MAPK activation waves reported in scratch-wound assays could help on the coordination of cell movements (Matsubayashi et al., 2004, 2011). But such coordinative role would presumable occur only in the presence of cell damage (Nikolić et al., 2006). Our data does not support Nikolic et al. hypothesis in this point. We show that there is a relationship between the displacement and the cell position relative to the gap (Figure 2. 28. E and Figure 2. 29. E). We propose that the coordination is accomplished by the actomyosin ring at the edge of the gap. In α-catenin knock-down cells and blebbistatin inhibition examples, such dependence is lost, as is the continuity between the cells. Thus, we believe that a supracellular coordination exists even in absence of damage-induced waves. As it has been previously discussed, some of the processes that occur during damage-induced migration can also occur in damage-free migration, but can be triggered by other signaling compounds.

4. Influence of the geometry of the gaps.

Epithelial gaps can appear in vitro and in vivo in various sizes as well as shapes. Dorsal closure in Drosophila, for example, presents an eye-shaped opening (Kiehart et al., 2000; Layton et al., 2009). Ventral closure, as well as other morphogenetic events, comprises ellipsoidal-like gaps (see Chapter 1 section II. 5. 2 and II. 5. 3). Epidermic wounds can display irregular shapes depending on the nature of the injury. On the other hand, in vitro gap closure studies usually consist on rectangular gaps (see Chapter 2 section 1. 1 and 1. 2). Thus, we have wondered about the effect of gap shape in our model of epithelial gap closure. Also, by varying the shape of the gap, we can study the influence of curvature in the extension of lamellipodia.

For this aim, we have fabricated squared and ellipsoidal-like pillars (hereafter referred as ellipsoidal pillars) of two different sizes (Figure 2. 30 A). Cells distribute randomly along the gap perimeter, with no preferential alignment of cells in areas of different curvature (Figure 2. 8. G-I). Live-cell microscopy shows that, regardless of the shape of the gaps, cells extend lamellipodia throughout closure and that these lamellipodia preferentially protrude along the edges with the lowest curvature (Figure 2. 30. B and C). We have analyzed the closure time of squared and ellipsoidal gaps relative to circular ones. Except in the case of the smallest square analyzed, gaps of ellipsoidal and squared shape close systematically faster than circular ones (Figure 2. 30. D). This faster response might be due to the enhancement of lamellipodial activity in regions of low curvature. A physical model has previously reported that epithelial cells can sense and respond to different global geometric conditions by detecting the curvature of the epithelial edge at a multicellular level (Mark et al., 2010).
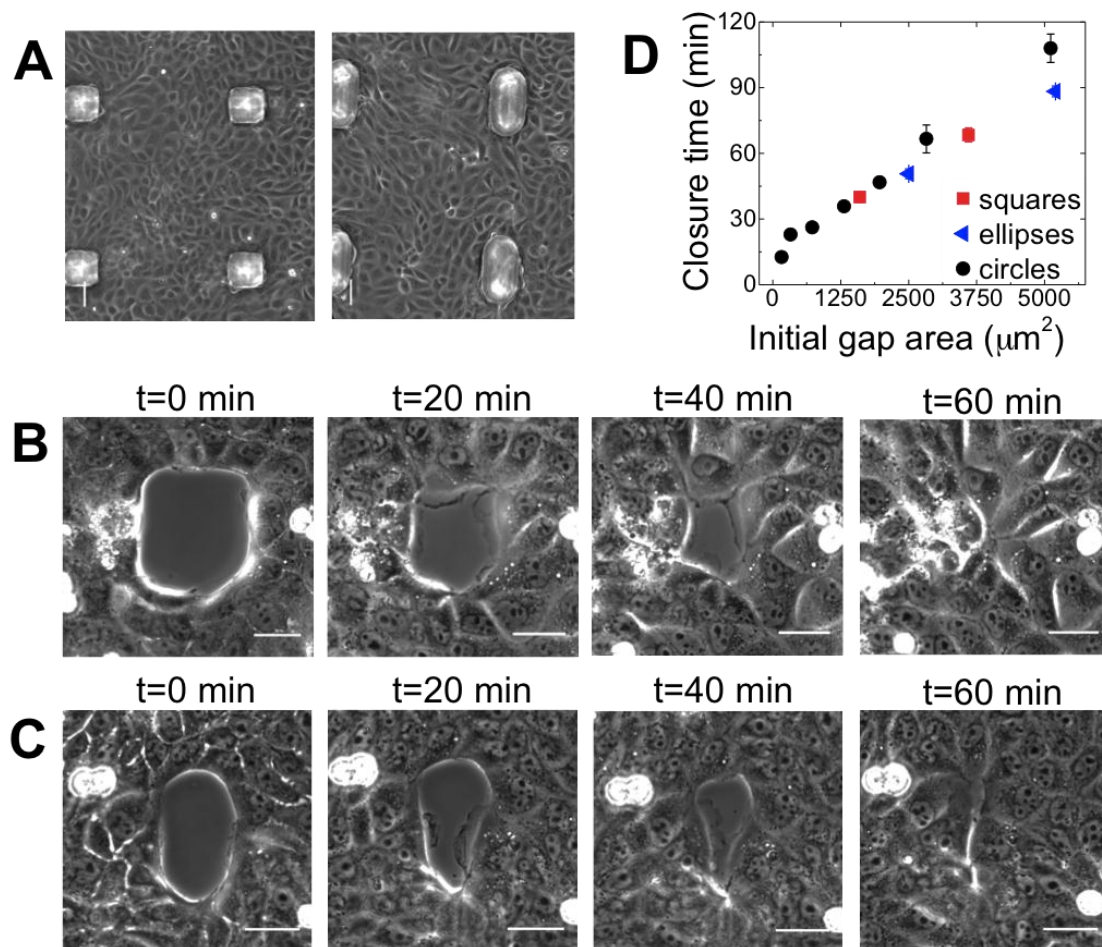
Figure 2. 30. Effect of geometry on gap closure. (*A*) Squared and ellipsoidal pillars were microfabricated following the same procedure as the circular pillars (PDMS molded from Si wafers) and squared and ellipsoidal gaps were patterned according to the described protocol for circles. (B) Sequence of phase-contrast micrographs showing the progression of a squared-gap closing. (C) Closure of an ellipsoidal gap. Scale bars are 20 μm. (*D*) Comparison of the closure time of the squared and ellipsoidal gaps with respect to circular. Data are means and standard errors for at least 12 gaps analyzed from different experiments.

Much as in the case of circular gap experiments, actin and phospho-myosin accumulate preferentially at areas in which lamellipodia do not protrude, thus a supracellular cable is not continuous (Figure 2. 31). Hence, these results indicate that the behavior observed in the closure of circular gaps applies also to different gap geometries. This result is in good agreement with previous studies showing that large wounds (i.e. lower curvature) are preferentially Rac-dependent whereas small ones (i.e. larger curvature) exhibit a purse-string mechanism (Fenteany et al., 2000; Tamada et al., 2007).
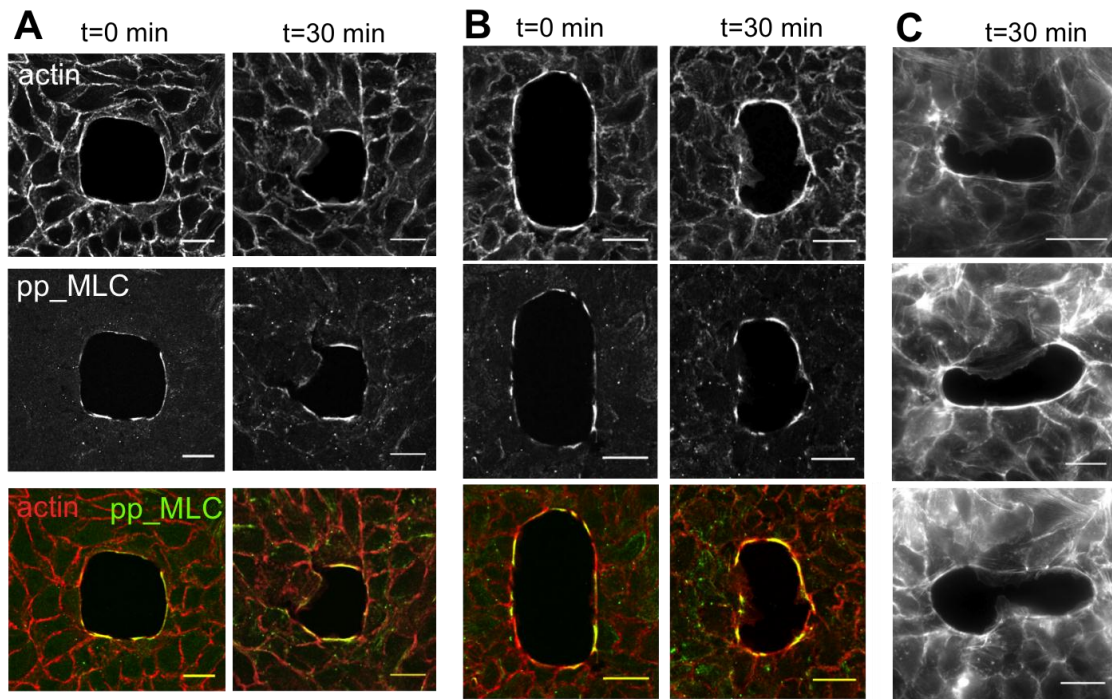
Figure 2. 31. Localization of actin and phospho-MLC (active myosin) right after removing the pillar and 30 min after the progression of closure. (A) Actin (shown by phalloidin staining) and phospho-MLC (immunostained) around squared gaps. (B) Actin and phospho-MLC around ellipsoidal gaps. (C) Epifluorescence micrographs of actin distribution in the closure of ellipsoidal gaps 30 min after pillar removal. All scale bars are 20 μm.

Along this line, we are currently working on the better characterization of the effect of curvature on the closure of gaps. We have observed that curvature has an impact on the extension of lamellipodia, as lamellipodial protrusions are boosted in straight edges rather than in highly curved areas. Thus, we will assess shapes containing differently curved areas and localize where lamellipodia are preferentially extended (Figure 2. 32. A and B). Moreover, there are theoretical models that predict the growth of a confined cell colony of a given geometry. For rectangular colonies the faster expansion is calculated to occur at the corners (Mark et al., 2010). However, such theoretical approaches have not addressed the closure of gaps, which represents the opposite situation to the expansion of a colony. In this regard, we will experimentally investigate where lamellipodia protrude preferentially for different shaped gaps. Furthermore, we will correlate the areas of different curvature with Rho and Rac activation. We will analyze as well if Rho and Rac activation depend only on the degree of curvature of the cell-gap interface or if they are also influenced by the convexity or concavity of a given curved region.
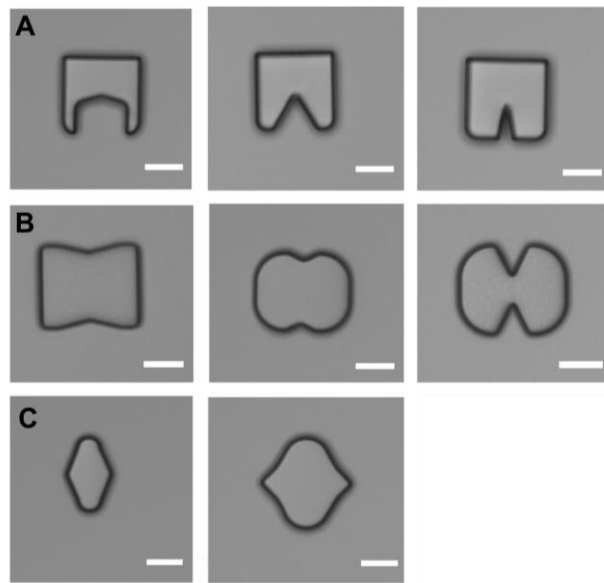
Figure 2. 32. Pillars produced to study the effect of gap shape in the closure. (A) These patterns with a preformed finger will be used to study the preferred direction of closure. (B) These patterns will be used to study differential zones of Rac and Rho activation. (C) These patterns will be used to analyze the effect of the angle at the canthi to see how it can promote a zippering activity at these edges. Scale bar is 50 μm.

Furthermore, by varying the shape of the gap we can also investigate the idea of a most-preferred gap shape. Given that openings can exist in various shapes in vivo, we wonder whether there is a mechanical rationale behind a given shape that can promote a faster closure by the surrounding cells. During development, for instance, most of the openings that occur are ellipsoidal or eye-shaped. In *Drosophila* dorsal closure, it has been proposed that the presence of canthis at the anterior and posterior limits of the opening help in the final zipping of the gap (Woolner et al., 2005; Jacinto et al., 2001). We will study to what extent the presence of canthis at the marings of the gap can promote a faster closure in our gap closure model. For this aim, we have microfabricated eye-shaped pillars with different angles at the canthis and different widths (Figure 2. 32. C).

5. Discussion

In this chapter, we have presented a novel approach to study gap closure in uninjured epithelia under well-defined experimental conditions. This approach provides a model for naturally occurring gaps in development, avoiding possible effects of cell death in gap closure. Such model experiments are also useful to discriminate between the different mechanisms proposed for epithelial gap closure (Tamada et al., 2007; Fenteany et al., 2000a; Garcia-Fernandez et al., 2009). By using a microfabricated stencil with an array of pillars, gaps of precise size and shape can be patterned in parallel in an epithelial cell culture. Thanks to the numerous pillars that can be fabricated in each stencil, one experiment can produce many gaps and thus retrieve high quality statistics. Besides, it is reasonably easy to vary the size and shape of the pillars to assess the effect of gap size and shape on the mechanism of closure.

By using our gap patterning protocol, we have observed that upon pillar removal, cells actively respond to the free space by extending lamellipodia and crawling into the gap. This is an interesting observation itself because it is the first reported case to show extension of lamellipodia during the closure of gaps of a single cell area. Previously, it had been assumed that small gaps were closed by a purse-string mechanism while only larger gaps (few cell sizes in diameter to infinitely large gaps) would present lamellipodia (Martin and Lewis, 1992; Tamada et al., 2007; *versus* Omelchenko et al., 2003; Fenteany et al., 2000; Poujade et al., 2007). We provide here evidence that gaps extend lamellipodia independently of their size. This response is due to the mere presence of free space, as it had been previously suggested (Nikolić et al., 2006; Poujade et al., 2007). We have also shown that the extension of lamellipodia is accompanied by changes in cell polarization and cell shape, mainly in the cells contacting the gap. We additionally showed that closure required that these lamellipodia would effectively pull on the substrate to propel cells inwards. In soft substrates, either we did not observe the formation of lamellipodia or they appeared smaller and shorter in time, and as a result cells could not close the gap. The closure mechanism is thus associated with stabilization of protruding lamellipodia that help to generate stronger forces at the leading edge (du Roure et al., 2005; Giannone et al., 2004). Altogether, these results indicate that gap closure is mainly due to an active and directed process governed by cells at the leading edge and triggered by the presence of the free space.

On the other hand, we found two different behavior and dynamics depending on the gap size. Gaps ≤20 µm presented different kinetics of closure compared to larger ones. Moreover, closure time of small gaps (15 µm in diameter) was affected by the increase in cell density, while larger gaps were irresponsive of cell density. Interestingly, such small gaps were insensitive to inhibition of the proposed gap closure regulators (Rac1, ROCK and MLCK). Altogether, these results pointed towards a mechanism of closure for small gaps that depends only on the unspecific spreading of cells at the gap edge, similar to how a rounded cell spreads in a substrate or how a drop splashes in a surface. In that manner, when cell density was increased and cells became more columnar, closure was faster due to a larger lateral area ready to spread.

Large gaps, on the contrary, showed a strong dependence on Rac1 to close, as inhibition of Rac1 drastically slowed down the closure. These results are in agreement as the work of Fenteany et al., where they found that activation of Rac1 was indispensable for the closure of scratch-induced wounds (Fenteany et al., 2000). Also, the prominent role of cell crawling over purse-string as the mechanism of closure observed in our approach is consistent with a recently proposed theoretical mechanical model for wound closure, in which crawling cells can close wounds without purse-string signaling, only because of their directed mechanical activity (Lee and Wolgemuth, 2011).

In addition, we showed that there is no continuous supracellular actomyosin cable connecting all the gap-bordering cells. Instead, actin and myosin accumulate only at areas where lamellipodia are not extruded. Nevertheless, the reported actin accumulation at the cell-gap interface, which is more prominent in this area and must thus be specifically triggered by the presence of empty space, is likely important during the closure. Actin accumulation could help in driving the gap margins together in a coordinated and isotropic manner, preventing the appearance of finger-like instabilities at the gap border, which are likely to appear during the advancement of straight edges (Poujade et al., 2007; Mark et al., 2010). As a consequence, when the actin-mediated continuity between cells is lost, i.e. in absence of cell-cell adhesions, the coordination of cellular movements is also lost. While cells lacking adherens junctions (α-catenin knock-down MDCK cells) can fill the space of the gap as they migrate as single cells, it is not clear how the final sealing is accomplished, and thus to what extent this process can be considered or not as a proper gap closure. In this regard, future experiments addressing the distribution of E-cadherin in both *wild-type* and α-catenin knock-down cells can help better establishing the final steps of the sealing, and study how junctional proteins form a stable adhesion from opposing lamellipodia when they contact.

Our results contrast with wound-induced gap closure experiments, purse-string mechanism has been found responsible for the closure of the wound. Purse-string has also been proposed for accounting for the extrusion of apoptotic cells (Rosenblatt et al., 2001), a process clearly related to death signaling, where the actomyosin cable formation is triggered through a caspase-mediated pathway (Andrade and Rosenblatt, 2011). Thus, evidence suggests that cell damage inflicted during the process of wound production is promoting the purse-string mechanism by affecting the neighboring cells. In concordance with this hypothesis, we showed here that in the absence of cell damage, purse-string is not the dominant mechanism, but the closure is mediated by a lamellipodial-driven crawling mechanism. However, similar situation where gaps are produced in the presence of cell damage or in the case of patterned wounds, the dynamics of closure differ from the closure of clean gaps. Interestingly, the closure of damage-associated gaps follow a trend similar to what reported for the purse-string contraction-driven closure of wounds, further suggesting the key role of death or damage factors in determining the mechanism of closure.

Finally, we show that squared and ellipsoidal gaps are closed faster than circular ones. Low curvature areas promote the protrusion of broad lamellipodia but a continuous purse-string is not formed in either squared or ellipsoidal gaps. Therefore closure of non-circular epithelial gaps also appears to be primarily driven by lamellipodial-mediated cell crawling.

The project will continue towards the study of the effect of geometry on gap closure. As it has been shown that curvature of the gap border can influence the extension of lamellipodia by boosting them in certain low curved areas, we will further explore such effects. For this aim, we have microfabricated a number of different-shaped pillars, as presented in Figure 2. 32. The method for gap production will be the same as described for this work. With this study, we aim at better understanding the relationship between shape and mechanism of closure. Also, we would like to address the concept of preferred shape, and thus investigate what is the shape that promotes a faster closure, and relate such shape effect in the in vivo gap closure situations. In this regard, we have produced eye-shaped pillars (similar to the opening in dorsal closure) to analyze the closure times and mechanism of closure of eye-shaped gaps.

Despite of the rich information extracted from the developed gap patterning method to study the closure of undamaged gaps in a controlled and systematic manner, this approach also presents its own drawbacks. The protocol is experimentally challenging and thus the success rate in producing the adequate gaps is far from 100% of the cases. The experimental success decreases with the

pillar diameter: for small pillars it becomes difficult to obtain proper gaps. Nevertheless, the main limitation that we have faced is the impossibility to measure traction forces with the pillar removal assay, since we have not been able to attach the PDMS stencil to an adequate substrate for traction force measurements (as will be described in Chapter 3 section 2). For that reason, in our attempt to calculate traction forces during closure we have adopted a different approach (see Chapter 3 section 2).

6. Conclusions

By studying the size and shape dependence of the closure of undamaged epithelial gaps we can conclude that:

- the mechanism of closure depends on the gap size: gaps ≤20 µm close by a passive or mechanism independently of any treatment assessed. Gaps > 20 µm are closed by Rac1-regulated cell crawling.

- damage factors play a critical role in determining the dynamics of the process. Gaps with damage associated close independently of Rac1 activity.

- gaps of different geometries are also closed by lamellipodia. Protrusion of lamellipodia are affected by differently curved gap-cells interfaces.

CHAPTER 3

Forces driving epithelial wound closure

1.Background

Traction forces are essential to a large variety of cellular processes, such as cell adhesion and migration. Migrating cells apply forces on the underlying substrate with at least two objectives: to sense the pliability of the ECM and to propel the cell body forward (Discher et al., 2005; Ananthakrishnan and Ehrlicher, 2007). For this reason, traction forces are a key parameter to understand cell migration processes, such as the previously described epithelial gap closure. Until now, studies addressing epithelial gap closure have been largely based on structural imaging and biochemical regulation. These studies have unveiled two mechanisms that contribute to gap closure: lamellipodia-driven cell crawling and contraction of a supracellular acto-myosin ring. While extensive and often contradictory evidence favoring each mechanism has accumulated, their relative contribution can only be ascertained through the direct measurement of the forces that drive gap closure.

We begin with the idea that the two proposed mechanisms of epithelial closure produce a different traction profile (Figure 3. 1). During the cell crawling-mediated closure, wound-bordering cells extend lamellipodia to promote the advancement of cells inwards (Figure 3. 1. A). According to studies of single and collective cell migration, such lamellipodia are expected to grab on the substrate in order to propel the cell body forward. If lamellipodia pull on the substrate, the forces exterted on the gel would be directed outwards. By contrast, if there were a purse-string response, cells would be drawn together by the contraction of a multicellular acto-myosin cable assembled at the wound margin (Figure 3. 1. B). Since the acto-myosin conforming the ring is part of the acto-myosin cytoskeleton, which is in turn anchored to the substrate through focal adhesions, the contraction of the cable could be transmitted to the substrate. Since the contraction of the cable drives the wound edges inwards, the forces observed on the substrate would be directed inwards.
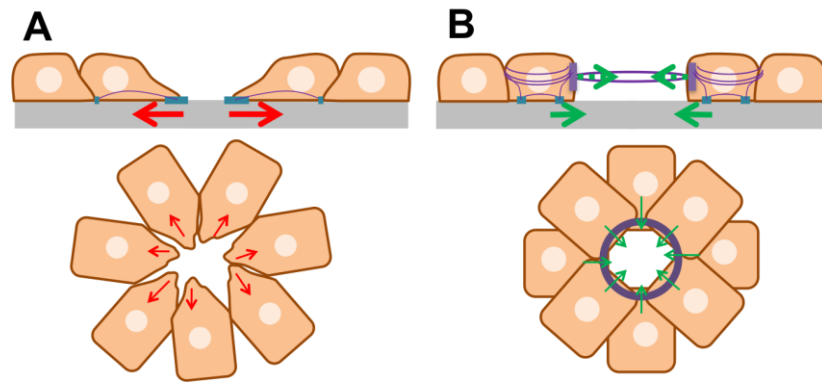
Figure 3. 1. Scheme of the proposed hypothesis to explain the possible mechanical scenarios during wound closure. (A) Lamellipodial crawling mechanism, top scheme lateral view, bottom scheme upper view. In blue, focal adhesions. Red depicts possible traction forces associated with this mechanis. (B) Purse-string mechanism. In purple, actin accumulation at the wound margin. In green, proposed traction forces.

The aim of the study has been to elucidate the forces that epithelial cells exert on the substrate during epithelial gap closure. The combination of the pillar removal assay described in Chapter 2 with a substrate adequate for the measurement of traction forces proved incompatible, at least in our hands, as will be discussed in section 5. For this reason, we have followed a different approach to produce gaps (wounds in this case) in an epithelium. In the present work, we have combined laser ablation to induce wounds in an epithelial monolayer with traction force microscopy to measure the traction forces in response to the generated wounds.

2. Experimental approach

2.1. Measuring cell traction forces: Traction force microscopy

The ability of cells to generate traction forces has been known for several decades. Harris and coworkers showed that an individual fibroblast can deform an elastic thin silicone sheet. The wrinkles caused by the fibroblast were the first direct qualitative evidence proving that single cells can generate detectable traction forces (Harris et al., 1981). Nowadays, there are many well-developed and well-characterized techniques to detect and quantify cell traction forces, such as the use of micropatterned deformable substrates (Balaban et al., 2001), deflectable cantilevers (Galbraith and Sheetz, 1997), microforce sensor arrays (Tan et al., 2003; du Roure et al., 2005), and traction force microscopy (Pelham and Wang, 1999; Munevar et al., 2001; Beningo and Wang, 2002). We will hereafter explain the technique of interest to the present work: traction force microscopy.
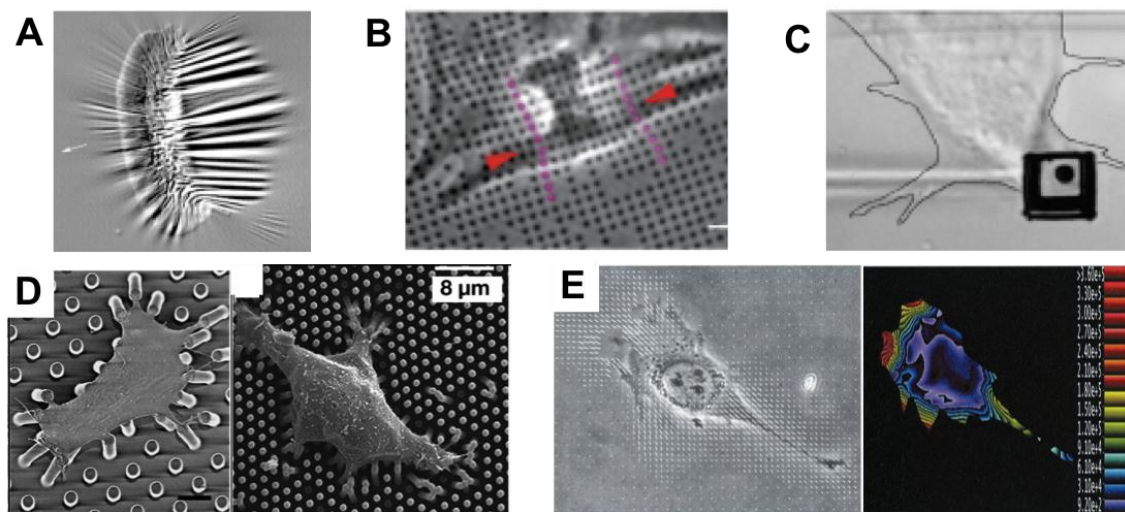

Figure 3. 2. Methods for calculating traction forces. (A) Wrinkles produced in a thin silicone film due to the forces exerted by a fish keratocyte. From (Beningo and Wang, 2002). (B) The forces exerted by a rat cardiac fibroblast distort a regular grid of micropatterned fiduciary markers on an elastic substrate. From (Balaban et al., 2001). (C) Trailing edge of a locomoting fibroblast migrating over a vertical force-sensing micropad From (Galbraith and Sheetz, 1997). (D) Microforce sensor array: vertically aligned micropillars are deflected by the cells pulling on them. Such discrete substrates avoid strain propagation across the substrate and thus facilitate the calculation of tractions from the displacement fields. From (Tan et al., 2003). An improvement of the technique allowed increasing the spatial density of micropillars, rendering a more spatial accurated calculation of forces. From (du Roure et al., 2005). (E) Traction force microscopy (force vector field overlapped to a phase contrast micrograph) of a migrating transformed fibroblast on a

polyacrylamide gel containing microspheres for the tracking of substrate deformations. The right image corresponds to the color-coded traction map. From (Munevar et al., 2001).

Traction force microscopy was inspired by the seminal works on thin rubber films, but was motivated by the need of quantifying the exerted traction forces. To achieve this goal, cells are plated on compliant substrates with embedded fluorescent beads. As cells migrate, they apply traction forces on the substrate and deform it. Such deformations are recorded by tracking the displacement of the fluorescent beads, and traction maps are computed from the displacement fields (Lee et al., 1994; Beningo et al., 2002; Pelham and Wang, 1999).

The typical substrates used for traction force microscopy are polyacrylamide (PA) gels, which are purely inert elastic hydrogels, coated with ECM molecules (Wang and Pelham, 1998). The stiffness or Young's modulus (E) of the gels can be adjusted by varying the ratio between acrylamide and its crosslinker bisacrylamide, thus rendering a stiffness range from hundreds of Pascals to tens of KiloPascals (Lo et al., 2000; Yeung et al., 2005). Substrate stiffness is tuned according to two criteria: it must be adapted to the cell contractility (certain tumor cells for instance produce significantly higher traction forces than their physiological counterparts) and it must match the compliance that cells sense in their physiological niche (Kraning-Rush et al., 2012; Pelham and Wang, 1997; Munevar et al., 2001; Engler et al., 2005).

Since PA gels are transparent, the displacement of fluorescent beads can be easily traced with fluorescence microscopy. For measuring the traction forces, images of the beads in the force-loaded mode (i.e. with cells crawling on top) are compared to null-force images (i.e. after cells have been removed by trypsinization) to obtain the displacement maps. Then, the traction forces are back-calculated by transforming the displacement field to the Fourier space and directly solving the equations. However, since PA gels are continuous substrates where deformations can propagate, the calculation of traction forces from the displacement fields is not trivial. Nowadays, reliable methods are available for the computation of traction forces for single cells and for cell monolayers (Dembo and Wang, 1999; Butler et al., 2002; Trepat et al., 2009). A more applied explanation of the experimental approach for traction force microscopy to the present work can be found in section 2.2 and 2.3.

2.2. Experimental design

Briefly, the experimental process is as follows. On the first day, PA gels are prepared, sterilized, and incubated with collagen overnight at 4°C. On the second

day, cells are seeded on the gels and kept in the incubator overnight. On the following day, once a monolayer of cells has formed, experiments can be started (Figure 3.3). Cell ablation is performed at the Advanced Microscopy Facility of the Institute for Research in Biomedicine (Barcelona). After ablation, the sample is brought back to the laboratory (a few meters away) to measure and analyze wound closure mechanics. Typically 3 wounds per sample are produced, and thus the recording is performed in the multiple stage positions mode. After complete closure, cells must be detached in order to obtain the relaxed bead positions for traction force calculation.
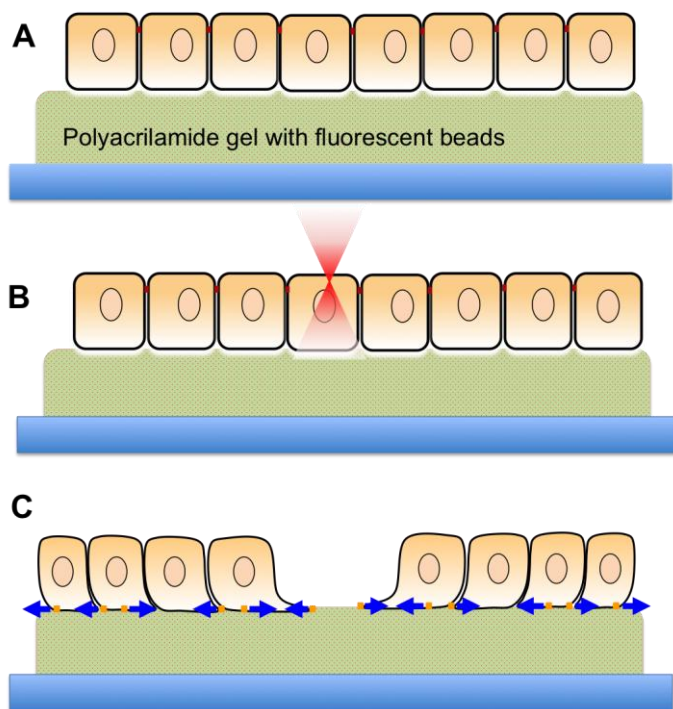

Figure 3. 3. Scheme of the experimental approach followed. (A) MDCK cells are seeded on soft PA gels containing fluorescent microspheres. (B) Laser is focused on the apical membrane of cells to disrupt it and create the wound. (C) Cells respond to the wound to close it.

2.3. Substrate preparation

Traction force microscopy is based on the use of PA gels as deformable substrates. For all the present experiments, we used gels of 9-12 KPa, which proved adequate for the calculation of traction forces exerted by the MDCK cells A detailed protocol for PA gel preparation can be found in Annex I.

Gels are functionalized with collagen thanks to the addition of N-hydroxisuccinimydil (NHS) to the gel. NHS creates an intermediary compound that is highly reactive, allowing the covalent linkage between amino groups of the PA gel and carboxylic groups of collagen. This NHS coating method has provided more homogeneous surface coating than those obtained with the traditionally used sulfo-SANPAH method (Kandow et al., 2007).

2.4. Laser ablation system

The laser ablation set-up used is based on a pulsed-UV laser coupled to the epi-fluorescence port of an inverted microscope. The laser is a Q-switched 3rd harmonic Nd:YAG with 355nm wavelength. According to manufacturing specifications, the pulse duration is shorter than 500 ps. The laser beam is aligned through mirrors to allow 2D beam steering across the field of view and enters the objective lens perfectly collimated to ensure diffraction-limited focusing. The microscope is an Axiovert 200M from Carl Zeiss (Germany), and an objective of high numerical aperture must be used to focus the laser down to a small focal volume, typically a 63x/1.2 NA water immersion lens. The efficient volume where laser damage is induced was estimated to be about 5.2 times the extent of the focal volume with a lateral extent of about 450 nm (estimations performed in glass). The laser cut was controlled through a home-made software, developed by Alfons Riedinger (EMBL, Heidelberg, Germany) and Julien Collombeli (IRB Barcelona, Spain). In the software, the target of ablation was defined as a single spot including between 1 and 3 laser pulses. The estimation of the ablation success is established by the appearance of cavitation or plasma bubbles, which result from the rapid and concentrated heat generated by the interaction of the focused laser with the cellular material. These cavitation bubbles appear as transient short-lived dark bubbles, and indicate that the plasma membrane has very likely been disrupted (Figure 3. 3). The ablation of one cell can imply few laser shots. However, the number of laser shots should be limited, since the fluorescent beads can photobleach at the ablation spot. For more details on the laser ablation procedure, see Annex K.

The typical ablated areas comprise between 5-10 cells. Smaller or larger wounds will be specifically stated in the text. Since the laser ablation system is located at a different facility from the confocal microscope used for measurements, there is always a delay of 15-20 min from the ablation of the cells to the start of closure monitoring. Therefore, we do not have access to the information related to the events directly occurring right after the ablation, which can also be of interest.

We gratefully acknowledge Julien Colombelli for his training on the use of the laser ablation set-up and for helping us in addressing technical issues related to the set-up.

2.5. Experimental measurements: confocal microscopy

In the present work, we have mainly used a laser-scanning confocal microscope (LSCM) to monitor the closure of the wounds. Confocal microscopy provides narrow optical sections thanks to the single-point illumination of the sample and the elimination of out-of-focus fluorescence arising from above and below the focal plane.

The illumination is based on scanning of the sample with a diffraction-limited focused laser beam through the objective lens. The fluorescence light emitted from the illuminated region is collected by the same focusing objective and enters the photodetector through a pinhole. Any light emanating from regions away from the illuminated point will be blocked by the aperture, thus eliminating out-of-focus interfering signal. The thickness of the optical section obtained is directly related to the pinhole size. In this way, a fine and sharp z-sectioning is achieved, and 3D images can be reconstructed in the software. A schematic of a confocal microscope is shown in Figure 3. 4.
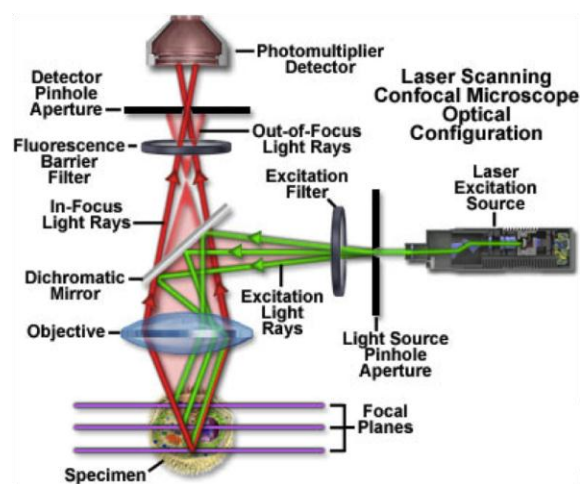
Figure 3. 4. Scheme of confocal microscopy.

Given that cells are typically several microns in height (5-15 μm depending on their spreading state), this approach is well suited to minimize background signal and enhance the image at a given focal plane. By sequential scanning at different z positions along the cell height, a 3D reconstruction of the cell will show improved resolution with respect to the equivalent wide-field epifluorescence image. This feature is particularly appealing to our study, since it will allow: 1) a better characterization of the actin signal during wound closure; and 2) a more precise recovery of the position of the fluorescence beads in the upper-most layer, thus optimizing the calculation of bead displacements and computation of traction forces.

2.6. Data analysis

Wound closure is typically recorded by double channel acquisition: for cell monitoring, a z-stack ranging from the apical part of the cell to its most-basal part is acquired. For bead displacement fields, a z-stack is obtained in order to compensate for possible defocusing events and to ensure recording the position of the upper-most layer of beads for force calculation, given that the cellular traction forces decay rapidly along the gel depth (Franck et al., 2011). For more details on confocal measurements, see Annex L.

Note that from this point onwards the computation of the traction forces from the bead measurements has been performed by Agusti Brugues, a PhD student involved in the project from the Integrative Cell and Tissue Dynamics lab in Barcelona. Traction maps are obtained using a method adapted from (Trepat et al., 2009). Bead images are registered to account for possible drifts in x and y, and aligned with the trypsin image. Given that for each xy position there is a stack of z-planes of beads, software was developed to select the first in-focus plane and the corresponding bead image after trypsin cell removal. The displacement of the beads is calculated by comparing the bead positions of each image with respect to the bead positions after trypsinization of the cells. The comparison is done using cross-correlation algorithms for small interrogation windows of the image that contain several beads. The shift between windows was measured using 2D correlation, and an overlap between two adjacent windows was set at 0,75. In order to back-calculate the traction force maps from the displacements, the displacement field is transformed to the Fourier space, where the elastostatic equations can be solved directly.

With the aim of achieving a clearer analysis of the traction forces, we base our analysis on the tractions in the perpendicular direction to the wound edge. To calculate these normal tractions, is the wound edge was obtained by thresholding the fluorescence images. Moreover, the angle of the traction forces with respect to the mask margin can be calculated. In this manner, inward-pointing forces (towards the center of the wound) can be discriminated from outward-pointing forces (towards the external part of the wound). This analysis is very useful for the interpretation of the traction maps.

3. Wound closure dynamics

Upon laser ablation, cells are activated to extrude the remnant cellular material and close the wound. In this situation, wound margin cells do not encounter a free space as reported in the pillar removal assay in Chapter 2, but dead cells instead (Figure 3. 5).
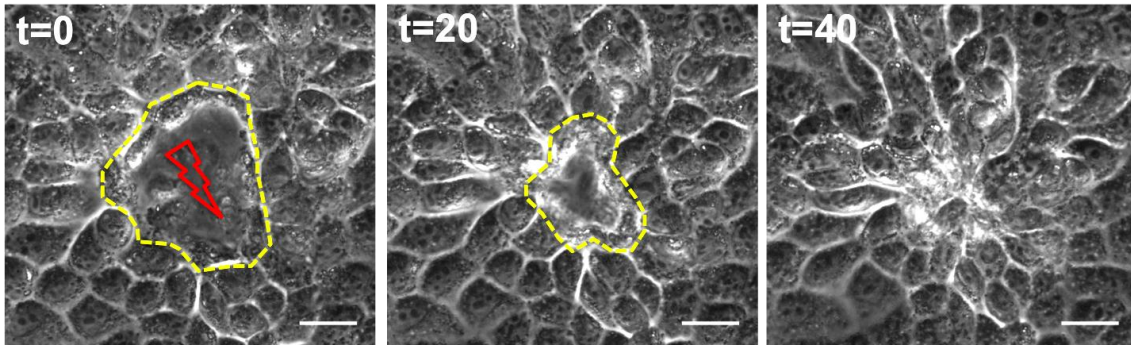

Figure 3. 5. Extrusion of the ablated cells. During the wound closure process, the remnant dead cells are shifted upwards. Red symbol represents the ablated area. Yellow dashed line outlines ablated cells. Scale bars are 20 μm.

3.1. Cell response: actin dynamics and cell reorganizations

Following wounding, wound-margin cells extend lamellipodia until the end of closure, when opposing lamellipodia contact (Figure 3. 6 and 3. 7). It is worth noticing that, unlike the case of the pillar removal assay, wound-margin cells also extend filopodia. The extension of such filopodia could be either a specific response to the presence of dead cells, to the differential coating of the substrate (collagen versus fibronectin), or it could be triggered by the soft compliance of the substrate in the laser ablation set-up.

Concomitantly, there is notable actin accumulation in the first row of cells, in particular at the wound-cell interface. From time-lapse confocal measurements we can observe that actin starts to accumulate approximately 15 min after starting the experiment, and increases as closure progresses. This actin accumulation is typically correlated with the formation of a supracellular actin cable along the wound margin. While this cable is traditionally positioned apically in the literature (Tamada et al., 2007; Bement et al., 1993), we observe actin accumulation primarily at the medial and basal sides of the wound-cell interface.
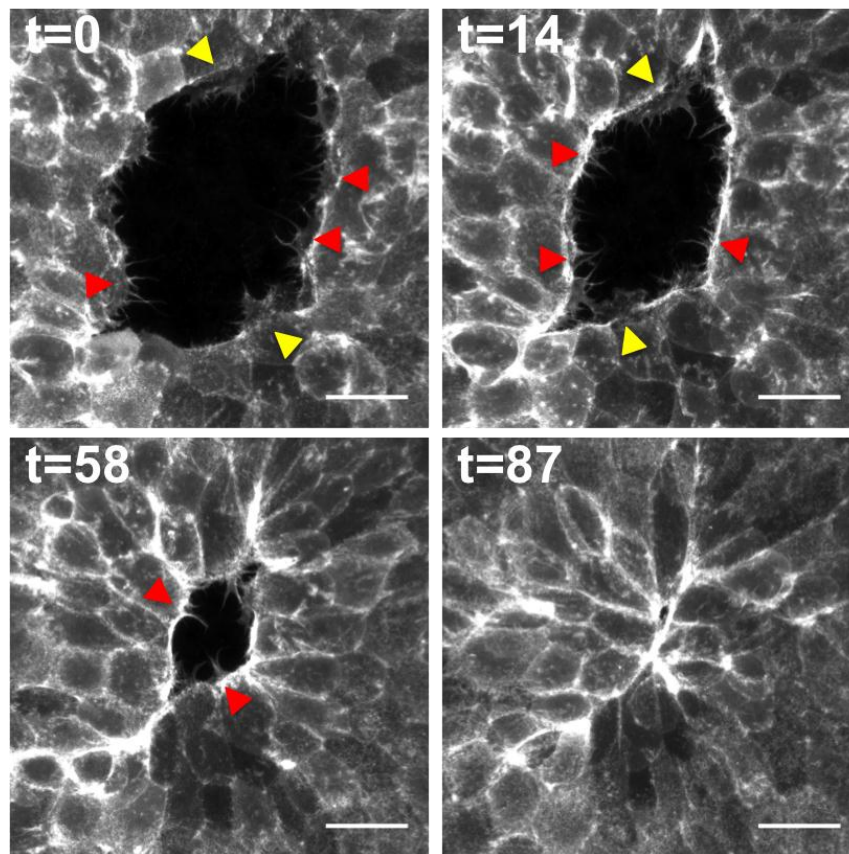
163

Figure 3. 6. Concomitant presence of lamellipodia and filopodia during wound closure. Yellow arrowheads indicate lamellipodia, red arrowheads indicate filopodia. Scale bars are 20 μm.

This model of actin accumulation at medial and basal parts is in better agreement with the proposed model for apoptotic cell extrusion. In this situation, actin has been proposed to accumulate all along the lateral membranes of the cells, thanks to actin assembly promoting-agents secreted by apoptotic cells and sensed by the surrounding healthy cells. However, note that in our experiments the wounded cells do not undergo an apoptotic process, but suffer necrosis. Nevertheless, it is possible that the laser-ablated cells can also trigger a similar program that results in actin accumulation along the lateral side of the cells.

In terms of cell morphology, cells elongate during the closure process, aligning in the direction of closure (Figure 3. 7). By the final stages, cells have formed a rosette-like structure, as recurrently found in the literature for wound closure events (Bement et al., 1993; Tamada et al., 2007; Meghana et al., 2011). Such cell alignment and rosette formation has been also proposed in the context of epithelial gap closure as shown in Figure 2. 18. C. Interestingly, while in small gaps only the first-row cells polarize and align in the direction of closure (as shown in Figure 2. 16), in large wounds cells up to 3 rows behind the wound change their shape and elongate along the direction of closure (Figure 3. 7).
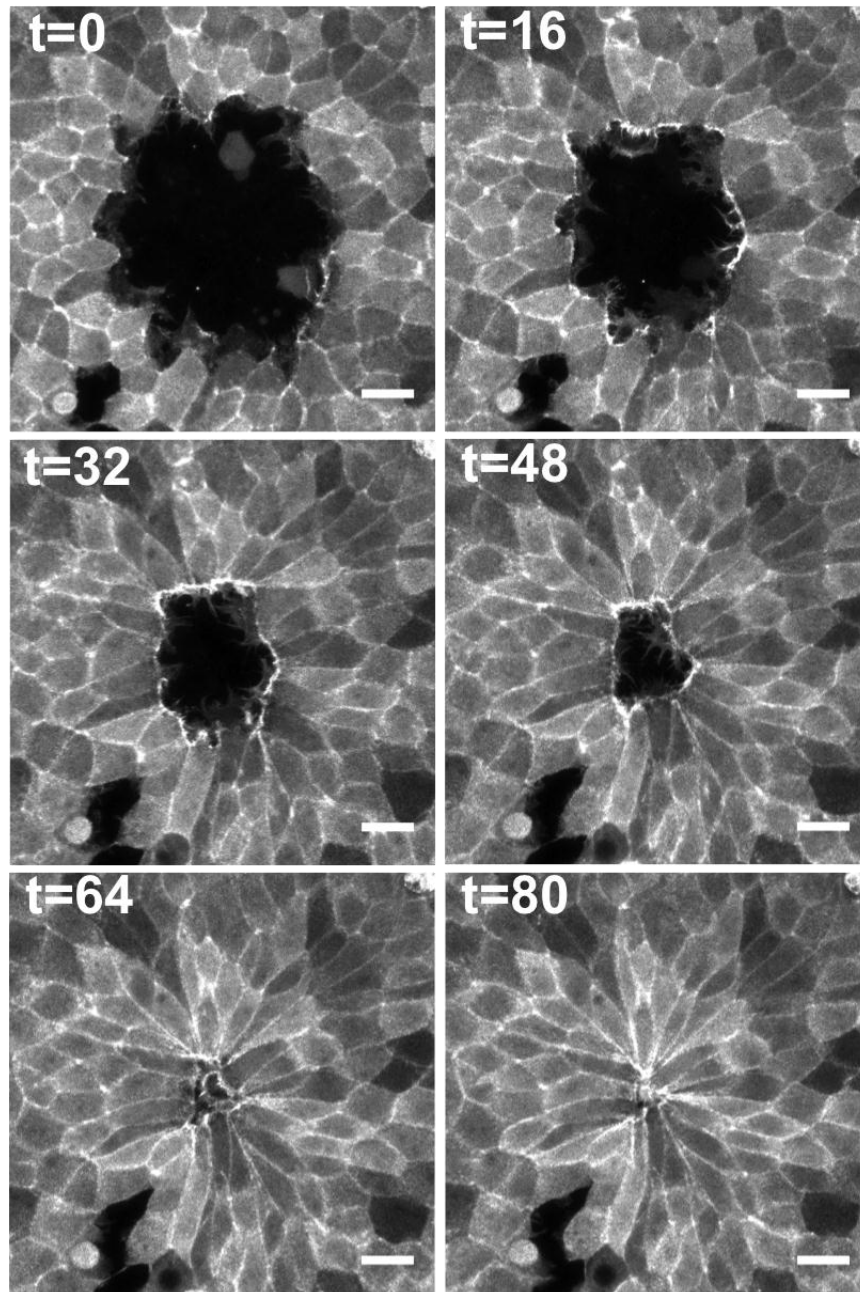
Figure 3. 7. Wound closure after laser ablating a monolayer of MDCK cells. Time is indicated in min after starting the measurements. Note, however, that t=0 represent 15-20 min after producing the wound. Scale bars are 20 μm.

3.2. Kinetics of wound closure

Similar to the case of gaps produced with the pillar removal approach in Chapter 2, we have also analyzed the decrease of the wound area as a function of time. This decrease is not linear, but follows an exponential-like decay instead. The trends of closure [*Ad(t)*] are quite homogeneous for wounds of 30-60 μm in diameter (700 to 3000 μm^2 in area) (Figure 3. 8. A). Interestingly, experiments

with low density of cells show a slower closure rate (Figure 3. 8. A). The closure times show high variability as a function of the initial area (Figure 3. 8. B). It is reasonable to speculate that given the presence of cell damage and debris, death factors can affect the closure in different ways.
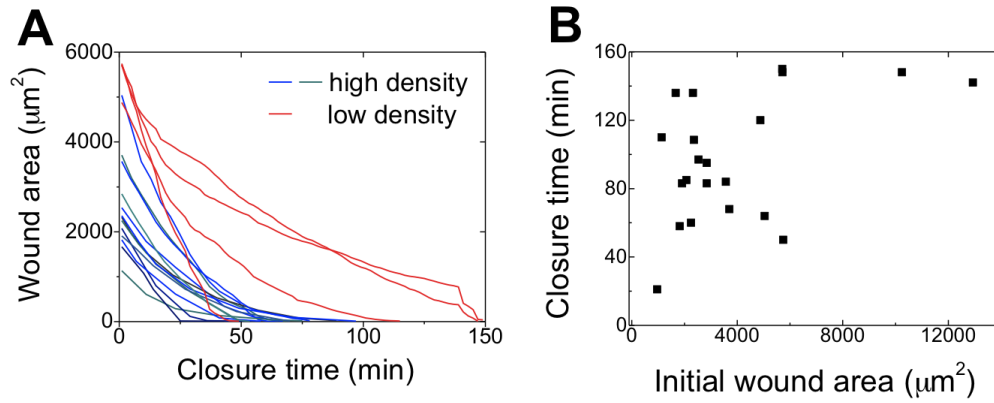

Figure 3. 8. Kinetics of wound closure. (A) Decrease of wound area as a function of time. A distinction is established depending on the cell density. (B) Closure time as a function of the initial wound area.

4. Traction forces during closure

We will hereafter present the results obtained by measuring the traction forces during wound closure, and provide evidence of how these forces are coupled to cellular responses.

4.1. Forces measured during wound closure

Figure 3. 9 shows traction maps superimposed to the confocal actin fluorescence images. For the sake of clarity, only those tractions with magnitude higher than a given threshold are depicted. Note that inward-pointing forces are colored in green, while outward-pointing forces are depicted in red.

The highest traction forces are located at the wound-cell interface. This observation could suggest a physical picture in which only one row of leader cells is involved in the active closure the wound. Note, however, the presence of high traction spots well behind the wound margin. These traction spots could originate from submarginal cells actively crawling into the wound. Alternatively, these spots could result from balancing the high-magnitude tractions exerted at the wound margin. According to Newton's laws, forces within an epithelium must be balanced at all times. As it has been explained in Chapter 1 section II. 4, leading-edge forces are not necessarily balanced at the cell rear or by second-row cells. Instead, forces can be balanced at long distances, since cells within an epithelium are engaged in a tug-of-war (Trepat et al., 2009; Serra-Picamal et al., 2012).

Note also the absence of significant forces at the end of closure. Hence, the high traction forces observed at the wound margin vanish once the wound has been sealed, further supporting a specific response to the presence of a wound in terms of traction force generation.
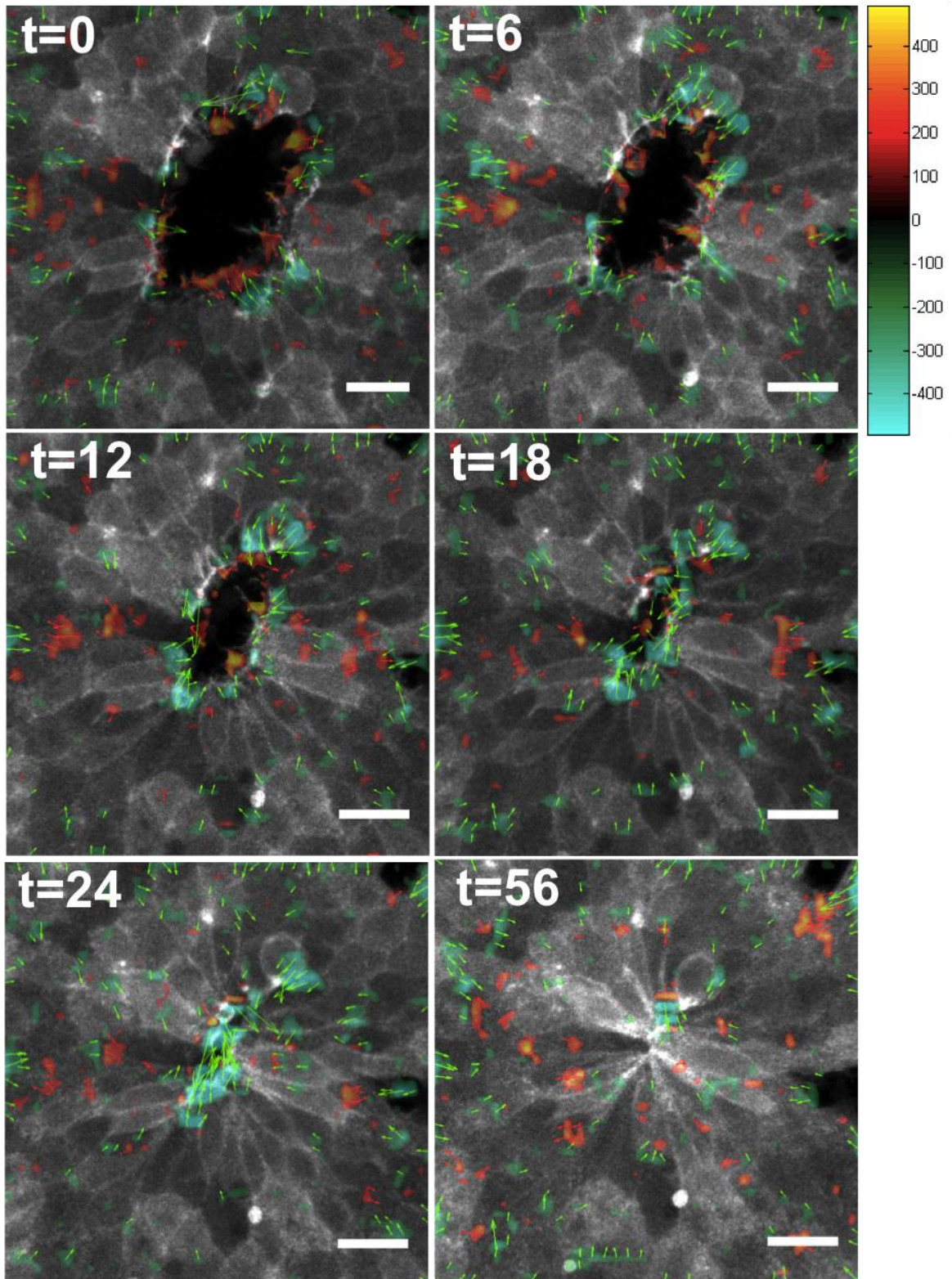
Figure 3. 9. Traction forces during wound closure. Actin fluorescence images are overlapped with the vectorial map of traction forces (red and green arrows) and a color-coded map of the magnitude of tractions. Traction values are reported in Pa. Time is reported in min. Scale bar is 20 μm.

4.2. Temporal evolution of traction forces.

We next analyzed how the measured traction forces evolve as wound closure progresses. In order to better analyze the temporal evolution of the forces, we averaged the radial component of the tractions at each time-point and plotted them as a function of the distance from the center of the wound. In this manner, we obtained spatio-temporal maps (kymographs), in which each line shows the average traction forces as a function of the distance from the center at a given time point. The stacking of the lines of averaged tractions shows the spatio-temporal evolution of forces (Figure 3. 10).

Traction kymographs show that at the beginning of closure, traction forces at the wound margin are outward pointing (i.e. red), and thus could hint a prominent role for lamellipodia-driven cell crawling during these first stages. After 15 min, inward-pointing tractions begin to appear. These inward-pointing tractions suggest that the actin cable becomes mechanically active only after lamellipodia have already started to close the wound. As closure progresses, inward-pointing tractions become dominant, although there always remains a narrow band of outward-pointing tractions at the very margin of the wound.

If we now take a look back at the results presented in Figure 3. 9, it becomes evident that there is a shift in the direction of the tractions at the wound edge: outward-pointing tractions (red) are very significant at the first stages of closure and located at the innermost part of the advancing edge (for t=0, t=6, t=12). Inward-pointing tractions (green) start to be more relevant at t=12 and dominate over red tractions at the final stages of closure (t=18 and t=24).

Thus, the kymograph-style representation of data has unveiled a fundamental feature in the mechanism of closure: there is a transition between outward-pointing forces (which dominate at the initial stages) to inward-pointing forces (more prevalent at the end).
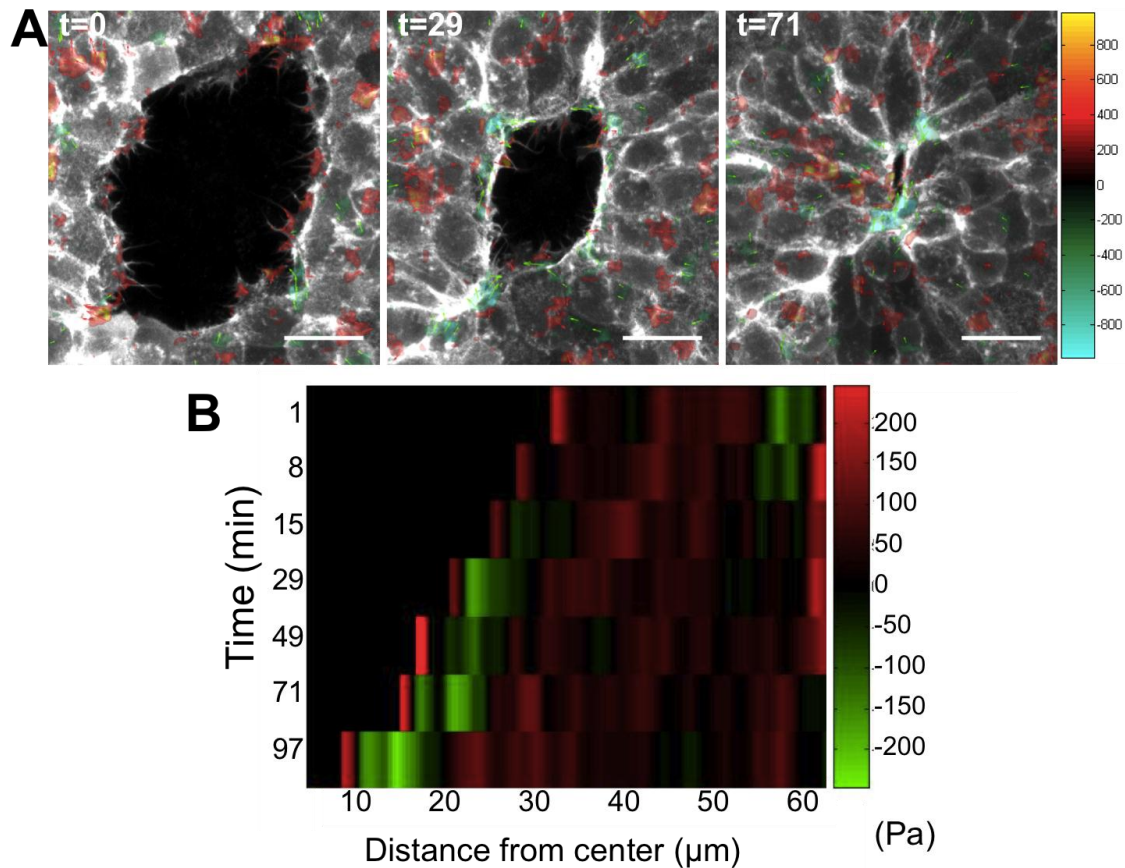
Figure 3. 10. Traction forces can be averaged radially for a given distance from the gap center. Traction forces from the experiment depicted in (A) are showed in a kymograph format in (B). In this manner, the two regimes clearly appear: first, red (outward-pointing) tractions dominate, while afterwards green (inward-pointing) tractions appear at the wound edge. Tractions are reported in Pa. Time is reported in min. Scale bars are 20 μm.

4.3. Correlation of traction forces and actin accumulation

In order to confirm that the inward-pointing forces are associated with the presence of a supracellular acto-myosin cable, we carefully followed the progression of the leading edge by displaying the lateral view of an xz orthogonal projection of a confocal z-stack. We then studied the colocalization of actin fluorescence images with traction forces. (Figure 3. 11).

Figure 3. 11. Advancement of the leading edge during closure. Top panels show the xz orthogonal projection (lateral view) of a confocal z-stack for two different sections analyzed, corresponding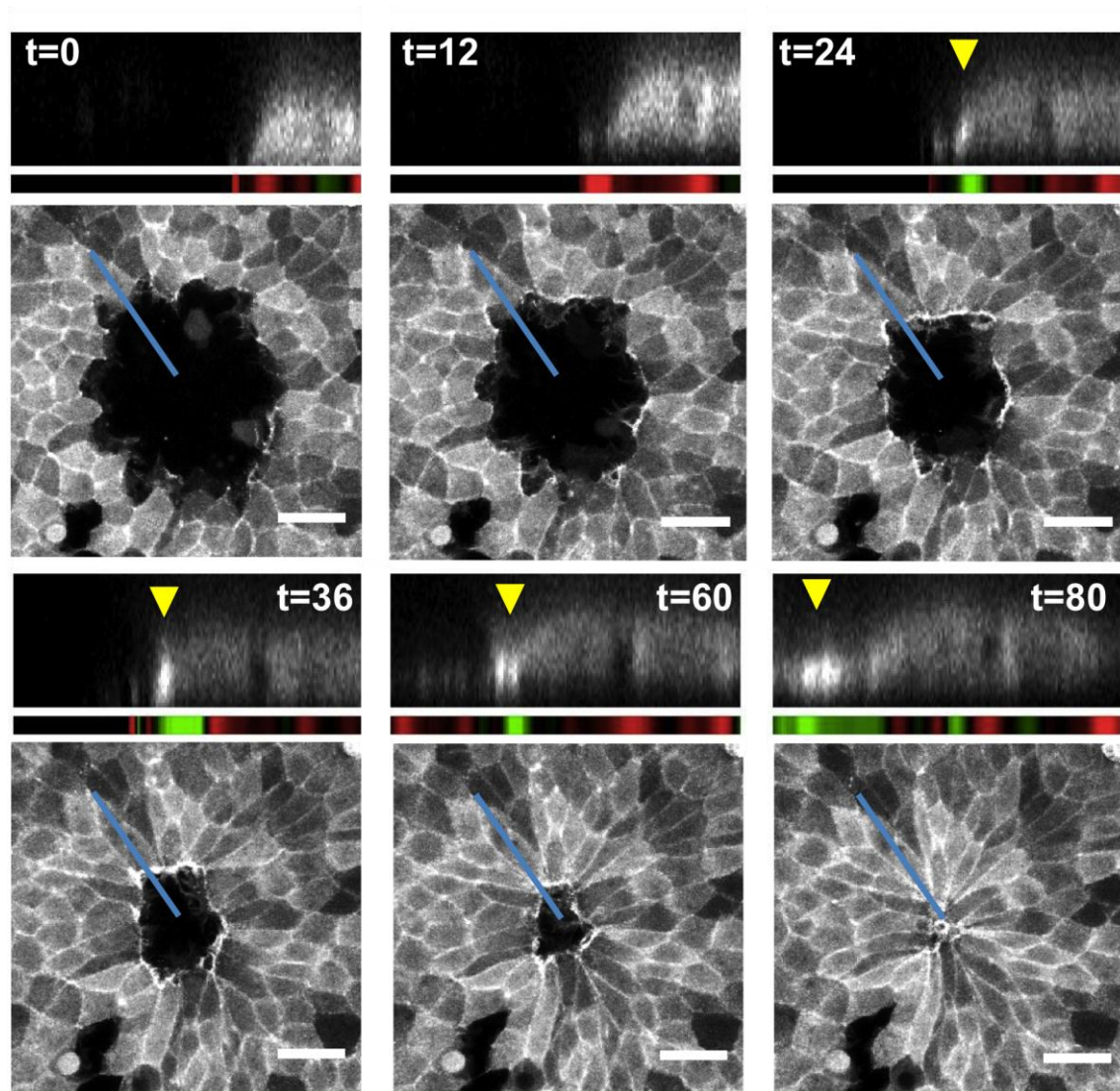 to the blue lines in the bottom images. Below each lateral view there is the profile of traction forces corresponding to the region, showing again inward-pointing forces in green and outward-pointing forces in red. Yellow arrowheads indicate areas of major actin accumulation in the lateral views. Scale bars are 20 μm.

At the beginning of closure (t=0 and t=12), tractions at the advancing edge are mostly outward-pointing and actin staining is diffuse. Such forces are most likely pulling forces exerted by lamellipodia on the substrate through focal adhesions. As closure progresses, actin starts to accumulate at the medial-basal region of the leading cell (for t=24, t=36) and the actin signal increases by the end of closure (t=60, and t=80). Interestingly, such actin accumulation correlates spatially and temporally with inward-pointing forces, further supporting that the actin cable is responsible for inward-pointing forces. Note, as well, that during closure there remains a narrow band of outward-pointing forces located before inward-pointing forces. We attribute this band to lamellipodia, which are present until the final

stages of closure. The positioning of the red band before the actin accumulation further reassures the spatial segregation of the lamellipodia at the front of the actin cable (for t=24, t=36 and t=60).

5. Discussion

In the present Chapter we have used a laser ablation set-up to produce wounds in an epithelial monolayer adherent to a soft polyacrylamide substrate. Using traction microscopy we have measured the forces that drive the process of wound closure. These forces indicate the transition between two regimes, one associated with cell crawling at early times, and one associated with contraction of a supracellular actin ring at later times.

Laser ablation has proven to be an adequate technique to inflict wounds in an epithelial monolayer over a substrate that allows the measurement of traction forces. The pillar removal assay presented in Chapter 2 could not be used with a compatible substrate for force measurement for the following reasons. First, the pillar stencil could not be used with the PA gel required for traction force microscopy. The PA gel is a hydrogel and thus cannot be plasma-treated in order to stick the pillar stencil to the substrate. Without a minimum degree of binding, the pillar stencil always slips over the PA gel. Given the small contact area of the pillars (that typically range from 15 to 60 µm in diameter), it results technically very challenging to stabilize the pillars on the gel throughout the gap patterning protocol and to ensure that pillar-bordering cells would not be disrupted.

On the other hand, we also tried to use PDMS as the substrate for traction force microscopy. In this way, we could stick the PDMS pillar stencil to the substrate, as was done in Chapter 2 section 3. 4. In this case, we encountered the problem of dispersing the beads in the substrate. Since PDMS is a highly hydrophobic material, fluorescent beads do not distribute homogeneously in the gel, but instead aggregate in large clusters, not suitable for traction force microscopy. Recently, we have been able to solve this problem by covalently attaching the fluorescent beads and obtaining a homogeneous distribution only at the surface of the PDMS substrate through silane chemistry. However, such approach conveyed an additional problem of substrate hydrophobicity. Since PDMS substrate was not hydrophilic enough after silane treatment, cells would not evenly disperse within the pillar stencil, and a monolayer did not form for at least 3 days.

Another alternative was the use of microforce sensor array as the substrate to culture cells and measure traction forces, but it has been again challenging to attach the PDMS pillar stencil on top of the micropillar array. Since the microforce

sensor array is made of pillars that can be deflected by cells, the pillar array is effectively soft, and thus the micropillars can be deformed when placing the pillar stencil on top of them. We experimentally addressed this possibility, but in only very few cases could we achieve the sandwich of micropillars for force sensing on the bottom and pillar stencil on the top. Moreover, when plating the cells inside the sandwich, cells would not disperse evenly across the pillar grid, but they rather stayed at the edges of the stencil. Since cells grow slower on micropillar force sensor arrays, we could not manage to obtain a confluent layer of cells in the space confined between the micropillar force sensor array and the inverted stencil of pillars.

For all the above-mentioned reasons, we could not measure the traction forces in our original experimental approach of undamaged epithelial gap closure. To overcome these difficulties we took another strategy. We measured traction forces using Traction force microscopy based on soft polyacrylamide gels, and produced our gaps by means of disrupting a group of cells in an epithelial monolayer with laser ablation. Accordingly, in this experimental approach, we are not producing gaps but wounds, given that targeted cells die upon ablation. In this case, the closure is based on the extrusion of these dead cells to the upper part of the monolayer.

Interestingly, this strategy will give us additional valuable information of the mechanisms of wound closure, which are more related to actual wound healing processes, given the presence of dead cells and dead factors. In addition, these experiments will be compared to the previous reported work to highlight common mechanisms and possible differences between the two situations (pillar removal assay versus laser ablation) in Chapter 4.

5. 1. Current working-model to explain wound closure

The combination of laser ablation with traction force microscopy has revealed novel features of wound closure. We have observed that cells within the wound margin experience a dramatic morphological and mechanical response. From the morphological perspective, these cells undergo shape reorganizations and elongate in the direction of closure while extending lamellipodia. Moreover, we have also shown a preferential accumulation of actin at the wound-cell interface, as it had been previously described (Martin and Lewis, 1992; Bement et al., 1993; Tamada et al., 2007). Regarding the mechanical behavior, cells at the wound margin display *de novo* relevant traction forces in response to wounding.

The traction profile evolution unveiled two regimes (Figure 3. 12). At the onset of closure, forces are mainly outward-pointing, associated with the pulling of lamellipodia that grab on the substrate to propel the cell forward. As closure progresses, inward-pointing tractions appear. These inward-pointing forces correlate spatially and temporally with accumulation of actin at the leading cells. As such, it appears that inward-pointing forces are the result of the contraction of a supracellular actin cable that drives the wound margins inwards. At the last steps of wound closure, the inward-pointing forces are prominent, as is the accumulation of actin, and progress until the final sealing of the wound.
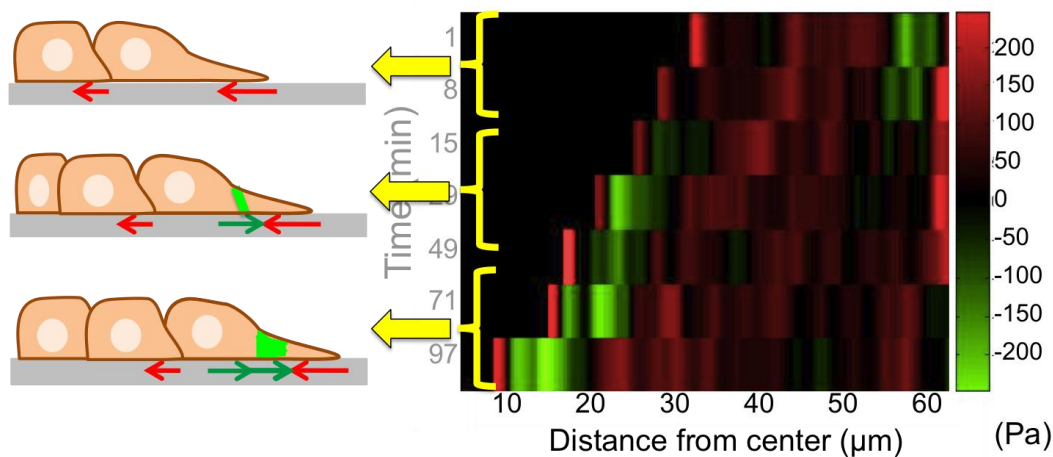

Figure 3. 12. Interpretation of the experimental results. Left panels show the schemes of our interpretation. Right panel shows the kymograph for the traction profile, as presented in Figure 3.9. B.

As a result, we have shown that, in our experimental conditions, the two main mechanisms proposed to explain wound closure play a role, but they are segregated spatially and temporally, and hence there is a transition from the lamellipodial-driven closure to the actin cable contraction-driven closure.

Note that, when the two regimes emerge (outward and inward pointing forces), the distance between the outward and inward-pointing forces is 5±1 μm, and is rather constant between the different analyzed experiments. This distance is in agreement with the spatial segregation of the structures responsible for these differently pointing tractions: the lamellipodia are located in front of the actin ring, as inward-pointing forces are located right after outward pointing forces (Figure 3. 12).

Insightful experiments in similar experimental conditions have shown before a prominent role of purse-string as the closure mechanism (Tamada et al., 2007). However, measuring the mechanics of wound closure has pointed out a central role of lamellipodia-driven cell crawling in the closure. Our findings thus raise the

question as to how both processes are coordinated to achieve efficient wound closure. Therefore, it is important to highlight the relevance of the mechanical component of cell migration as a way to both better understand a given process and to uncover hidden mechanisms that might not be evident in an approach based only on chemical treatments.

Interestingly, wound-margin cells exert traction forces with a magnitude above that of a resting monolayer. Such higher mechanical activity had been traditionally assumed to be a feature of leader cells, which are imagined to pull a resting monolayer and drive its advancement (Khalil and Friedl, 2010). In this regard, direct measurement of the traction forces in an expanding monolayer ruled out the assumption that leader marginal cells exert much higher forces than follower sub-marginal cells. Instead, these studies showed that all cells in the expanding monolayer exert significant forces and engage in a tug-of-war (Trepat et al., 2009; Tambe et al., 2011). Under our experimental conditions, we showed that leading marginal cells exert higher forces than those located further from the wound. This could be due to the presence of the multicellular actin cable that connects the wound-margin cells. Intuitively, the actin belt must confer a higher level of coordination between the first-row cells with respect to innermost cells (as shown also in Chapter 2 section 3. 8). Also, the contractile cable can provide an additional traction force resulting in a traction profile with a traction peak at the first-row cells.

In addition to the magnitude of the traction forces of the wound-margin cells, the direction of these forces is also noteworthy. This is the first time that forces in the same direction of migration (what we have named inward-pointing forces because they are oriented towards the centre of the gap) have been reported at a leading edge. Typically, advancing edges are associated with forces directed in the opposite direction, as first-row cells grab on the substrate. However, in our experimental conditions we have shown that first-row cells form an actin cable at the wound margin. Most likely, this additional supracellular coordination and the contraction of this cable determine the resulting inward-pointing forces. This assumption brings the following question: if the inward-pointing forces are due to such supracellular coordination, will they exist in the absence of actin cable, or even in the absence of cell-cell connections? To address this question, we are planning on using a-catenin knock down MDCK cells, which do not form cell-cell adhesions. Since actin cable needs to be anchored at cell-cell junctions to be functional, cells that are not physically connected between them could not account for the multicellular coordination and contractility of the actin cable. Thus, we will investigate the closure mechanics in the absence of cell-cell junctions to verify our current working model.

6. Conclusions

By relating the mechanical results to the structural reorganization that takes place during wound closure, we can conclude that:

-   cells actively respond to wounding by morphological reorganization and specific mechanical activity.

-   there is a transition between two mechanical regimes: in the first regime tractions are directed away from the wound. In the second regime, tractions are inward-pointing.

-   the first regime is associated with the pulling of lamellipodia on the substrate, while the second regime is associated with the contraction of a supracellular actin cable.

CHAPTER 4

General conclusions

and outlook

The present work has been focused in understanding how epithelial cells maintain the integrity of the epithelial barrier by addressing situations where discontinuities in the epithelia appear and must be closed by the surrounding epithelial cells. The process by which epithelial cells respond to discontinuities is termed epithelial gap closure, and is the focus of the present work. Such discontinuities can arise both naturally (like developmental process involving sealing of openings, or extrusion of cells during homeostatic processes) or induced (in cases of injury, like a skin cut or a disruption of lung epithelia by external agents). Due to the importance of epithelial gap closure, many studies have addressed the issue in different situations, from embryonic to adult gap closure, in naturally occurring gaps or in artificially produced wounds, in in vivo and in vitro scenarios. Despite two mechanisms have been proposed to drive epithelial closure (purse-string and cell crawling), the complexity of the process overshadows a clear picture of the closure, so that there is still no clear agreement on the mechanism of closure. There are few parameters that could determine the activation of one or the other mechanism, such as the size and the shape of the gap, the presence of death factors during closure, the matrix where cells lye on, among others. Moreover, it is not clear yet if both mechanisms could coexist simultaneously, or segregated in time. Up to date, there is no work addressing these parameters in a systematic manner.

Since many of the controversies about the epithelial closure mechanism arise from the high variability in the experimental conditions when studying in vitro models of gap closure, Chapter 2 describes a novel approach to study the mechanisms of epithelial gap closure in well-defined and tunable conditions. We have used a PDMS pillar stencil to produce gaps in an epithelial monolayer, where the gap size and shape can be precisely controlled and gaps are patterned without cell damage associated. By using this approach, we have shown that gap-bordering cells extend lamellipodia to the free space and polarize in order to actively migrate into the gap. By varying the size of the gap we unveiled two different regimes: small gaps (≤ 20 μm) are closed independently of any treatment applied. Such small gaps might possess redundant mechanism or they could be closed by physical means not controlled by the classical regulators. Large gaps, on the other hand, close by a Rac-dependent cell crawling mechanism. Lamellipodial-driven migration is also the dominating mechanism during the closure of different gap geometries, and is actually boosted by areas of low curvature. This observation opens many questions on the curvature-sensing mechanism. In this regard, it will be interesting to further address the relationship between curvature at the cells-gap interface and lamellipodial extension. Such dependence could be mediated by a differential organization of the actin cortex depending on the membrane

curvature contacting the gap, and also by a differential distribution of geometry-sensing proteins, such as IRSp53 or I-BAR domain-containing proteins (Scita et al., 2008; Bhatia et al., 2010). We have started addressing this point by producing pillars with differently curved regions, and with convex and concave areas. Besides, it would be interesting to study the role of cell-cell adhesions in the sealing of the gap in order to better characterize the final closure steps. Cadherins have been proposed to drive the initiation of a cell-cell contact between close lamellipodia (Yamada and Nelson, 2007). Our model appears as a good scenario to study the formation of junctions from various lamellipodia converging at a vertex, and could be compared to the formation of adherens junctions from two opposing lamellipodia in the closure of an ellipsoidal gap.

As we show in Chapter 2, gap closure strongly depends on the lamellipodial-mediated migration of cells, and since migration is ultimately a mechanical process, it appears evident that measuring the traction forces during epithelial closure can provide valuable insights, as it has for cases of collective cell migration (du Roure et al., 2005; Trepat et al., 2009 Tambe et al., 2011; Serra-Picamal et al., 2012). The pillar removal assay has proven to be very useful to gain insight on the size and shape dependence of the closure mechanisms, but it is not an appropriate method to characterize the mechanics of the process. The use of a PDMS stencil for gap patterning requires a very specific substrate for the interaction of the stencil with the substrate. Neither polyacrylamide gels nor micropillar arrays could be attached to the PDMS stencil for traction force measurements. Given that our aim is obtaining the mechanical component of epithelial gap closure, we have used another approach that enables the measurement of the traction forces during epithelial closure.

In Chapter 3, we have taken advantage of a laser ablation set-up to produce wounds in an epithelial monolayer that is seeded in a polyacrylamide gel, where traction forces can be measured. In response to the inflicted wound, surrounding cells respond and extrude the cell remnants upwards, completely sealing the wound. By measuring the traction forces during the closure, we have unveiled the presence of the two closure mechanisms, lamellipodial crawling and purse-string, spatially and temporally segregated. In a first stage, lamellipodia protrude and exert forces while pulling on the substrate as they propel the cells forward. In a second stage, forces arising from the contraction of a supracellular actin cable take over and drive the final sealing. During this last step, the effect of the purse-string results in inward-pointing forces, which, to our knowledge, have never been described before. Inward-pointing forces can only result from a multicellular coordination that could only exist in circular wounds of small area. Given that multicellular coordination through the supracellular actin cable appears to play an

important role in wound closure, it begs the question: would inward-pointing forces exist in the absence of a supracellular actin cable? In order to address this question, we are working on the characterization of the traction forces when cell-cell adhesions are disrupted. If cells cannot form adhesions, the multicellular coordination and the supracellular actin cable cannot exist. If the inward-pointing forces are due to the purse-string, they should disappear or at least diminish when the actin cable is absent.

When comparing the two presented works in Chapter 2 and Chapter 3, some differences arise. A key difference between both set-ups is the presence of death factors: in the laser ablation approach the closure process is actually the extrusion of dead cells, while in the pillar removal assay the closure process is the occupation of a denuded area without death or damage signaling. As we have pointed out, there were already some studies hinting towards a relationship between purse-string and wounded or apoptotic cells (Rosenblatt et al., 2001; Tamada et al., 2007). Indeed, we show here that the presence of death factors conveys an important contribution of the actin cable contraction during wound closure, as it can be observed on the mechanical characterization of wound closure. In the absence of death factors cell crawling has a more prevalent role, and while actin also accumulates in gap-margin cells, purse-string seems to be less relevant.

On the other hand, we observe some differences in the dynamics and kinetics of migration between both epithelial closure models. As we show in Figure 4.1, the closure time as a function of the initial gap area highlights the differences between both approaches. In the gap pillar removal assay, the closure time is linearly related to the initial area, and since initial conditions are very well-defined, the variability in the data is low. However, the closure of gaps or wounds with damage associated shows more variability in the closure time depending on the initial area (Figure 4.1, blue data points versus black and red data points). Such variability increases in larger gaps (> 4000 μm^2). The variability of the data is related to the difficulty of controlling the initial conditions of the gap or wound, and also to an intrinsic variability of the closure process, since the presence of debris and death factors can affect the closure in many different ways. Besides the difference between damage-associated and damage-free situations, note that the closure times seem to indicate that wounds are sealed at slower paces than gaps (Figure 4.1., blue and red data points versus black data points). This could be related to the stiffness of the substrate: wounds are closed by cells crawling in a soft (9-12KPa) PA gel, while gaps are closed by cells migrating over glass, an infinitely stiff substrate. Moreover, we also showed in Chapter 2 that soft PDMS substrates dramatically affect the closure of epithelial gaps. In soft PDMS substrates, gap

closure is significantly slower and even impaired. Wounds in soft PA substrates close slower but always seal the gap. These differences can be due to the presence of death factors in this latter case that would trigger the contraction of the actin cable, which would help in the final sealing of the wound. Thus, these experiments hints toward a key role of substrate stiffness in affecting closure process. Indeed, literature recurrently shows that cells migrate faster on stiff than on soft substrates (Lo et al., 2000; Pelham and Wang 1997).
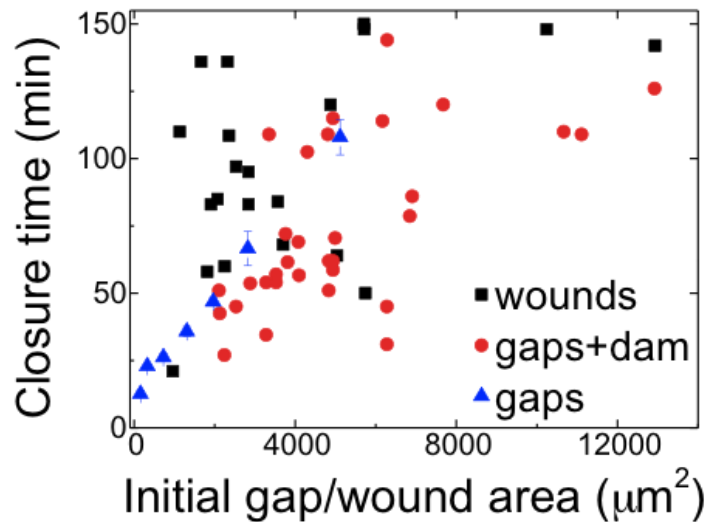

Figure 4. 1. Closure time as a function of the initial gap or wound area. Blue triangles show the gaps produced by the pillar removal assay, as explained in Chapter 2. Data are means and standard errors. Red circles show the gaps with damage associated produced by crushing or ripping the cells, as explained in Chapter 2. Black squares show the wounds produced by the laser ablation set-up, as explained in Chapter 3. For red and black data sets, data points are single experiments.

The presented work has provided insightful knowledge on the gap size relevance and on the mechanical aspect of epithelial gap closure that could only be addressed in an *in vitro* system. However, great effort should be put now in translating all the knowledge available in in vitro systems to the *in vivo* situations. In this regard, our studies hint towards the relevant parameters that should be carefully assessed. It would be of great interest to systematically characterize the closure of gaps depending on the size of such gaps in embryonic closure (for example in *Drosophila* and *C. elegans* embryos) and in adult closure. Given that systematic analysis in adult tissues could present more difficulties, in these case tissue explants could be of interest. However, in these approaches the gap would be necessarily produced by puncture or scratching (as to our knowledge surface masking techniques seem challenging to implement in developing embryos or adult tissues), which would imply damage factors affecting the closure process.

Another relevant parameter that should be assessed is the underlying substrate where cells migrate over in in vivo epithelial closure. Up to date, there is no available information on the mechanical properties of the amnioserosa cells over which epithelial cells migrate during Drosophila dorsal closure (Y. Toyama, personal communication). Likewise, there is very limited information about the stiffness of the wound bed over which epithelial cells crawl during epidermic wound healing. In this case, it is reasonable to speculate that such matrix would be stiff, given the high content of crosslinked fibrin and collagen and the observed stiffening of scarred tissue. Besides the key role of the underlying substrate mechanical properties (stiffness, but also visco-elastic properties), the recent work of Solon et al. suggested an implication of the pulsatile contractility of the amnioserosa cells in driving dorsal closure. Similarly, it appears that myofibroblasts in the dermis below an injured area could help in the closure by contracting the wound bed and bringing wound edges closer (Chaponnier and Gabbiani, 2005; Hinz, 2007). Such observations pinpoint a relevant contribution of the underlying substrate that could be passive (because of the stiffness of the matrix or underlying cells) but also active (contractility of underlying cells). In these regards, experiments in co-culture of cells, where the lower layer could be a mixture of contractile cells such as myofibroblasts and matrix, and the upper layer could be epithelial cells, could be useful.

On the other hand, deciphering the mechanics of gap closure in vivo would represent an important breakthrough. While up-to-date approaches to measure traction forces in tissues in vivo are lacking, inputs from laser drilling experiments to infer tension in tissues (as the experiments performed in Kiehart's group) or from careful tracking of cell movements could help in deciphering the physics of the process (Kiehart et al., 2000; Benazeraf et al., 2010).

In conclusion, careful observation of in vivo epithelial closure processes can provide us some clues and hint hypothesis than can be then further tested and fully characterized in in vitro models. In the present work we have tried our best to fill such gap: from a thorough investigation of the established notions in epithelial gap closure, we have further analyzed the key questions arising form in vivo studies in a well-characterized in vitro model. Then, the insights gained in systematic in vitro studies should be verified and validated in the in vivo organism to fully ascertain universal mechanisms. As such, we let room for developmental biologists and biophysicists to pursue future investigations.

Author contributions

Main articles from the PhD:

Anon, E., Serra-Picamal, X., Hersen, P., Gaulthier, N., Sheetz, M., Trepat, X. & Ladoux, B. (2012). *Cell crawling mediates collective cell migration to close undamaged epithelial gaps.* Proceedings of the National Academy of Sciences, July 3, 2012 vol. 109 no. 27, 10891-10896

The forces driving wound healing. *Manuscript in preparation.*

Co-authored articles:

I contributed minorly to these articles, which correspond to projects carried out by other lab members with whom I collaborated, or that were already advanced when I joined the lab.

Serra-Picamal, X., Conte, V., Vincent, R., Anon, E., Tambe, D., Bazellières, E., Butler, J., Fredberg, J., Trepat, X. (2012)*. Mechanical waves during tissue expansion*. Nature Physics. In press.

Saez, A., Anon, E., Ghibaudo, M., du Roure, O., Di Meglio, J. M., Hersen, P., Silberzan, P., Buguin, A., Ladoux, B. *Traction forces exerted by epithelial cell sheets.* Journal of Physics Condensed Matter. 2010 May 19:22(19);194119.

Ladoux, B., Anon, E., Lambert, M., Rabdozey, A., Hersen, P., Buguin, A., Silberzan, P., Mege, R. M. *Strength Dependence of Cadherin-Mediated Adhesions.* Biophysical Journal. 2010 Feb 17;98(4):534-42.

Conference contributions:

- From cells to organs, Symposium. *Apr 16-17, 2012;* Barcelona, Spain. Oral contribution.
- American Society for Cell Biology. *Dec 03-05, 2011*; Denver, US. Poster contribution.
- CellMech 2011. *Oct 17-19, 2011*; Amsterdam, The Netherlands. Oral contribution. Awarded for best presentation.
- Biophysical Society conference on Actin, cytoskeleton and nucleus. Nov 9-12, 2010. Singapore. Oral contribution.
- World Congress Biomechanics. *Aug 01-06, 2010.* Singapore. Poster contribution. Awarded for best poster
- WEH workshop in Cell mechanics. *Oct 19-21, 2009*; Bad Honnef, Germany. Poster contribution
- IBEC symposium in Bionengineering and Nanomedicine. *Apr 14-15, 2009.* Barcelona, Spain

List of figures and tables

Protocols

ANNEX A. MICROFABRICATION OF SU8 MASTERS

The following protocol has been optimized for the manufacturing of SU8 pillars in glass substrates. Although it can be used as a guideline for other related microfabrication process, some parameters might need to be adapted.

1. Clean glass slides with successive baths of acetone, ethanol and MilliQ water, during 5 min under sonication. Dry under nitrogen flow.

    a. The substrates used are regular microscopy glass slides, either 2x6 or 4x6 cm. Should there be a problem with SU8 not being enough attached to the glass substrate, or SU8 features being removed during the developing step, silicon wafer might be used.

    b. For small features, it is recommendable to clean the slides with Piranha solution (sulfuric acid with hydrogen peroxide at 3:1 proportion), by incubating the slides in the piranha solution for 30 min. Dry under nitrogen flow.

    Piranha solution is a very aggressive treatment and should thus be handed very carefully and always under a chemical hood. Before discarding, let deactivate by adding MilliQ water and letting it settle for few hours.

2. Spin SU8-50 (MicroChem) on top of the slides (2-steps program: 5 sec, 500 rpm, a=300; 30 sec, 3500 rpm, a=1500)

3. Soft bake: 6 min at 65°C, 20 min at 95°C

4. If the desired final height of the features is 100 μm, repeat again steps 2 and 3. Otherwise proceed to step 5.

5. Place the transparency mask or the glass mask on the photolithography holder

    a. For relatively large features (>80 μm), the photolithography mask can be a simple transparency (printed at high resolution quality). In this case, stick the transparency mask on the lower side of the glass in the photolithography holder with tape. Be careful on having the mask in total contact with glass, to avoid diffraction effects.

    b. For smaller features, a quarz-chrome mask is recommended.

6. Align the slides below the mask and raise them until they slightly contact the mask.

7. Expose to the UV light for 5 sec.

Given that SU8-50 is a negative photoresist, the areas of the photoresist exposed to UV result crosslinked, and thus insoluble to liquid developers.

For large features (>150 µm), 10 sec of exposure is recommended.

8. Bake: 1 min at 65°C, 9 min at 95°C

9. Development: place the glass slides in the SU-8 developer for 3 min. Check if the developing process has completed by rinsing one slide corner with isopropanol. If the liquid is white, it means that unreticulated SU-8 is still present. Then put the slide back in SU-8 developer for 1 extra min and repeat the verification until the slide appears transparent when rinsed with isopropanol.

    a. If the features produced are pillars, the majority of the glass slide will be covered of unreticulated SU8 that must be dissolved. This can increase the developing time.

    b. The developing process is faster under agitation. The glass slide can be hold with tweezers and moved vigorously inside the developer-containing cuvette.

10. Dry under nitrogen flow.

11. An extra step of baking can improve the adhesiveness of SU8 to the glass substrate. If desired, bake the slides on a hotplate for 30 min at 100°C.

12. Silanize the master: place the slides in a vacuum jar together with few drops of silane (1H,1H,2H,2H-Perfluorooctyl-trichlorosilane 97%) on a coverslip. Apply vacuum during 30 min. After, close vacuum and let it incubate for 1 hour.

ANNEX B. SOFT LITHOGRAPHY

1. Weight few grams of PDMS base (Sylgard 184, Dow-Corning)

2. Add the reticulant at a ratio of 1 part per 10 parts of base

3. Mix thoroughly for a couple of minutes. Air bubbles will appear.

4. Degass in a vacuum jar for 30 min approx. Air bubbles should emerge to the surface and burst.

5. Pour PDMS on the wafer or master. Degass again until all bubbles have disappeared.

6. Cure at 80°C for 2 hours or at 60°C overnight.

    The curing time of PDMS depend on the temperature. The higher the temperature, the faster it cures. It also depends on the thickness of PDMS. For thin membranes or stencils, the curing time is shorter. Big blocks of PDMS might take longer times.

7. Carefully peel off from the wafer or master with tweezers. Store in clean Petri dishes.

ANNEX C. GAP PATTERNING PROTOCOL

1. Cut the PDMS stencils by the very edge of the pillars grid. Ensure that the PDMS piece only contains the pillars, and no extra PDMS roof. Typically, the PDMS stencil will measure few mm x few mm.

   This is important because cells must be seeded at the very edge of the pillars grid, to ensure that cells drop will enter the grid by capillarity and thus distribute evenly beneath the stencil. Otherwise, if cells do not enter the pillars grid at first and are seeded only at the margins of the grid, it will take longer time for cells to form a monolayer beneath the stencil. Increasing the culture time to more than 48h will promote the appearance of dying cells.

2. Coat MatTek petri dishes (or any other glass bottom petri dish) with fibronectin by incubating them with a drop of 100 µl of 20 µg/ml fibronectin in PBS for 1h at room temperature or 20 min at 37°C. After, rinse with PBS and let dry.

   Alternatively, the substrate can be a glass coverslip, depending on the type of experiment. For immunostaining, glass coverslip are more convenient. In this case, glass coverslips must be thoroughly cleansed, even if taken from they are brand new. Fibronectin coating applies equally.

3. Place PDMS stencils with pillars facing upwards and MatTek dishes in the plasma cleaner. Apply oxygen plasma at medium power for 30 sec.

   The power and time of oxygen plasma required depends highly:

   a. on the plasma cleaner machine itself. It is important to ensure the appearance of oxygen plasma, but not too strong. Violet plasma is the most adequate. White plasma (pure oxygen) would result in too strong bonding. Pink plasma (air) does not work.

   b. on the age of silicon wafers used for PDMS pillar stencil molding. The more times the silicon wafers have been used, the worse the PDMS pillars attach to the glass substrate. For the SU8 masters, we did not observe such ageing effect, although SU8 masters were not used as long as the silicon wafers.

   Thus, an optimization step when using a different plasma machine might be required.

4. Carefully attach PDMS pillar stencil to the glass substrate with tweezers. To ensure the proper degree of attachment between pillars and glass substrate, place the PDMS stencil in contact with glass, wait 30 sec, remove the stencil and place it again. If the PDMS stencil cannot be removed, indicating it is too strongly attached, discard the sample.

5. Let the effect of oxygen plasma fade away from the PDMS for 1 hour.

6. Incubate with Pluronics 0.3% in PBS for 1 hour at room temperature. The time must be strictly controlled.

   a. Shorter Pluronics incubation time will not properly prevent cell attachment at the pillars walls, thus cells will be teared when peeling off PDMS stencil

   b. Longer incubation times will passivate all surfaces, PDMS stencil and glass substrate. Thus, cells will not be able to attach on the fibronectin-coated glass.

7. Rinse carefully 3 times with PBS. After the last cleaning step, aspirate completely PBS with a yellow tip connected with a vacuum pump.

8. Sterilize under UV for 10 min.

9. Incubate with fibronectin at 20 μg/ml for 20 min in the incubator. After, aspirate fibronectin and rinse once with cell media. Aspirate all media with vacuum. Leave the samples in the hood uncovered.

10. Trypsinize cells, centrifuge, and resuspend in small volume of cell medium (200 μl aprox).

11. Place a drop of cells at the glass substrate, right at the side of a PDMS stencil. Make sure cell suspension is distributed all beneath the PDMS stencil. Cell solution appears cloudy so it is easy to observe its distribution.

12. Let cells sit and attach to the substrate in the incubator. After 30 min, add 2 ml of medium and leave overnight.

13. On the following day, perform the experiment. Peel off the PDMS stencil with tweezers by holding the PDMS stencil between the tweezers and pulling up, always perpendicular to the glass substrate. Try not to move the stencil horizontally to avoid damaging cells.

14. If fluorescent experiments are performed, change the media to free-of-phenol red media.

15. Proceed to time-lapse microscopy measurements.

ANNEX D. WOUND PATTERNING PROTOCOL

1. RIPPED GAPS

The protocol is the same as the described above, except for the step of Pluronics incubation. Without the Pluronics incubation, cells attach to the PDMS pillars walls, and thus when the stencil is peeled off, the cells attached to the pillars are torn and ripped, producing a gap with surrounded damaged/dead cells.

1. Proceed with steps 1 to 4 of the previous protocol.

2. After attaching PDMS pillar stencil to the substrate, the second fibronectin coating can be performed straight away. No Pluronics incubation.

3. Continue with steps 9-15.

2. CRUSHED GAPS

The method consists on crushing a monolayer of cells with the PDMS pillar stencil, so that the cells beneath the pillars will be squeezed and thus killed. Such dead cell islands appear with a different texture under the microscope, with more granules, and their actin fluorescence mostly disappears.

1. Coat MatTek petri dishes with fibronectin by incubating them with a drop of 100 μl of 20 μg/ml fibronectin in PBS for 1h at room temperature or 20 min at 37°C.

2. Seed cells in the MatTek dishes. Leave them in the incubator overnight.

3. Prepare thick PDMS stencils: pour a large quantity of PDMS in the wafer. This is to ensure that PDMS stencils have a thick roof, which will be convenient afterwards.

4. On the following day, ensure a confluent monolayer has formed. At this point, experiment can start.

5. Hold the PDMS stencils with a needle on the opposite side where pillars are. The stencil can be now easily manipulated by the pinched needle.

6. Place the PDMS pillar stencil in slight contact with the cell sample. Be careful in not sliding the PDMS stencil horizontally, so it would rip or tear cells. Do so without removing the cell media.

7. Check under the microscope if an array of wounds has appeared. Islands of dead cells should appear with a different texture. If that would not occur, the squeezing process can be repeated.

8. Proceed with time-lapse microscopy monitoring.

ANNEX E. Cy3-FIBRONECTIN

The kit used for the fluorescent labelling of fibronectin is from Amersham. Fibronectin is from Sigma.

1. Prepare 800 ml of 0.1 M sodium carbonate buffer by mixing:

   - 300 ml 0.2M $NaHCO_3$
   - 70 ml 0.2M Na_2CO_3
   - 400 ml H_2O

2. Adjust pH at 9.3

3. Dyalise 1 ml of fibronectin in 400 ml of sodium carbonate buffer ON at 4°C. The dyalise membranes and supports are provided by Amersham kit.

4. On the next morning, change the buffer for new 400 ml of sodium carbonate buffer. Let the dyalisis ON at 4°C.

5. Mix the dyalized fibronectin with the aliquot of Cy3 provided by Amersham. Cover with foil.

6. Let react for 30 min at room temperature and gently vortex every 10 min.

7. Dyalize the labelled fibronectin in 400 ml of PBS, let ON at 4°C.

8. On the next morning, recover the labelled fibronectin and store at 4°C until use.

   For the functionalization of substrates with labelled fibronectin, mix the fluorescent fibronectin with regular fibronectin at a ratio of 1:10 (fluo:non-fluo).

ANNEX F. NUCLEI TRACKING

For nuclei labelling for posterior tracking, use DAPI (Invitrogen). Hoescht33342 is not recommended.

1. Dilute in DAPI in medium at a final concentration of 1:250 from a stock solution of 1 mg/ml of DAPI.

2. Let incubate for 4-6 hours

3. Before starting the experiment, rinse thoroughly with medium.

4. Perform experiment with medium without phenol red.

5. For the acquisition, take good care in exposing the mínimum to UV light. Set the intensity of fluorescent light at mínimum and do not expose longer tan 60-80 ms. Time lapses with acquisition intervals of 1 time point/min can last up to 2 hours. For longer experiments, increase the acquisition interval.

   For an automated tracking, nuclei must be completely separated one from each other. Thus, high densitites, where nuclei of different cells contact each other, are not suitable for automated tracking. The analysis of nuclei displacement and polarization is done in Fiji.

6. Adjust the images for a proper intensity and contrast.

7. Threshold the images so that each single nuclei are outlined, and create a binary mask. Each mask must correspond to a single nucleus.

8. In the menu Measure, select a range for the posible area that nuclei can have. This will avoid selecting two nuclei together as a single particle, as the area would be too large to be included.

ANNEX G. IMMUNOSTAININGS

Before starting the staining protocol, rinse 3 times with PBS.

1. Fixation: incubate cells with 4% paraformaldehyde (in PBS) for 15 min at room temperature. Rinse 3 times with PBS

    After fixing the cells, the sample can be stored at 4ºC for few days.

2. Permeabilization: incubate with 0,25% Triton X100 (in PBS) for 5-15 min at room temperature. Rinse once with PBS.

3. Saturation: incubate with 1% BSA (in PBS) for 30 min at room temperature. BSA should be prepared fresh every time. Rinse once with PBS

4. Stainings

5. Immunolabelling:

    a. Antibody labeling:

        i. Primary antibody (dilution depending on the antibody, see below) in 0,5% BSA (in PBS). When the sample is on a glass coverslip, 50 µl of the primary antibody dilution should be placed in a clean parafilm and the glass coverslip placed on top of the drop. Incubation can be done during 2 hours at room temperature or overnight at 4ºC.Rinse 3 times with PBS for 5 min.

        ii. Secondary antibody (typically at 1:200 dilution) in PBS. Same procedure as for the previous step.

    b. Actin staining: incubate with Alexa Fluor 564-conjugated phalloidin at 1:1000 dilution in PBS for 30 min at room temperature. Rinse with PBS.

    c. Nuclei staining: incubate with Hoescht at 1:1000 dilution in PBS for 30 min at room temperature. Rinse with PBS.

6. Mounting: put a drop of 50 µl of Mowiol in a glass slide and place the coverslip on top. Let it reticulate overnight and image the day after.

Antibodies used

Primary antibodies:

- primary rabbit antibody against phospho-MLC (Cell Signaling), dilution 1:200

- primary rabbit antibody against fibronectin (Invitrogen), dilution 1:200

- primary rabbit antibody against laminin (Invitrogen), dilution 1:200

- primary mouse against E-cadherin (BD Transduction Laboratories), dilution 1:1000

- primary rabbit against ZO-1 (Zymed, Invitrogen) , dilution 1:1000

Secondary antibodies:

- secondary polyclonal anti-rabbit conjugated with 488-Alexa Fluor (Invitrogen), dilution 1:200

- secondary polyclonal anti-mouse conjugated with 488-Alexa Fluor (Invitrogen), dilution 1:200

- secondary polyclonal anti-mouse conjugated with 405-Alexa Fluor (Invitrogen), dilution 1:200

H. CONFOCAL ACQUISITION SETTINGS

For confocal acquisition of fixed samples, we typically used the following settings:

- z-stack depth: 10-15 μm depending on the height of the cells. The stack would always comprise all the cells height plus 2 μm above and below.

- z step: given by Nyquist criterion

- pixel dwell: adjust experimentally depending on the sample

- average frame: 2

Images were acquired and processed with NIS Elements software.

I. POLYACRYLAMIDE GELS

1. Prepare BindSilane mixture: mix BindSilane with acetic acid and ethanol in 1:1:7 proportions. BindSilane should be prepared fresh every week.

2. Incubate MatTek Petri dishes (or any glass-bottom dishes) with BindSilane mixture for 5 min.

   Incubation with BindSilane enables the attachment of the polyacrylamide gel to the glass substrate.

3. Remove BindSilane and rinse 3 times with ethanol. Let it air dry.

4. Prepare polyacrylamide mix (see Table I for the volumes required of each component):

   a. 40% acrylamide (varying volume depending on desired stiffness)

   b. 2% bis-acrylamide (varying volume depending on desired stiffness)

   c. 100 μl of N-hydroxisuccinimidil (NHS)

   d. beads (Invitrogen Fluospheres)

   e. 2,5 μl of Amoniunm Persulfate (APS)

   f. 0,25 μl of N,N,N,N-Tetramethylethylenediamine (TEMED)

   g. The resting volume up to 500 μl of final volume is HEPES 10 mM

      APS and TEMED must be added at the last moment, since they trigger the polymerization.

   Note that the mixture can also be prepared to a final volume of 250 μl in order to not waste reagents. In this case, all volumes must be divided by 2. Final volume should not be less than 250 μl in order to have a minimum of 0,125 μl of TEMED. Less TEMED volume would not polymerize the mix.

5. Place a drop of 12 μl (for gels of x mm diameter) or 20 μl drop (for gels of 22 mm) on the center of the MatTek dishes and flatten with a coverslip of the according size.

6. Let polymerize for 30-45 min.

7. Fill the MatTek dishes with HEPES 10 mM.

8. Remove the glass coverslip with the help of a razor blade and tweezers.

9. Aspirate the liquid, leave only a thin film covering the gel.

10. Sterilize by UV light in the cell culture hood for 10 min.

11. Add aprox 100 μl of sterile collagen at a concentration of 0,1 μg/ml, enough to cover the gel.

12. Leave it incubating overnight at 4ºC.

On the following day, seed cells:

13. Trypsinize cells.

14. While cells are being trypsinized, remove the collagen from the gel and rinse once with PBS and once with medium. Remove the medium and let the gel dry slightly (for no more than 10 min)

15. Centrifuge cells. After removing the trypsine supernatant, resuspend the cell pellet with 50 μl of medium.

16. Seed the 50 μl drop of cells in the gel.

17. Let the cells sit and attach to the gel for 20 min.

18. After 20 min, when the cells have started to attach, cover the Petri dish with 2 ml of medium.

19. Leave the cells overnight and proceed with the experiment on the day after.

	0,2	0,7	4,5	9	12	16	35	E (KPa)
HEPES 10mM	340,25	327,75	272,5	266,5	254	222,75	185,25	(μL)
NHS	100	100	100	100	100	100	100	(μL)
Acrilamide 40%	37,5	50	75	93,75	93,75	125	125	(μL)
Bisacrilamide 2%	7,5	7,5	37,5	25	37,5	37,5	75	(μL)
beads	12	12	12	12	12	12	12	(μL)
APS	2,5	2,5	2,5	2,5	2,5	2,5	2,5	(μL)
TEMED	0,25	0,25	0,25	0,25	0,25	0,25	0,25	(μL)

Table I. PA gel recipe for the different gel stiffnesses.

ANNEX J. TRANSFECTION METHODS

1. ELECTROPORATION

Elecroporation is performed with the Neon Transfection System, from Life Technologies. A kit with all reagents and utensils is provided.

1. Add 3 ml of Transfection Buffer E2 to the cuvette in the electroporator

2. Trypsinize cells, centrifuge, resuspend in PBS.

3. Count the cells and calculate the concentration of cells/ml. Adjust to a final cell number of 20.000. Centrifuge again and discard the supernatant completely.

4. Resuspend the 20.000 cells in 100 μl of Resuspension Buffer and pipette thoroughly to disassemble cell aggregates.

5. Add 2-6 μl of plasmid and mix thoroughly with the cells.

6. Pipette the cell suspension with the appropriate transfection tip. Be careful to not produce any bubbles. Should there be any bubble, add 10 μl more of resuspension buffer so it is easier to avoid the bubbles.

7. The transfection parameters for transfecting MDCK cells must be set to: 1650 mV, 20 ms pulse, 1 pulse

8. After the transfection has been performed, place the cell suspension in a 6-well plate. Fill the well with 2 ml of medium.

9. Expression of the transfected protein starts to be visible after 24 h aprox, and can last up to 5 days.

2. TRANSFECTION BY CELL LIGHT REAGENTS®

1. Seed cells at low density. Transfection can be performed 12-24h after.

2. For the transfection, mix 10 μl of Cell Light Talin with 2 ml of medium.

3. Substitute the cell media for the media containing Cell Light Talin.

4. Transfected cells can be used after 16h. Transfection lasts for about 5-7 days

ANNEX K. LASER ABLATION PROTOCOL

Laser ablation of cells was performed in collaboration with Julien Collombeli, at the Advanced Digital Microscopy core, at Institut Recerca Biomedica (IRB) in Barcelona, Spain.

1. Calibrate the laser to ensure the laser beam shoots at the spot highlighted in the software.

2. Focus at the very apical part of the cell and shine a laser pulse.

   The laser shot is effective when a cavitation bubble appears, seen as a transient black bubble being released from the ablated cell.

3. Repeat laser shot until cell appears dead. To make sure the cell is dead, actin fluorescence must have faded and cell appears rough in transmitted light.

   a. If the laser is focused too apically, it will not interact with the cellular material, no cavitation bubble will appear.

   b. If the laser is focused too basally, there is a high risk of photobleaching the fluorescent beads.

   Thus, a compromise in the region of ablation must be reached: the more apical the shooting, the less effective ablation is; by contrast, basal laser targeting will very likely ablate the cell and photobleach the beads.

   It is advisable to start the ablation process at the apical-most part of cells and proceed to the basal part if cell disruption is not accomplished.

4. In order to check for possible photobleaching of the fluorescent beads, image on the channel for beads fluorescence. Photobleached beads will appear as a black region in the spot of the ablation target. All area devoided of fluorescent beads cannot be used for traction force calculation, thus mechanical information will be missing.

ANNEX L. CONFOCAL MICROSCOPY MEASUREMENT FOR TRACTION FORCE CALCULATIONS.

Monitoring of the closure is performed in a CLSM Nikon A1R.

- For cell monitoring, we acquire a z-stack of ≈8 z–planes of 1.5 μm z-step, ranging from the apical part of the cell to its most-basal part. The number of planes can vary according to cell's height.

  For an improved resolution in the z-direction, z-step should be around 0.3 μm. This is particularly relevant to track the position of the actin ring from a lateral view in an ortogonal xz reconstruction, as shown in Figure 3. 11.

  Acquiring a stack of different z-planes allows us for a better spatial determination of the localization of actin, and a good resolution when reconstructing the total cell volume.

- For bead monitoring, we acquire a z-stack of ~12 z planes, 0.3 μm z-step. This stack typically ranges from around 1 μm above the position of the beads, to 3 μm deep inside the gel.

  By having a stack of the beads we can compensate for possible defocusing events. Take good care in obtaining always the upper-most layer of fluorescent beads, which is critical for traction force calculation.

Abbreviations

ABP: Actin-Binding Proteins

Arp2/3: Actin Related Proteins 2 and 3

CIL: Contact Inhibition of Locomotion

Cx: Connexin

CXCR: Chemokine Receptor

DRIE: Deep Reactive Ion Etching

ECM: Extracellular Matrix

EGF: Epidermal Growth Factor

EMT: Epitelial to Mesenchymal Transition

ERK: Extracellular signal-Regulated Kinase, synonym of MAPK

FA: focal adhesion, FC: focal complex

FAK: Focal Adhesion Kinase

FGF: Fibroblast Growth Factor

FITC: fluoresce   in isothyacianate

FRET: Förster or Fluorescence Resonance Energy Transfer

GAP: GTPase Activating Factor

GEF: Guanine nucleotide Exchange Factor

GDI: Guanine nucleotide Dissociation Inhibitor

HGF: hepatocyte growth factor

IRSp53: Insulin-receptor tyrosine kinase Susbtrate p53

JAM: Junctional Adhesion Molecule

JNK: c-Jun N-terminal Kinase

KGF: Keratinocyte Growth Factor

LIMK: LIM Kinase

MAPK: Microtubule-Associated Protein Kinase

MDCK: Madin-Darby Canine Kidney

MET: Mesenchymal to Epithelial Transition

MHC: Myosin Heavy Chain

MLC: Myosin light Chain

MRC: Myosin Regulatory Chain

MLCK: Myosin Light Chain Kinase

MMP: Matrix MetalloProteinases

MRCK: Myotonic dystrophy kinase Related Cdc42-binding Kinase

MTOC: Microtubule Organizing Centre

MYPT: Myosin Phosphatase Targeting Protein

NF-KB: nuclear factor kappa-light-chain-enhancer of activated B cells

NHS: N-hydroxisuccinimydil

NPF: Nucleation-Promoting Factor

PA: polyacrylamide

PAK: p21 Activated Kinase

PDGF: Platelet-Derived Growth Factor

PDMS: PolyDiMethylSiloxane

PIP2: PhosphatidylInositol 4,5-bisPhosphate or PtdIns(4,5)P_2

PI3K: PhosphatidylInositol 3-Kinase

PKC: Protein Kinase C

ROCK: Rho-associated protein Kinase

ROS: Reactive Oxygen Species

S1P: Sphingosine-1-Phosphate

TNF-α: tumor necrosis factor α

TGF-β: Transforming Growth factor beta

VEGF: Vascular Endotelial Growth Factor

ZIPK: Zipper-Interacting Protein Kinase

Bibliography

Abe, K., and Takeichi, M. (2007). EPLIN mediates linkage of the cadherin – catenin complex to F-actin and stabilizes the circumferential actin belt. *Proceedings of the National Academy of Sciences 105*, 13–19.

Abercrombie, M., and Heaysman, J. (1953). Observations on the social behaviour of cells in tissue culture: I. Speed of movement of chick heart fibroblasts in relation to their mutual contacts. *Experimental cell research 5*, 111–131.

Abraham, V. C., Krishnamurthi, V., Taylor, D. L., and Lanni, F. (1999). The actin-based nanomachine at the leading edge of migrating cells. *Biophysical journal 77*, 1721–1732.

Abrams, J. M., White, K., Fessler, L. I., and Steller, H. (1993). Programmed cell death during Drosophila embryogenesis. *Development 117*, 29–43.

Abreu-Blanco, M. T., Verboon, J. M., and Parkhurst, S. M. (2011). Cell wound repair in Drosophila occurs through three distinct phases of membrane and cytoskeletal remodeling. *The Journal of cell biology 193*, 455–464.

Abreu-Blanco, M. T., Watts, J. J., Verboon, J. M., and Parkhurst, S. M. (2012). Cytoskeleton responses in wound repair. *Cellular and molecular life sciences : CMLS*. In press

Ahmed, S., Goh, W. I., and Bu, W. (2010). I-BAR domains, IRSp53 and filopodium formation. *Seminars in cell & developmental biology 21*, 350–356.

Alexander, S., Koehl, G. E., Hirschberg, M., Geissler, E. K., and Friedl, P. (2008). Dynamic imaging of cancer growth and invasion : a modified skin-fold chamber model. *Histochemistry and cell biology 130*, 1147–1154.

Alexandrova, A. Y., Arnold, K., Schaub, S., Vasiliev, J. M., Meister, J.-J., Bershadsky, A. D., and Verkhovsky, A. B. (2008). Comparative dynamics of retrograde actin flow and focal adhesions: formation of nascent adhesions triggers transition from fast to slow flow. *PloS one 3*, e3234.

Altan, Z. M., and Fenteany, G. (2004). c-Jun N-terminal kinase regulates lamellipodial protrusion and cell sheet migration during epithelial wound closure by a gene expression-independent mechanism. *Biochemical and Biophysical Research Communications 322*, 56–67.

Aman, A., and Piotrowski, T. (2010). Cell migration during morphogenesis. *Developmental biology 341*, 20–33.

Amann, K. J., and Pollard, T. D. (2001). The Arp2/3 complex nucleates actin filament branches from the sides of pre-existing filaments. *Nature cell biology 3*, 306–310.

Ananthakrishnan, R., and Ehrlicher, A. (2007). The forces behind cell movement. *International journal of biological sciences 3*, 303–317.

Andrade, D., and Rosenblatt, J. (2011). Apoptotic regulation of epithelial cellular extrusion. *Apoptosis : an international journal on programmed cell death 16*, 491–501.

Andrew, D. J., and Ewald, A. J. (2010). Morphogenesis of epithelial tubes: Insights into tube formation, elongation, and elaboration. *Developmental biology 341*, 34–55.

Angelini, T. E., Hannezo, E., Trepat, X., Marquez, M., Fredberg, J. J., and Weitz, D. a (2011). Glass-like dynamics of collective cell migration. *Proceedings of the National Academy of Sciences 108*, 4714–4719.

Balaban, N. Q., Schwarz, U. S., Riveline, D., Goichberg, P., Tzur, G., Sabanay, I., Mahalu, D., Safran, S., Bershadsky, a, Addadi, L., et al. (2001). Force and focal adhesion assembly: a close relationship studied using elastic micropatterned substrates. *Nature cell biology 3*, 466–472.

Bao, J., Ma, X., Liu, C., and Adelstein, R. S. (2007). Replacement of nonmuscle myosin II-B with II-A rescues brain but not cardiac defects in mice. *The Journal of biological chemistry 282*, 22102–22111.

Batchelder, E. L., Hollopeter, G., Campillo, C., Mezanges, X., Jorgensen, E. M., Nassoy, P., Sens, P., and Plastino, J. (2011). Membrane tension regulates motility by controlling lamellipodium organization. *108*, 11429–11434.

Bell, C., and Waizbard, E. (1986). Variability of cell size in primary and metastatic human breast carcinoma. *Invasion Metastasis 6*, 11–20.

Bement, W. M., Forscher, P., and Mooseker, M. S. (1993). A novel cytoskeletal structure involved in purse string wound closure and cell polarity maintenance. *The Journal of cell biology 121*, 565–578.

Bement, W. M., Mandato, C. A., and Kirsch, M. N. (1999). Wound-induced assembly and closure of an actomyosin purse string in Xenopus oocytes. *Current biology 9*, 579–587.

Bement, W. M., Yu, H.-Y. E., Burkel, B. M., Vaughan, E. M., and Clark, A. G. (2007). Rehabilitation and the single cell. *Current opinion in cell biology 19*, 95–100.

Bénazéraf, B., Francois, P., Baker, R. E., Denans, N., Little, C. D., & Pourquié, O. (2010). A random cell motility gradient downstream of FGF controls elongation of an amniote embryo. *Nature*, 466(7303), 248-52.

Beningo, K. a, Dembo, M., Kaverina, I., Small, J. V., and Wang, Y. L. (2001). Nascent focal adhesions are responsible for the generation of strong propulsive forces in migrating fibroblasts. *The Journal of cell biology 153*, 881–888.

Benink, H. a, and Bement, W. M. (2005). Concentric zones of active RhoA and Cdc42 around single cell wounds. *The Journal of cell biology 168*, 429–439.

Benjamin, J. M., Kwiatkowski, A. V., Yang, C., Korobova, F., Pokutta, S., Svitkina, T., Weis, W. I., and Nelson, W. J. (2010). AlphaE-catenin regulates actin dynamics independently of cadherin-mediated cell-cell adhesion. *The Journal of cell biology 189*, 339–352.

Benseñor, L. B., Kan, H.-M., Wang, N., Wallrabe, H., Davidson, L. a, Cai, Y., Schafer, D. a, and Bloom, G. S. (2007). IQGAP1 regulates cell motility by linking growth factor signaling to actin assembly. *Journal of cell science 120*, 658–669.

Bianco, A., Poukkula, M., Cliffe, A., Mathieu, J., Luque, C. M., Fulga, T. a, and Rørth, P. (2007). Two distinct modes of guidance signalling during collective migration of border cells. *Nature 448*, 362–365.

Binamé, F., Pawlak, G., Roux, P., and Hibner, U. (2010). What makes cells move: requirements and obstacles for spontaneous cell motility. *Molecular bioSystems 6*, 648–661.

Bindschadler, M., and McGrath, J. L. (2007). Sheet migration by wounded monolayers as an emergent property of single-cell dynamics. *Journal of cell science 120*, 876–884.

Blanchoin, L., Amann, K. J., Higgs, H. N., Marchand, J.-baptiste, Kaiser, D. A., and Pollard, T. D. (2000). Direct observation of dendritic actin complex and WASP / Scar proteins. *Nature 171*, 1007–1011.

Blaser, H., Eisenbeiss, S., Neumann, M., Reichman-Fried, M., Thisse, B., Thisse, C., and Raz, E. (2005). Transition from non-motile behaviour to directed migration during early PGC development in zebrafish. *Journal of cell science 118*, 4027–4038.

Block, E. R., and Klarlund, J. K. (2008). Wounding Sheets of Epithelial Cells Activates the Epidermal Growth Factor Receptor through Distinct Short- and Long-Range Mechanisms. *Molecular biology of the cell 19*, 4909–4917.

Block, E. R., Matela, A. R., SundarRaj, N., Iszkula, E. R., and Klarlund, J. K. (2004). Wounding induces motility in sheets of corneal epithelial cells through loss of spatial constraints: role of heparin-binding epidermal growth factor-like growth factor signaling. *The Journal of biological chemistry 279*, 24307–24312.

Bloor, J. W., and Kiehart, D. P. (2002). Drosophila RhoA regulates the cytoskeleton and cell-cell adhesion in the developing epidermis. Development 129, 3173–3183.

Braga, V. M., Del Maschio, a, Machesky, L., and Dejana, E. (1999). Regulation of cadherin function by Rho and Rac: modulation by junction maturation and cellular context. Molecular biology of the cell, 10(1), 9-22.

Brandt, B., Junker, R., Griwatz, C., Junker, R., Heidi, S., Brinkmann, O., Semjonow, A., Assmann, G., and Zã, S. (1996). Isolation of Prostate-derived Single Cells and Cell Clusters from Human Peripheral Blood. *Cancer research*, 4556–4561.

Bridgman, P. C., Dave, S., Asnes, C. F., Tullio, a N., and Adelstein, R. S. (2001). Myosin IIB is required for growth cone motility. *The Journal of neuroscience 21*, 6159–6169.

212

Brock, J., Midwinter, K., Lewis, J., and Martin, P. (1996). Demonstration of a Requirement for Rho Activation. Journal of Cell Biology *135*, 1097–1107.

Buchsbaum, R. J. (2007). Rho activation at a glance. *Journal of cell science 120*, 1149–1152.

Bugyi, B., and Carlier, M.-F. (2010). Control of actin filament treadmilling in cell motility. *Annual review of biophysics 39*, 449–470.

Bugyi, B., Le Clainche, C., Romet-Lemonne, G., and Carlier, M.-F. (2008). How do in vitro reconstituted actin-based motility assays provide insight into in vivo behavior? *FEBS letters 582*, 2086–2092.

Burridge, K., and Chrzanowska-Wodnicka, M. (1996). Focal adhesions, contractility, and signaling. *Annual review of cell and developmental biology 12*, 463–518.

Butcher, D. T., Alliston, T., and Weaver, V. M. (2009). A tense situation: forcing tumour progression. *Nature reviews Cancer 9*, 108–122.

Butler, J. P., Tolić-Nørrelykke, I. M., Fabry, B., and Fredberg, J. J. (2002). Traction fields, moments, and strain energy that cells exert on their surroundings. *American journal of physiology. Cell physiology,* 282(3), C595–605.

Byers, S. W., Sommers, C. L., Hoxter, B., Mercurio, a M., and Tozeren, a (1995). Role of E-cadherin in the response of tumor cell aggregates to lymphatic, venous and arterial flow: measurement of cell-cell adhesion strength. *Journal of cell science* 108, 5, 2053–2064.

Cai, Y., Biais, N., Giannone, G., Tanase, M., Jiang, G., Hofman, J. M., Wiggins, C. H., Silberzan, P., Buguin, A., Ladoux, B., et al. (2006). Nonmuscle myosin IIA-dependent force inhibits cell spreading and drives F-actin flow. *Biophysical journal 91*, 3907–3920.

Cai, Y., and Sheetz, M. P. (2009). Force propagation across cells: mechanical coherence of dynamic cytoskeletons. *Current opinion in cell biology 21*, 47–50.

Campellone, K. G., and Welch, M. D. (2010). A nucleator arms race: cellular control of actin assembly. *Nature reviews. Molecular cell biology 11*, 237–251.

Campos, I., Geiger, J. a, Santos, A. C., Carlos, V., and Jacinto, A. (2010). Genetic screen in Drosophila melanogaster uncovers a novel set of genes required for embryonic epithelial repair. *Genetics 184*, 129–140.

Carlier, M. F., Laurent, V., Santolini, J., Melki, R., Didry, D., Xia, G. X., Hong, Y., Chua, N. H., and Pantaloni, D. (1997). Actin depolymerizing factor (ADF/cofilin) enhances the rate of filament turnover: implication in actin-based motility. *The Journal of cell biology 136*, 1307–1322.

Carmona-Fontaine, C., Matthews, H. K., Kuriyama, S., Moreno, M., Dunn, G. a, Parsons, M., Stern, C. D., and Mayor, R. (2008). Contact inhibition of locomotion in vivo controls neural crest directional migration. *Nature 456*, 957–961.

Caussinus, E., Colombelli, J., and Affolter, M. (2008). Tip-cell migration controls stalk-cell intercalation during Drosophila tracheal tube elongation. *Current biology 18*, 1727–1734.

Cavey, M., Rauzi, M., Lenne, P.-F., and Lecuit, T. (2008). A two-tiered mechanism for stabilization and immobilization of E-cadherin. *Nature 453*, 751–756.

Chaffer, C. L., Thompson, E. W., and Williams, E. D. (2007). Mesenchymal to epithelial transition in development and disease. *Cells, tissues, organs 185*, 7–19.

Chan, C., and Odde, D. J. (2008). Traction Dynamics of Filopodia on. Science *322*, 1687–1691.

Chaponnier, C., and Gabbiani, G. (2005). Tissue repair, contraction , and the myofibroblast. *Wound repair and regeneration*, 13, 7-12.

Chen, C. S. (2008). Mechanotransduction - a field pulling together? *Journal of cell science 121*, 3285–3292.

Cheney, R. E., Riley, M. A., and Mooseker, M. S. (1993). Phylogenetic Analysis of the Myosin Superfamily. *Cell Motility and the Cytoskeleton 223*, 215–223.

Chidgey, M., and Dawson, C. (2007). Desmosomes: a role in cancer? British journal of cancer 96, 1783–1787.

Chiu, D. T., Jeon, N. L., Huang, S., Kane, R. S., Wargo, C. J., Choi, I. S., Ingber, D. E., and Whitesides, G. M. (2000). Patterned deposition of cells and proteins onto surfaces by using three-dimensional microfluidic systems. *Proceedings of the National Academy of Sciences of the United States of America*. 97, 2408–2413.

Choi, C. K., Vicente-Manzanares, M., Zareno, J., Whitmore, L. a, Mogilner, A., and Horwitz, A. R. (2008). Actin and alpha-actinin orchestrate the assembly and maturation of nascent adhesions in a myosin II motor-independent manner. *Nature cell biology 10*, 1039–1050.

Christiansen, J. J., and Rajasekaran, A. K. (2006). Reassessing epithelial to mesenchymal transition as a prerequisite for carcinoma invasion and metastasis. *Cancer research 66*, 8319–8326.

Chrzanowska-Wodnicka, M., and Burridge, K. (1996). Rho-stimulated contractility drives the formation of stress fibers and focal adhesions. *The Journal of cell biology 133*, 1403–1415.

Clark, A. G., Miller, A. L., Vaughan, E., Yu, H.-Y. E., Penkert, R., and Bement, W. M. (2009). Integration of single and multicellular wound responses. *Current biology 19*, 1389–1395.

Colas, J., and Schoenwolf, G. (2001). Towards a cellular and molecular understanding of neurulation. *Developmental dynamics 145*, 117–145.

Coles, E. G., Taneyhill, L. a, and Bronner-Fraser, M. (2007). A critical role for Cadherin6B in regulating avian neural crest emigration. *Developmental biology 312*, 533–544.

Connolly, B. A., Rice, J., Feig, L. A., Rachel, J., and Buchsbaum, R. J. (2005). Tiam1-IRSp53 Complex Formation Directs Specificity of Rac-Mediated Actin Cytoskeleton Regulation. *Molecular and Cellular Biolgy 25*, 4602.

Conti, M. a., and Adelstein, R. S. (2008). Nonmuscle myosin II moves in new directions. *Journal of Cell Science 121*, 404–404.

Cooper, J. a (1987). Effects of cytochalasin and phalloidin on actin. *The Journal of cell biology 105*, 1473–1478.

Copp, A. J. (2005). Neurulation in the cranial region--normal and abnormal. *Journal of anatomy 207*, 623–635.

Copp, A. J., and Greene, N. D. E. (2010). Defining a PARticular Pathway of Neural Tube Closure. *Developmental Cell 18*, 1–2.

Corfe, B. M., Dive, C., and Garrod, D. R. (2000). Changes in intercellular junctions during apoptosis precede nuclear condensation or phosphatidylserine exposure on the cell surface. *Cell death and differentiation 7*, 234–235.

Costa, M., Raich, W., Agbunag, C., Leung, B., Hardin, J., and Priess, J. R. (1998). A Putative Catenin–Cadherin System Mediates Morphogenesis of the. *The Journal of cell biology 141*, 297–308.

Cowin, A. J., Adams, D., Geary, S. M., Wright, M. D., Jones, J. C. R., and Ashman, L. K. (2006). Wound healing is defective in mice lacking tetraspanin CD151. *The Journal of investigative dermatology 126*, 680–689.

Cramer, L. P. (1997). Molecular mechanism of actin-dependent retrograde flow in lamellipodia of motile cells. *Frontiers in bioscience 2*, d260–70.

Cuvelier, D., Théry, M., Chu, Y.-S., Dufour, S., Thiéry, J.-P., Bornens, M., Nassoy, P., and Mahadevan, L. (2007). The universal dynamics of cell spreading. *Current biology 17*, 694–699.

Czuchra, A., Wu, X., Meyer, H., Hengel, J. V., Schroeder, T., Geffers, R., Rottner, K., and Brakebusch, C. (2005). Cdc42 Is Not Essential for Filopodium Formation , Directed Migration , Cell Polarization , and Mitosis in Fibroblastoid. *Molecular biology of the cell 16*, 4473–4484.

Czyz, J. (2008). The stage-specific function of gap junctions during tumourigenesis. *Cellular and molecular biology letters*, 13(1), 92-102.

Danjo, Y., and Gipson, I. K. (1998). Actin "purse string" filaments are anchored by E-cadherin-mediated adherens junctions at the leading edge of the epithelial wound, providing coordinated cell movement. *Journal of cell science 111 Pt 2*, 3323–3332.

Danjo, Y., and Gipson, I. K. (2002). Specific transduction of the leading edge cells of migrating epithelia demonstrates that they are replaced during healing. *Experimental eye research 74*, 199–204.

Davidson, L. A., and Keller, R. E. (1999). Neural tube closure in Xenopus laevis involves medial migration, directed protrusive activity, cell intercalation and convergent extension. *Development 126*, 4547–4556.

Davidson, L. A, Ezin, A. M., & Keller, R. (2002). Embryonic wound healing by apical contraction and ingression in Xenopus laevis. *Cell motility and the cytoskeleton*, 53(3), 163-76.

del Rio, A., Perez-Jimenez, R., Liu, R., Roca-Cusachs, P., Fernandez, J. M., and Sheetz, M. P. (2009). Stretching single talin rod molecules activates vinculin binding. *Science 323*, 638–641.

Dent, E. W., Kwiatkowski, A. V., Mebane, L. M., Philippar, U., Barzik, M., Rubinson, D. a, Gupton, S., Van Veen, J. E., Furman, C., Zhang, J., et al. (2007). Filopodia are required for cortical neurite initiation. *Nature cell biology 9*, 1347–1359.

de Rooij, J., Kerstens, A., Danuser, G., Schwartz, M. a, and Waterman-Storer, C. M. (2005). Integrin-dependent actomyosin contraction regulates epithelial cell scattering. *The Journal of cell biology 171*, 153–164.

Desai, L. P., Aryal, A. M., Ceacareanu, B., Hassid, A., and Waters, C. M. (2004). RhoA and Rac1 are both required for efficient wound closure of airway epithelial cells. *American journal of physiology. Lung cellular and molecular physiology 287*, L1134–44.

Dickinson, R. B., Caro, L., and Purich, D. L. (2004). Force generation by cytoskeletal filament end-tracking proteins. *Biophysical journal 87*, 2838–2854.

Didry, D., Carlier, M. F., and Pantaloni, D. (1998). Synergy between actin depolymerizing factor/cofilin and profilin in increasing actin filament turnover. *The Journal of biological chemistry 273*, 25602–25611.

Discher, D. E., Janmey, P., and Wang, Y.-L. (2005). Tissue cells feel and respond to the stiffness of their substrate. *Science 310*, 1139–1143.

Dokukina, I. V., and Gracheva, M. E. (2010). A model of fibroblast motility on substrates with different rigidities. *Biophysical journal 98*, 2794–2803.

Douezan, S., Dumond, J., and Brochard-Wyart, F. (2012). Wetting transitions of cellular aggregates induced by substrate rigidity. *Soft Matter 8*, 4578.

Drees, F., Pokutta, S., Yamada, S., Nelson, W. J., and Weis, W. I. (2005). Alpha-catenin is a molecular switch that binds E-cadherin-beta-catenin and regulates actin-filament assembly. *Cell 123*, 903–915.

du Roure, O., Saez, A., Buguin, A., Austin, R. H., Chavrier, P., Silberzan, P., Siberzan, P., and Ladoux, B. (2005). Force mapping in epithelial cell migration. *Proceedings of the National Academy of Sciences of the United States of America 102*, 2390–2395.

Eisenhoffer, G. T., Loftus, P. D., Yoshigi, M., Otsuna, H., Chien, C.-B., Morcos, P. a, and Rosenblatt, J. (2012). Crowding induces live cell extrusion to maintain homeostatic cell numbers in epithelia. *Nature 484*, 546–549.

Ellis, S., and Mellor, H. (2000). The novel Rho-family GTPase rif regulates coordinated actin-based membrane rearrangements. *Current biology 10*, 1387–1390.

Engler, A. J., Sen, S., Sweeney, H. L., and Discher, D. E. (2006). Matrix elasticity directs stem cell lineage specification. *Cell 126*, 677–689.

Etienne-Manneville, S., and Hall, A (2001). Integrin-mediated activation of Cdc42 controls cell polarity in migrating astrocytes through PKCz. *Cell 106*, 489–498.

Etienne-manneville, S. (2002). Rho GTPases in cell biology. *Nature 420*, 629–635.

Even-Ram, S., Doyle, A. D., Conti, M. A., Matsumoto, K., Adelstein, R. S., and Yamada, K. M. (2007). Myosin IIA regulates cell motility and actomyosin-microtubule crosstalk. *Nature Cell Biology 9*, 299–309.

Ewald, A. J., Brenot, A., Duong, M., Chan, B. S., and Werb, Z. (2008). Collective epithelial migration and cell rearrangements drive mammary branching morphogenesis. *Developmental cell 14*, 570–581.

Farge, E. (2003). Mechanical Induction of Twist in the Drosophila Foregut / Stomodeal Primordium. *Current Biology 13*, 1365–1377.

Farooqui, R., and Fenteany, G. (2005). Multiple rows of cells behind an epithelial wound edge extend cryptic lamellipodia to collectively drive cell-sheet movement. *Journal of cell science 118*, 51–63.

Fenteany, G., Janmey, P. A., and Stossel, T. P. (2000). Signaling pathways and cell mechanics involved in wound closure by epithelial cell sheets. *Current biology 10*, 831–838.

Florian, P., Schoneberg, T., Schulzke, J. D., Fromm, M., and Gitter, a H. (2002). Single-cell epithelial defects close rapidly by an actinomyosin purse string mechanism with functional tight junctions. *The Journal of Physiology 545*, 485–499.

Fouchard, J., Mitrossilis, D., and Asnacios, A. (2011). Acto-myosin based response to stiffness and rigidity sensing. *Cell adhesion & migration 5*, 16–19.

Franco, S. J., and Huttenlocher, A. (2005). Regulating cell migration: calpains make the cut. *Journal of cell science* 118, 3829–3838.

Franck, C., Maskarinec, S. a, Tirrell, D. a, and Ravichandran, G. (2011). Three-dimensional traction force microscopy: a new tool for quantifying cell-matrix interactions. *PloS one*, 6(3), e17833

Franke, J. D., Montague, R. a, and Kiehart, D. P. (2005). Nonmuscle myosin II generates forces that transmit tension and drive contraction in multiple tissues during dorsal closure. Current biology 15, 2208–2221.

Friedl, P. (2004). Prespecification and plasticity: shifting mechanisms of cell migration. *Current opinion in cell biology 16*, 14–23.

Friedl, P., and Alexander, S. (2011). Cancer invasion and the microenvironment: plasticity and reciprocity. *Cell 147*, 992–1009.

Friedl, P., and Gilmour, D. (2009). Collective cell migration in morphogenesis, regeneration and cancer. *Nature reviews. Molecular cell biology 10*, 445–457.

Friedl, P., Hegerfeldt, Y., and Tusch, M. (2004). Collective cell migration in morphogenesis and cancer. *The International journal of developmental biology 48*, 441–449.

Friedl, P., and Wolf, K. (2010). Plasticity of cell migration: a multiscale tuning model. *The Journal of cell biology 188*, 11–19.

Friedl, P., and Wolf, K. (2003). Tumour-cell invasion and migration: diversity and escape mechanisms. *Nature reviews. Cancer 3*, 362–374.

Gabbiani, G. (2003). The myofibroblast in wound healing and fibrocontractive diseases. *The Journal of pathology 200*, 500–503.

Gaggioli, C., Hooper, S., Hidalgo-Carcedo, C., Grosse, R., Marshall, J. F., Harrington, K., & Sahai, E. (2007). Fibroblast-led collective invasion of carcinoma cells with differing roles for RhoGTPases in leading and following cells. *Nature cell biology*, 9(12), 1392–400.

Galbraith, C. G., Yamada, K. M., and Sheetz, M. P. (2002). The relationship between force and focal complex development. *The Journal of cell biology 159*, 695–705.

Galko, M. J., and Krasnow, M. a (2004). Cellular and genetic analysis of wound healing in Drosophila larvae. *PLoS biology 2*, E239.

Ganz, A., Lambert, M., Saez, A., Silberzan, P., Buguin, A., Mège, R. M., and Ladoux, B. (2006). Traction forces exerted through N-cadherin contacts. *Biology of the cell 98*, 721–730.

Garcia-Fernandez, B., Campos, I., Geiger, J., Santos, A. C., and Jacinto, A. (2009). Epithelial resealing. *The International journal of developmental biology 53*, 1549–1556.

Gardel, M. L., Sabass, B., Ji, L., Danuser, G., Schwarz, U. S., and Waterman, C. M. (2008). Traction stress in focal adhesions correlates biphasically with actin retrograde flow speed. *The Journal of cell biology 183*, 999–1005.

Garlick, J., and Taichman, L. (1994). Effect of TGF-b1 on re-epithelialization of human keratinocytes in vitro: an organotypic model. *Journal for investigative dermatology* 103 (4) 553-559.

Gauthier, N. C., Fardin, M. A., Roca-Cusachs, P., and Sheetz, M. P. (2011). Temporary increase in plasma membrane tension coordinates the activation of exocytosis and contraction during cell spreading. *Proceedings of the National Academy of Sciences of the United States of America 108*, 14467–14472.

216

Geiger, B., Spatz, J. P., and Bershadsky, A. D. (2009). Environmental sensing through focal adhesions. *Nature reviews. Molecular cell biology 10*, 21–33.

Georges, P. C., and Janmey, P. a (2005). Cell type-specific response to growth on soft materials. *Journal of applied physiology 98*, 1547–1553.

Gerbal, F., Chaikin, P., Rabin, Y., and Prost, J. (2000). An elastic analysis of Listeria monocytogenes propulsion. *Biophysical journal 79*, 2259–2275.

Ghabrial, A. S., and Krasnow, M. a (2006). Social interactions among epithelial cells during tracheal branching morphogenesis. *Nature 441*, 746–749.

Ghibaudo, M., Saez, A., Trichet, L., Xayaphoummine, A., Browaeys, J., Silberzan, P., Buguin, A., and Ladoux, B. (2008). Traction forces and rigidity sensing regulate cell functions. *Soft Matter 4*, 1836.

Giannone, G., Dubin-Thaler, B. J., Döbereiner, H.-G., Kieffer, N., Bresnick, A. R., and Sheetz, M. P. (2004). Periodic lamellipodial contractions correlate with rearward actin waves. *Cell 116*, 431–443.

Giannone, G., Dubin-Thaler, B. J., Rossier, O., Cai, Y., Chaga, O., Jiang, G., Beaver, W., Döbereiner, H.-G., Freund, Y., Borisy, G., et al. (2007). Lamellipodial actin mechanically links myosin activity with adhesion-site formation. *Cell 128*, 561–575.

Giannone, G., Mège, R.-M., and Thoumine, O. (2009). Multi-level molecular clutches in motile cell processes. *Trends in cell biology 19*, 475–486.

Godin, L. M., Vergen, J., Prakash, Y. S., Pagano, R. E., and Hubmayr, R. D. (2011). Spatiotemporal dynamics of actin remodeling and endomembrane trafficking in alveolar epithelial type I cell wound healing. *American journal of physiology. Lung cellular and molecular physiology 300*, L615–23.

Golomb, E., Ma, X., Jana, S. S., Preston, Y. a, Kawamoto, S., Shoham, N. G., Goldin, E., Conti, M. A., Sellers, J. R., and Adelstein, R. S. (2004). Identification and characterization of nonmuscle myosin II-C, a new member of the myosin II family. *The Journal of biological chemistry 279*, 2800–2808.

Gorshkova, I., He, D., Berdyshev, E., Usatyuk, P., Burns, M., Kalari, S., Zhao, Y., Pendyala, S., Garcia, J. G. N., Pyne, N. J., et al. (2008). Protein kinase C-e regulates sphingosine 1-phosphate-mediated migration of human lung endothelial cells through activation of phospholipase D2, protein kinase C-z, and Rac1. *The Journal of biological chemistry 283*, 11794–11806.

Gough, W., Hulkower, K. I., Lynch, R., McGlynn, P., Uhlik, M., Yan, L., and Lee, J. a (2011). A quantitative, facile, and high-throughput image-based cell migration method is a robust alternative to the scratch assay. *Journal of biomolecular screening 16*, 155–163.

Gov, N. S. (2007). Collective cell migration patterns: follow the leader. *Proceedings of the National Academy of Sciences of the United States of America 104*, 15970–15971.

Grasso, S., Hernández, J. a, and Chifflet, S. (2007). Roles of wound geometry, wound size, and extracellular matrix in the healing response of bovine corneal endothelial cells in culture. American journal of physiology. *Cell physiology 293*, C1327–37.

Gregorc, U., Ivanova, S., Thomas, M., Guccione, E., Glaunsinger, B., Javier, R., Turk, V., Banks, L., and Turk, B. (2007). Cleavage of MAGI-1, a tight junction PDZ protein, by caspases is an important step for cell-cell detachment in apoptosis. *Apoptosis : an international journal on programmed cell death 12*, 343–354.

Grinnel, F., Ho, C., and Wysocki, A. (1992). Degradation of fibronectin and vitronectin in chronic wound fluid: analysis by cell blotting, immunoblotting, and cell adhesion assays. *Journal for investigative dermatology*.98 (4) 410-416.

Grose, R., Hutter, C., Bloch, W., Thorey, I., Watt, F. M., Fässler, R., Brakebusch, C., and Werner, S. (2002). A crucial role of β1 integrins for keratinocyte migration in vitro and during cutaneous wound repair. *Development 2315*, 2303–2315.

Grutnert, S., Jechlinger, M., and Beug, H. (2003). Diverse cellular and molecular mechanisms contribute to epithelial plasticity and metastasis. *Nature Reviews Molecular Cell Biology 4*, 657–665.

Gu, Y., Forostyan, T., Sabbadini, R., and Rosenblatt, J. (2011). Epithelial cell extrusion requires the sphingosine-1-phosphate receptor 2 pathway. *The Journal of cell biology 193*, 667–676.

Gumbiner, B. M. (2005). Regulation of cadherin-mediated adhesion in morphogenesis. *Nature reviews. Molecular cell biology 6*, 622–634.

Guo, W., and Giancotti, F. G. (2004). Integrin signalling during tumour progression. *Nature reviews. Molecular cell biology 5*, 816–826.

Guo, W.-hui, Frey, M. T., Burnham, N. a, and Wang, Y.-li (2006). Substrate rigidity regulates the formation and maintenance of tissues. *Biophysical journal 90*, 2213–2220.

Gupton, S. L., Anderson, K. L., Kole, T. P., Fischer, R. S., Ponti, A., Hitchcock-DeGregori, S. E., Danuser, G., Fowler, V. M., Wirtz, D., Hanein, D., et al. (2005). Cell migration without a lamellipodium: translation of actin dynamics into cell movement mediated by tropomyosin. *The Journal of cell biology 168*, 619–631.

Gupton, S. L., and Waterman-Storer, C. M. (2006). Spatiotemporal feedback between actomyosin and focal-adhesion systems optimizes rapid cell migration. *Cell 125*, 1361–1374.

Gurtner, G. C., Werner, S., Barrandon, Y., and Longaker, M. T. (2008). Wound repair and regeneration. *Nature 453*, 314–321.

Haas, P., and Gilmour, D. (2006). Chemokine signaling mediates self-organizing tissue migration in the zebrafish lateral line. *Developmental cell 10*, 673–680.

Halbleib, J. M., and Nelson, W. J. (2006). Cadherins in development: cell adhesion, sorting, and tissue morphogenesis. *Genes & development 20*, 3199–3214.

Hall, A. (1998). Rho GTPases and the Actin Cytoskeleton. *Science 279*, 509–514.

Hall, P. A. (1999). Assessing apoptosis: a critical survey. *Endocrine-related cancer 6*, 3–8.

Hall, S. E., Savill, J. S., Henson, P. M., and Haslett, C. (1994). Apoptotic neutrophils are phagocytosed by fibroblasts with participation of the fibroblast vitronectin receptor and involvement of a mannose/fucose-specific lectin. *The Journal of Immunology* 5, 3218-3226

Harden, N. (2002). Signaling pathways directing the movement and fusion of epithelial sheets: lessons from dorsal closure in Drosophila. *Differentiation 70*, 181–203.

Harden, N., Lee, J., Loh, H. Y., Ong, Y. M., Tan, I., Leung, T., Manser, E., and Lim, L. (1996). A Drosophila homolog of the Rac- and Cdc42-activated serine/threonine kinase PAK is a potential focal adhesion and focal complex protein that colocalizes with dynamic actin structures. *Molecular and cellular biology 16*, 1896–1908.

Harden, N., Ricos, M., Ong, Y. M., Chia, W., and Lim, L. (1999). Participation of small GTPases in dorsal closure of the Drosophila embryo: distinct roles for Rho subfamily proteins in epithelial morphogenesis. *Journal of cell science 112 Pt 3*, 273–284.

Hartsock, A., and Nelson, W. J. (2009). Adherens and tight junctions: structure, function and connections to the actin cytoskeleton. *Biochimica et biophysica acta 1778*, 660–669.

Hartwig, J. H., Stossel, T. P., Kwiatkowski, D. J., di Nardo, A., and Cicchetti, G. (2005). Arp2,3 complex-deficient mouse fibroblasts are viable and have normal leading-edge actin structure and function. *Proceedings of the National Academy of Sciences of the United States of America* (10) 16263-16268.

Heasman, S. J., and Ridley, A. J. (2008). Mammalian Rho GTPases: new insights into their functions from in vivo studies. *Nature reviews. Molecular cell biology 9*, 690–701.

Heath, J. P., and Holifield, B. F. (1991). Cell Locomotion : New Research Tests Old Ideas on Membrane and Cytoskeletal Flow. *Cell Motility and the Cytoskeleton 257*, 245–257.

Hegerfeldt, Y., Tusch, M., Bröcker, E.-b, Strategies, M., and Friedl, P. (2002). Collective Cell Movement in Primary Melanoma Explants : Plasticity of Cell-Cell Interaction , β 1-Integrin Function , and Migration Strategies Collective Cell Movement in Primary Melanoma Explants : Plasticity of Cell-Cell. *Cancer Research*, 2125–2130.

Hertle, M., Kubler, M., Leigh, I., Watt, F. M., and Watts, F. (1992). Aberrant Integrin Expression during epidermal wound healing and in psoriatic epidermis. *Journal Clinical Investigation* 8 (23) 1892-1901.

Higgs, H. N., and Pollard, T. D. (2001). Regulation of actin filament network formation through Arp2/3 complex: activation by a diverse array of proteins. *Annual review of biochemistry 70*, 649–676.

Hinz, B. (2007). Formation and function of the myofibroblast during tissue repair. *The Journal of investigative dermatology*, 127(3), 526-37.

Homsy, J. G., Jasper, H., Peralta, X. G., Wu, H., Kiehart, D. P., and Bohmann, D. (2006). JNK signaling coordinates integrin and actin functions during Drosophila embryogenesis. *Developmental dynamics 235*, 427–434.

Hotulainen, P., and Lappalainen, P. (2006). Stress fibers are generated by two distinct actin assembly mechanisms in motile cells. *The Journal of cell biology 173*, 383–394.

Huber, M. a, Kraut, N., and Beug, H. (2005). Molecular requirements for epithelial-mesenchymal transition during tumor progression. *Current opinion in cell biology 17*, 548–558.

Hulpiau, P., and van Roy, F. (2009). Molecular evolution of the cadherin superfamily. *The international journal of biochemistry & cell biology* 41, 349–369.

Hunter, J. A., Savin, J., & Dahl, M. V. (2003). *Clinical dermatology*.

Hutson, M. S., Tokutake, Y., and Chang, M.-shien (2003). Forces for Morphogenesis Investigated with Laser Microsurgery and. *Science* 300, 145–149.

Huttenlocher, A., and Horwitz, A. R. (2011). Integrins in cell migration. *Cold Spring Harbor perspectives in biology 3*, a005074.

Insall, R. H., and Higgs, H. N. (2011). Dogma bites back – the evidence for branched actin Discussing the morphology of actin filaments in lamellipodia. *Trends in cell biology*, 21 (1) 3–5.

Isenberg, B. C., Dimilla, P. a, Walker, M., Kim, S., and Wong, J. Y. (2009). Vascular smooth muscle cell durotaxis depends on substrate stiffness gradient strength. *Biophysical journal 97*, 1313–1322.

Jacinto, a, Martinez-Arias, A., and Martin, P. (2001). Mechanisms of epithelial fusion and repair. *Nature cell biology 3*, E117–23.

Jacinto, A., Woolner, S., and Martin, P. (2002). Dynamic analysis of dorsal closure in Drosophila: from genetics to cell biology. *Developmental cell 3*, 9–19.

Jankovics, F., and Brunner, D. (2006). Transiently reorganized microtubules are essential for zippering during dorsal closure in Drosophila melanogaster. *Developmental cell 11*, 375–385.

Jiang, G., Huang, A. H., Cai, Y., Tanase, M., and Sheetz, M. P. (2006). Rigidity sensing at the leading edge through alphavbeta3 integrins and RPTPalpha. *Biophysical journal* 90, 1804–1809.

Joanny, J.-F., and Prost, J. (2009). Active gels as a description of the actin-myosin cytoskeleton. *HFSP journal 3*, 94–104.

Jung, H. S., Komatsu, S., Ikebe, M., and Craig, R. (2008). Head – Head and Head – Tail Interaction : A General Mechanism for Switching Off Myosin II Activity in Cells. *Molecular biology of the cell 19*, 3234–3242.

Jurado, C., Haserick, J. R., and Lee, J. (2005). Slipping or gripping? Fluorescent speckle microscopy in fish keratocytes reveals two different mechanisms for generating a retrograde flow of actin. *Molecular biology of the cell 16*, 507–518.

Kaibuchi, K., Shinya, K., Masaki, F., and Masato, N. (1999). Regulation of cadherin-mediated cell – cell adhesion by the Rho family GTPases Kozo. *Current opinion in cell biology,* 11, 591-596.

Kametani, Y., and Takeichi, M. (2007). Basal-to-apical cadherin flow at cell junctions. *Nature cell biology 9*, 92–98.

Kasza, K. E., Rowat, A. C., Liu, J., Angelini, T. E., Brangwynne, C. P., Koenderink, G. H., and Weitz, D. (2007). The cell as a material. *Current opinion in cell biology* 19, 101–107.

Kasza, K. E., and Zallen, J. a (2011). Dynamics and regulation of contractile actin-myosin networks in morphogenesis. *Current opinion in cell biology 23*, 30–38.

Keese, C., Wegener, J., Walker, S., and Giaever, L. (2004). Electrical wound-healing assay for cells in vitro. *Proceedings of the National Academy of Sciences of the United States of America 101*, 1554–1559.

Kelley, C. A., Sellers, J. R., Gard, D. L., Bui, D., Adelstein, R. S., and Baines, I. C. (1996). Xenopus nonmuscle myosin heavy chain isoforms have different subcellular localization and enzymatic activities. *Journal of Cell Biology 134*, 675–687.

Keren, K. (2011). Membrane tension leads the way. *108*, 14379–14380.

Kiehart, D. P. (1999). Wound healing: The power of the purse string. *Current biology 9*, R602–5.

Kiehart, D. P., Galbraith, C. G., Edwards, K. A., Rickoll, W. L., and Montague, R. (2000). Multiple forces contribute to cell sheet morphogenesis for dorsal closure in Drosophila. *The Journal of cell biology 149*, 471–490.

Klarlund, J. K., and Block, E. R. (2011). Free edges in epithelia as cues for motility. *Cell Adhesion & Migration* 5, 106–110.

Klepeis, V. E., Cornell-Bell, a, and Trinkaus-Randall, V. (2001). Growth factors but not gap junctions play a role in injury-induced Ca^{2+} waves in epithelial cells. *Journal of cell science 114*, 4185–4195.

Klepeis, V. E., Weinger, I., Kaczmarek, E., and Trinkaus-Randall, V. (2004). P2Y receptors play a critical role in epithelial cell communication and migration. *Journal of cellular biochemistry 93*, 1115–1133.

Kobayashi, T., and Sokabe, M. (2010). Sensing substrate rigidity by mechanosensitive ion channels with stress fibers and focal adhesions. *Current opinion in cell biology 22*, 669–676.

Koestler, S. a, Auinger, S., Vinzenz, M., Rottner, K., and Small, J. V. (2008). Differentially oriented populations of actin filaments generated in lamellipodia collaborate in pushing and pausing at the cell front. *Nature cell biology 10*, 306–313.

Kolega, J. (2003). Asymmetric Distribution of Myosin IIB in Migrating Endothelial Cells Is Regulated by a rho-dependent Kinase and Contributes to Tail Retraction. *Molecular biology of the cell 14*, 4745–4757.

Kolega, J. (1986). Effects of mechanical tension on protrusive activity and microfilament and intermediate filament organization in an epidermal epithelium moving in culture. *The Journal of cell biology 102*, 1400–1411.

Kollmannsberger, P., Mierke, C. T., Fabry, B. (2011). Nonlinear viscoelasticity of adherent cells is controlled by cytoskeletal tension. *Soft Matter 7*: 3127-3132.

Korn, E. D., Carlier, M. F., and Pantaloni, D. (1987). Actin polymerization and ATP hydrolysis. Science 238, 638–644.

Kraning-Rush, C. M., Califano, J. P., and Reinhart-King, C. (2012). Cellular traction stresses increase with increasing metastatic potential. *PloS one*, 7(2), e32572.

Kraynov, V. S. (2000). Localized Rac Activation Dynamics Visualized in Living Cells. Science *290*, 333–337.

Kress, H., Stelzer, E. H. K., Holzer, D., Buss, F., Griffiths, G., and Rohrbach, A. (2007). Filopodia act as phagocytic tentacles and pull with discrete steps and a load-dependent velocity. *Proceedings of the National Academy of Sciences of the United States of America 104*, 11633–11638.

Kumar, S., Maxwell, I. Z., Heisterkamp, A., Polte, T. R., Lele, T. P., Salanga, M., Mazur, E., and Ingber, D. E. (2006). Viscoelastic retraction of single living stress fibers and its impact on cell shape, cytoskeletal organization, and extracellular matrix mechanics. *Biophysical journal* 90, 3762–3773.

Kupfer, a, Louvard, D., and Singer, S. J. (1982). Polarization of the Golgi apparatus and the microtubule-organizing center in cultured fibroblasts at the edge of an experimental wound. *Proceedings of the National Academy of Sciences of the United States of America 79*, 2603–2607.

LaBonne, C., Burke, B., and Whitman, M. (1995). Role of MAP kinase in mesoderm induction and axial patterning during Xenopus development. *Development 121*, 1475–1486.

LaBonne, C., and Bronner-Fraser, M. (1999). Molecular mechanisms of neural crest formation. *Annual review of cell and developmental biology,* 15, 81-112.

Ladoux, B., Anon, E., Lambert, M., Rabodzey, A., Hersen, P., Buguin, A., Silberzan, P., and Mège, R.-M. (2010). Strength dependence of cadherin-mediated adhesions. *Biophysical journal 98*, 534–542.

Lauffenburger, D. a, and Horwitz, a F. (1996). Cell migration: a physically integrated molecular process. *Cell 84*, 359–369.

Layton, A. T., Toyama, Y., Yang, G.-Q., Edwards, G. S., Kiehart, D. P., and Venakides, S. (2009). Drosophila morphogenesis: tissue force laws and the modeling of dorsal closure. *HFSP journal 3*, 441–460.

220

LeClainche, C., and Carlier, M.-france (2008). Regulation of Actin Assembly Associated With Protrusion and Adhesion in Cell Migration. *Physiology Review*, 489–513.

Lecaudey, V., and Gilmour, D. (2006). Organizing moving groups during morphogenesis. *Current opinion in cell biology 18*, 102–107.

Lecuit, T., and Le Goff, L. (2007). Orchestrating size and shape during morphogenesis. *Nature 450*, 189–192.

Lecuit, T., and Lenne, P.-F. (2007). Cell surface mechanics and the control of cell shape, tissue patterns and morphogenesis. *Nature reviews. Molecular cell biology 8*, 633–644.

le Duc, Q., Shi, Q., Blonk, I., Sonnenberg, A., Wang, N., Leckband, D., and de Rooij, J. (2010). Vinculin potentiates E-cadherin mechanosensing and is recruited to actin-anchored sites within adherens junctions in a myosin II-dependent manner. *The Journal of cell biology* 189, 1107–1115.

Lee, J., Leonard, M., Oliver, T., Ishihara, a, and Jacobson, K. (1994). Traction forces generated by locomoting keratocytes. *The Journal of cell biology*, 127(6 Pt 2), 1957–64.

Lee, P., and Wolgemuth, C. W. (2011). Crawling cells can close wounds without purse strings or signaling. *PLoS computational biology 7*, e1002007.

Levental, K. R., Yu, H., Kass, L., Lakins, J. N., Egeblad, M., Erler, J. T., Fong, S. F. T., Csiszar, K., Giaccia, A., Weninger, W., et al. (2009). Matrix crosslinking forces tumor progression by enhancing integrin signaling. *Cell 139*, 891–906.

Li, G., Gustafson-Brown, C., Hanks, S. K., Nason, K., Arbeit, J. M., Pogliano, K., Wisdom, R. M., and Johnson, R. S. (2003). c-Jun is essential for organization of the epidermal leading edge. *Developmental cell 4*, 865–877.

Lidke, D. S., Lidke, K. a, Rieger, B., Jovin, T. M., and Arndt-Jovin, D. J. (2005). Reaching out for signals: filopodia sense EGF and respond by directed retrograde transport of activated receptors. *The Journal of cell biology 170*, 619–626.

Lin, C. H., Espreafico, E. M., Mooseker, M. S., and Forscher, P. (1997). Myosin drives retrograde F-actin flow in neuronal growth cones. *The Biological bulletin 192*, 183–185.

Lo, C. M., Wang, H. B., Dembo, M., and Wang, Y. L. (2000). Cell movement is guided by the rigidity of the substrate. *Biophysical journal 79*, 144–152.

Lo, C., Buxton, D. B., Chua, G. C. H., Dembo, M., Adelstein, R. S., and Wang, Y. L. (2004). Nonmuscle Myosin IIB Is Involved in the Guidance of Fibroblast Migration. *Molecular biology of the cell 15*, 982–989.

Ma, X., Lynch, H. E., Scully, P. C., and Hutson, M. S. (2009). Probing embryonic tissue mechanics with laser hole drilling. *Physical biology 6*, 036004.

Machacek, M., Hodgson, L., Welch, C., Elliott, H., Pertz, O., Nalbant, P., Abell, A., Johnson, G. L., Hahn, K. M., and Danuser, G. (2009). Coordination of Rho GTPase activities during cell protrusion. *Nature 461*, 99–103.

Machesky, L. M., and Insall, R. H. Scar1 and the related Wiskott-Aldrich syndrome protein, WASP, regulate the actin cytoskeleton through the Arp2/3 complex. *Current biology 8*, 1347–1356.

Madara, A. (1990). Maintenance of the macromolecular barrier at cell extrusion sites in intestinal epithelium: physiological rearrangement of tight junctions. *Journal of membrane biology 116*, 177–184.

Magie, C. R., Meyer, M. R., Gorsuch, M. S., and Parkhurst, S. M. (1999). Mutations in the Rho1 small GTPase disrupt morphogenesis and segmentation during early Drosophila development. *Development 126*, 5353–5364.

Mallavarapu, a, and Mitchison, T. (1999). Regulated actin cytoskeleton assembly at filopodium tips controls their extension and retraction. *The Journal of cell biology 146*, 1097–1106.

Mandato, C. A., and Bement, W. M. (2003). Actomyosin Transports Microtubules and Microtubules Control Actomyosin Recruitment during Xenopus Oocyte Wound Healing. *Current Biology 13*, 1096–1105.

Mandato, C. a, and Bement, W. M. (2001). Contraction and polymerization cooperate to assemble and close actomyosin rings around Xenopus oocyte wounds. *The Journal of cell biology 154*, 785–797.

Marcy, Y., Prost, J., Carlier, M.-F., and Sykes, C. (2004). Forces generated during actin-based propulsion: a direct measurement by micromanipulation. *Proceedings of the National Academy of Sciences of the United States of America 101*, 5992–5997.

Mark, S., Shlomovitz, R., Gov, N. S., Poujade, M., Grasland-Mongrain, E., and Silberzan, P. (2010). Physical model of the dynamic instability in an expanding cell culture. *Biophysical journal 98*, 361–370.

Martin, A. C., Gelbart, M., Fernandez-Gonzalez, R., Kaschube, M., and Wieschaus, E. F. (2010). Integration of contractile forces during tissue invagination. *The Journal of cell biology, 188*(5), 735–49.

Martin, P. (1997). Wound healing--aiming for perfect skin regeneration. *Science 276*, 75–81.

Martin, P., D'Souza, D., Martin, J., Grose, R., Cooper, L., Maki, R., and McKercher, S. R. (2003). Wound healing in the PU.1 null mouse--tissue repair is not dependent on inflammatory cells. *Current biology* 13(13), 1122-8.

Martin, P., and Leibovich, S. J. (2005). Inflammatory cells during wound repair: the good, the bad and the ugly. *Trends in cell biology 15*, 599–607.

Martin, P., and Lewis, J. (1992). Actin cables and epidermal movement in embryonic wound healing. *Nature 360*, 179–183.

Martin, P., and Parkhurst, S. M. (2004). Parallels between tissue repair and embryo morphogenesis. *Development 131*, 3021–3034.

Martinac, B. (2004). Mechanosensitive ion channels: molecules of mechanotransduction. *Journal of cell science 117*, 2449–2460.

Martín-Blanco, E., and Knust, E. (2001). Epithelial morphogenesis: filopodia at work. *Current biology 11*, R28–31.

Masuda-Hirata, M., Suzuki, A., Amano, Y., Yamashita, K., Ide, M., Yamanaka, T., Sakai, M., et al. (2009). Intracellular polarity protein PAR-1 regulates extracellular laminin assembly by regulating the dystroglycan complex. *Genes to cells, 14* (7), 835-50.

Matsubayashi, Y., Ebisuya, M., Honjoh, S., and Nishida, E. (2004). ERK Activation Propagates in Epithelial Cell Sheets and Regulates Their Migration during Wound Healing. *Current Biology 14*, 731–735.

Matsubayashi, Y., Razzell, W., and Martin, P. (2011). "White wave" analysis of epithelial scratch wound healing reveals how cells mobilise back from the leading edge in a myosin-II-dependent fashion. *Journal of cell science 124*, 1017–1021.

Matsumura, F. (2005). Regulation of myosin II during cytokinesis in higher eukaryotes. *Trends in cell biology 15*, 371–377.

Mayor, R., and Carmona-Fontaine, C. (2010). Keeping in touch with contact inhibition of locomotion. *Trends in cell biology 20*, 319–328.

McCluskey, J., and Martin, P. (1995). Analysis of the tissue movements of embryonic wound healing. *Developmental biology 170*, 102–114.

McNeil, P. L., Muthukrishnan, L., Warder, E., and D'Amore, P. a (1989). Growth factors are released by mechanically wounded endothelial cells. *The Journal of cell biology 109*, 811–822.

McNeil, P. L., and Steinhardt, R. a (2003). Plasma membrane disruption: repair, prevention, adaptation. *Annual review of cell and developmental biology 19*, 697–731.

Medalia, O., Beck, M., Ecke, M., Weber, I., Neujahr, R., Baumeister, W., and Gerisch, G. (2007). Organization of actin networks in intact filopodia. *Current Biology 17*, 79–84.

Meghana, C., Ramdas, N., Hameed, F. M., Rao, M., Shivashankar, G. V., and Narasimha, M. (2011). Integrin adhesion drives the emergent polarization of active cytoskeletal stresses to pattern cell delamination. *Proceedings of the National Academy of Sciences of the United States of America 108*, 9107–9112.

Mellor, H. (2010). The role of formins in filopodia formation. *Biochimica et biophysica acta 1803*, 191–200.

Meşe, G., Richard, G., and White, T. W. (2007). Gap junctions: basic structure and function. *The Journal of investigative dermatology,* 127(11), 2516-24.

Miki, H., Yamaguchi, H., Suetsugu, S., and Takenawa, T. (2000). IRSp53 is an essential intermediate between Rac and WAVE in the regulation of membrane ruffling. *Nature 408*, 1–4.

Millard, T. H., and Martin, P. (2008). Dynamic analysis of filopodial interactions during the zippering phase of Drosophila dorsal closure. *Development 135*, 621–626.

Mills, J. C., Stone, N. L., Erhardt, J., and Pittman, R. N. (1998). Apoptotic membrane blebbing is regulated by myosin light chain phosphorylation. *The Journal of cell biology 140*, 627–636.

Mine, N., Iwamoto, R., and Mekada, E. (2005). HB-EGF promotes epithelial cell migration in eyelid development. *Development 132*, 4317–4326.

Mitchison, T. J., and Kirsch, M. N. (1988). Cytoskeletal dynamics and nerve growth. Neuron. 1 761-776

Mitrossilis, D., Fouchard, J., Guiroy, A., Desprat, N., Rodriguez, N., Fabry, B., and Asnacios, A. (2009). Single-cell response to stiffness exhibits muscle-like behavior. *Proceedings of the National Academy of Sciences of the United States of America 106*, 18243–18248.

Mitrossilis, D., Fouchard, J., Pereira, D., Postic, F., Richert, A., Saint-Jean, M., and Asnacios, A. (2010). Real-time single-cell response to stiffness. *Proceedings of the National Academy of Sciences of the United States of America 107*, 16518–16523.

Miyake, K., McNeil, P. L., Suzuki, K., Tsunoda, R., and Sugai, N. (2001). An actin barrier to resealing. *Journal of cell science 114*, 3487–3494.

Mogilner, a, and Oster, G. (1996). Cell motility driven by actin polymerization. *Biophysical journal 71*, 3030–3045.

Montell, D. J. (2003). Border-cell migration: the race is on. *Nature reviews. Molecular cell biology 4*, 13–24.

Muliyil, S., Krishnakumar, P., and Narasimha, M. (2011). Spatial, temporal and molecular hierarchies in the link between death, delamination and dorsal closure. *Development 138*, 3043–3054.

Munevar, S., Wang, Y., and Dembo, M. (2001). Traction force microscopy of migrating normal and H-ras transformed 3T3 fibroblasts. *Biophysical journal*, 80(4), 1744–57.

Murrell, M., Kamm, R., and Matsudaira, P. (2011). Substrate viscosity enhances correlation in epithelial sheet movement. *Biophysical journal 101*, 297–306.

Mège, R.-M., Gavard, J., and Lambert, M. (2006). Regulation of cell-cell junctions by the cytoskeleton. *Current opinion in cell biology 18*, 541–548.

Nabeshima, K., Inoue, T., Shimao, Y., Kataoka, H., and Koono, M. (1999). Cohort migration of carcinoma cells: differentiated colorectal carcinoma cells move as coherent cell clusters or sheets. *Histology and Histopathology 14*, 1183–1197.

Nabeshima, K., Inoue, T., Shimao, Y., and Sameshima, T. (2002). Matrix metalloproteinases in tumor invasion : Role for cell migration. *Pathology International 52*, 255–264.

Narumiya, S., Ishizaki, T., and Uehata, M. (2000). Use and properties of ROCK-specific inhibitor Y-27632. *Methods in enzymology 325*, 273–284.

Naumanen, P., Lappalainen, P., and Hotulainen, P. (2008). Mechanisms of actin stress fibre assembly. *Journal of microscopy 231*, 446–454.

Nicholson-Dykstra, S. M., and Higgs, H. N. (2008). Arp2 depletion inhibits sheet-like protrusions but not linear protrusions of fibroblasts and lymphocytes. *Cell motility and the cytoskeleton 65*, 904–922.

Nicolás, F. J., Lehmann, K., Warne, P. H., Hill, C. S., Downward, J., and Nicolas, F. J. (2003). Epithelial to mesenchymal transition in Madin-Darby canine kidney cells is accompanied by down-regulation of Smad3 expression, leading to resistance to transforming growth factor-beta-induced growth arrest. *The Journal of biological chemistry 278*, 3251–3256.

Niedergang, F., and Chavrier, P. (2004). Signaling and membrane dynamics during phagocytosis: many roads lead to the phagos(R)ome. *Current opinion in cell biology 16*, 422–428.

Nikolić, D. L., Boettiger, A. N., Bar-Sagi, D., Carbeck, J. D., and Shvartsman, S. Y. (2006). Role of boundary conditions in an experimental model of epithelial wound healing. *American journal of physiology. Cell physiology 291*, C68–75.

Ninov, N., Chiarelli, D. a, and Martín-Blanco, E. (2007). Extrinsic and intrinsic mechanisms directing epithelial cell sheet replacement during Drosophila metamorphosis. *Development 134*, 367–379.

Nishimura, T., Honda, H., and Takeichi, M. (2012). Planar cell polarity links axes of spatial dynamics in neural-tube closure. *Cell, 149* (5), 1084–97.

Nobes, C. D., and Hall, a (1995). Rho, rac, and cdc42 GTPases regulate the assembly of multimolecular focal complexes associated with actin stress fibers, lamellipodia, and filopodia. *Cell 81*, 53–62.

Nozumi, M. (2002). Differential localization of WAVE isoforms in filopodia and lamellipodia of the neuronal growth cone. *Journal of Cell Science 116*, 239–246.

Nusrat, A., Brown, G. T., Tom, J., Drake, A., Bui, T. T. T., Quan, C., and Mrsny, R. J. (2005). Extracellular Loop Domains of the Tight Junction Protein Occludin. *Molecular biology of the cell*, 16, 1725-1734.

Oakes, P. W., Beckham, Y., Stricker, J., and Gardel, M. L. (2012). Tension is required but not sufficient for focal adhesion maturation without a stress fiber template. *The Journal of cell biology 196*, 363–374.

O'Brien, L. E., Jou, T. S., Pollack, a L., Zhang, Q., Hansen, S. H., Yurchenco, P., and Mostov, K. E. (2001). Rac1 orientates epithelial apical polarity through effects on basolateral laminin assembly. *Nature cell biology*, 3(9), 831-8.

Ochsner, M., Dusseiller, M. R., Grandin, H. M., Luna-Morris, S., Textor, M., Vogel, V., and Smith, M. L. (2007). Micro-well arrays for 3D shape control and high resolution analysis of single cells. *Lab on a chip* 7, 1074–1077.

Omelchenko, T., Vasiliev, J. M., Gelfand, I. M., Feder, H. H., and Bonder, E. M. (2003). Rho-dependent formation of epithelial "' leader '" cells. *Proceedings of the National Academy of Sciences of the United States of America*. 100 (19) 10788-10793

Otto, I. M., Raabe, T., Rennefahrt, U. E., Bork, P., Rapp, U. R., and Kerkhoff, E. (2000). The p150-Spir protein provides a link between c-Jun N-terminal kinase function and actin reorganization. *Current biology 10*, 345–348.

Palazzo, a F., Cook, T. a, Alberts, a S., and Gundersen, G. G. (2001). mDia mediates Rho-regulated formation and orientation of stable microtubules. *Nature cell biology 3*, 723–729.

Palazzo, a F., Joseph, H. L., Chen, Y. J., Dujardin, D. L., Alberts, A. S., Pfister, K. K., Vallee, R. B., and Gundersen, G. G. (2001). Cdc42, dynein, and dynactin regulate MTOC reorientation independent of Rho-regulated microtubule stabilization. *Current biology 11*, 1536–1541.

Palecek, S., Loftus, J., Ginsberg, M., Lauffenburger, D., and Horwitz, A. (1997). Integrin-ligand binding properties govern cell migration speed through cell-substratum adhesiveness. *Nature*. 385 537-540

Pantaloni, D. (2001). Mechanism of Actin-Based Motility. *Science 292*, 1502–1506.

Parsons, J. T., Horwitz, A. R., and Schwartz, M. a (2010). Cell adhesion: integrating cytoskeletal dynamics and cellular tension. *Nature reviews. Molecular cell biology 11*, 633–643.

Parsons, M., Monypenny, J., Ameer-beg, S. M., Millard, T. H., Machesky, L. M., Peter, M., Keppler, M. D., Schiavo, G., Watson, R., Chernoff, J., et al. (2005). Spatially Distinct Binding of Cdc42 to PAK1 and N-WASP in Breast Carcinoma Cells. *Molecular and Cellular Biolgy 25*, 1680–1695.

Pasapera, A. M., Schneider, I. C., Rericha, E., Schlaepfer, D. D., and Waterman, C. M. (2010). Myosin II activity regulates vinculin recruitment to focal adhesions through FAK-mediated paxillin phosphorylation. *The Journal of cell biology 188*, 877–890.

Paszek, M. J., Boettiger, D., Weaver, V. M., and Hammer, D. a (2009). Integrin clustering is driven by mechanical resistance from the glycocalyx and the substrate. *PLoS computational biology 5*, e1000604.

Paszek, M. J., Zahir, N., Johnson, K. R., Lakins, J. N., Rozenberg, G. I., Gefen, A., Reinhart-King, C. a, Margulies, S. S., Dembo, M., Boettiger, D., et al. (2005). Tensional homeostasis and the malignant phenotype. *Cancer cell 8*, 241–254.

Pelham, R. J., and Wang, Y. L. (1998). Cell locomotion and focal adhesions are regulated by the mechanical properties of the substrate. Biological Bulletin *194*, 348–9

Pelham, R J , Wang, Y. L. (1997). Cell locomotion and focal adhesions are regulated by. *Proceedings of the National Academy of Sciences of the United States of America* 94, 13661–13665.

Pelham, R. J., and Wang, Y. L. (1999). High resolution detection of mechanical forces exerted by locomoting fibroblasts on the substrate. *Molecular biology of the cell*, 10(4), 935–45.

Pellegrin, S., and Mellor, H. (2007). Actin stress fibres. *Journal of cell science 120*, 3491–3499.

Pellegrini, S., and Mellor, H. (2005). The Rho Family GTPase Rif Induces Filopodia through mDia2. *Current Biology 15*, 129–133.

Peralta Soler, A., Mullin, J., Knudsen, K., and Marano, C. (1996). Tissue remodeling during tumor necrosis factor-induced apoptosis in LLC-PK1 renal epithelial cells. *American journal of physiology. Cell physiology 270*, 869–879.

Pertz, O. (2010). Spatio-temporal Rho GTPase signaling - where are we now? *Journal of cell science 123*, 1841–1850.

Pertz, O., Hodgson, L., Klemke, R. L., and Hahn, K. M. (2006). Spatiotemporal dynamics of RhoA activity in migrating cells. *Nature 440*, 1069–1072.

Petroll, W. M., Ma, L., Jester, J. V., Cavanagh, H. D., and Bean, J. (2001). Organization of junctional proteins in proliferating cat corneal endothelium during wound healing. *Cornea 20*, 73–80.

Peyton, S. R., and Putnam, A. J. (2005). Extracellular matrix rigidity governs smooth muscle cell motility in a biphasic fashion. *Journal of cellular physiology 204*, 198–209.

Pollard, T. D. (2007). Regulation of actin filament assembly by Arp2/3 complex and formins. *Annual review of biophysics and biomolecular structure 36*, 451–477.

Pollard, T. D., and Borisy, G. G. (2003). Cellular motility driven by assembly and disassembly of actin filaments. *Cell 112*, 453–465.

Pollard, T. D., and Cooper, J. a (2009). Actin, a central player in cell shape and movement. *Science 326*, 1208–1212.

Ponti, A., Machacek, M., Gupton, S. L., Waterman-Storer, C. M., and Danuser, G. (2004). Two distinct actin networks drive the protrusion of migrating cells. *Science 305*, 1782–1786.

Poujade, M., Grasland-Mongrain, E., Hertzog, A., Jouanneau, J., Chavrier, P., Ladoux, B., Buguin, A., and Silberzan, P. (2007). Collective migration of an epithelial monolayer in response to a model wound. *Proceedings of the National Academy of Sciences of the United States of America 104*, 15988–15993.

Prager-Khoutorsky, M., Lichtenstein, A., Krishnan, R., Rajendran, K., Mayo, A., Kam, Z., Geiger, B., and Bershadsky, A. D. (2011). Fibroblast polarization is a matrix-rigidity-dependent process controlled by focal adhesion mechanosensing. *Nature cell biology 13*, 1457–1465.

Raftopoulou, M., and Hall, A. (2004). Cell migration: Rho GTPases lead the way. *Developmental Biology 265*, 23–32.

Raich, W. B., Agbunag, C., and Hardin, J. (1999). Rapid epithelial-sheet sealing in the Caenorhabditis elegans embryo requires cadherin-dependent filopodial priming. *Current biology 9*, 1139–1146.

Reddy, K. B., Nabha, S. M., and Atanaskova, N. (2003). Role of MAP kinase in tumor progression and invasion. *Cancer metastasis reviews 22*, 395–403.

Reed, B. H., Wilk, R., and Lipshitz, H. D. (2001). Downregulation of Jun kinase signaling in the amnioserosa is essential for dorsal closure of the Drosophila embryo. *Current biology 11*, 1098–1108.

Regen, C. M., and Horwitz, a F. (1992). Dynamics of beta 1 integrin-mediated adhesive contacts in motile fibroblasts. *The Journal of cell biology 119*, 1347–1359.

Revenu, C., and Gilmour, D. (2009). EMT 2.0: shaping epithelia through collective migration. *Current opinion in genetics & development 19*, 338–342.

Ricos, M. G., Harden, N., Sem, K. P., Lim, L., and Chia, W. (1999). Dcdc42 acts in TGF-beta signaling during Drosophila morphogenesis: distinct roles for the Drac1/JNK and Dcdc42/TGF-beta cascades in cytoskeletal regulation. *Journal of cell science 112 Pt 8*, 1225–1235.

Ridley, a J., and Hall, a (1992). The small GTP-binding protein rho regulates the assembly of focal adhesions and actin stress fibers in response to growth factors. *Cell 70*, 389–399.

Ridley, a J., Paterson, H. F., Johnston, C. L., Diekmann, D., and Hall, a (1992). The small GTP-binding protein rac regulates growth factor-induced membrane ruffling. *Cell 70*, 401–410.

Ridley, A. J. (2001). Rho family proteins: coordinating cell responses. Trends in cell biology *11*, 471–477.

Ridley, A. J., Schwartz, M. a, Burridge, K., Firtel, R. a, Ginsberg, M. H., Borisy, G., Parsons, J. T., and Horwitz, A. R. (2003). Cell migration: integrating signals from front to back. *Science 302*, 1704–1709.

Riesgo-Escovar, J. R. (1997). Common and Distinct Roles of DFos and DJun During Drosophila Development. *Science 278*, 669–672.

Riveline, D., Zamir, E., Balaban, N. Q., Schwarz, U. S., Ishizaki, T., Narumiya, S., Kam, Z., Geiger, B., and Bershadsky, a D. (2001). Focal contacts as mechanosensors: externally applied local mechanical force induces growth of focal contacts by an mDia1-dependent and ROCK-independent mechanism. *The Journal of cell biology 153*, 1175–1186.

Roh-Johnson, M., Shemer, G., Higgins, C. D., McClellan, J. H., Werts, A. D., Tulu, U. S., Gao, L., et al. (2012). Triggering a Cell Shape Change by Exploiting Preexisting Actomyosin Contractions. *Science 335*, 1232-1235

Rohatgi, R., Ma, L., Miki, H., Lopez, M., Kirchhausen, T., Takenawa, T., and Kirschner, M. W. (1999). The interaction between N-WASP and the Arp2/3 complex links Cdc42-dependent signals to actin assembly. *Cell 97*, 221–231.

Rojas, R., Ruiz, W. G., Leung, S. M., Jou, T. S., and Apodaca, G. (2001). Cdc42-dependent modulation of tight junctions and membrane protein traffic in polarized Madin-Darby canine kidney cells. *Molecular biology of the cell*, 12(8), 2257-74.

Rosenblatt, J., Raff, M. C., and Cramer, L. P. (2001). An epithelial cell destined for apoptosis signals its neighbors to extrude it by an actin- and myosin-dependent mechanism. *Current biology 11*, 1847–1857.

Rugh, R. (1990). The mouse: its reproduction and development. 1990. Oxford University Press.

Russo, J. M., Florian, P., Shen, L. E., Graham, W. V., Tretiakova, M. S., Gitter, A. H., Mrsny, R. J., Turner, J. R., and Maria, S. (2005). Distinct temporal-spatial roles for rho kinase and myosin light chain kinase in epithelial purse-string wound closure. *Gastroenterology 128*, 987–1001.

Rämet, M., Lanot, R., Zachary, D., and Manfruelli, P. (2002). JNK signaling pathway is required for efficient wound healing in Drosophila. *Developmental biology 241*, 145–156.

Rørth, P. (2009). Collective cell migration. *Annual review of cell and developmental biology 25*, 407–429.

Saarikangas, J., Zhao, H., and Lappalainen, P. (2010). Regulation of the Actin Cytoskeleton-Plasma Membrane Interplay by Phosphoinositides. *Physiology Review*, 259–289.

Saez, A., Buguin, A., Silberzan, P., and Ladoux, B. (2005). Is the mechanical activity of epithelial cells controlled by deformations or forces? *Biophysical journal 89*, L52–4.

Saez, A., Ghibaudo, M., Buguin, A., Silberzan, P., and Ladoux, B. (2007). Rigidity-driven growth and migration of epithelial cells on microstructured anisotropic substrates. *Proceedings of the National Academy of Sciences of the United States of America 104*, 8281–8286.

Sahai, E., and Marshall, C. J. (2003). Differing modes of tumour cell invasion have distinct requirements for Rho/ROCK signalling and extracellular proteolysis. *Nature Cell Biology 5*, 711–719.

Saitoh, T., Takemura, S., Ueda, K., Hosoya, H., Nagayama, M., Haga, H., Kawabata, K., Yamagishi, a, and Takahashi, M. (2001). Differential localization of non-muscle myosin II isoforms and phosphorylated regulatory light chains in human MRC-5 fibroblasts. *FEBS letters 509*, 365–369.

Salbreux, G., Prost, J., and Joanny, J. (2009). Hydrodynamics of Cellular Cortical Flows and the Formation of Contractile Rings. *Physical Review Letters 103*, 1–4.

Sammak, P. J., Hinman, L. E., Tran, P. O., Sjaastad, M. D., and Machen, T. E. (1997). How do injured cells communicate with the surviving cell monolayer? *Journal of cell science 110 Pt 4*, 465–475.

Sawada, Y., Tamada, M., Dubin-Thaler, B. J., Cherniavskaya, O., Sakai, R., Tanaka, S., and Sheetz, M. P. (2006). Force sensing by mechanical extension of the Src family kinase substrate p130Cas. *Cell 127*, 1015–1026.

Schlessinger, K., McManus, E. J., and Hall, A. (2007). Cdc42 and noncanonical Wnt signal transduction pathways cooperate to promote cell polarity. *The Journal of cell biology 178*, 355–361.

Schwaiger, I., Sattler, C., Hostetter, D. R., and Rief, M. (2002). The myosin coiled-coil is a truly elastic protein structure. *Nature materials 1*, 232–235.

Schwartz, M. a, and Horwitz, A. R. (2006). Integrating adhesion, protrusion, and contraction during cell migration. *Cell 125*, 1223–1225.

Schwarz, U. (2007). Soft matters in cell adhesion: rigidity sensing on soft elastic substrates. *Soft Matter 3*, 263.

Scuderi, A., and Letsou, A. (2005). Amnioserosa is required for dorsal closure in Drosophila. *Developmental dynamics 232*, 791–800.

Serra-Picamal, X., Conte, V., Vincent, R., Anon, E., Tambe, D., Bazellieres, E., Butler, J., Fredberg, J., and Trepat, X. (2012). Mechanical waves during tissue expansion. *Nature Physics* in press.

Shah, M., Foreman, D. M., and Ferguson, M. W. (1992). Control of scarring in adult wounds by neutralising antibody to transforming growth factor beta. *Lancet*, 339(8787), 213-4.

Sharma, G.-D., He, J., and Bazan, H. E. P. (2003). p38 and ERK1/2 coordinate cellular migration and proliferation in epithelial wound healing: evidence of cross-talk activation between MAP kinase cascades. *The Journal of biological chemistry 278*, 21989–21997.

Shaw, T. J., and Martin, P. (2009). Wound repair at a glance. *Journal of cell science 122*, 3209–3213.

Sheetz, M. P., Felsenfeld, D. P., and Galbraith, C. G. (1998). Cell migration : regulation of force on extracellular- complexes. *Trends in cell biology 8,* 51-54.

Siddique, M. S. P., Mogami, G., Miyazaki, T., Katayama, E., Uyeda, T. Q. P., and Suzuki, M. (2005). Cooperative structural change of actin filaments interacting with activated myosin motor domain, detected with copolymers of pyrene-labeled actin and acto-S1 chimera protein. *Biochemical and biophysical research communications 337*, 1185–1191.

Siegrist, S. E., and Doe, C. Q. (2007). Microtubule-induced cortical cell polarity. *Genes & development 21*, 483–496.

Simpson, K. J., Selfors, L. M., Bui, J., Reynolds, A., Leake, D., Khvorova, A., and Brugge, J. S. (2008). Identification of genes that regulate epithelial cell migration using an siRNA screening approach. *Nature cell biology 10*, 1027–1038.

Simpson, D. M., and Ross, R. (1972). The neutrophilic leukocyte in wound repair a study with antineutrophil serum. *The Journal of clinical investigation*, 51(8), 2009-23.

Sit, S.-T., and Manser, E. (2011). Rho GTPases and their role in organizing the actin cytoskeleton. *Journal of cell science 124*, 679–683.

Slattum, G., McGee, K. M., and Rosenblatt, J. (2009). P115 RhoGEF and microtubules decide the direction apoptotic cells extrude from an epithelium. *The Journal of cell biology 186*, 693–702.

Small, J. V. (2010). Dicing with dogma: de-branching the lamellipodium. *Trends in cell biology 20*, 628–633.

Small, J. V., Herzog, M., and Anderson, K. (1995). Actin filament organization in the fish keratocyte lamellipodium. *The Journal of cell biology 129*, 1275–1286.

Small, J. V., Stradal, T., Vignal, E., and Rottner, K. (2002). The lamellipodium: where motility begins. *Trends in cell biology 12*, 112–120.

Smalley, K. S. M., Brafford, P., Haass, N. K., Brandner, J. M., Brown, E., and Herlyn, M. (2005). Up-regulated expression of zonula occludens protein-1 in human melanoma associates with N-cadherin and contributes to invasion and adhesion. *The American journal of pathology*, 166(5), 1541-54.

Smutny, M., Cox, H. L., Leerberg, J. M., Kovacs, E. M., Conti, M. A., Ferguson, C., Hamilton, N. a, Parton, R. G., Adelstein, R. S., and Yap, A. S. (2010). Myosin II isoforms identify distinct functional modules that support integrity of the epithelial zonula adherens. *Nature cell biology 12*, 696–702.

Soderholm, J., and Heald, R. (2005). Scratch n' screen for inhibitors of cell migration. *Chemistry & biology 12*, 263–265.

Solanas, G., Cortina, C., Sevillano, M., and Batlle, E. (2011). Cleavage of E-cadherin by ADAM10 mediates epithelial cell sorting downstream of EphB signalling. *Nature cell biology 13*, 1100–1107.

Solon, J., Kaya-Copur, A., Colombelli, J., and Brunner, D. (2009). Pulsed forces timed by a ratchet-like mechanism drive directed tissue movement during dorsal closure. *Cell 137*, 1331–1342.

Solon, J., Levental, I., Sengupta, K., Georges, P. C., and Janmey, P. (2007). Fibroblast adaptation and stiffness matching to soft elastic substrates. *Biophysical journal 93*, 4453–4461.

Steffen, A., Faix, J., Resch, G. P., Linkner, J., Wehland, J., Small, J. V., Rottner, K., and Stradal, T. E. B. (2006). Filopodia Formation in the Absence of Functional WAVE- and Arp2/3-Complexes. *Molecular biology of the cell 17*, 2581–2591.

Stricker, J., Aratyn-Schaus, Y., Oakes, P. W., and Gardel, M. L. (2011). Spatiotemporal constraints on the force-dependent growth of focal adhesions. *Biophysical journal 100*, 2883–2893.

Stronach, B., and Perrimon, N. (2002). Activation of the JNK pathway during dorsal closure in Drosophila requires the mixed lineage kinase , slipper. *Genes & development 16*, 377–387.

Suraneni, P., Rubinstein, B., Unruh, J. R., Durnin, M., Hanein, D., and Li, R. (2012). The Arp2/3 complex is required for lamellipodia extension and directional fibroblast cell migration. *The Journal of cell biology 197*, 239–251.

Suzanne, M., and Steller, H. (2009). Letting go: modification of cell adhesion during apoptosis. *Journal of biology 8*, 49.

Svitkina, T. M., and Borisy, G. G. (1999). Organization and Treadmilling of Actin Filament Array in Lamellipodia. *The Journal of Cell Biology 145*, 1009–1026.

Svitkina, T. M., Bulanova, E. a, Chaga, O. Y., Vignjevic, D. M., Kojima, S.-ichiro, Vasiliev, J. M., and Borisy, G. G. (2003). Mechanism of filopodia initiation by reorganization of a dendritic network. *The Journal of cell biology 160*, 409–421.

Szabó, B., Szöllösi, G., Gönci, B., Jurányi, Z., Selmeczi, D., and Vicsek, T. (2006). Phase transition in the collective migration of tissue cells: Experiment and model. *Physical Review E 74*, 1–5.

Szpaderska, a M., Zuckerman, J. D., and DiPietro, L. a. (2003). Differential injury responses in oral mucosal and cutaneous wounds. *Journal of dental research*, 82(8), 621-6.

Takaishi, K., Sasaki, T., Kotani, H., Nishioka, H., and Takai, Y. (1997). Regulation of cell-cell adhesion by rac and rho small G proteins in MDCK cells. *The Journal of cell biology*, 139(4), 1047-59.

Tamada, M., Perez, T. D., Nelson, W. J., and Sheetz, M. P. (2007). Two distinct modes of myosin assembly and dynamics during epithelial wound closure. *The Journal of cell biology 176*, 27–33.

Tambe, D. T., Hardin, C. C., Angelini, T. E., Rajendran, K., Park, C. Y., Serra-Picamal, X., Zhou, E. H., Zaman, M. H., Butler, J. P., Weitz, D. a, et al. (2011). Collective cell guidance by cooperative intercellular forces. *Nature materials 10*, 469–475.

Tan, J. L., Tien, J., Pirone, D. M., Gray, D. S., Bhadriraju, K., and Chen, C. S. (2003). Cells lying on a bed of microneedles: an approach to isolate mechanical force. *Proceedings of the National Academy of Sciences of the United States of America 100*, 1484–1489.

Teddy, J. M., and Kulesa, P. M. (2004). In vivo evidence for short- and long-range cell communication in cranial neural crest cells. *Development 131*, 6141–6151.

Tee, S.-Y., Bausch, A., and Janmey, P. (2009). The mechanical cell. *Current Biology* 19 (17): R745-748

Tee, S.-Y., Fu, J., Chen, C. S., and Janmey, P. (2011). Cell shape and substrate rigidity both regulate cell stiffness. *Biophysical journal 100*, L25–7.

Thiery, J. P., Acloque, H., Huang, R. Y. J., and Nieto, M. A. (2009). Epithelial-mesenchymal transitions in development and disease. *Cell 139*, 871–890.

Thiery, J. P., and Sleeman, J. P. (2006). Complex networks orchestrate epithelial-mesenchymal transitions. *Nature reviews. Molecular cell biology 7*, 131–142.

Todaro, G., Lazar, G., and Green, H. (1965). The initiation of cell division in a contact inhibited mammalian cell line. *Journal of Cellular and Comparative Physiology* 66, 325–333.

Togo, T. (2006). Disruption of the plasma membrane stimulates rearrangement of microtubules and lipid traffic toward the wound site. *Journal of cell science 119*, 2780–2786.

Togo, T., and Steinhardt, R. A. (2004). Nonmuscle Myosin IIA and IIB Have Distinct Functions in the Exocytosis-dependent Process of Cell Membrane Repair. *Molecular biology of the cell 15*, 688–695.

Tomasek, J. J., Gabbiani, G., Hinz, B., Chaponnier, C., and Brown, R. a (2002). Myofibroblasts and mechano-regulation of connective tissue remodelling. *Nature reviews. Molecular cell biology 3*, 349–363.

Toriseva, M., and Kähäri, V.-M. (2009). Proteinases in cutaneous wound healing. *Cellular and molecular life sciences : CMLS 66*, 203–224.

Tracqui, P. (2009). Biophysical models of tumour growth. *Reports on Progress in Physics 72*, 056701.

Trappmann, B., Gautrot, J. E., Connelly, J. T., Strange, D. G. T., Li, Y., Oyen, M. L., Cohen Stuart, M. a, Boehm, H., Li, B., Vogel, V., et al. (2012). Extracellular-matrix tethering regulates stem-cell fate. *Nature materials 11*, 642–649.

Trepat, X., Chen, Z., and Jacobson, K. (2012). Cell Migration. *Comprehensive Physiology 2*, 1–24.

Trepat, X., Deng, L., An, S., Navajas, D., Tschumperlin, D., Gertho,W., Butler, J., Fredberg, J. (2007). Universal physical responses to stretchin the living cell. *Nature 447* (3), 592{596.

Trepat, X., Wasserman, M. R., Angelini, T. E., Millet, E., Weitz, D. a., Butler, J. P., and Fredberg, J. J. (2009). Physical forces during collective cell migration. *Nature Physics 5*, 426–430.

Trichet, L., Le Digabel, J., Hawkins, R. J., Vedula, S. R. K., Gupta, M., Ribrault, C., Hersen, P., Voituriez, R., and Ladoux, B. (2012). Evidence of a large-scale mechanosensing mechanism for cellular adaptation to substrate stiffness. *Proceedings of the National Academy of Sciences of the United States of America*. 108 (18) 6933-6938.

Unal-Cevik, I., Kilinç, M., Can, A., Gürsoy-Ozdemir, Y., and Dalkara, T. (2004). Apoptotic and necrotic death mechanisms are concomitantly activated in the same cell after cerebral ischemia. *Stroke; a journal of cerebral circulation 35*, 2189–2194.

Urban, E., Jacob, S., Nemethova, M., Resch, G. P., and Small, J. V. (2010). Electron tomography reveals unbranched networks of actin filaments in lamellipodia. *Nature cell biology 12*, 429–435.

Vallotton, P., Gupton, S. L., Waterman-Storer, C. M., and Danuser, G. (2004). Simultaneous mapping of filamentous actin flow and turnover in migrating cells by quantitative fluorescent speckle microscopy. *Proceedings of the National Academy of Sciences of the United States of America 101*, 9660–9665.

Vallotton, P., and Small, J. V. (2009). Shifting views on the leading role of the lamellipodium in cell migration: speckle tracking revisited. *Journal of cell science 122*, 1955–1958.

Vasioukhin, V., Bauer, C., Yin, M., and Fuchs, E. (2000). Directed actin polymerization is the driving force for epithelial cell-cell adhesion. *Cell 100*, 209–219.

Vasioukhin, V., and Fuchs, E. (2001). Actin dynamics and cell-cell adhesion in epithelia. *Current opinion in cell biology 13*, 76–84.

Vaughan, E. M., Miller, A. L., Yu, H.-Y. E., and Bement, W. M. (2011). Control of local Rho GTPase crosstalk by Abr. *Current biology 21*, 270–277.

Vedula, S. R. K., Leong, M. C., Lai, T. L., Hersen, P., Kabla, A. J., Lim, C. T., and Ladoux, B. (2012). Emerging modes of collective cell migration induced by geometrical constraints. *Proceedings of the National Academy of Sciences of the United States of America*, In press.

Verkhovsky, a B., Svitkina, T. M., and Borisy, G. G. (1999). Self-polarization and directional motility of cytoplasm. *Current biology 9*, 11–20.

Vicente-Manzanares, M., Ma, X., Adelstein, R. S., and Horwitz, A. R. (2009). Non-muscle myosin II takes centre stage in cell adhesion and migration. *Nature reviews. Molecular cell biology 10*, 778–790.

Vicente-Manzanares, M., Zareno, J., Whitmore, L., Choi, C. K., and Horwitz, A. F. (2007). Regulation of protrusion, adhesion dynamics, and polarity by myosins IIA and IIB in migrating cells. *The Journal of cell biology 176*, 573–580.

Villar, C., and Zhao, X. (2010). Candida albicans induces early apoptosis followed by secondary necrosis in oral epithelial cells. *Molecular Oral Microbiology 25*, 215–225.

Vitorino, P., and Meyer, T. (2008). Modular control of endothelial sheet migration. *Genes & development 1*, 3268–3281.

Vogel, V., and Sheetz, M. P. (2009). Cell fate regulation by coupling mechanical cycles to biochemical signaling pathways. *Current opinion in cell biology 21*, 38–46.

Walcott, S., and Sun, S. X. (2010). A mechanical model of actin stress fiber formation and substrate elasticity sensing in adherent cells. *Proceedings of the National Academy of Sciences of the United States of America 107*, 7757–7762.

Walsh, S. V., Hopkins, A. M., Chen, J., Narumiya, S., Parkos, C. a., and Nusrat, A. (2001). Rho Kinase Regulates Tight Junction Function and Is Necessary for Tight Junction Assembly in Polarized Intestinal Epithelia. *Gastroenterology*, 121(3), 566-579.

Wang, Y. L. (1985). Exchange of actin subunits at the leading edge of living fibroblasts: possible role of treadmilling. *The Journal of cell biology 101*, 597–602.

Wang, Y. L., and Pelham, R. J. (1998). Preparation of a flexible, porous polyacrylamide substrate for mechanical studies of cultured cells. *Methods in enzymology*, 298, 489–96

Watanabe, N., and Mitchison, T. J. (2002). Single-Molecule Speckle Lamellipodia. *Science 295*, 1083–1086.

Webb, D. J., Parsons, J. T., and Horwitz, A. F. (2002). Adhesion assembly, disassembly and turnover in migrating cells -- over and over and over again. *Nature cell biology 4*, E97–100.

Weijer, C. J. (2009). Collective cell migration in development. *Journal of cell science 122*, 3215–3223.

Werner, S., and Grose, R. (2003). Regulation of Wound Healing by Growth Factors and Cytokines. *Physiology Review*, 835–870.

Wheeler, A. P., Wells, C. M., Smith, S. D., Vega, F. M., Henderson, R. B., Tybulewicz, V. L., and Ridley, A. J. (2006). Rac1 and Rac2 regulate macrophage morphology but are not essential for migration. *Journal of cell science 119*, 2749–2757.

Williams-Masson, E. M., Malik, a N., and Hardin, J. (1997). An actin-mediated two-step mechanism is required for ventral enclosure of the C. elegans hypodermis. *Development 124*, 2889–2901.

Wodarz, a, Hinz, U., Engelbert, M., and Knust, E. (1995). Expression of crumbs confers apical character on plasma membrane domains of ectodermal epithelia of Drosophila. *Cell 82*, 67–76.

Wong, I., and Ho, C.-M. (2009). Surface molecular property modifications for poly(dimethylsiloxane) (PDMS) based microfluidic devices. *Microfluidics and nanofluidics 7*, 291–306.

Wood, W., Jacinto, A., Grose, R., Woolner, S., Gale, J., Wilson, C., and Martin, P. (2002). Wound healing recapitulates morphogenesis in Drosophila embryos. Nature cell biology *4*, 907–912.

Woolner, S., Jacinto, A., and Martin, P. (2005). The small GTPase Rac plays multiple roles in epithelial sheet fusion--dynamic studies of Drosophila dorsal closure. *Developmental biology 282*, 163–173.

Xia, Y., and Kao, W. W.-Y. (2004). The signaling pathways in tissue morphogenesis: a lesson from mice with eye-open at birth phenotype. *Biochemical pharmacology 68*, 997–1001.

Xia, Y., and Karin, M. (2004). The control of cell motility and epithelial morphogenesis by Jun kinases. *Trends in cell biology* 14, 94–101.

Xu, S., and Chisholm, A. D. (2011). A Gαq-Ca2+ signaling pathway promotes actin-mediated epidermal wound closure in C. elegans. *Current biology*, 21(23), 1960–7.

Yamada, S., Pokutta, S., Drees, F., Weis, W. I., and Nelson, W. J. (2005). Deconstructing the cadherin-catenin-actin complex. *Cell* 123, 889–901.

Yamanaka, T., Horikoshi, Y., Suzuki, a, Sugiyama, Y., Kitamura, K., Maniwa, R., Nagai, Y., et al. (2001). PAR-6 regulates aPKC activity in a novel way and mediates cell-cell contact-induced formation of the epithelial junctional complex. *Genes to cells* 6(8), 721-31.

Yang, C., Czech, L., Gerboth, S., Kojima, S.-ichiro, Scita, G., and Svitkina, T. (2007). Novel roles of formin mDia2 in lamellipodia and filopodia formation in motile cells. *PLoS biology 5*, e317.

Yang, N., Higuchi, O., Ohashi, K., Nagata, K., Ada, A., Kangawa, K., Nishida, E., and Mizuno, K. (1998). Cofilin phosphorylation by LIM-kinase 1 and its role in Rac-mediated actin reorganization. *Nature 393*, 809–812.

Yarrow, J. C., Perlman, Z. E., Westwood, N. J., and Mitchison, T. J. (2004). A high-throughput cell migration assay using scratch wound healing, a comparison of image-based readout methods. *BMC biotechnology 4*, 21.

Yin, J., Xu, K., Zhang, J., Kumar, A., and Yu, F.-S. X. (2007). Wound-induced ATP release and EGF receptor activation in epithelial cells. *Journal of cell science 120*, 815–825.

Yonemura, S., Wada, Y., Watanabe, T., Nagafuchi, A., and Shibata, M. (2010). alpha-Catenin as a tension transducer that induces adherens junction development. Nature cell biology *12*, 533–542.

Zaidel-Bar, R., and Geiger, B. (2010). The switchable integrin adhesome. *Journal of cell science 123*, 1385–1388.

Zamir, E., and Geiger, B. (2001). Molecular complexity and dynamics of cell-matrix adhesions. *Journal of cell science 114*, 3583–3590.

Zavadil, J., and Böttinger, E. P. (2005). TGF-beta and epithelial-to-mesenchymal transitions. *Oncogene 24*, 5764–5774.

Zemel, A, Rehfeldt, F., Brown, a E. X., Discher, D. E., and Safran, S. a (2010). Optimal matrix rigidity for stress fiber polarization in stem cells. *Nature physics 6*, 468–473.

Zenz, R., Scheuch, H., Martin, P., Frank, C., Eferl, R., Kenner, L., Sibilia, M., and Wagner, E. F. (2003). c-Jun regulates eyelid closure and skin tumor development through EGFR signaling. *Developmental cell 4*, 879–889.

Zhang, H., Gally, C., & Labouesse, M. (2010). Tissue morphogenesis: how multiple cells cooperate to generate a tissue. *Current opinion in cell biology*, *22* (5), 575-82

Zhang, H., Landmann, F., Zahreddine, H., Rodriguez, D., Koch, M., and Labouesse, M. (2011). A tension-induced mechanotransduction pathway promotes epithelial morphogenesis. *Nature 471*, 99–103.

Zheng, J. Q., Wan, J. J., and Poo, M. M. (1996). Essential role of filopodia in chemotropic turning of nerve growth cone induced by a glutamate gradient. *The Journal of neuroscience 16*, 1140–1149.